

Gaseous detectors

A watercolor illustration of a courtyard. In the foreground, a paved walkway leads towards a large, multi-story building with a series of arched windows. To the left, there is a covered walkway or bridge structure. The background shows more buildings and greenery under a light sky. The overall style is artistic and painterly.

M. Abbrescia

EURIZON School on particle detection technologies

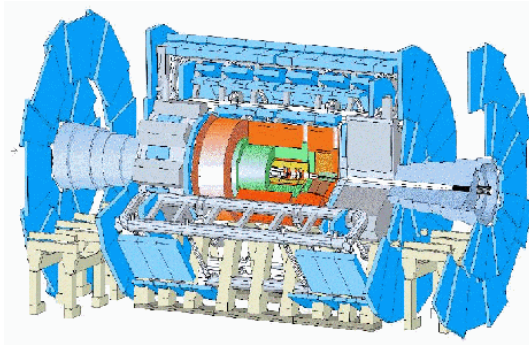
Why studying gaseous detectors?

Many times the replacement of gaseous detectors by solid state detectors, and their progressive elimination was predicted

ALL the times, this prediction turned out to be wrong!

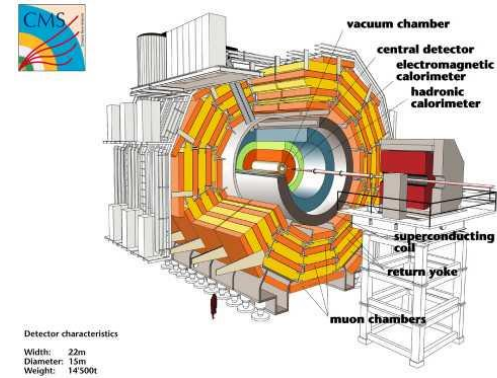
- ✓ Silicon detectors **have replaced** gaseous detectors for vertex detection
- ✓ Gaseous **detectors are still dominating in the muon systems** at large radii
 - to date it is totally unrealistic to replace such a system by Si detectors
- ✓ The Time Projection Chamber (TPC) for Heavy Ion Physics **is unbeatable** in terms of radiation length and channel number economy
- ✓ Gaseous detectors **have even regained territory** that was occupied by other technologies
 - Examples: Resistive Plate Chambers (RPCs) **replacing scintillators** for triggering and time of flight measurements, or Micro-Pattern Gaseous Detectors (MPGDs) **proposed to be used** for precision tracking.

Gaseous detectors @ LHC



ATLAS Gaseous Detectors:

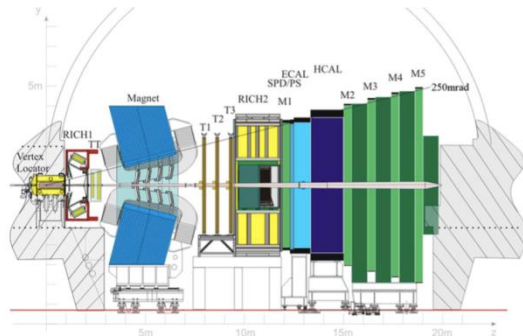
- MDT, RPC, CSC, TGC, MM



Detector characteristics
Width: 22m
Diameter: 13m
Weight: 14500t

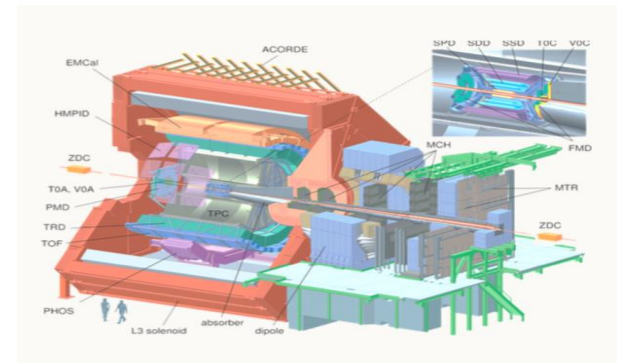
CMS Gaseous Detectors:

- DT, RPC, CSC, GEM



LHCb Gaseous Detectors:

- MWPC, GEM



ALICE Gaseous Detectors:

- RPC, MRPC, TPC

Gas Detector History



Geiger Counter
H. Geiger W. Mueller 1928

PPC
Parallel Plate Counter

PC
Proportional Counter

Pestov Counter
V. Pestov 1982

RPC
Resistive Plate Chambers
R. Santonico R. Cardarelli 1981



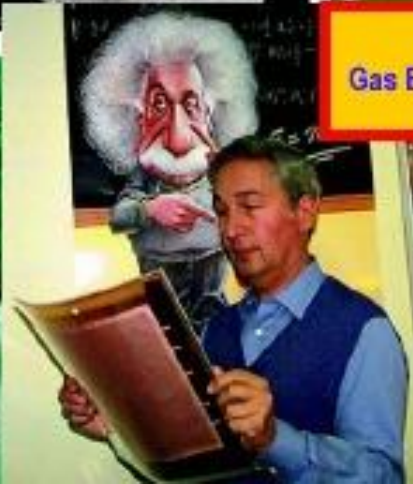
MWPC
Multiwire Proportional Chamber
G. Charpak et al 1958

TPC
Time Projection Chamber
D.R. Nygren et al 1974

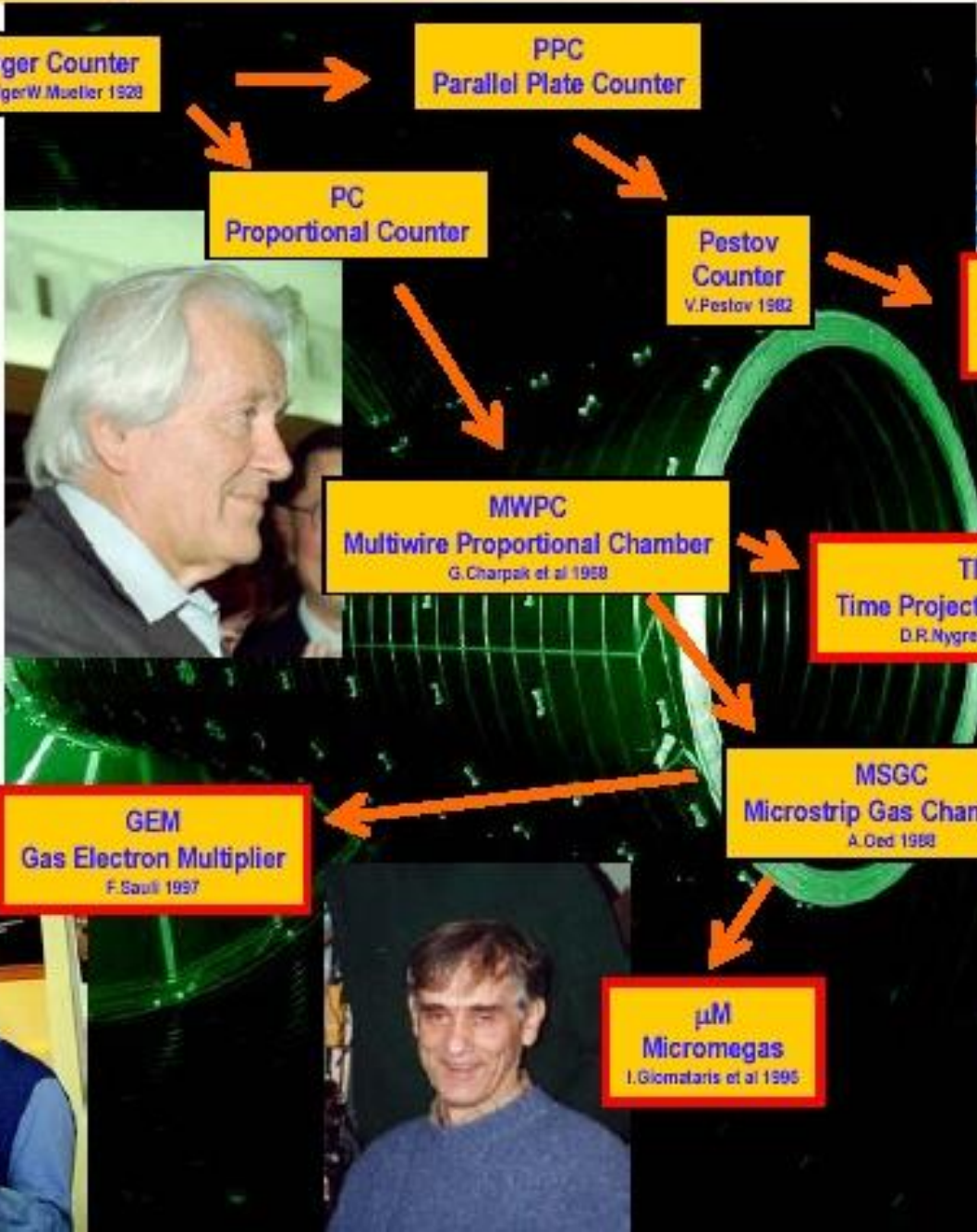


GEM
Gas Electron Multiplier
F. Sauli 1997

MSGC
Microstrip Gas Chambers
A. Oed 1988

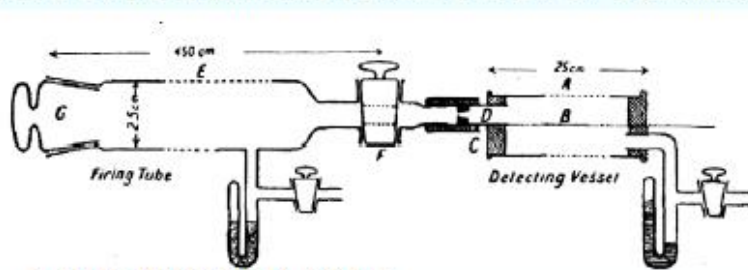


μM
Micromegas
I. Giomataris et al 1995



100 years of glorious tradition

1908: FIRST WIRE COUNTER USED BY RUTHERFORD IN THE STUDY OF NATURAL RADIOACTIVITY

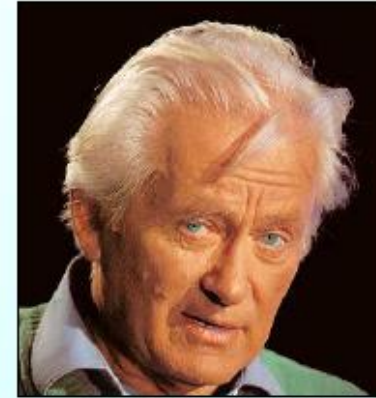
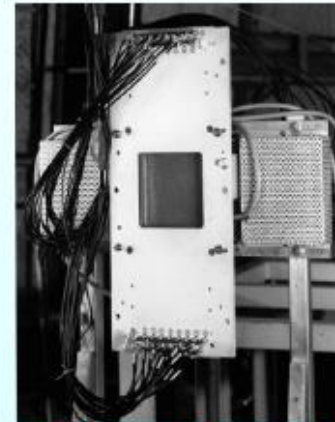


E. Rutherford and H. Geiger,
Proc. Royal Soc. A81 (1908) 141



Nobel Prize in Chemistry in 1908

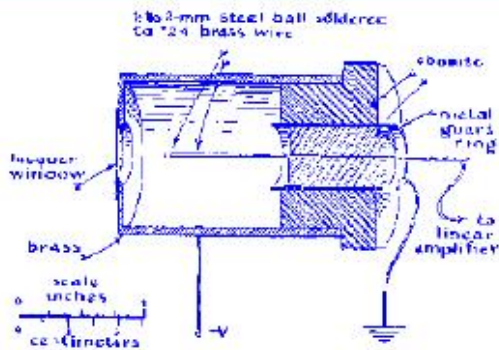
1968: MULTIWIRE PROPORTIONAL CHAMBER



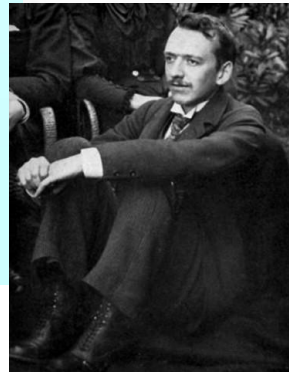
Nobel Prize in 1992

G. Charpak, *Proc. Int. Symp. Nuclear Electronics (Versailles 10-13 Sept 1968)*

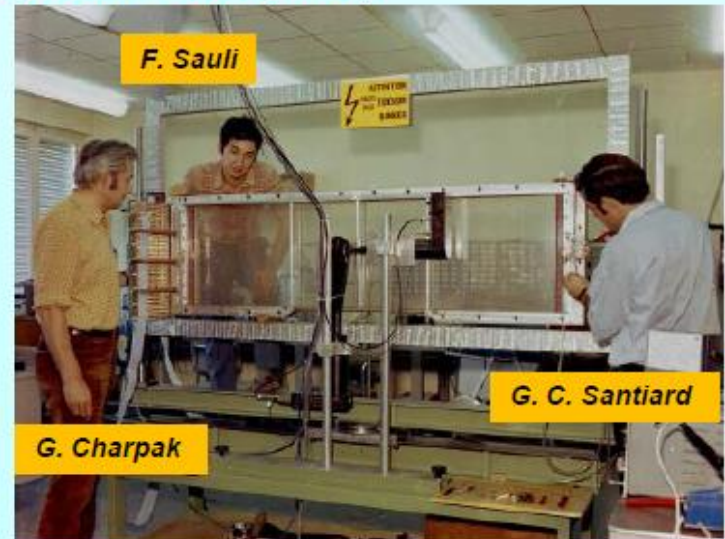
1928: GEIGER COUNTER SINGLE ELECTRON SENSITIVITY



H. Geiger and W. Müller,
Phys. Zeits. 29 (1928) 839

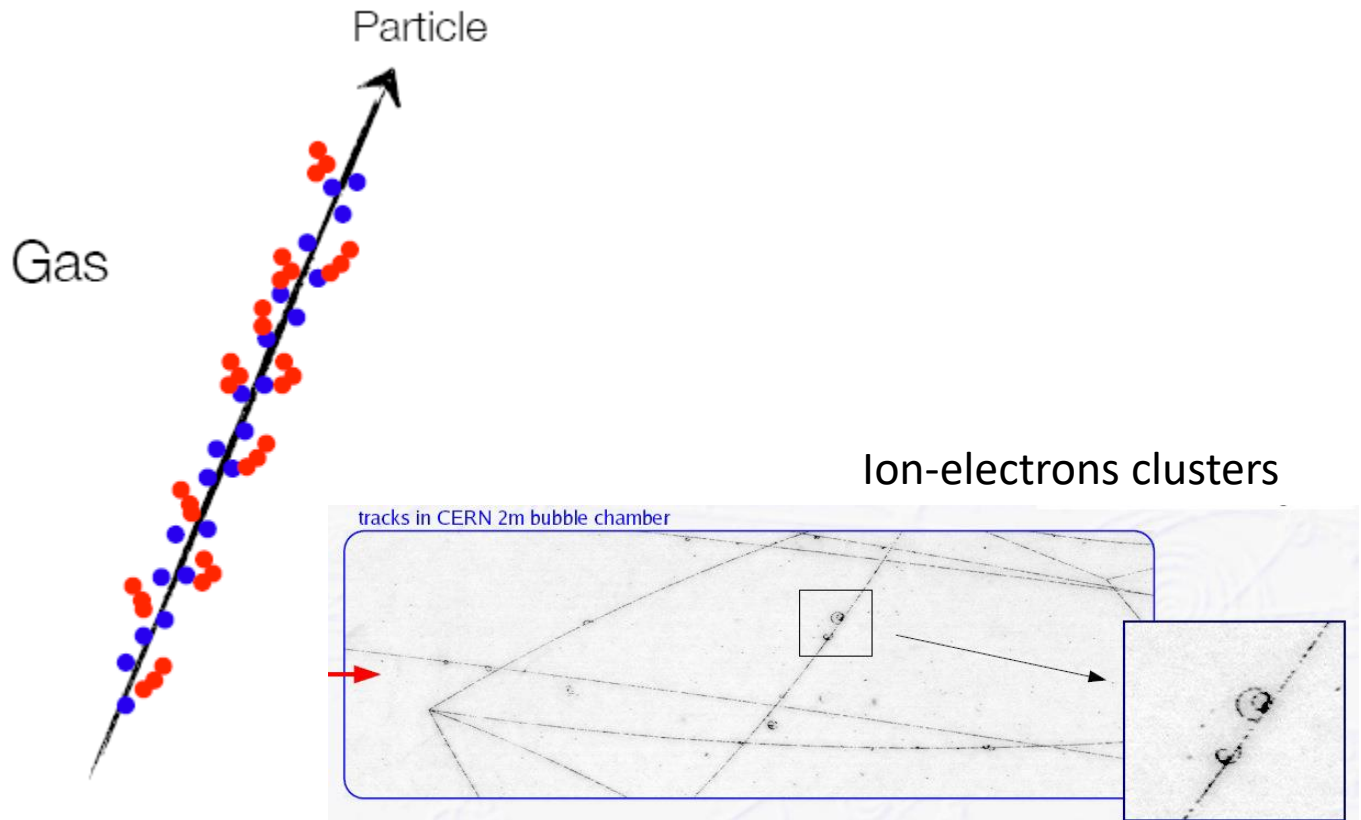


C.T.R. Wilson,
aged 20,
Nobel prize
in 1927



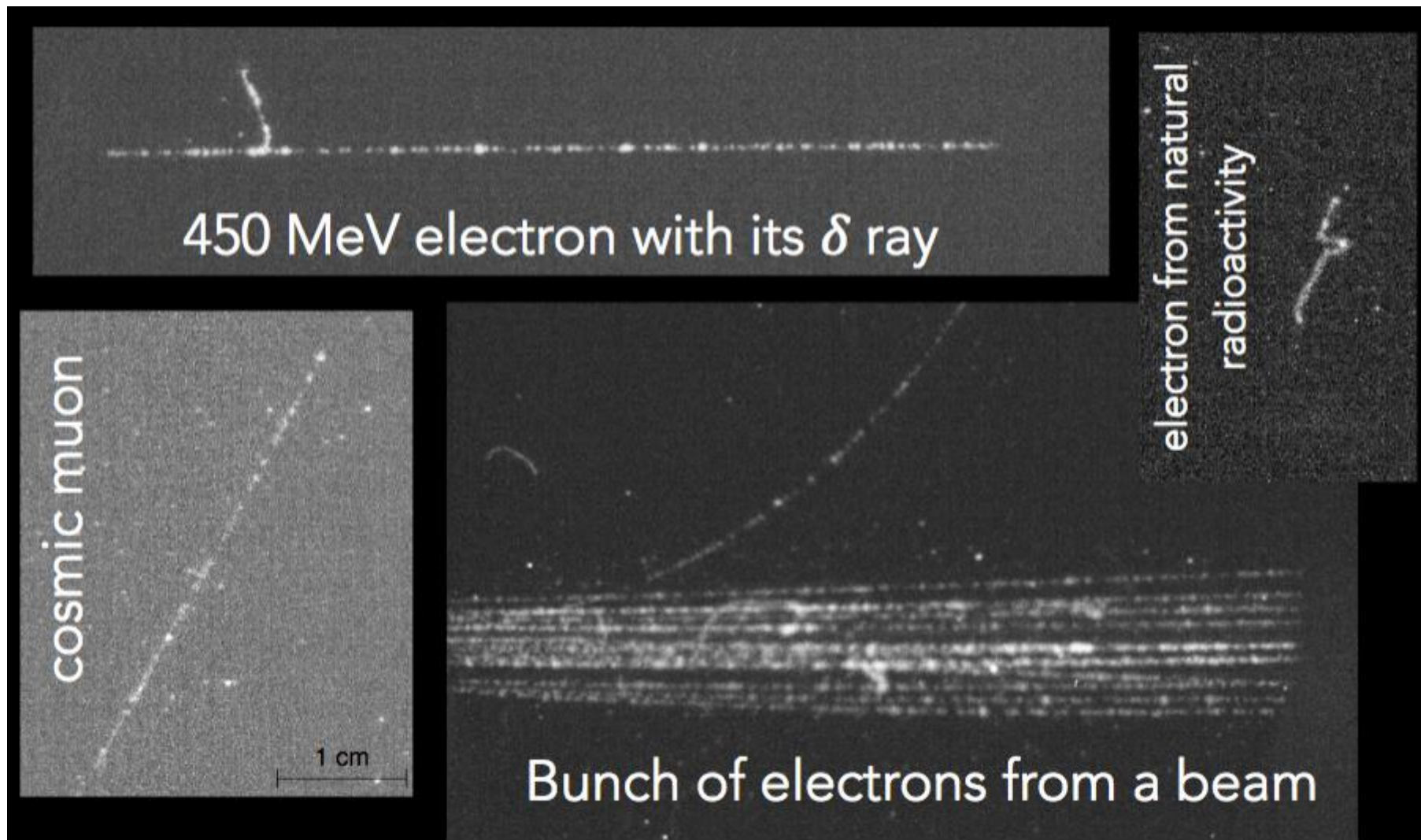
Schematic principle of gaseous detectors

“Core” of a gaseous detector is a volume of gas, or gas mixture, where a charged ionizing particle leaves a trail of ion-electron pairs. Some electrons can further ionize the gas, creating “clusters” of ions electron pairs.



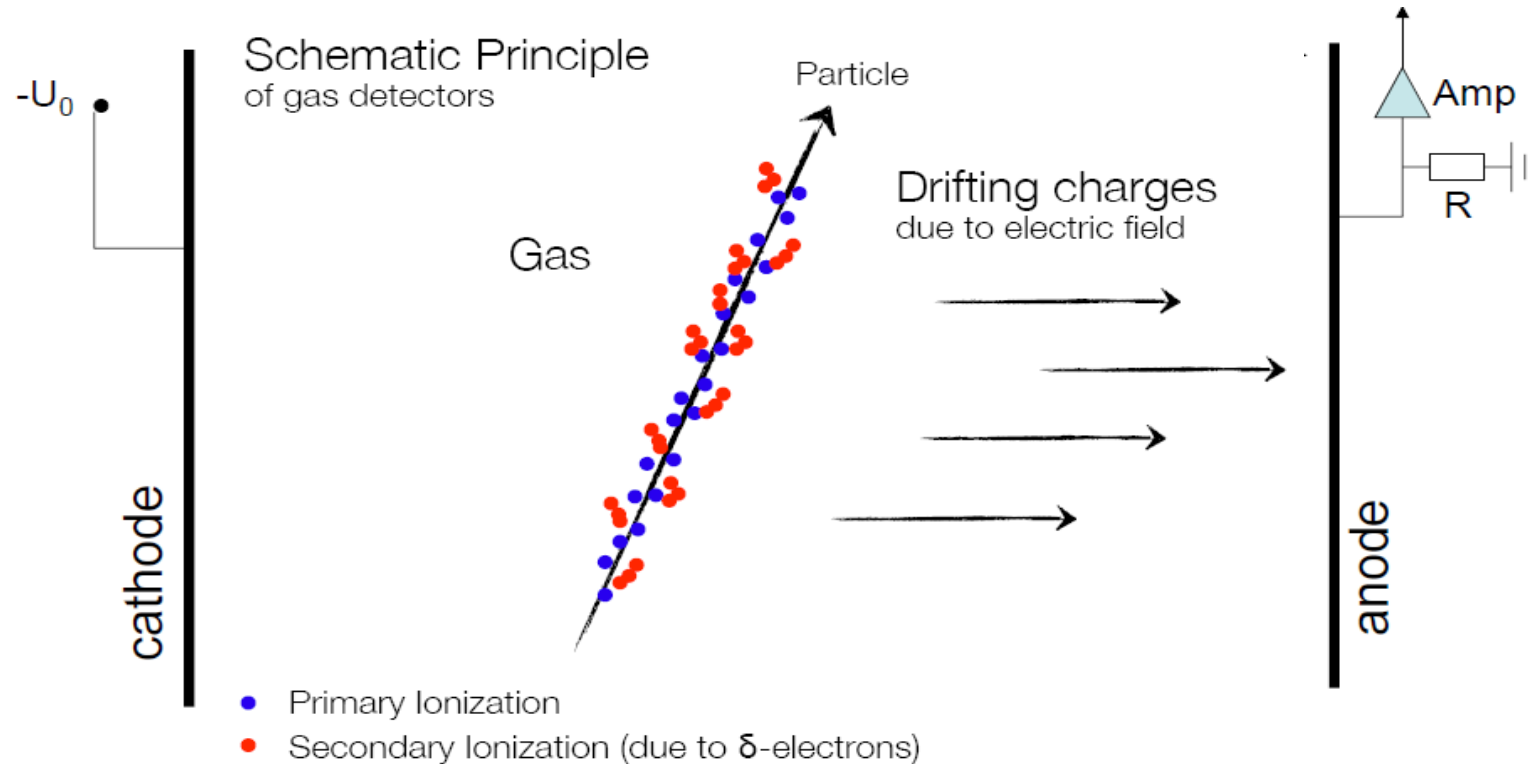
- Primary Ionization
- Secondary Ionization (due to δ -electrons)

Particle tracks in a gaseous detector



Triple-GEM: we will see it later on.

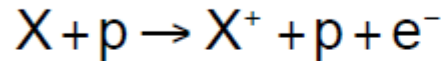
Working principle of gaseous detectors



- An electric field is applied: due to its presence, electrons and ions move toward anode and cathode, respectively.
- If the electric field is intense enough multiplication processes take place (Townsend avalanches)
- Signal is produced by **induction** from the movement of charges in the gas

Ionization

Primary ionization

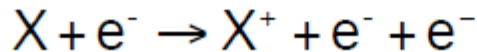


p = charge particle traversing the gas

X = gas atom

e^- = delta-electron (δ)

Secondary ionization



if E_δ is high enough ($E_\delta > E_i$)

Ionization energy

: I_0

Average energy/ion pair

: W_i

Average number of primary ion pairs [per cm]

: n_p

Average number of ion pairs [per cm]

: n_T

$$\langle n_T \rangle = \frac{L \cdot \left\langle \frac{dE}{dx} \right\rangle_i}{W_i}$$

[about 2-6 times n_p]

[L: layer thickness]

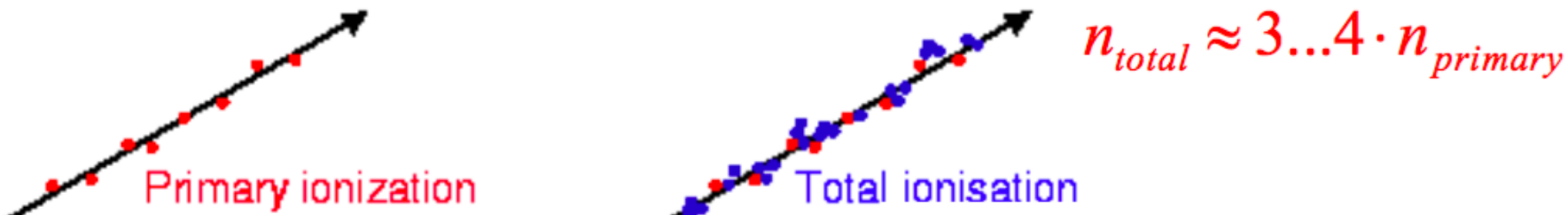
Note: $I_0 \neq W_i$, because **not the whole energy** lost by the impinging particle goes in ionization processes; a part (roughly half) goes **in excitation** of the gas molecules.

→ The average energy W_i needed to create an ion-electron pair is $\approx 2-3 I_0$

Typical values: $W_i \approx 30 \text{ eV} \rightarrow 100 \text{ e}^-/\text{ion pairs}$ for 3 keV of energy lost by the particle

Secondary ionization

Quite often the extracted electrons have kinetic energy enough to generate secondary ionization: they are usually called δ -rays. Other ion-electron pairs are produced close to the track.



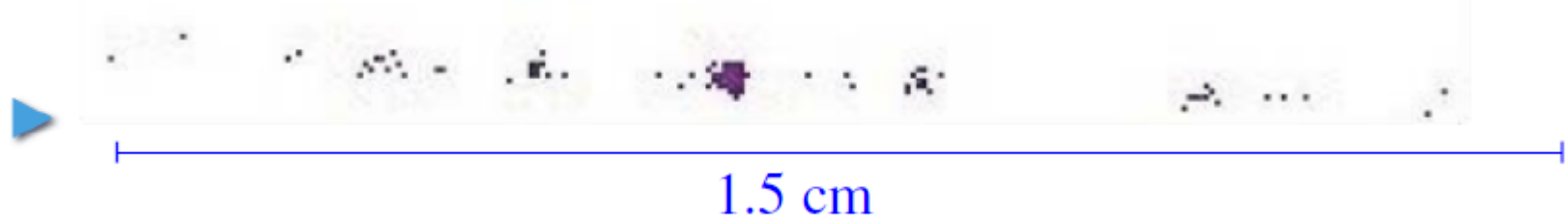
$$n_T = \frac{\Delta E}{W_i}$$

- ΔE : total energy loss
- W_i : energy needed to create one ion/electron pair (**typically few tens of eV, depending on the gas**)
- n_T : total number of ion/electron pairs generated (**typically 100 pairs/cm**)

The total number of electron/ion pairs created is proportional to the total energy deposited in the gas. Moreover: $n_T = n_p + n_s$.

Characteristic of ionization

Electrons are not evenly spaced, not even exponentially:



▶ 25-30 clusters/cm

Ar

δ -electrons

▶ Deposits are not always “lumps”:



Number of primary ionising interactions per cm in Ar,

- ▶ by μ^\pm at minimum ionising energy,
- ▶ at 300 K and 1 atm,

according to

- ▶ Degrad: 23.1 / cm
- ▶ Heed: 24.1 / cm
- ▶ Rieke-Prepejchal: 24.3 / cm
- ▶ CERN 77-9: 29.4 / cm

Various simulations programs do exist to computer gas parameters

Parameters of most common gases

Gas	ρ (g/cm ³) (STP)	I_0 (eV)	W_i (eV)	dE/dx (MeVg ⁻¹ cm ²)	n_ρ (cm ⁻¹)	n_t (cm ⁻¹)
H ₂	$8.38 \cdot 10^{-5}$	15.4	37	4.03	5.2	9.2
He	$1.66 \cdot 10^{-4}$	24.6	41	1.94	5.9	7.8
N ₂	$1.17 \cdot 10^{-3}$	15.5	35	1.68	(10)	56
Ne	$8.39 \cdot 10^{-4}$	21.6	36	1.68	12	39
Ar	$1.66 \cdot 10^{-3}$	15.8	26	1.47	29.4	94
Kr	$3.49 \cdot 10^{-3}$	14.0	24	1.32	(22)	192
Xe	$5.49 \cdot 10^{-3}$	12.1	22	1.23	44	307
CO ₂	$1.86 \cdot 10^{-3}$	13.7	33	1.62	(34)	91
CH ₄	$6.70 \cdot 10^{-4}$	13.1	28	2.21	16	53
C ₄ H ₁₀	$2.42 \cdot 10^{-3}$	10.8	23	1.86	(46)	195

for MIPs

of ion-electron pairs in gas mixtures

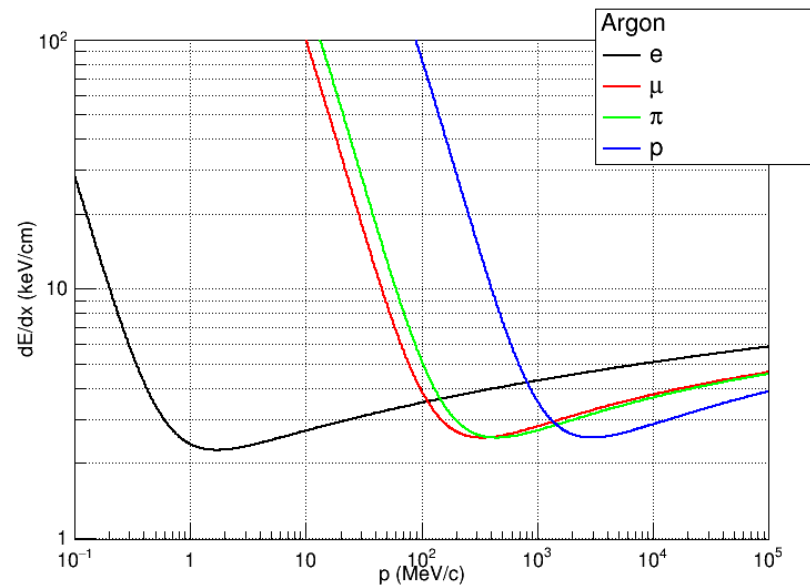
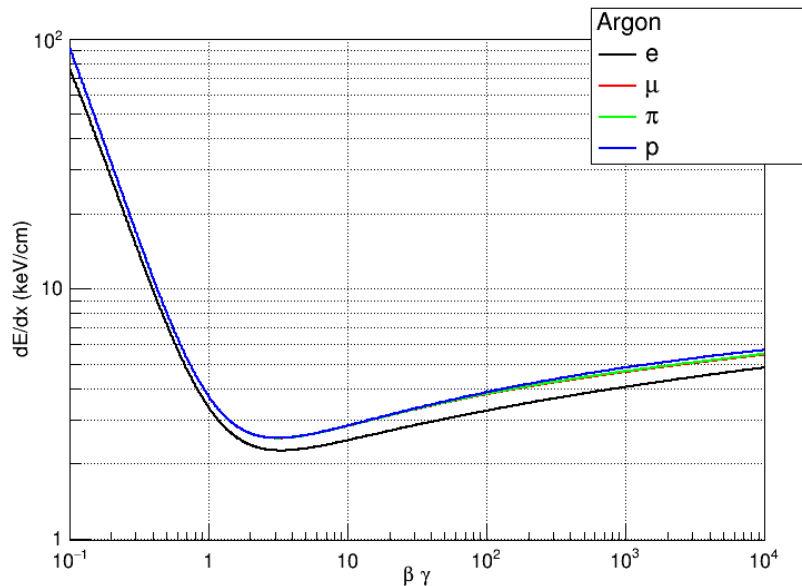
The number of primary and total ion-electron pairs in gas mixtures can be computed taking into account the fractional gas composition (in volume) and the values for the individual gases.

Example: gas mixture Ar/C₄H₁₀ 70/30

$$n_T = 0.7 \times 91 + 0.3 \times 195 = 122 \text{ pairs/cm}$$

$$n_p = 0.7 \times 34 + 0.3 \times 46 = 38 \text{ pairs/cm}$$

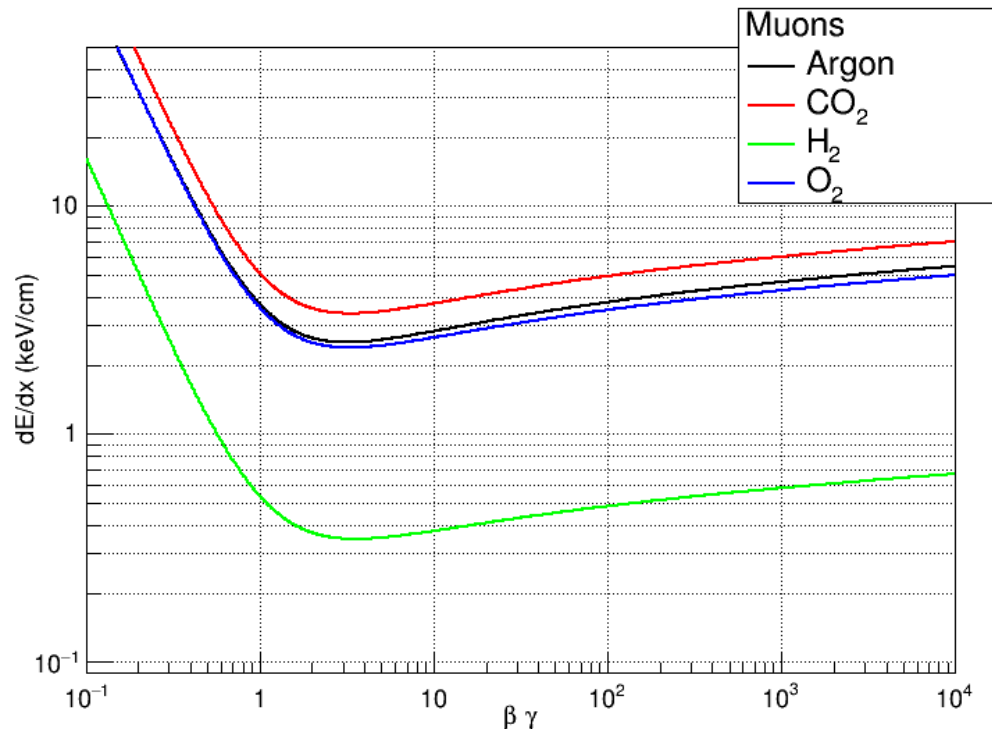
Energy loss in Ar



Energy loss is usually computed by means of the Bethe-Block formula (whose non quantum mechanical version was obtained by Bohr in 1907)

- The minimum energy loss for electrons is slightly lower than the minimum of heavier particles.

Energy loss in various gases



- Although $Z/A=1$, the energy loss in hydrogen is significantly lower than in other gases due to the lower density.

Statistics of ion-electron pair production

Primary ionization events are independent and therefore follow

Poisson statistics.

- Each time an impinging particle crosses a layer of gas, it has a certain probability to produce a certain number of primary electrons
- If n_p is the average number of primary electrons (ions), the probability $P(k)$ to have k electrons (ions) is:

$$P(k) = e^{-n_P} \frac{n_P^k}{k!}$$

Therefore there is always a finite probability to produce no electron-ion pairs: $P(0) = e^{-n_P}$

→ What happens in these cases?

Note: of course n_p is proportional to the gas layer thickness and the energy loss.

Diffusion of electrons and ions in gases

After ionization, electrons and ions quickly lose their energy due to collisions with the gas molecules → thermalize

-Electrons and ions energy (and velocity) distribution are well described by a Maxwell distribution

$$P(E) \propto \sqrt{E} e^{-\frac{E}{kT}}$$

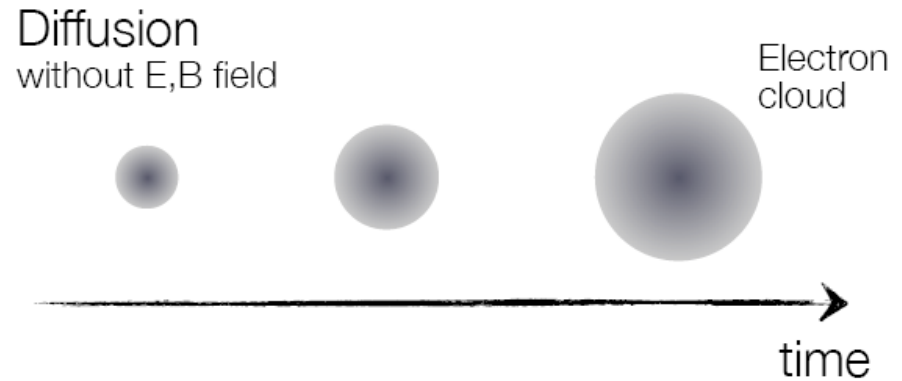
- Mean velocity according to Maxwell distribution: $v = \sqrt{\frac{8kT}{\pi m}}$ m=mass of particle

-Their average kinetic energy at room temperature is $E \approx 3/2 kT \approx 26 \text{ meV}$

Immediately, ions and electrons undergo diffusion processes, like “a drop of ink in clear water”.

Diffusion of electrons and ions in gases

Diffusion processes in gases are well described by the kinetic theory of gases. After a time t from ionization, electrons (ions) density is well described by a Gaussian distribution:



$$\frac{dN}{dr} = \frac{N_0}{\sqrt{4\pi Dt}} \exp\left(-\frac{r^2}{4Dt}\right)$$

whose σ is related to the diffusion coefficient D by:

$$\sigma(r) = \sqrt{6Dt}$$

Diffusion takes place in 3D:

- considering diffusion just in one direction: $\sigma_x = \sqrt{2Dt}$

Diffusion coefficient is given by the following expression:

$$D = \frac{1}{3} v \lambda = \frac{2}{3\sqrt{\pi}} \frac{1}{P\sigma_0} \sqrt{\frac{(kT)^3}{m}}$$

D depends on gas temperature T and pressure P
 λ = electron (ion) mean free path in the gas

Diffusion of electrons and ions in gases

- This table shows the mean free path, the average velocity, the diffusion coefficients and the mobilities (see later on) of ions in their own gases at NTP
- Electrons move faster than ions (because of their much lower mass) with average thermal velocities of the order of 10^7 cm/s.

Gas	$\lambda(\text{cm})$	$u(\text{cm/s})$	$D^+(\text{cm}^2/\text{s})$	$\mu^+(\text{cm}^2\text{s}^{-1}\text{V}^{-1})$
H_2	1.8×10^{-5}	2.0×10^5	0.34	13
He	2.8×10^{-5}	1.4×10^5	0.26	10.2
Ar	1.0×10^{-5}	4.4×10^4	0.04	1.7
O_2	1.0×10^{-5}	5.0×10^4	0.06	2.2
H_2O	1.0×10^{-5}	7.1×10^4	0.02	0.7

Diffusion of electrons and ions in gases

While diffusing, electrons and ions do not have an easy life.

Possible interaction of positive ions:

- Neutralization with a negative charge carrier (either an electron or a negative ion)
- Neutralization after the extraction of an electron from the walls of the detector
- Charge transfer
 - to a molecule of its own gas ($A^+ + A \rightarrow A + A^+$)
 - to a molecule of another gas with lower ionization potential ($A^+ + B \rightarrow A + B^+$)

Possible interactions of electrons:

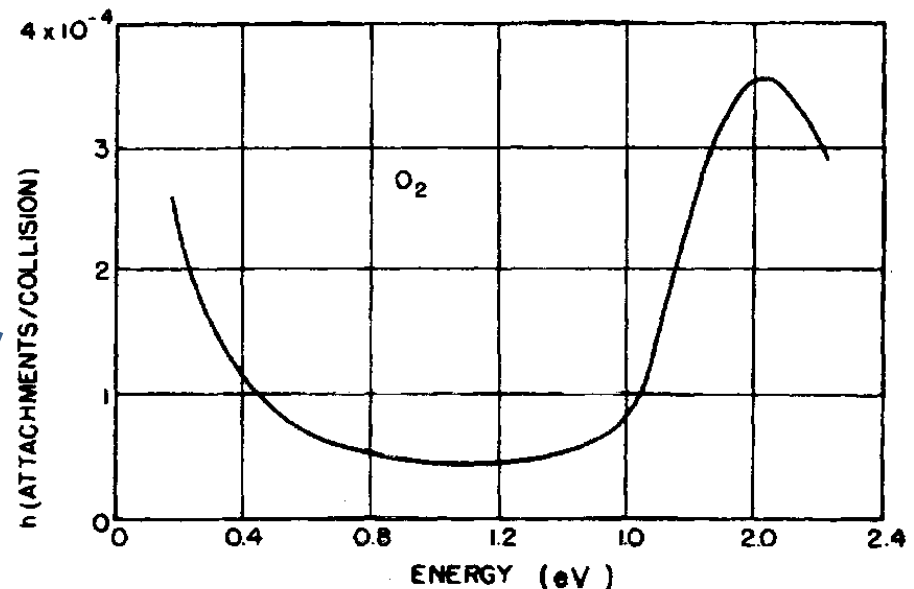
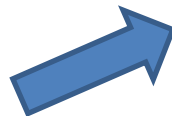
- Neutralization with a positive ion ($e + A^+ \rightarrow A$)
- Attachment to a molecule with negative electron affinity ($e + A \rightarrow A^-$)
 - This attachment probability is negligible for noble gases and hydrogen
 - Oxygen is a gas with strong electronegative affinity
 - The attachment coefficient depends strongly on the electric field (if any)
- Absorption in the walls of the detector

Effects of electronegative gases

- Some gases, like O_2 , Cl_2 , H_2O vapour, etc., are characterized by a high probability to capture drifting electrons and form negative ions;
- The net effect is reducing the total number of drifting electrons → electronegative gases
- The probability of capture per collision (or per unit length) is called "attachment coefficient"

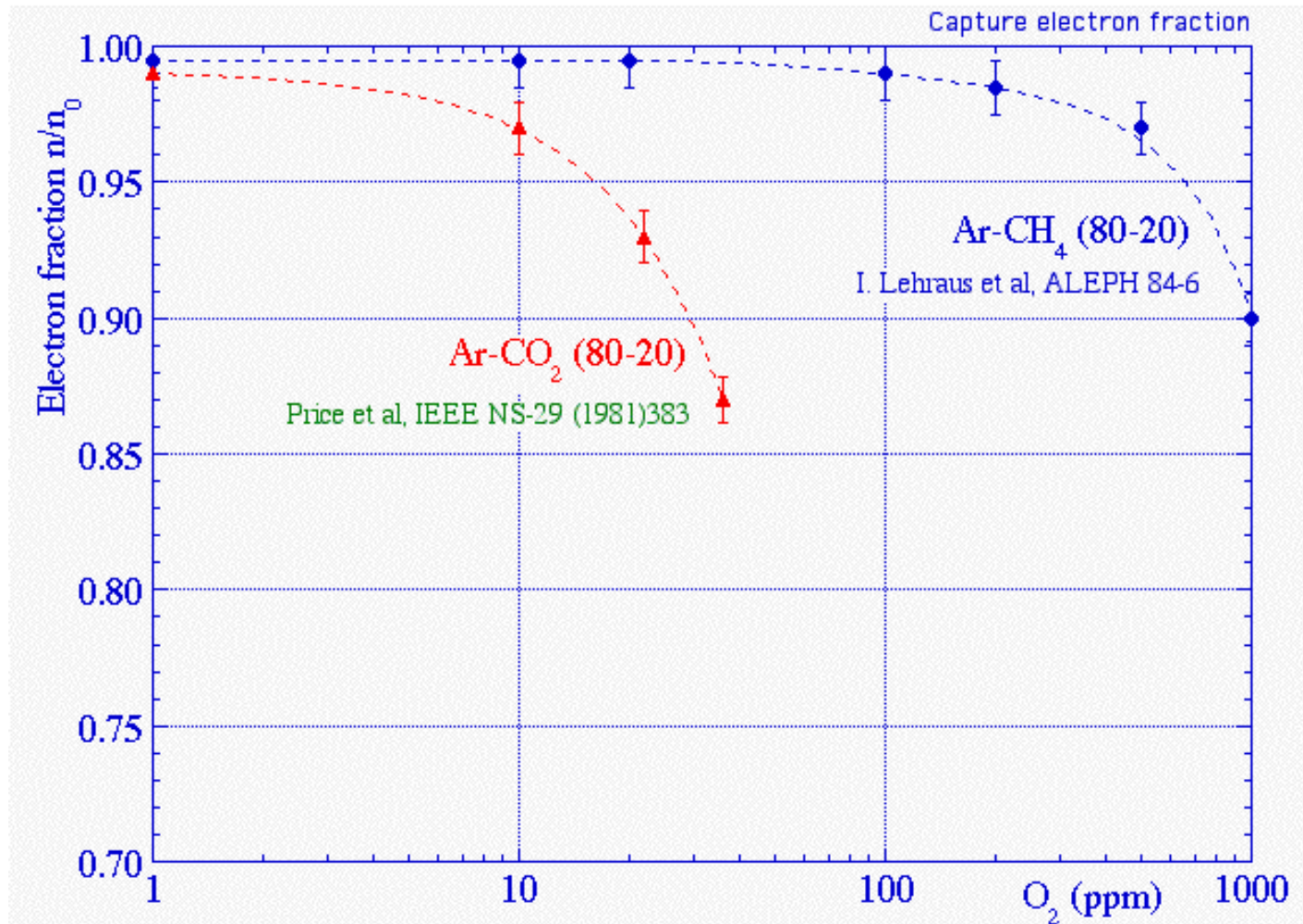
The attachment coefficient strongly depends on electron energy .

Attachment coefficient of electrons in Oxygen, vs. electron kinetic energy



Effects of electronegative gases

Fraction of electrons surviving after a drift of 20 cm in two gas mixtures, as a function of the contamination of O_2 , under the action of $E = 200$ V/cm



Drift in electric fields

When an electric field is applied, the electron-ion pairs drift along the electric field lines, and this motion is superimposed to the chaotic thermal motion.

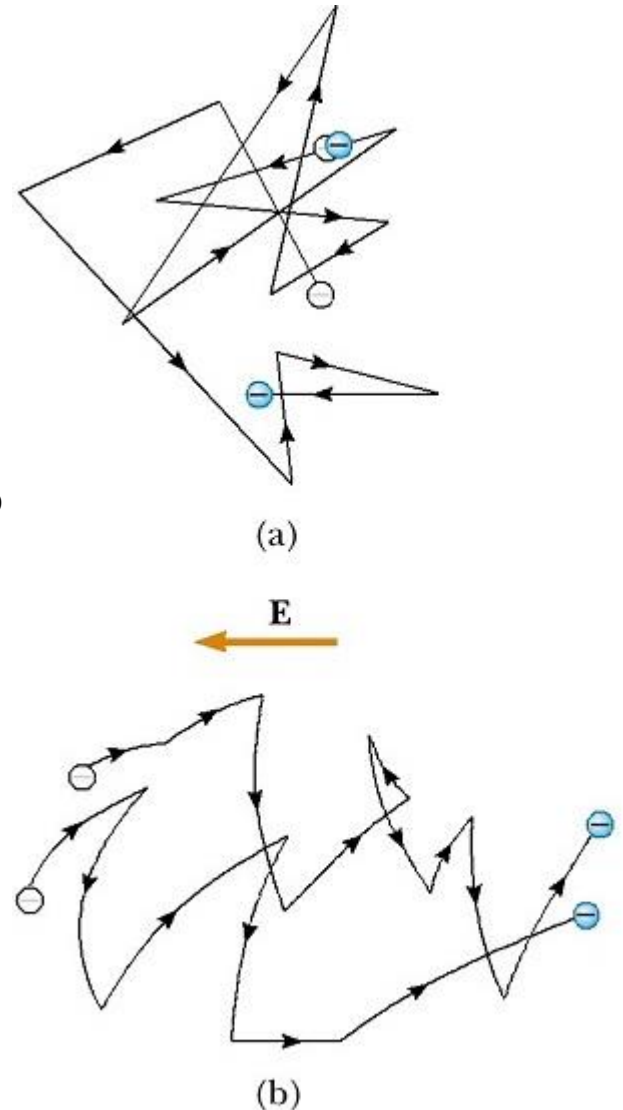
- Acceleration is interrupted by collisions with gas atoms
- This limits the drift velocity \rightarrow mean drift velocity v_D
- The drift velocity is roughly proportional to the time between two subsequent collisions

$$\vec{v}_D = \frac{q}{m} \cdot \tau(\vec{E}, \sigma) \cdot \vec{E}$$

q, m ... charge and mass

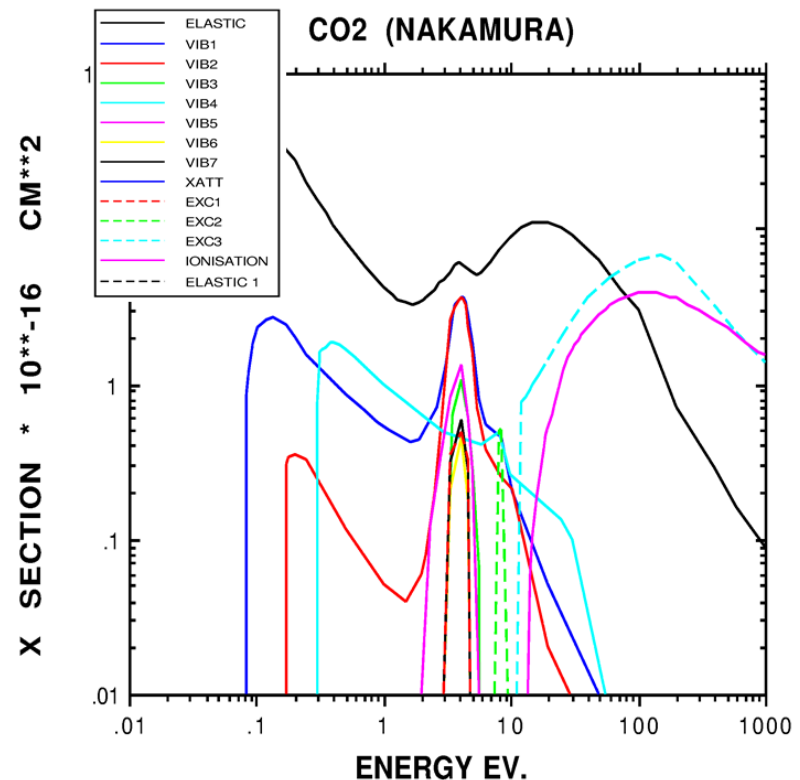
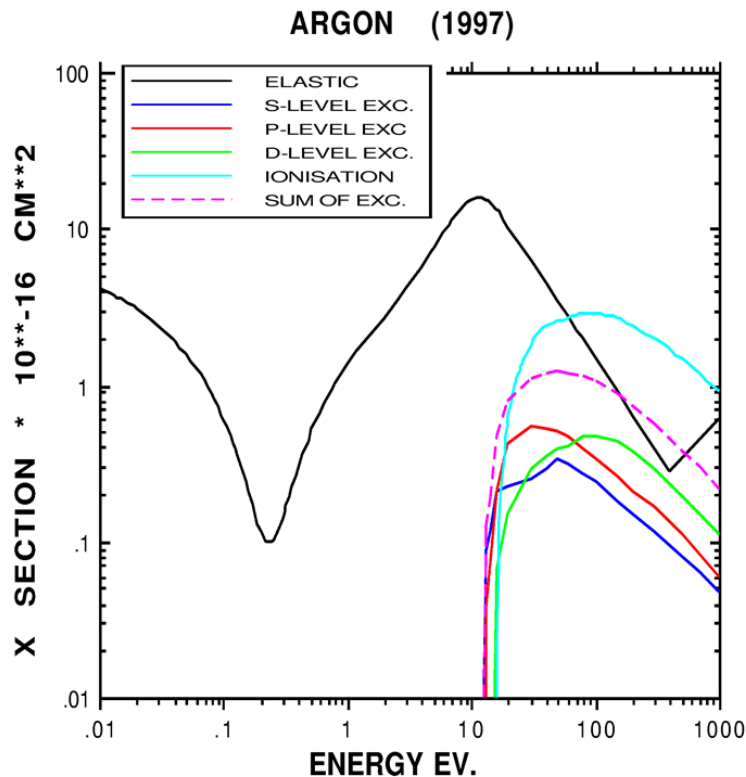
E ... electric field

τ ... mean time between collisions

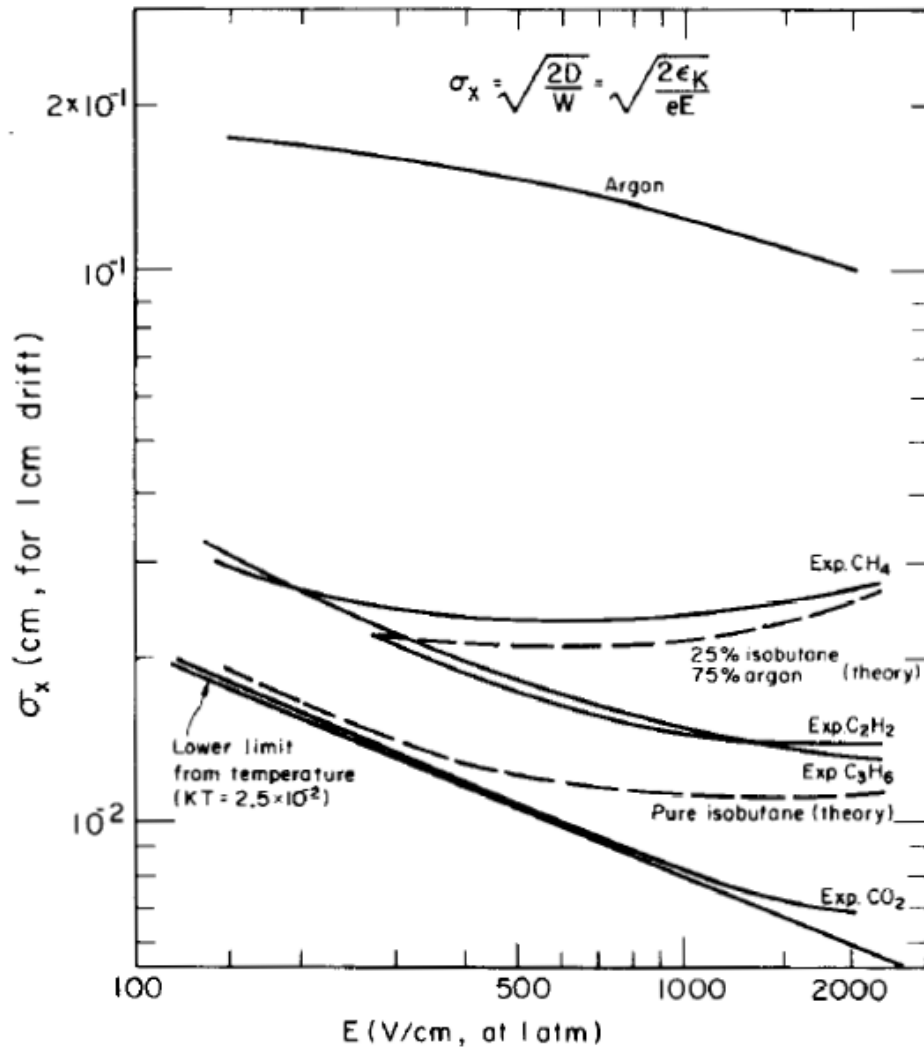


Drift of electrons in gases

- v_d is just **the average velocity** in the direction of the electric field; a random thermal movement is superimposed \rightarrow diffusion while drifting
- While drifting, electrons **can undergo several processes** (excitation, ionization, and others), whose cross section depends in complicated ways on the electron kinetic energy due to quantum mechanical effects and the structure of the molecules of the gas.

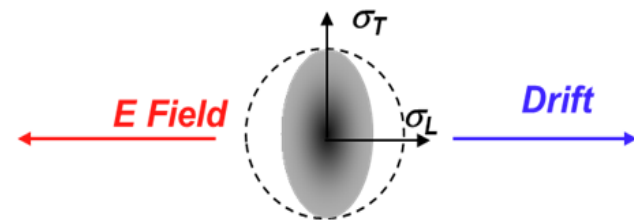


Diffusion in electric field



Drift in direction of E-field superimposed to statistical diffusion

- Extra velocity **influences longitudinal diffusion**
- Transverse diffusion not affected



Drifting induces a reduced diffusion in the longitudinal direction

Diffusion in magnetic field

The presence of a magnetic field changes the drift properties of a swarm of electrons

- The trajectories between collisions are **no more rectilinear**;
- The energy distribution can be changed
- The drift velocity **is smaller** with respect to the absence of a magnetic field and can be approximated as:

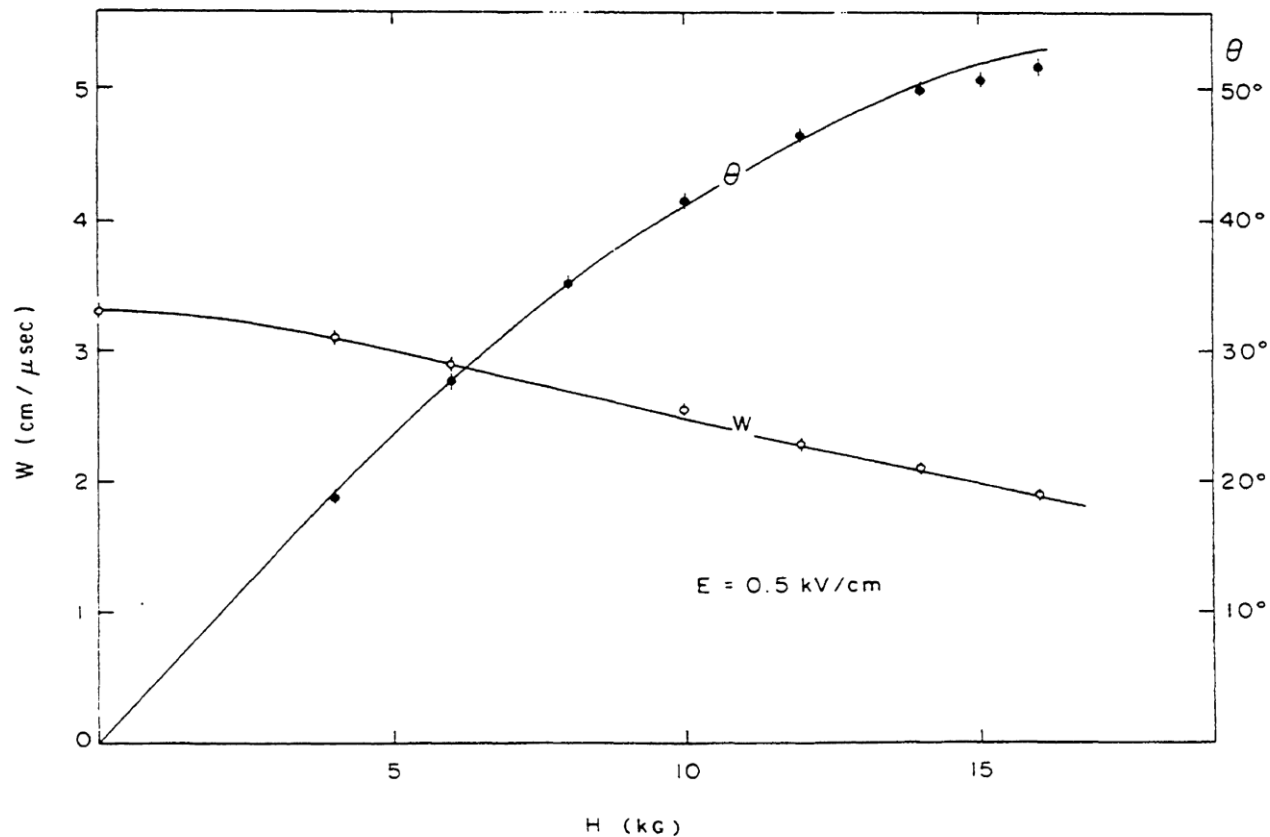
$$v_D^B = \frac{v_D}{\sqrt{1 + \omega^2 \tau^2}} \quad \text{where} \quad \omega = \frac{eB}{m} \quad \text{is the Larmour frequency}$$

and τ is the average time between two subsequent electron collisions.

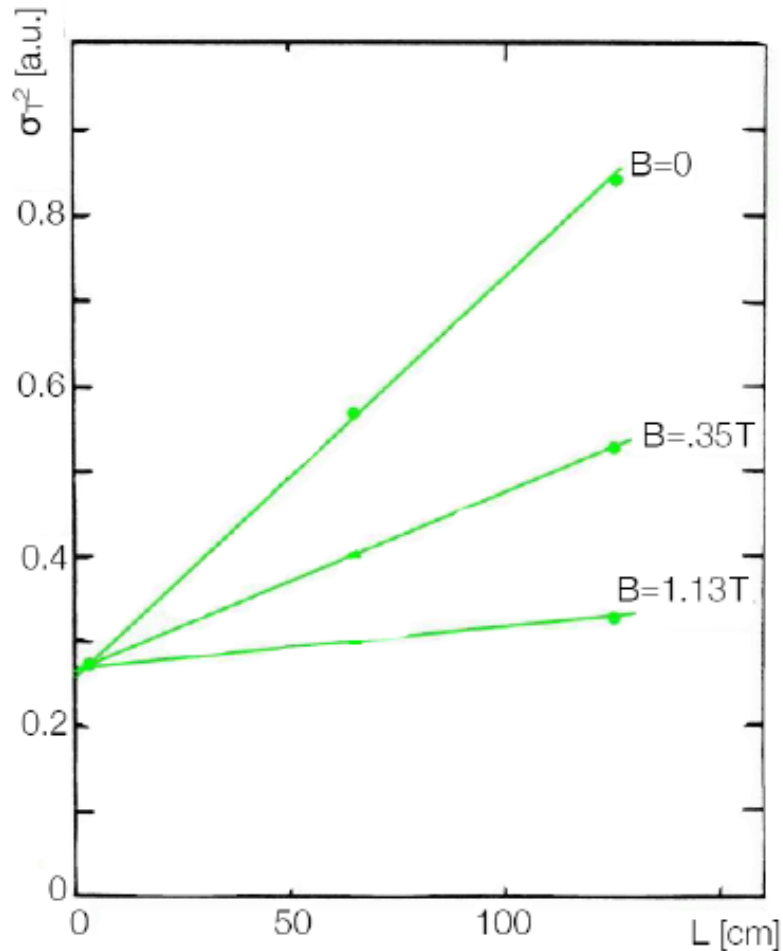
- **Electrons do not drift anymore along the electric field lines**
 - the angle between \mathbf{v}_D and \mathbf{E} is called the Lorentz angle

Effects of a magnetic field

Dependance of the electron drift velocity and Lorentz angle on the magnetic field for a mixture of Ar/C₄H₁₀/methyal 67.2/30.3/2.5 (an electric field of 500 V/m is applied).

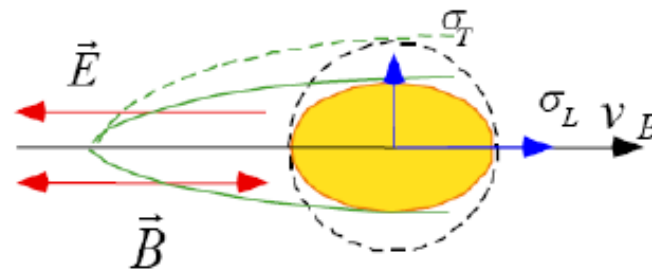


Diffusion in magnetic fields



In the presence of a B-field different effects on longitudinal and transverse diffusion

No Lorentz force along B-field direction



Transverse diffusion as function of drift length for different B fields

B-Field can substantially reduce diffusion in transverse direction

Drift of ions/electrons in gases

On **average** electrons/ions move along the field lines of the electric field E . Sometimes, one finds that v_d is roughly proportional to E -field, the mobility μ (for ions and electrons) is usually introduced, relating drift velocity and applied electric field:

$$\vec{v}_D = \mu_{\pm} |\vec{E}| \quad [\text{cm s}^{-1} \text{ V}^{-1}]$$

Note: μ_{\pm} usually depend also on gas T and p .

Mobility behaves differently for the case of ions and electrons.

μ_+ : ion mobility

- for ions $v_D \propto E$, i.e. mobility is really constant

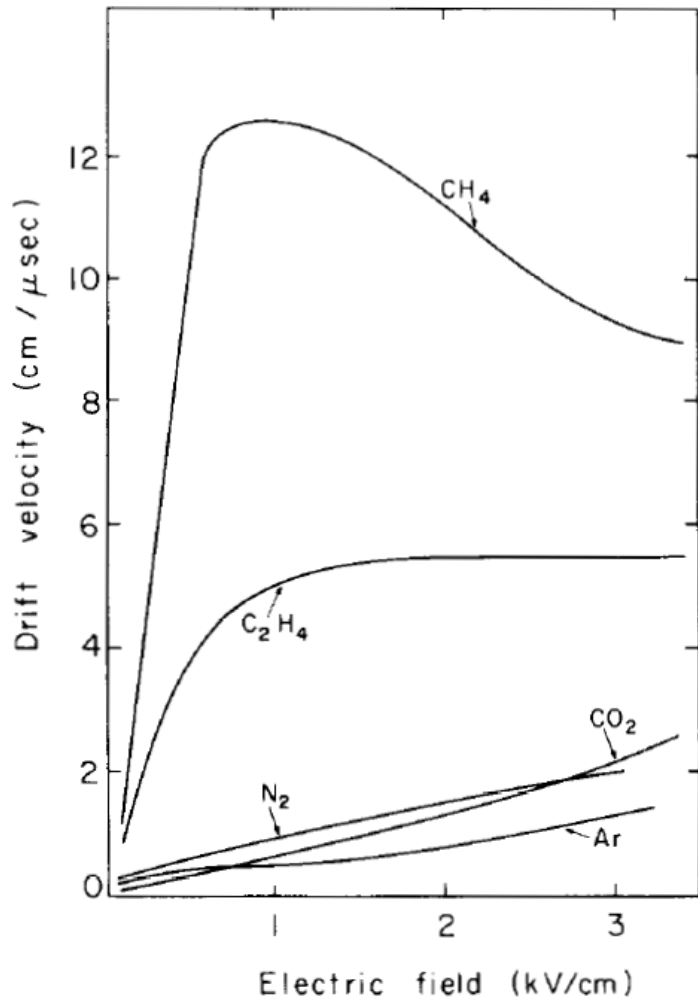
μ_- : electron mobility

- in cold gas approximation ($T_{\text{kin}} \approx kT$) $\rightarrow v_D \propto E \rightarrow \mu = \text{const.}$

- in hot gas ($T_{\text{kin}} \gg kT$) $\rightarrow v_D =, \text{const.} \rightarrow \mu = \text{not const.}$

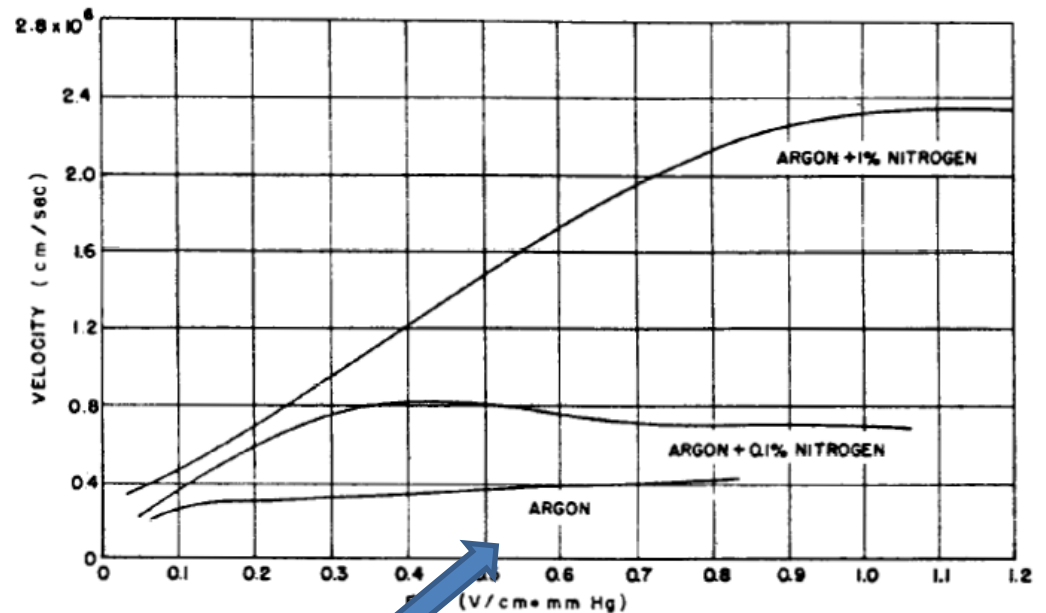
i.e., at high E , electron drift velocity typically tend to saturate.

Electron drift velocity



Drift velocity of electrons in several gases at normal conditions

Use gas mixture to obtain constant v_D
 Important for applications using drift time to get spatial information



Small contaminants in the gas significantly affect drift velocity

E-Field/pressure

Mobility and diffusion coefficients of electrons and ions in gases

Typical drift velocities for electrons are **3 orders of magnitude larger** than drift velocity for ions (due to the different mass):

- Electrons, v_d of the order of cm/ μ s
- Ions, v_d of the order of cm/ms

Mobility of ions is related to diffusion coefficient by the Einstein equation:

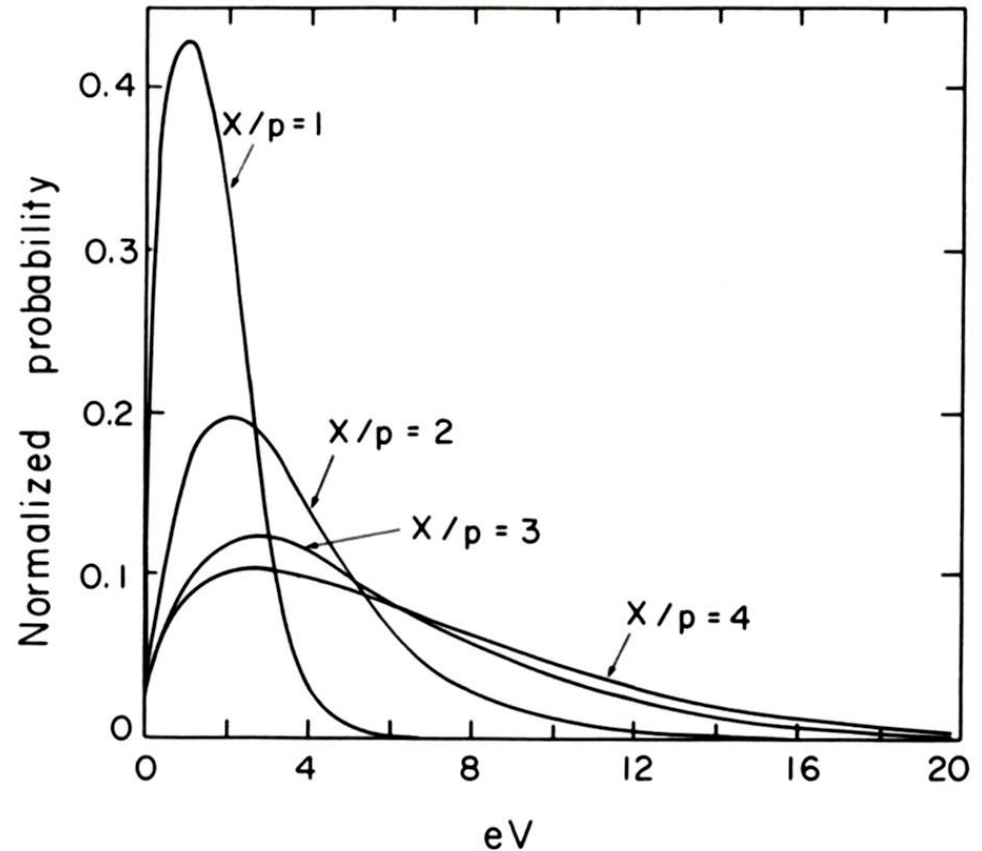
$$\frac{D}{\mu} = \frac{kT}{e}$$

valid for ideal gases in thermal equilibrium.

In principle, this should be valid also for electrons, but electrons immediately deviate from thermal equilibrium while drifting under the action of an electric field, except for very low fields.

Energy distribution of electrons in electric fields

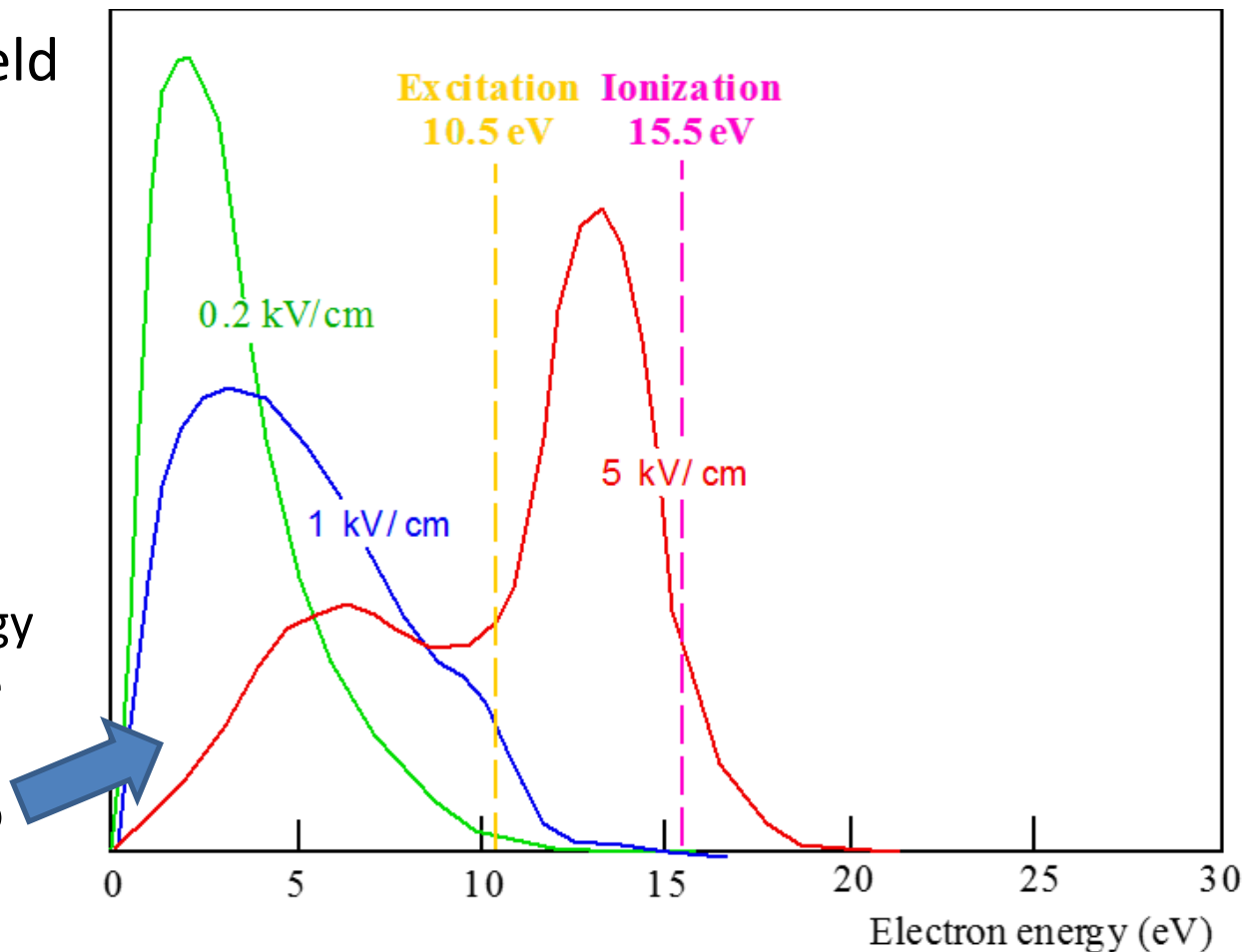
- Increasing the electric field, the electron energy distributions deviate significantly from the Maxwellian shape, and the average energy can exceed of several orders of magnitude the thermal value
- The plot shows the energy distributions of electrons in He for different values of the reduced electric field E/p ;
- In the plot X is the electric field in units of V/cm and p is the pressure in units of 760 Torr
 $X/p = 1$ means $E=760$ V/cm at atmospheric pressure



High E fields: excitation and ionization

- When the electric field exceeds few kV/cm, more and more electrons can reach enough energy to produce excitation and ionization.

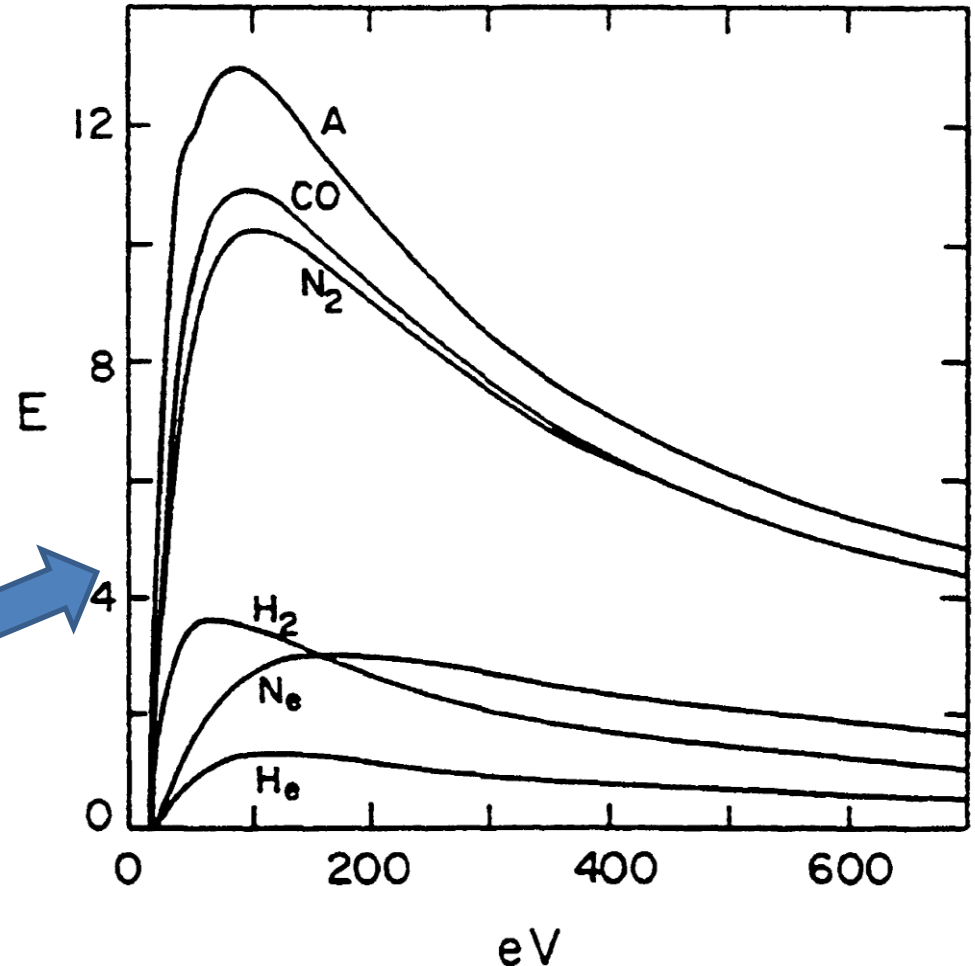
- The plot shows the energy distribution in Ar for three different values of the electric field, compared to the energy needed for excitation and ionization



High E fields: ionization

When electron energy is above the first ionization potential, the collisions can yield new electron ion pairs, while the "primary" electrons continue their path

- The plot shows the ionization probability (in arbitrary units) as a function of the electron energy in various gases
- The maximum ionization probability is reached around 100 eV



First Townsend coefficient

The first Townsend coefficient is defined as the inverse of the ionisation mean free path:

$$\alpha = \frac{1}{\lambda_{ion}}$$

- it represent the average number of pairs produced per unit length

The ionization mean free path is given:

$$\lambda_{ion} = \frac{1}{N\sigma}$$

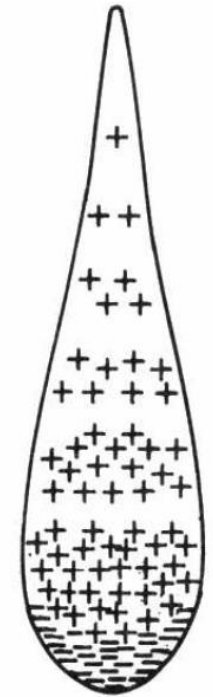
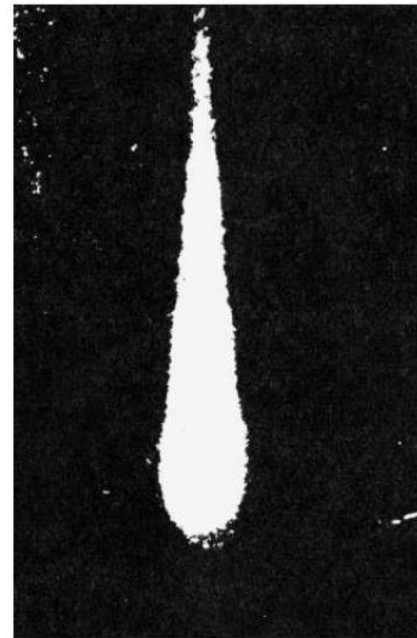
N = number of particles per unit volume

σ = ionization cross section

The first Townsend coefficient strongly depends on the electric field

The presence of electronegative gases (β = attachment coefficient), reduces the number of electrons $\rightarrow \eta = \alpha - \beta$ = effective Townsend coefficient

Townsend avalanche

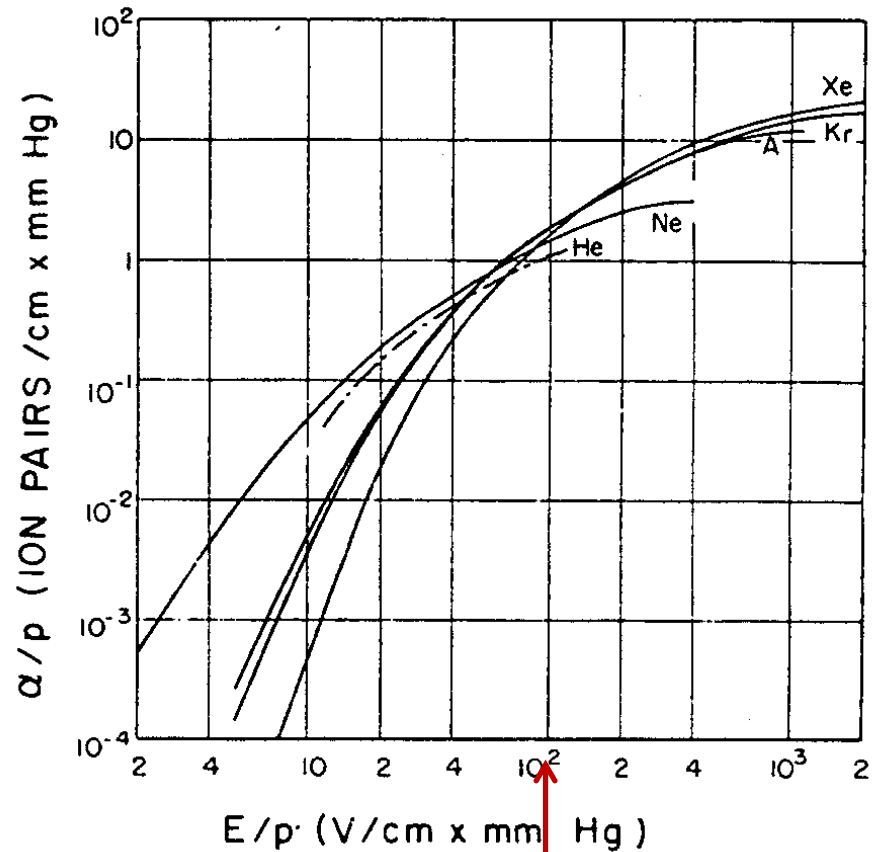
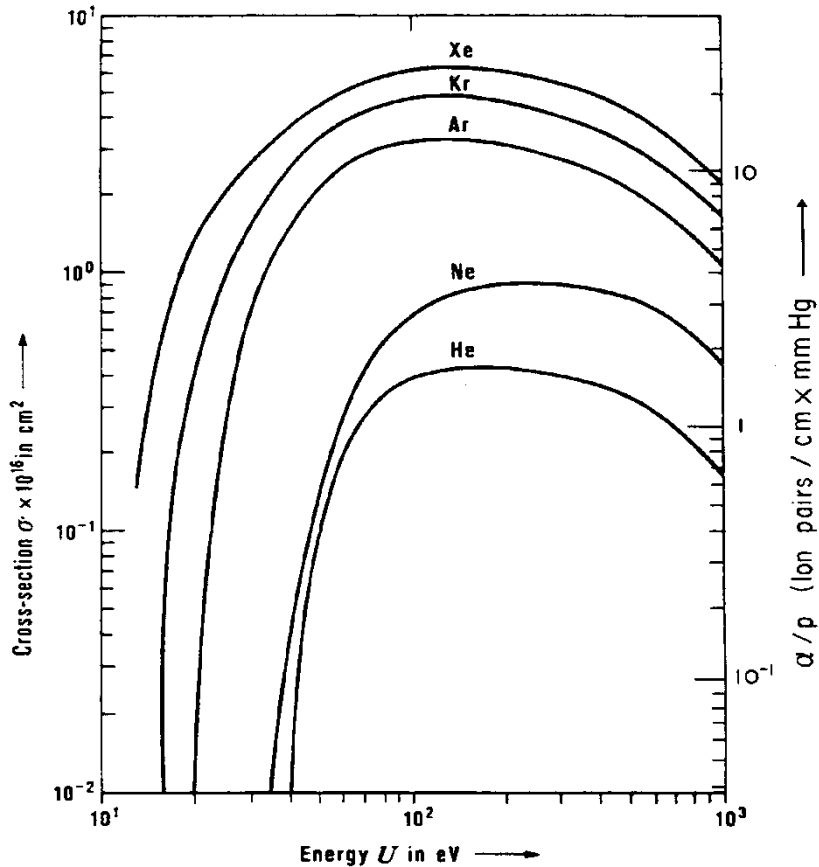


Drop-like shape of an avalanche

Left: cloud chamber picture

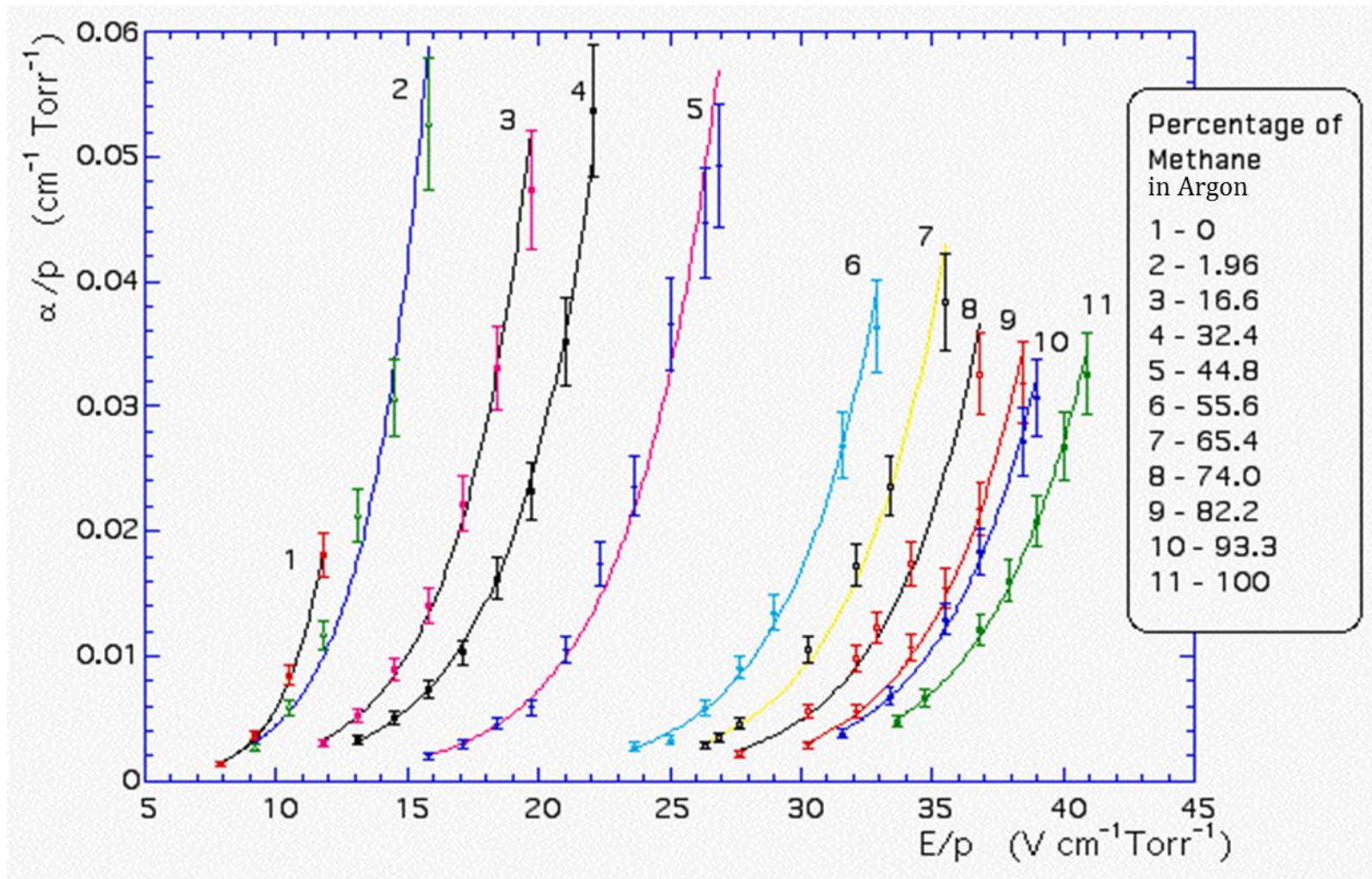
Right: schematic view

Ionization cross section and first Townsend coefficient



$E \approx 75 \text{ kV/cm}$ needed to reach $\alpha \approx 1$

First Townsend coefficient in Ar-CH₄



Korff approximation

A simple parametrization for the first Townsend coefficient was introduced by Korff:

$$\frac{\alpha}{p} = A \exp\left(-\frac{Bp}{E}\right)$$

- A and B are numerical coefficients

An alternative model is the following:

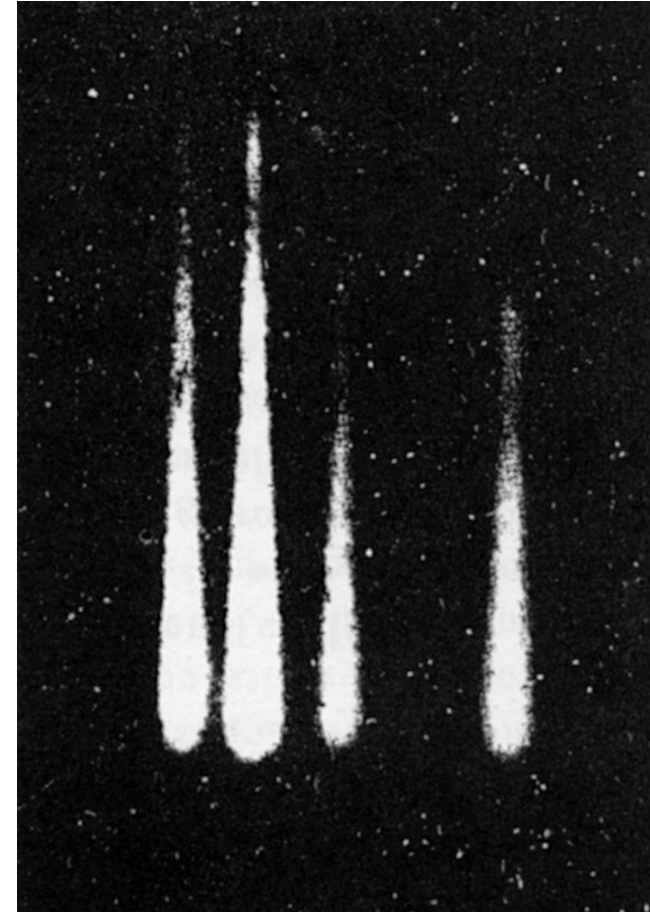
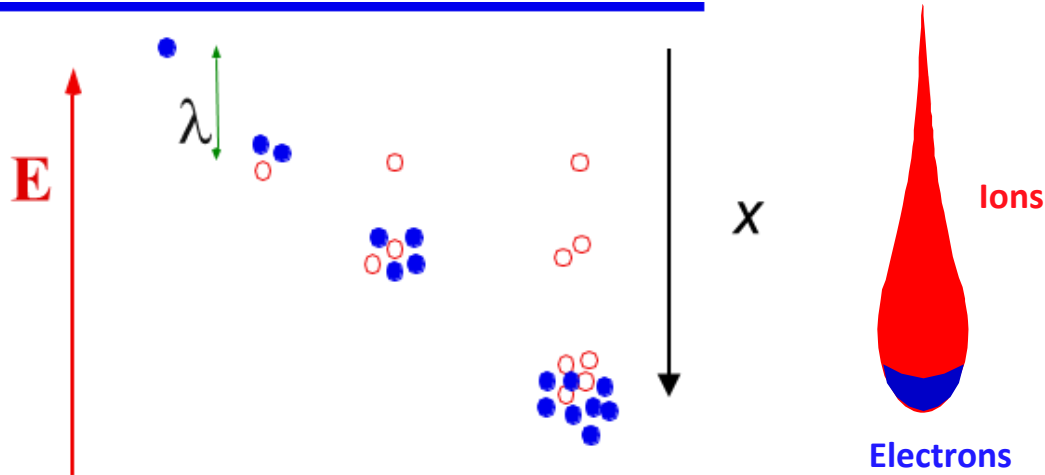
$$\alpha = kN\varepsilon$$

- Here k is a numerical coefficient, N is the number of gas molecules per unit volume and ε is the mean electron energy

Gas	A ($\text{cm}^{-1}\text{Torr}^{-1}$)	B ($\text{cm}^{-1}\text{Torr}^{-1}$)	k ($\text{cm}^2\text{eV}^{-1}$)
He	3	34	0.11×10^{-17}
Ne	4	100	0.14×10^{-17}
Ar	14	180	1.81×10^{-17}
Xe	16	350	
CO ₂	20	466	

Avalanche shape

Uniform electric field



- Since the electron drift velocity is ≈ 1000 times larger than the ion drift velocity, at any given time electrons will be on the front of a drop-like distribution, while ions will be left on the tail

Electron gain in gases

Indicating with n the electrons at the position x , the electrons produced between x and $x + dx$ are:

$$dn = \alpha n dx$$

If α is independent on x (uniform electric field), the previous differential equation can be easily integrated to get:

$$n(x) = n_0 e^{\alpha x}$$

n_0 = initial number of electrons

In the general case of non-uniform electric field, the result is:

$$n(x) = n_0 e^{\int_0^x \alpha(x) dx}$$

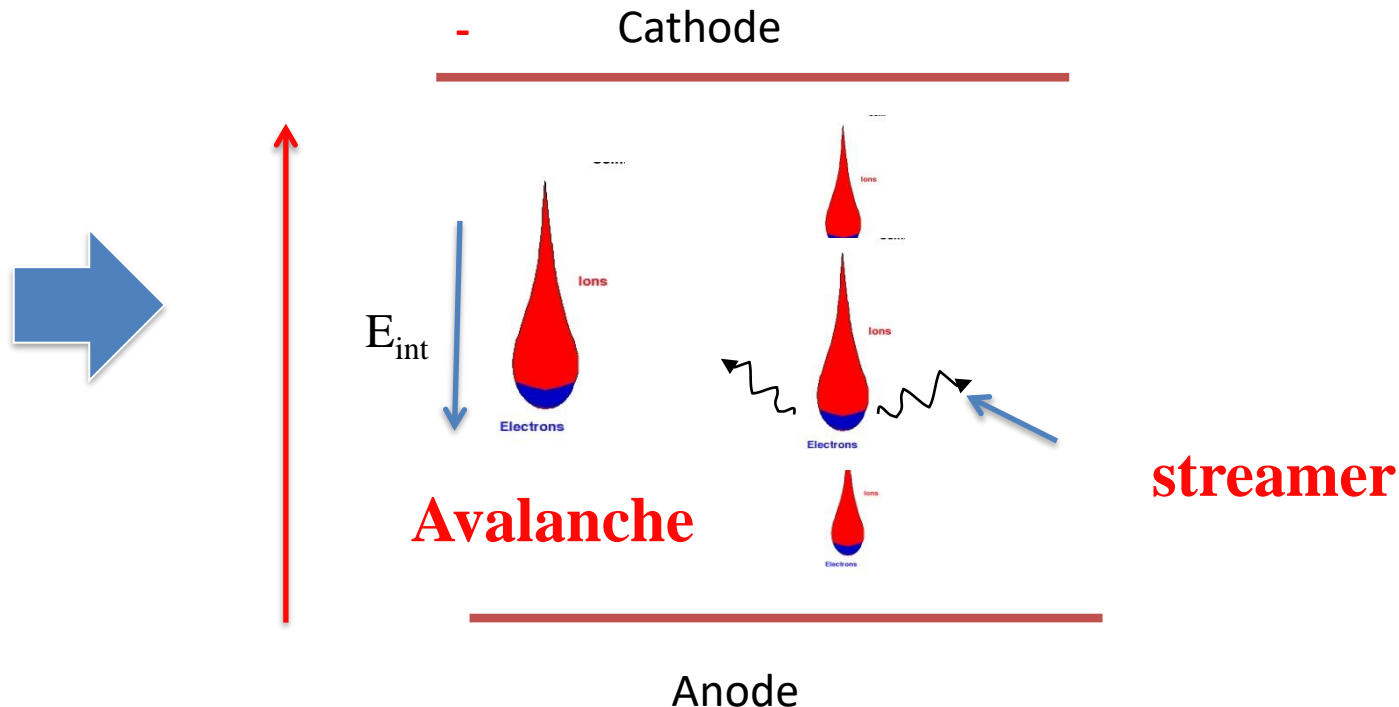
The multiplication factor (also simply called gain) is given by:

$$M = \exp \left\{ \int_0^x \alpha(x) dx \right\}$$

Streamer formation

Between the front and the tail of an avalanche an internal E_{int} forms, directly in the opposite direction as the applied E_{appl} . When the $E_{int} = E_{appl}$... the multiplication process stops.

- Ion and electrons recombine with **photon emission**.
- New secondary avalanches can be produced, forming a streamline of continuous flow of charges from one electrode: the “**streamer**”



Breakdown

The net effect is that the gain cannot be increased at will

→ Beyond a certain limit a continuous discharge sets in

Raether empirically proposed the “Raether limit” for the transition between “avalanche” operating mode, to “streamer mode”.

→ In practice, sometimes a small percentage of streamer can be acceptable during operation of gaseous detectors, but beyond a certain limit, depending on the precise configuration and gas, breakdown occurs.

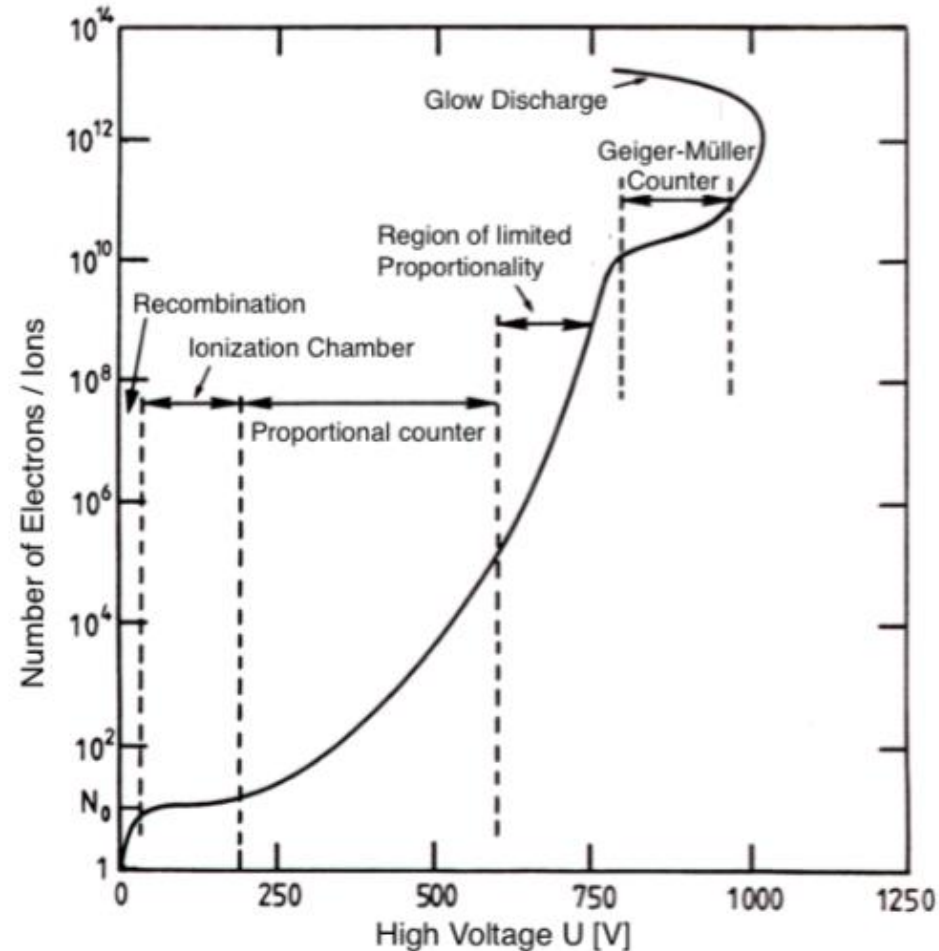
Raether limit: $\alpha x \approx 20$ ($M \approx 10^8$)

→ In practise sometimes breakdown sets in even for gains much lower than 10^8 (down to 10^6).

Operation modes

Gas counters may be operated in different operation modes depending on the applied high voltage:

- **Recombination:** electric field is not enough to collect all the charge, electrons and ions will recombine.
- **Ionization chambers** are operated at a voltage which allows full collection of charges, but below the threshold of secondary ionization (**no amplification**).



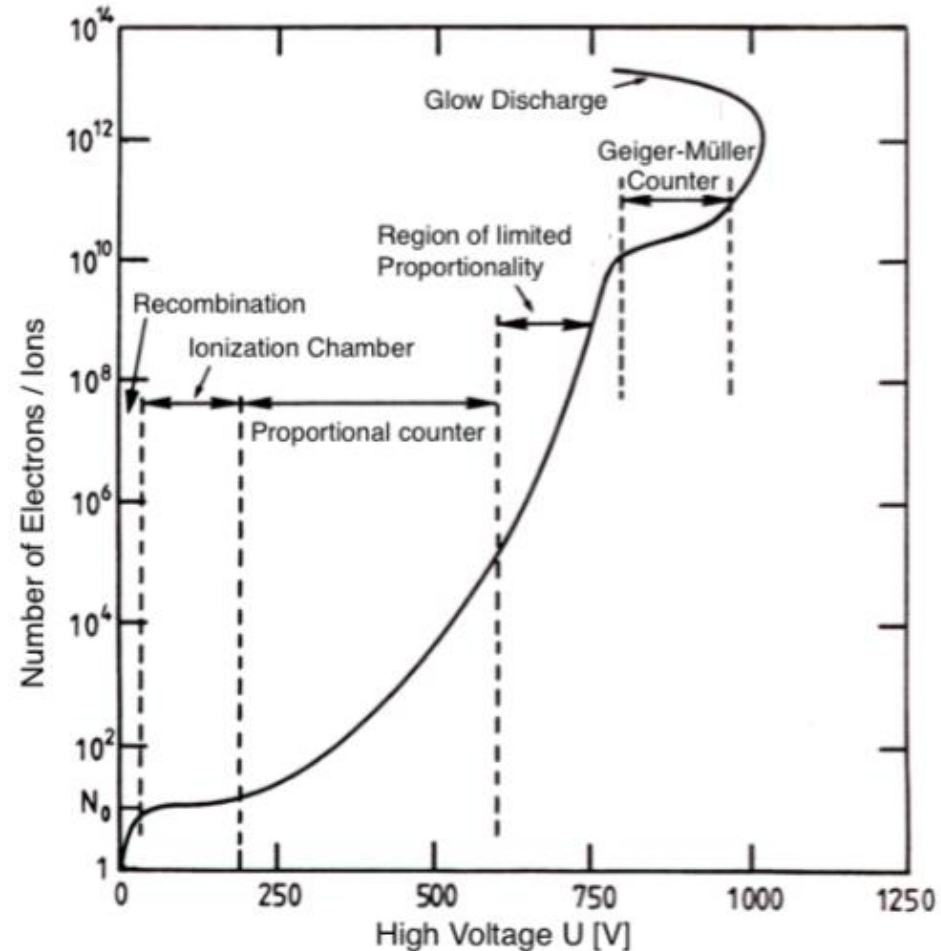
(Original: W. Price, *Nuclear Radiation Detection*, McGraw-Hill, 1958)

E.g. operation range of a cylindrical gas counter with central anode wire as function of the high voltage;

Operation modes

Gas counters may be operated in different operation modes depending on the applied high voltage:

- **Proportional chambers:**
 - ❖ signal amplification through secondary ionization, proportional to the primary ionization.
 - ❖ **Amplification factors 10^4 – 10^6**
 - ❖ Limit is reached when electrons produced by the photo-effect are no longer negligible
 - ❖ The effect of photons is reduced with admixtures of a “quenching” gas (e.g. **CH₄, CO₂**) which absorbs UV photons.



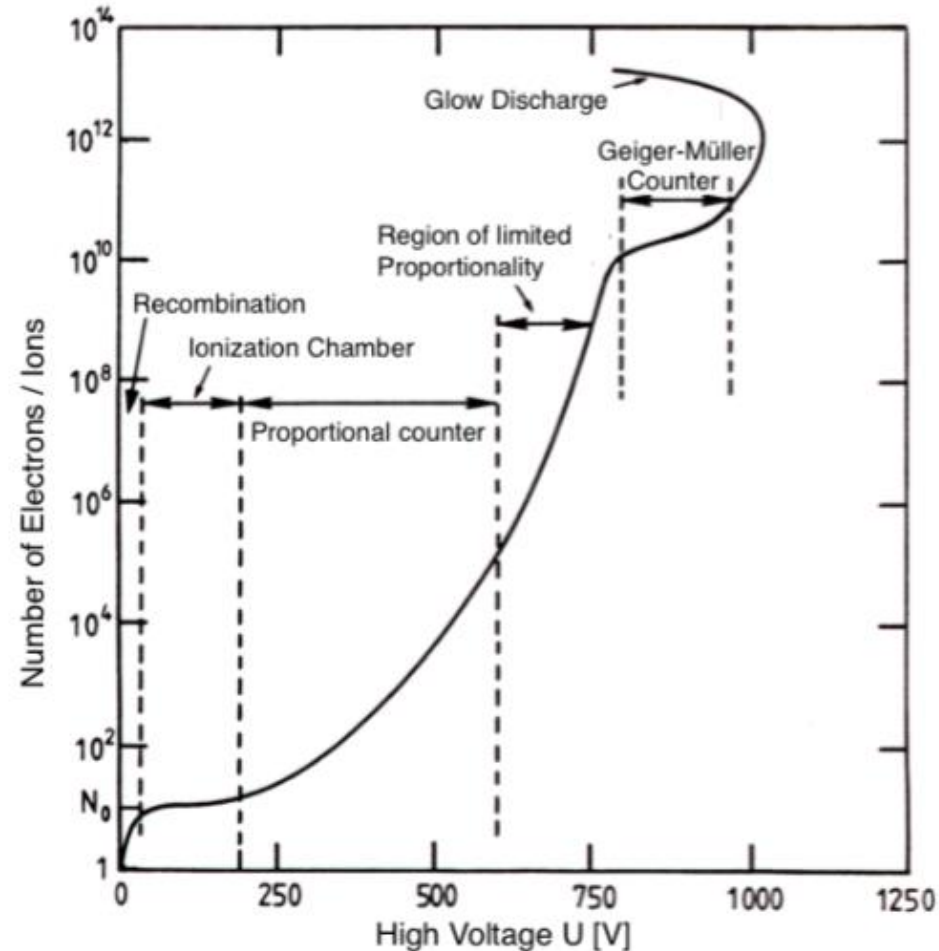
(Original: W. Price, *Nuclear Radiation Detection*, McGraw-Hill, 1958)

E.g. operation range of a cylindrical gas counter with central anode wire as function of the high voltage;

Operation modes

Gas counters may be operated in different operation modes depending on the applied high voltage:

- **Geiger- Muller counter:**
- The UV photons are spreading transversal to the field and create photoelectrons in the whole gas volume: the discharge is no longer localized.
- ❖ The produced total charge is independent from the primary ionization
- ❖ **Amplification factor $10^8 - 10^{10}$**
- **Discharge region:** UV photons avalanches are created everywhere, discharge even without particle crossing



(Original: W. Price, *Nuclear Radiation Detection*, McGraw-Hill, 1958)

E.g. operation range of a cylindrical gas counter with central anode wire as function of the high voltage; number of e^- ion pairs for primary ionizing electrons:

Choice of the gas filling

- Noble gases** are preferentially used due to the absence of vibrational and rotational states → **ionization dominates.**

(Polyatomic gas have non-ionizing de-excitation modes available)

→ Possible electron multiplication at low electric field

→ Choose cheap noble gases with low ionization potential

Gas	ρ (g/cm ³) (STP)	I_0 (eV)	W_i (eV)	dE/dx (MeVg ⁻¹ cm ²)	n_t (cm ⁻¹)
H ₂	$8.38 \cdot 10^{-5}$	15.4	37	4.03	9.2
He	$1.66 \cdot 10^{-4}$	24.6	41	1.94	7.8
N ₂	$1.17 \cdot 10^{-3}$	15.5	35	1.68	56
Ne	$8.39 \cdot 10^{-4}$	21.6	36	1.68	39
Ar	$1.66 \cdot 10^{-3}$	15.8	26	1.47	94
Kr	$3.49 \cdot 10^{-3}$	14.0	24	1.32	192
Xe	$5.49 \cdot 10^{-3}$	12.1	22	1.23	307
CO ₂	$1.86 \cdot 10^{-3}$	13.7	33	1.62	91
CH ₄	$6.70 \cdot 10^{-4}$	13.1	28	2.21	53
C ₄ H ₁₀	$2.42 \cdot 10^{-3}$	10.8	23	1.86	195

Expensive and rare



The drift velocity depends very strongly on the nature of the gas, namely on the detailed structure of the elastic and inelastic electron-molecule cross-sections. Sometimes it **saturates at high electric fields.**

Choice of the gas filling

If only a noble gas is used to fill the counter, it can operate at relatively low gains ($M \approx 10^3 - 10^4$) before entering the permanent discharge regime

When the avalanche forms, excited Ar atoms are created, which can return to the ground state only emitting UV photons

- The energy of these photons can be sometimes larger than the energy needed to extract electrons from the cathode walls (7.7 eV for copper)
- Photoelectrons can be extracted from the walls, which cause further ionization of the gas

Possible spurious delayed pulses due to ions neutralizing on the cathode

- Ar⁺ ions reaching the cathode are neutralized and extract an electron from the walls
- The neutral Ar atom is produced in an excited state, decays emitting UV photons
- An additional electron can also be extracted from the wall

Both processes induce spurious delayed pulses

Use of quencher gases

The problem is solved by adding to noble gas percentages of other polyatomic gases, usually called "quenchers"

✓ Gas quencher molecules have non-radiative (rotational and vibrational) mode and can absorb UV photons in a wide energy range.

- CH₄ absorbs photons between 7.9 and 14.5 eV

- Other polyatomic gases used are freons, CO₂, BF₃, C₄H₁₀, etc.

✓ Polyatomic gases dissipate energy by elastic collisions

Sometimes quenchers can dissociate resulting in simpler molecules, sometimes harmful to the detector, like HF → aging

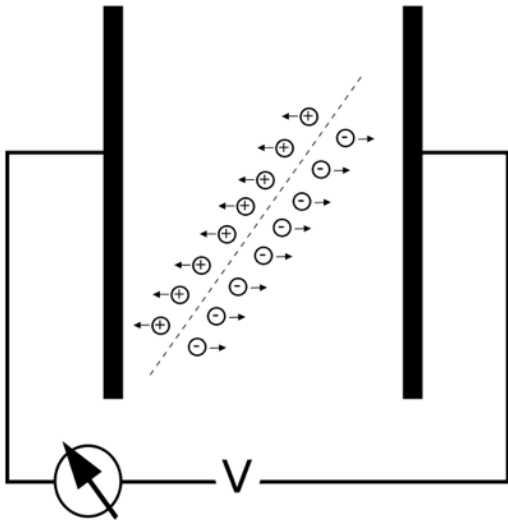
Even small quantities of quencher allow to operate these detectors up to gain of 10⁶ without discharges.

Use of quencher gases

Also electronegative gases are used as quenchers, like many freons (CF_3Br), ethyl-bromide ($\text{C}_2\text{H}_5\text{Br}$), etc. which help operate detectors at high gain without discharges.

- They are characterized by an electron capture mean free path that is less than typical anode-cathode distance (≈ 1 cm) and larger than avalanche size (few μm)
- These gases capture electrons possibly extracted at the cathode forming negative ions, preventing the formation of spurious delayed avalanches
- Also these gases can dissociate, sometimes forming solid or liquid polymers which can deposit on the electrodes, altering their properties
 - Malter effect, where the E field close to the electrode is distorted, causing undesired discharges
 - Aging effects (one of the main issues in all particle detectors)

(Some) geometries of gaseous detectors

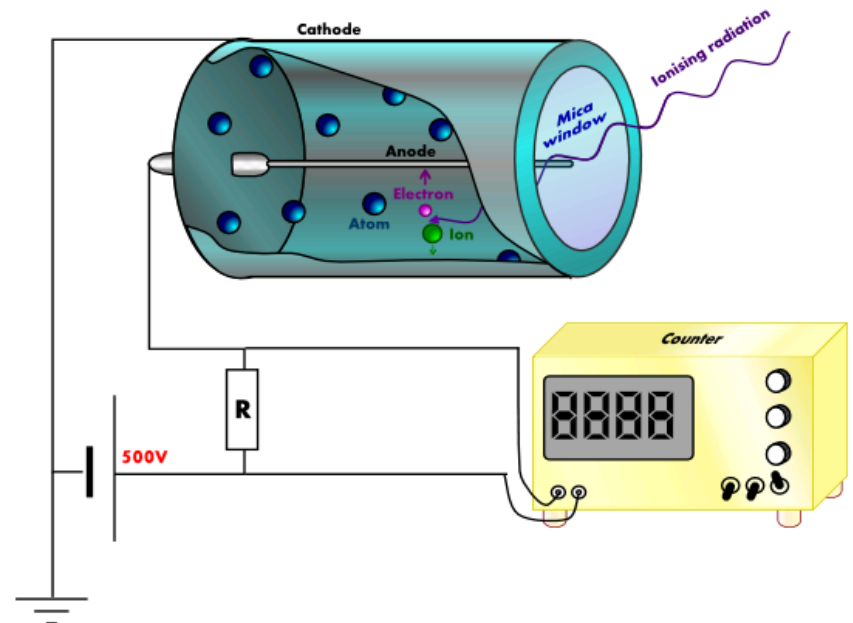


Planar geometry

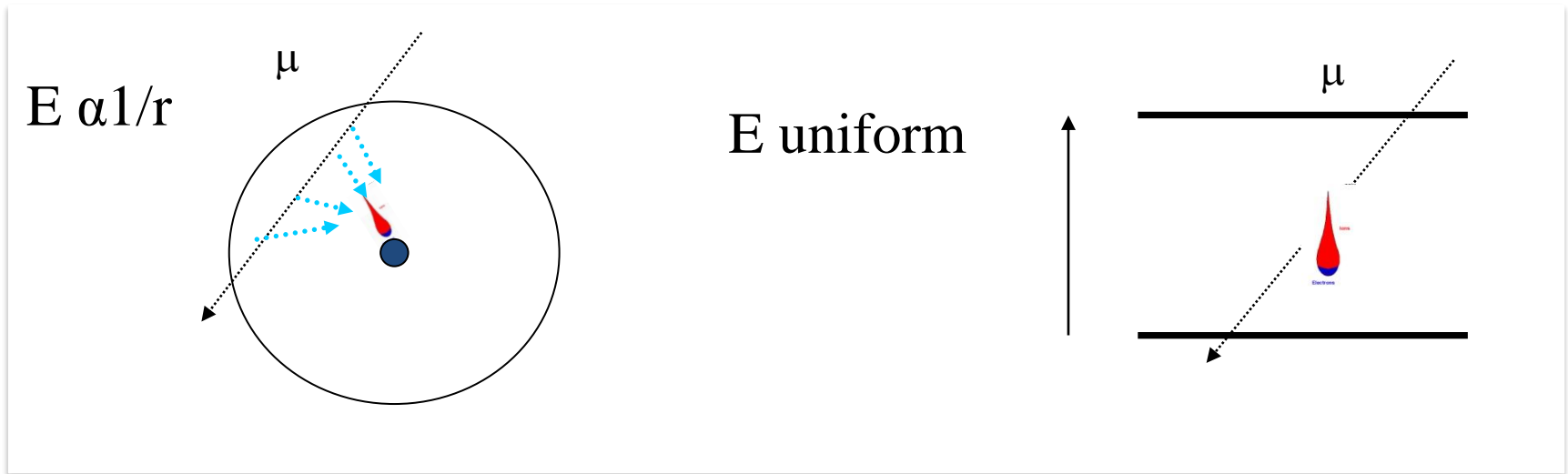
- E uniform and perpendicular to the electrodes
- Amount of ionization produced proportional to path length in the detector
- Signal depends on the point(s) where the ionization occurs → **not proportional to energy released** in the detector

Cylindrical geometry:

- Anode wire surrounded by a cylindrical cathode
- $E \propto 1/r$: weak field far from the wire
- electrons/ions drift in the gas volume
- **multiplication occurs only near the anode** → signal proportional to energy released in the detector



Cylindrical vs. planar geometry



Detectors with cylindrical geometry have an important limitation: primary electrons have to drift close to the wire before the charge multiplication can start

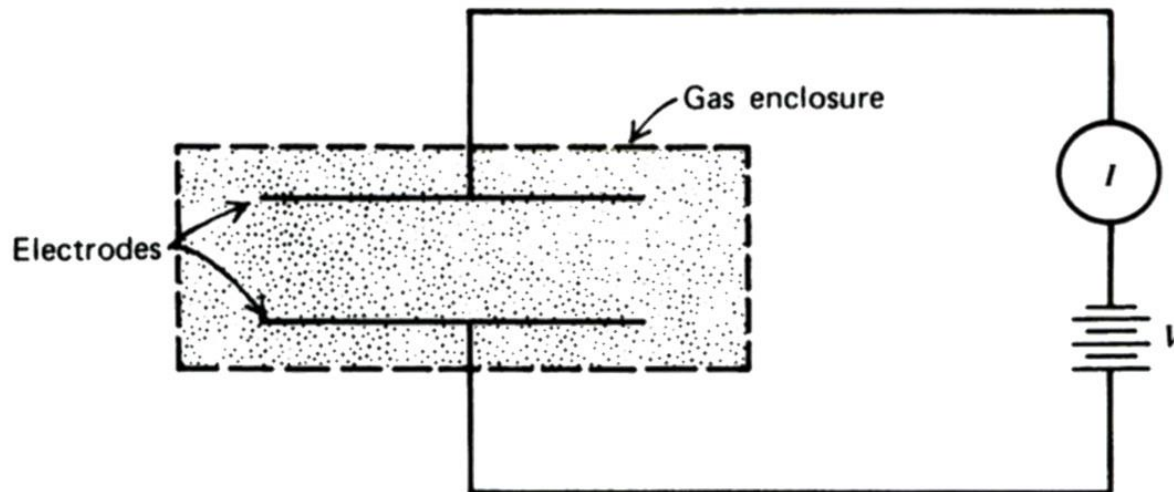
→ limit in the time resolution

In a parallel plate geometry (as the RPC) the charge multiplication starts immediately because all the gas volume is active.

→ **much better time resolution (~ 1 ns)**

Ionization chamber: the simplest gaseous detector

- The ionization chamber operates in the charge collection region
- Generally, a planar geometry is used
 - Range of applied voltages varies from ≈ 10 V to ≈ 1 kV
- It can be operated **with almost any gas**, including electronegative gases (i.e. air, or more dense gases, to increase ionization prob.)
- At equilibrium, the current flowing in the external circuit is equal to the ionization current



Current mode of operation

No current is observed when the applied voltage is null

- No electric field → recombination of ions and electrons

Increasing the applied voltage, the current also increases

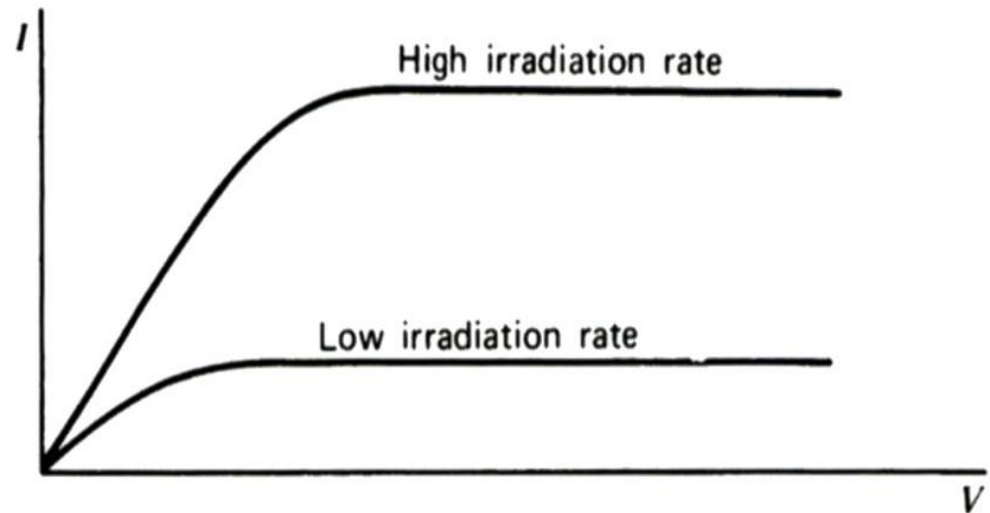
- The electric field separates the ions and the probability of recombination at the production point is reduced

- The drift velocity also increases, thus reducing the probability of recombination along the path between the production point and the collection electrodes

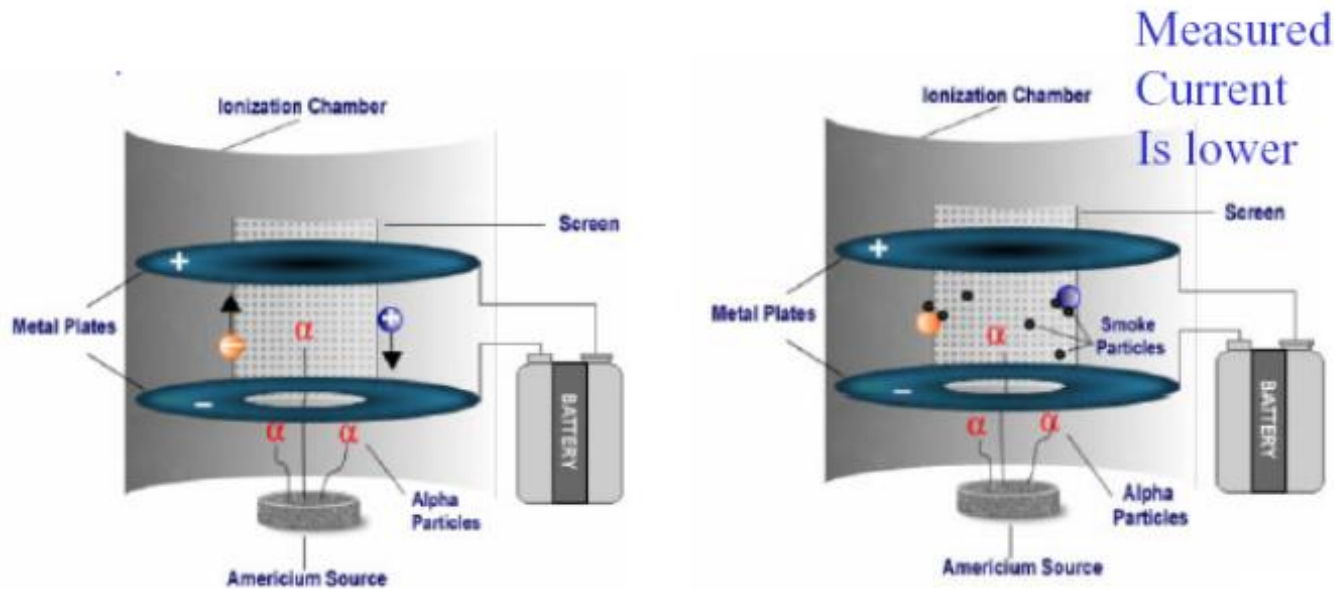
A further increase of the applied voltage leads to a saturation of the current

Recombination is suppressed, and all the charges produced are collected at the electrodes

The saturation current is proportional to the charge formation rate



Ionization chambers as smoke detectors



Detect the decrease of induced charge by the alpha source

$1 \mu\text{Cu} (\sim 0.3 \mu\text{g})$ of ^{241}Am
 $\tau = 432 \text{ y}$

- α passing through ionization air-chamber produce constant current
- **smoke absorbs α 's \Rightarrow reduced ionization, lower signal, alarm ..**
- α 's have low penetrability: they are stopped by the plastic of detector

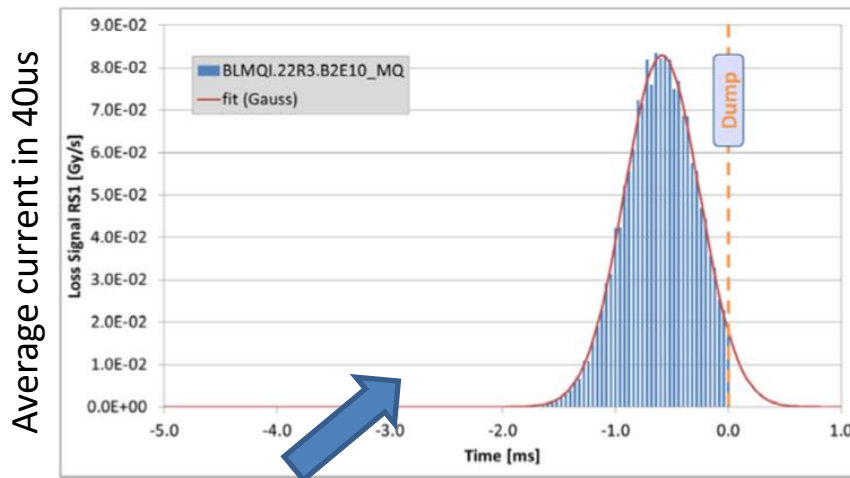
Ionization chamber



Inside a basic ionization smoke detector. The black, round structure at the right is the ionization chamber. The white, round structure at the upper left is the piezoelectric buzzer that produces the alarm sound.

Ionization chambers as beam monitors

- Used for the LHC beam loss monitors (3520 objects).
- Alternating layers of HV and GND with 5 mm distance, 1.5kV filled with N_2 . 300 ns electron drift time, 80 μs ion drift time
- The total current averaged over times of 40 μs to 2.5 ms is read out in order to measure the beam losses.



LHC UFO event 2010

Ionization chambers can be used to detect also single particle, or bunches of particles
→ pulse mode of operation

Limits of ionization chambers

Detecting single particles with **ionization chambers is difficult**

- Output signal is a **current read by a galvanometer**
- This current is proportional to the charge collected, proportional to the energy lost by the particle in the gas
- Signals in ionization chambers are generally very small

$$1 \text{ MeV particle stopping in the gas} \rightarrow N_e \simeq \frac{10^6 \text{ eV}}{35 \text{ eV}} \simeq 3 \cdot 10^4$$

Considering the detector like a planar capacitor of 10^{-10} F capacity, the arrival of $3 \cdot 10^4$ electrons implies a change in potential: $\frac{3 \cdot 10^4 \cdot 1.6 \cdot 10^{-19} \text{ C}}{10^{-10} \text{ F}} = 4.6 \cdot 10^{-5} \text{ V}$

- The galvanometer must be capable of measuring **the very small output current** which is in the region of fA to pA, depending on chamber design, particle considered, etc.
- Time duration of the signal is related to time needed to collect electrons/ions (μs or ms)

Proportional counters

A cylindrical geometry is adopted

- The anode is a thin wire, on the cylinder axis
- The cathode is the metallic wall of the cylinder

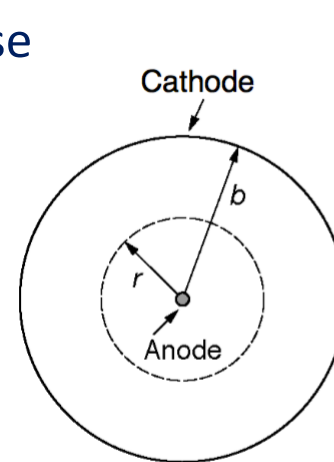
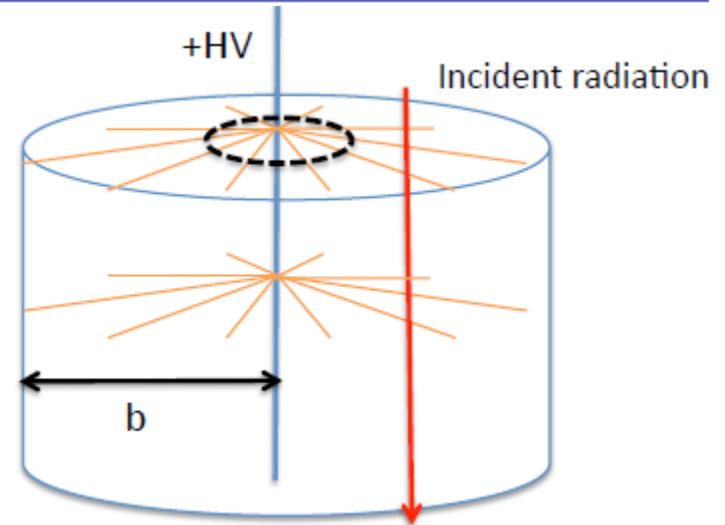
In most part of the counter, the electric field is not enough to trigger avalanche processes

- Electrons drift toward the anode
- Ions drift toward the cathode

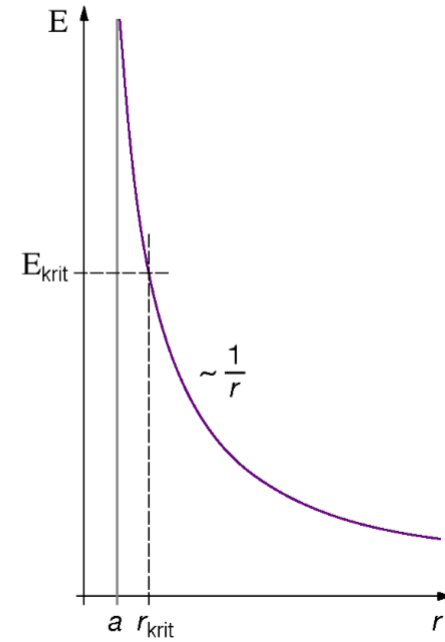
When electrons get close to the wire (usually at a few wire radii), the electric field becomes intense enough to trigger multiplication processes

- A drop-like avalanche develops, with electrons in front and ions left behind
- Due to diffusion, the avalanche surrounds the wire

Electrons are collected at the anode, while positive ions keep drifting toward the cathode

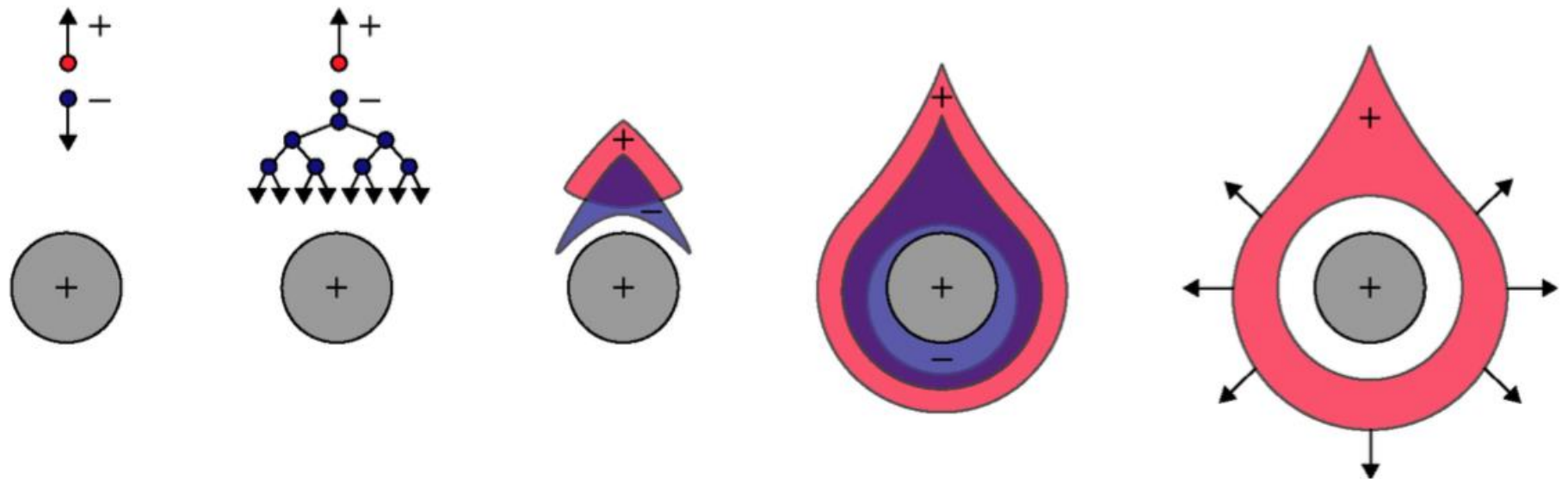


a ... radius anode wire
b ... radius cathode



Avalanche development close to the wire

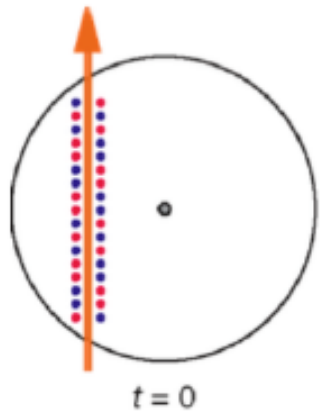
Time development of an avalanche near the wire of a proportional counter



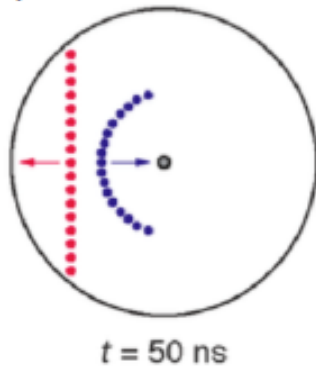
- a) a single primary electron proceeds towards the wire anode,
- b) in the region of increasingly high field the electron experiences ionizing collisions (avalanche multiplication),
- c) electrons and ions are subject to lateral diffusion,
- d) a drop-like avalanche develops which surrounds the anode wire,
- e) the electrons are quickly collected, while the ions begin drifting towards the cathode generating the signal at the electrodes.

Avalanche development

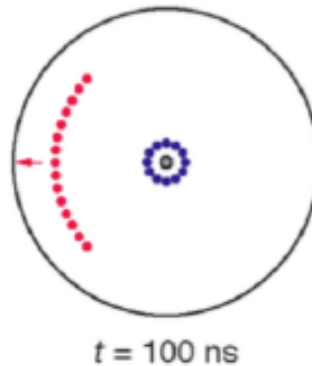
Charged particle produces primary ionization along the track



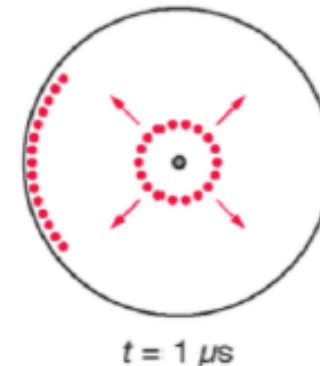
Primary e- drift quickly to the anode wire. Ions drift much slower to the cathode cylinder.



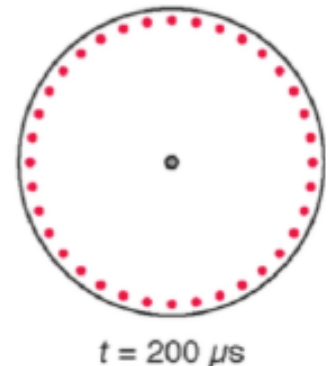
The primary e- reach the region of high field and produce secondary ionization charge carrier avalanche around the wire. The primary ions continue to drift to the cathode.



The ions produced in the secondary ionization drift also to the cathode. The secondary e- are generated close to the anode.



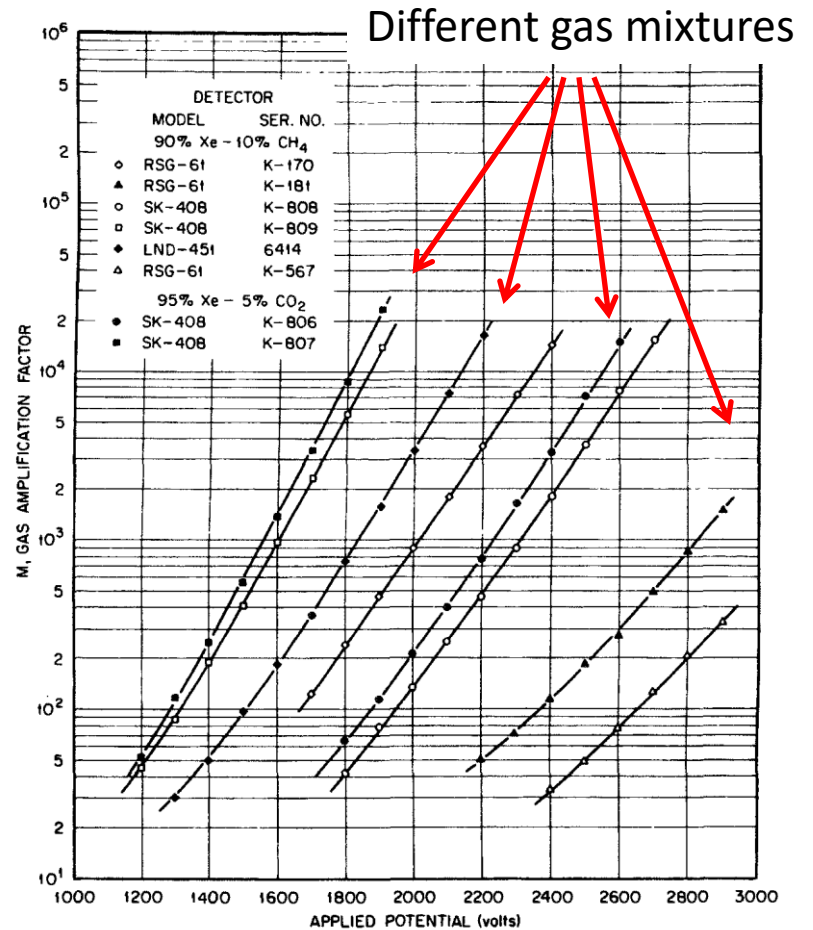
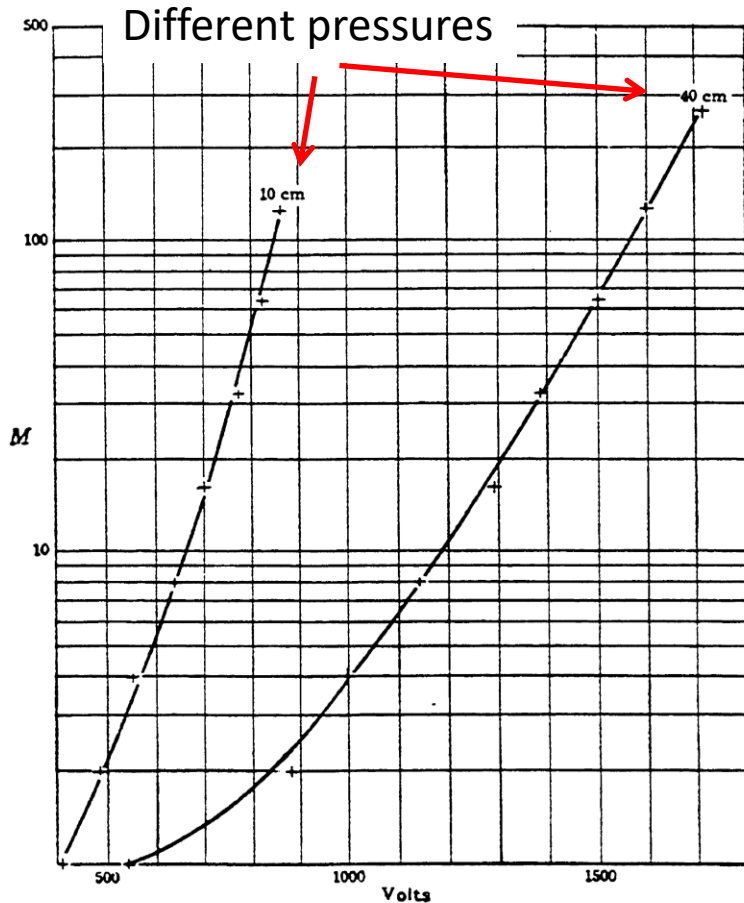
Finally also the secondary ions reach the cathode.



• ... positive ions • ... electrons

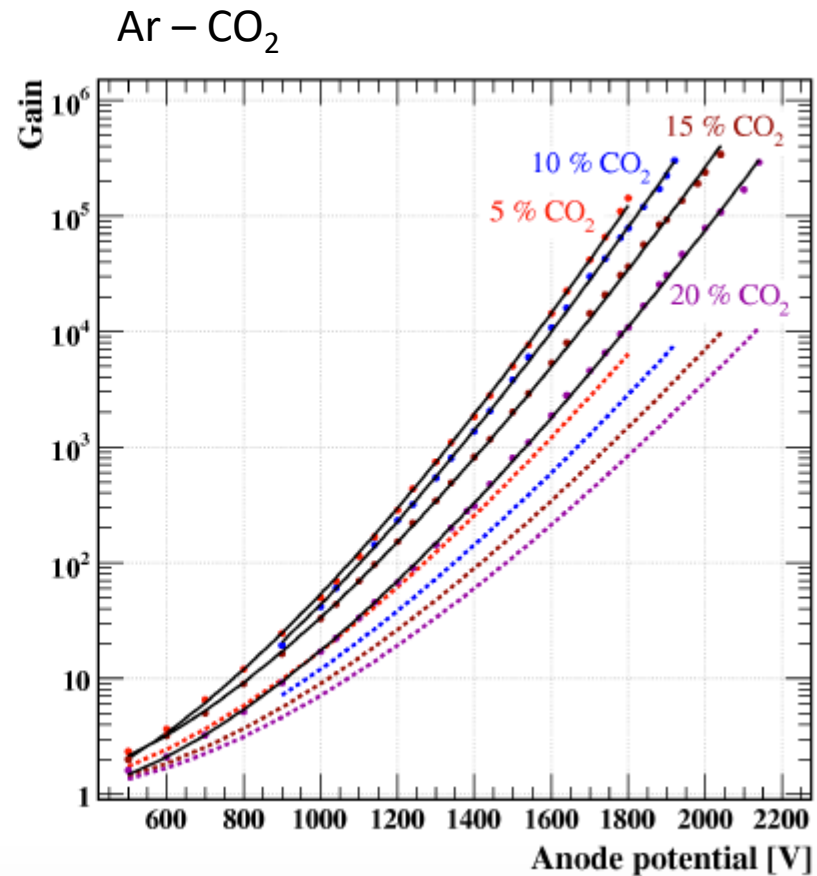
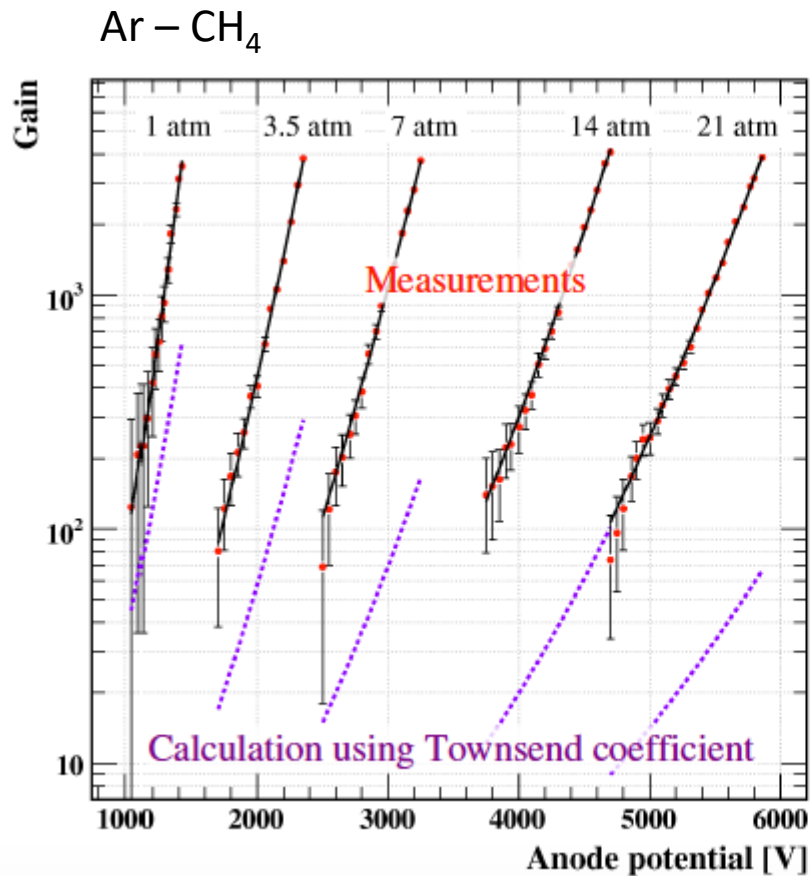
- Signal in proportional counters is mainly due to ions drifting to the cathode
- Of course, increasing the operating voltage, so that $M > 10^4$, causes the presence of space charge around the wire, distorting E , and losing proportionality

Gain in proportional counters



Comparison between predictions (lines, Diethorn formula) and experimental results (points)

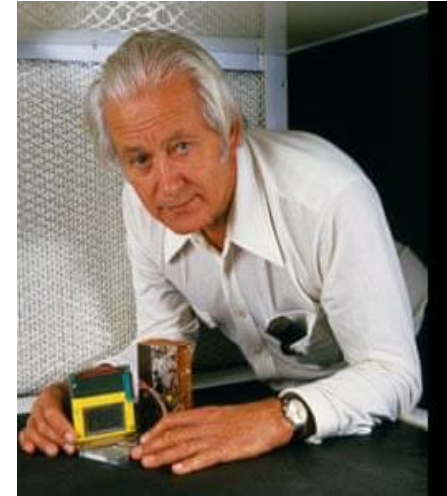
Gain in proportional counters



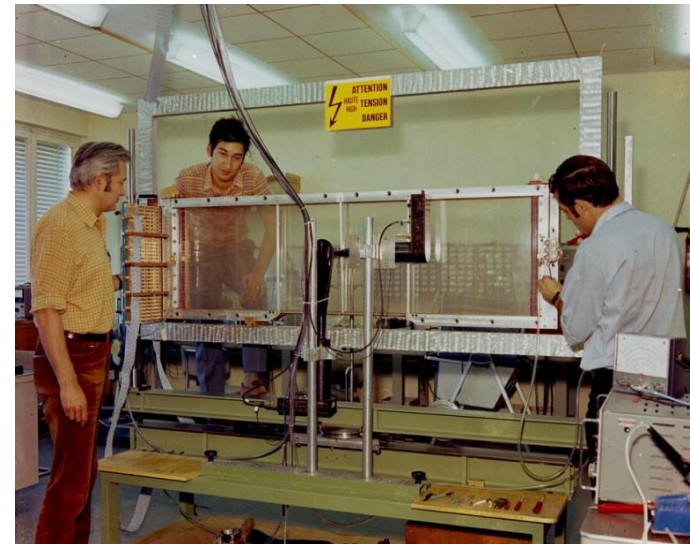
Comparison between predictions (lines) and experimental results (points)

Multi-wire proportional chambers

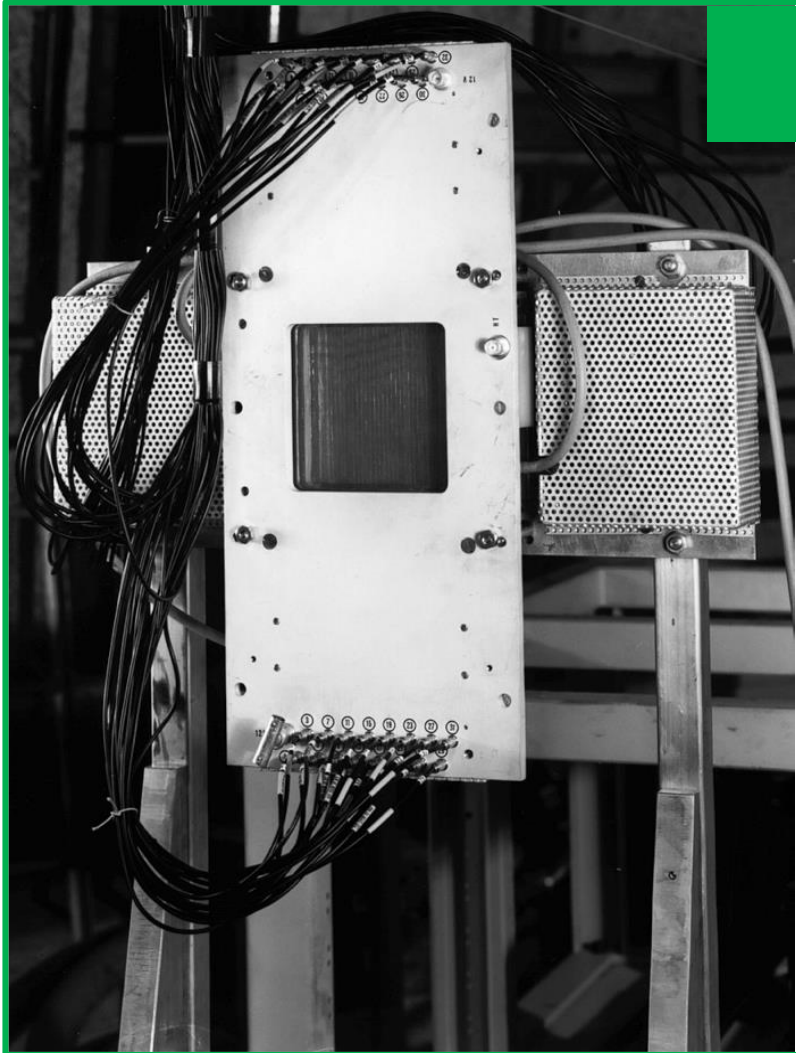
The invention of the Multi Wire Proportional Chamber (MWPC) by Georges Charpak in 1968 was a game changer, earning him the 1992 Nobel Prize in Physics. Suddenly, experimenters had access to large-area charged particle detectors with millimeter spatial resolution and staggering MHz-rate capability. Crucially, the emerging integrated-circuit technology could deliver amplifiers so small in size and cost to equip many thousands of proportional wires.



This ingenious and deceptively simple detector is relatively easy to construct. The workshops of many university physics departments could master the technology, attracting students and “democratising” particle physics. So compelling was experimentation with MWPCs that within a few years, large detector facilities with tens of thousands of wires were constructed [...].



Examples of MWPCs



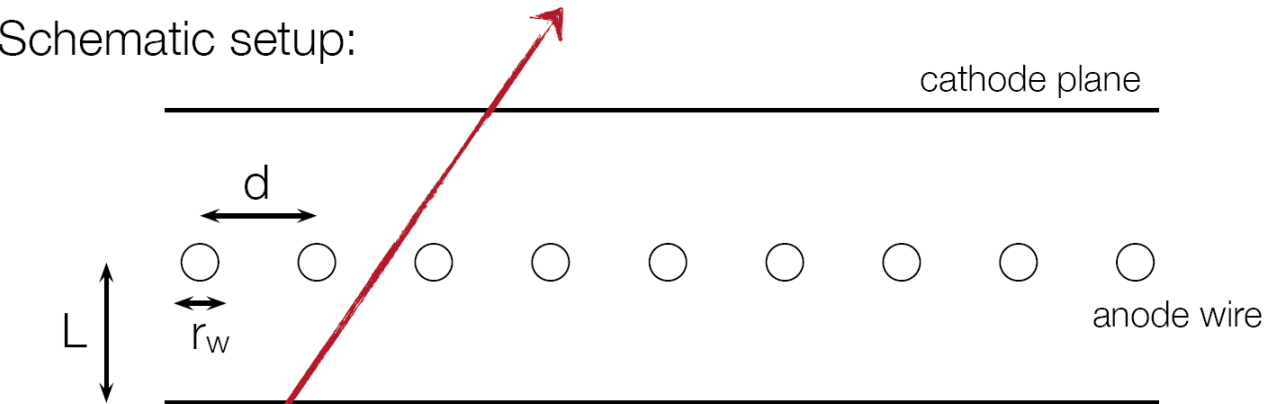
First prototype of MWPC
(Charpak 1968)

A telescope of MWPCs



Multi-Wire Proportional Chambers (MWPC)

Schematic setup:



Parameters:

d = 2 - 4 mm
 r_w = 20 - 25 μm
 L = 3 - 6 mm
 U_0 = several kV
Total area: $O(\text{m}^2)$

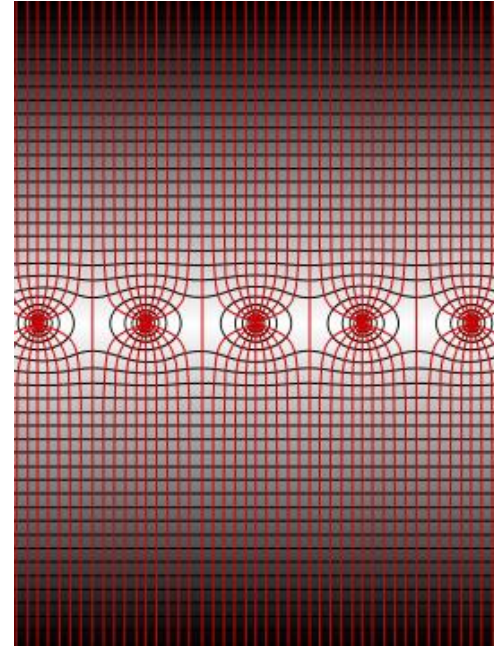
Features:

Tracking of charged particles
Some PID capabilities via dE/dx
Large area coverage
High rate capabilities

- A MWPC consists in **a set of anode wires**, equally spaced and kept at the same potential, symmetrically placed in between two cathode planes
- In first prototypes **anodes were grounded and the cathode were kept at negative potential**
 - **Each wire acts as an independent proportional counter**
 - Distance between the planes usually is 3-4 time wire pitch

Multi Wire Proportional Chambers

- E field essentially uniform in most of the detector
- It becomes very intense close to the anode
 - Avalanche
- Every anode wire is connected to an amplifier and the signals can be processed electronically.

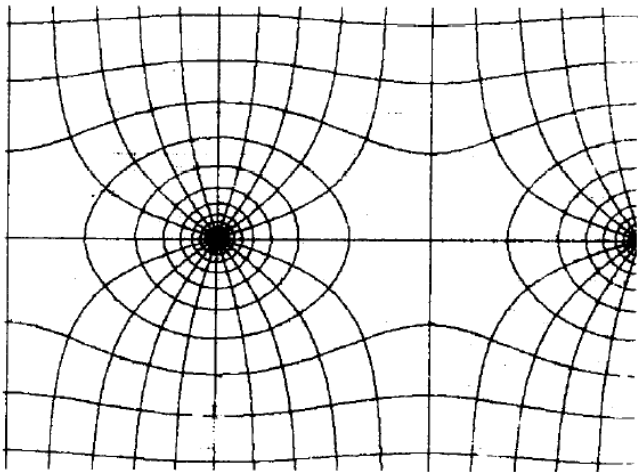


Diameter of anode wires 10 – 50 μm
Distances between wires 1 – 5 mm
Each wire connected to an amplifier
Typical gas amplification in MWPC is 10^5

Position resolution:
Depends on wire distance
e.g. for $d = 2 \text{ mm}$
By simply using the wire position
$$\sigma(x) = \frac{d}{\sqrt{12}} = 577 \mu\text{m}$$

Electric field in a MWPC

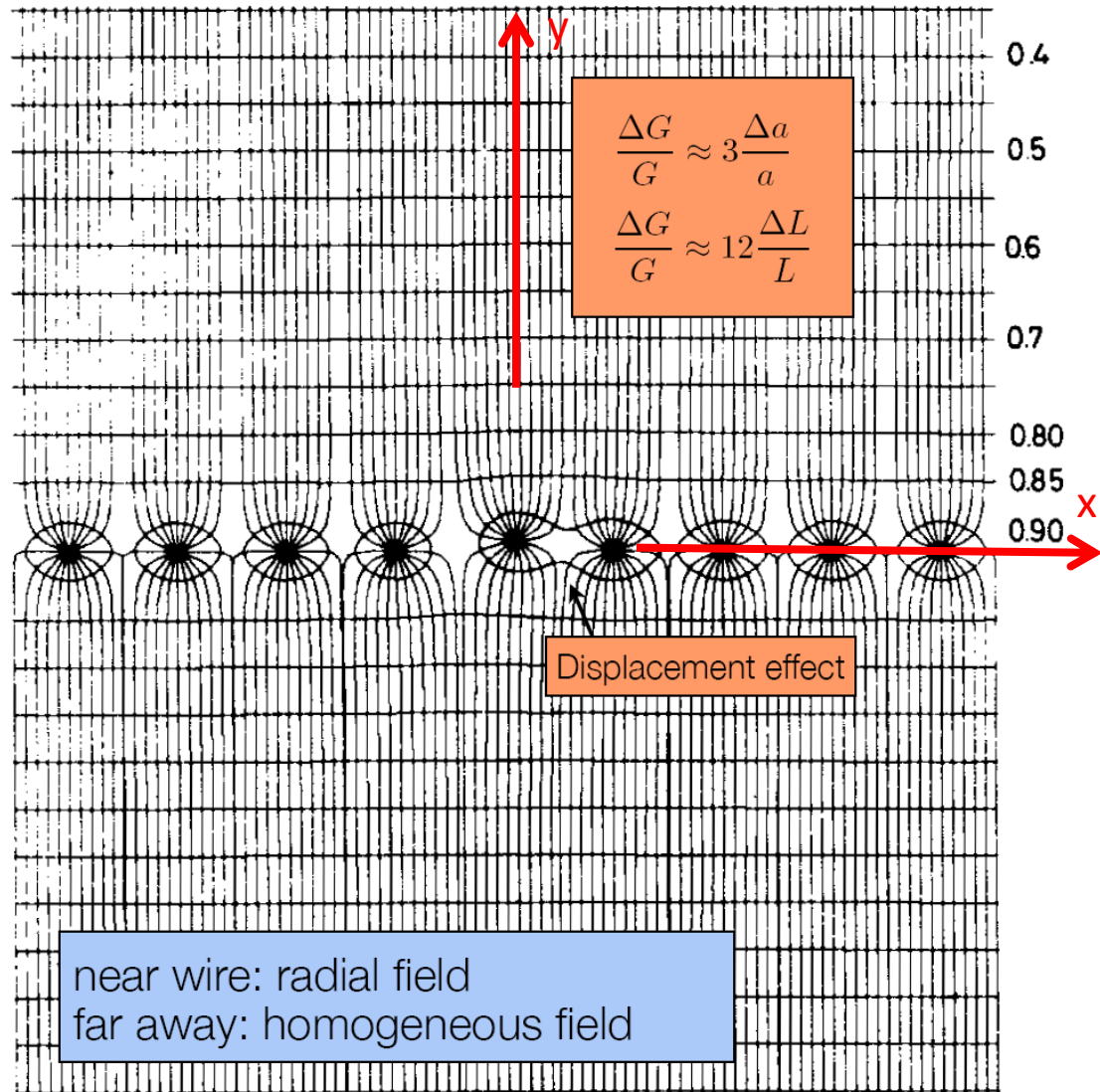
Electric field lines
and equipotentials



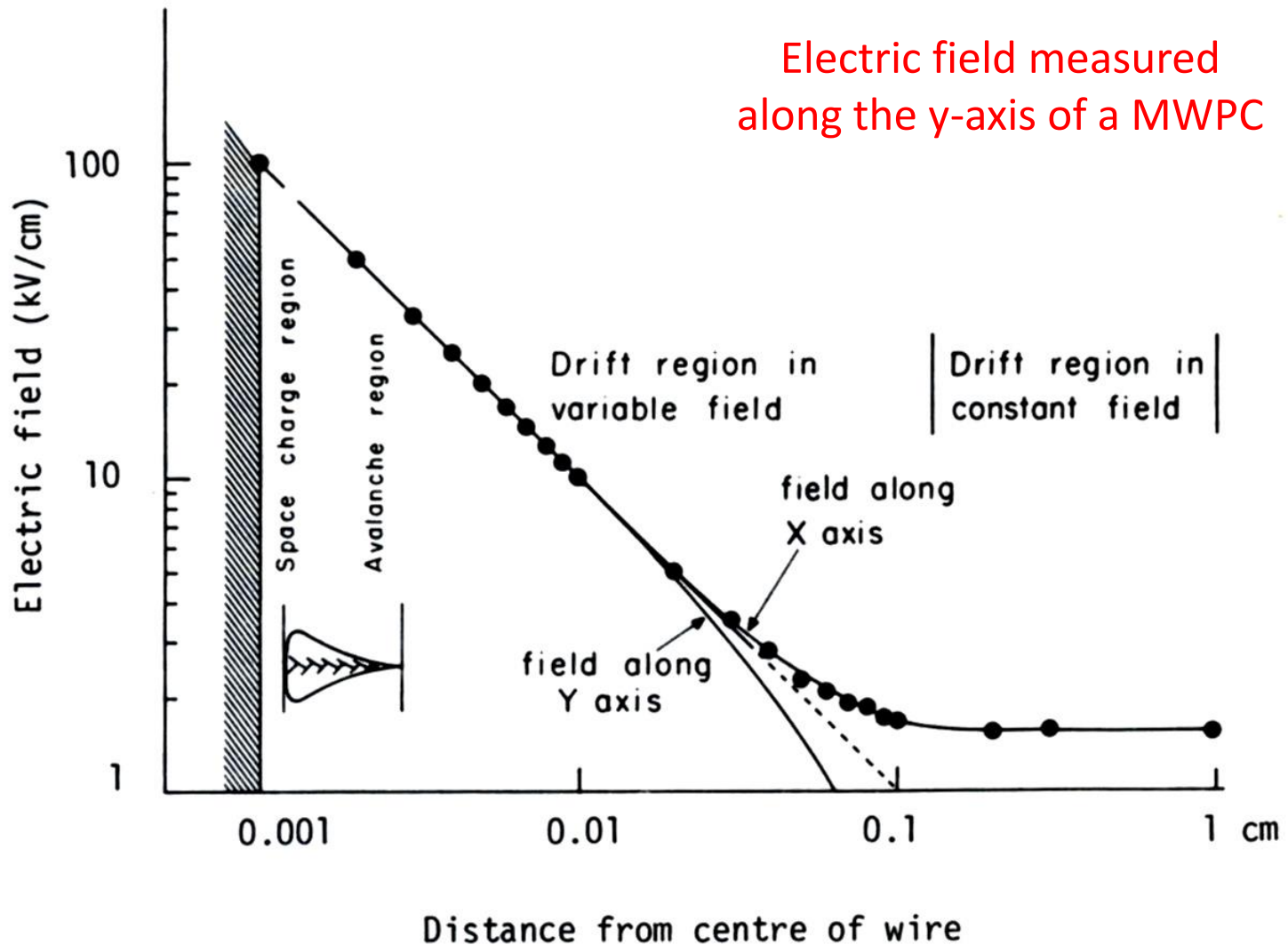
Small wire displacements
reduce field quality ...

Need high mechanical precision
both for geometry and wire tension ...

[electrostatics and gravitation; wire sag]



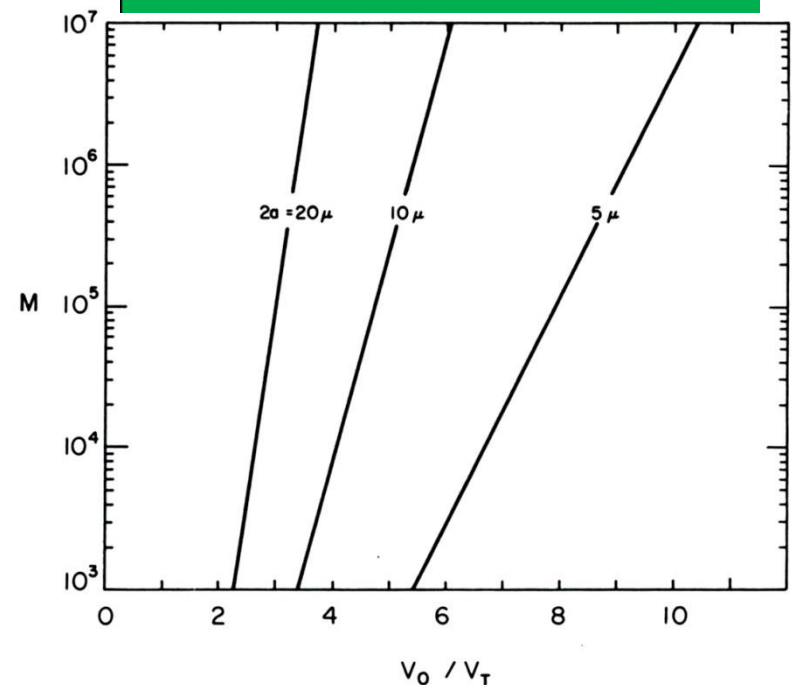
Electric field in a MWPC



Choice of the geometry

- The accuracy of localization depends on the wire spacing
 - MWPCs with spacings less than 2mm are difficult to operate
 - As s decreases, the capacitance also decreases, and to keep the same gain the high voltage should be increased since $\ln M \propto CV_0$
 - Increasing high voltage above a few kV can lead to security issues!
 - Another option is that of scaling down all the geometrical parameters of the MWPC (a, s, l)
 - The mean free path for ionization is invariant \rightarrow need to increase the gas pressure!
- Thick anode wires allow to increase the gain
 - Thick wires are easier to handle than thin ones
 - If the gain curve is steep, the probability of discharge in any section of the chamber can be high

Dependence of the gain on the HV for a MWPC with $s = 2mm$ and $l = 8mm$. The gain is plotted for three values of the diameter $2a$ of the anode wires

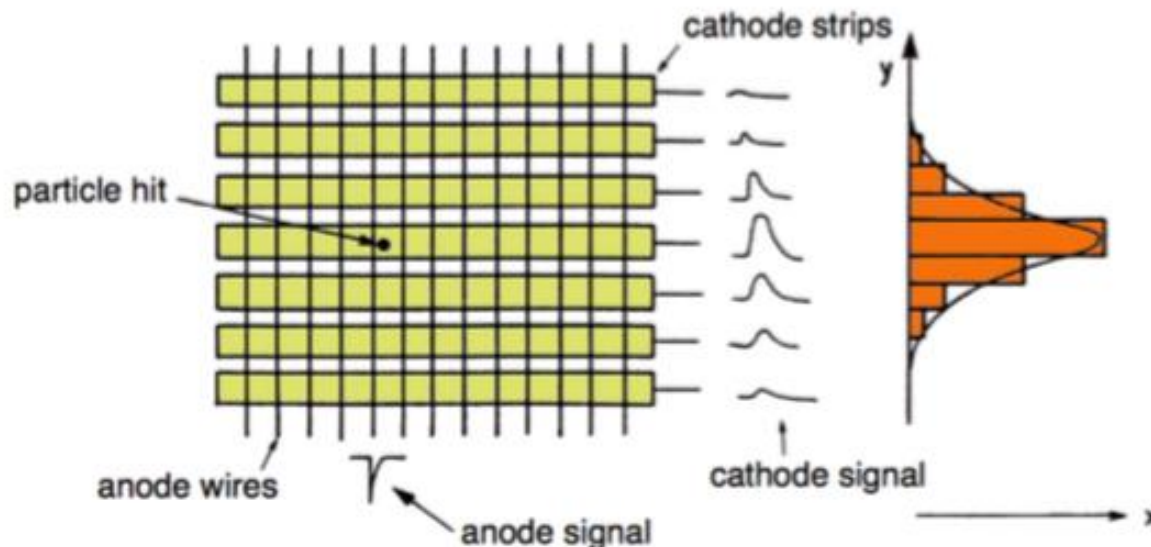


Multi Wire Proportional Chamber as Cathode Strip Chamber

A MWPC can only measure the coordinate perpendicular to the wires. No position measurement along the wires.

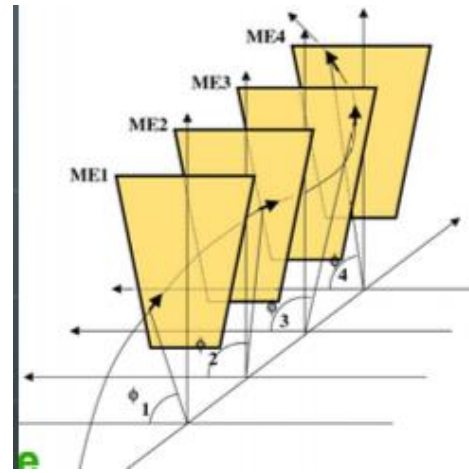
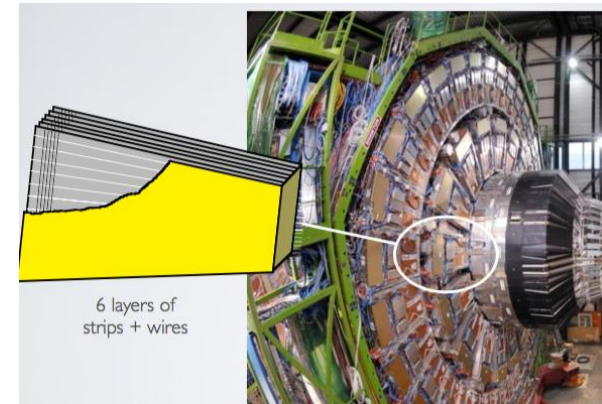
If the cathode is segmented, perpendicular to the wires, the signal induced can be used to determine the second coordinate.

Employing a center of charge calculation a position resolution of $50\ \mu\text{m}$ is achievable.

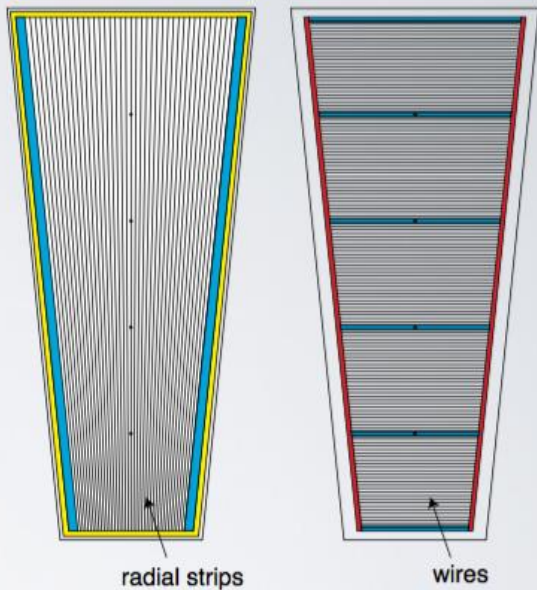


CSC: example from CMS

The 4 Endcap CMS stations are equipped with CSCs. Each CSC has 6 gas gaps and with 6 layer of strips (radial) and wires.



The CMS CSC geometry

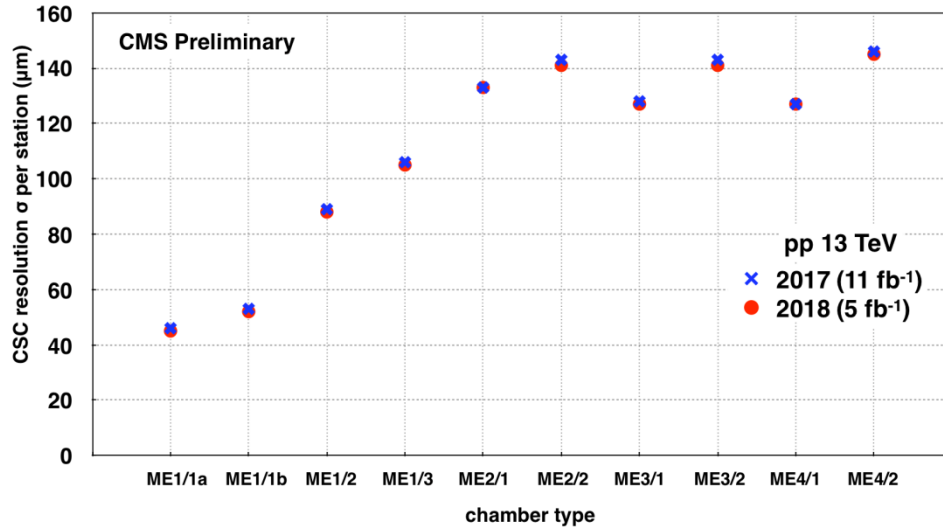


The main goal of CSCs is to define the bending angle of muon in the magnetic field of steel disks → crucial a good space resolution in direction perpendicular to the radius of a disk.

CSC chosen due to presence of high and inhomogeneous magnetic field and high particle rates.

CMS CSC performance

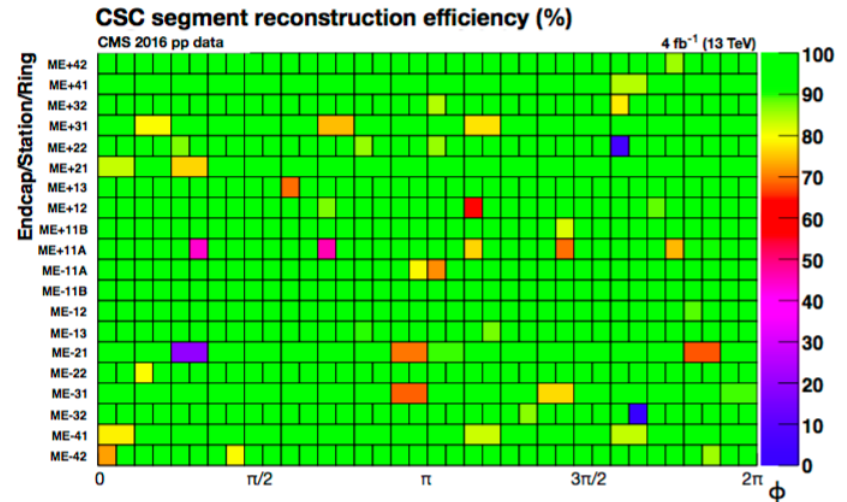
CSC Spatial Resolution



CSC station spatial resolution :

- Between 40–140 μm (depending by the strips pitch)
- stable performance

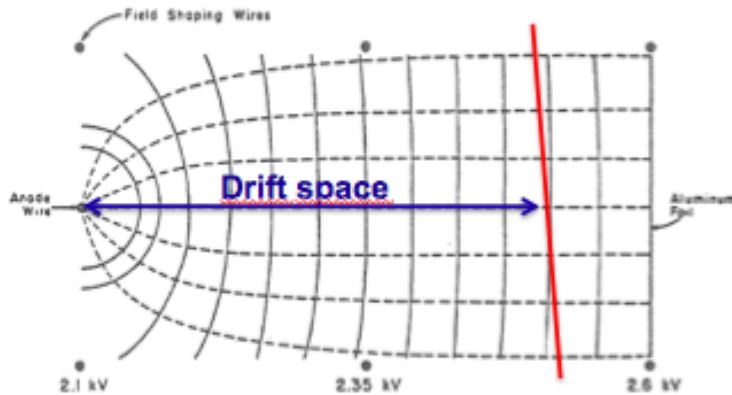
Segment reconstruction efficiency



Drift Chambers

Drift chambers are wire chamber with a long path:

1. Charged particle traversing the gas produce ionization
2. Electrons drift to the anode wire
3. Electrons close to the wire give rise to avalanche multiplication processes



Trigger system

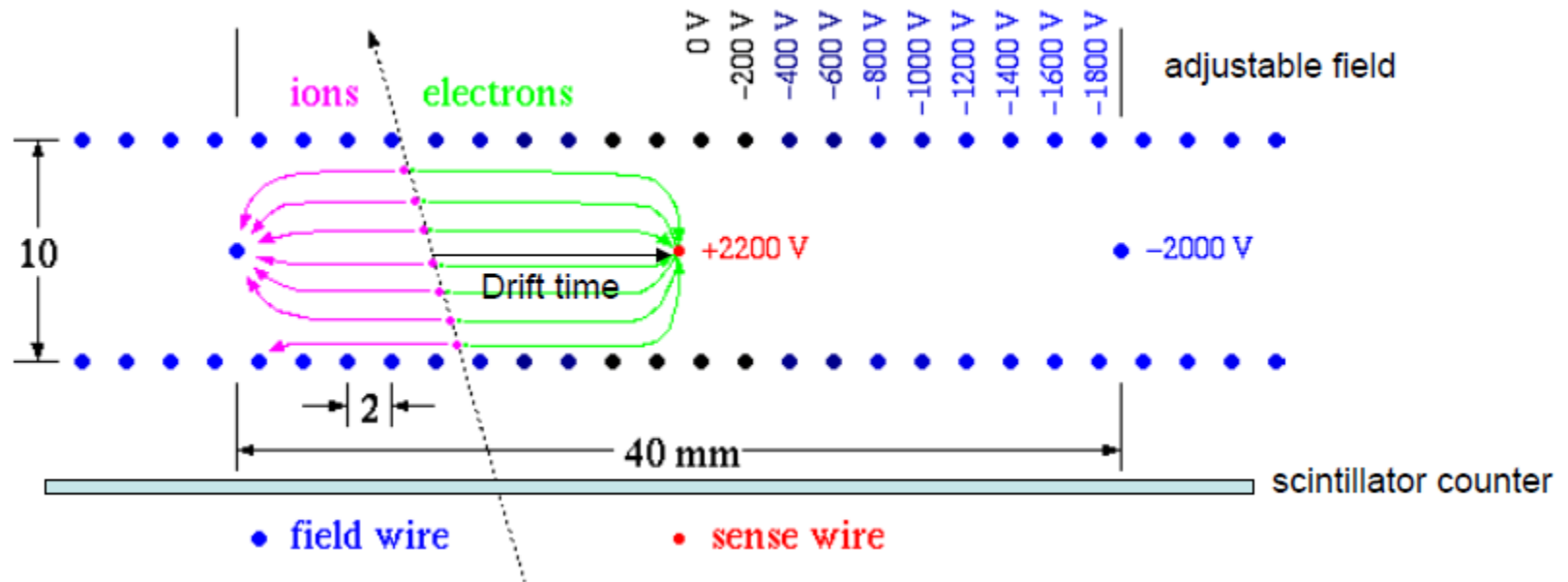
➤ Hit position defined by the linear relation between the drift velocity (about 50 $\mu\text{m}/\text{ns}$) and the time of arrival on the anode wire

$$x = v \cdot \Delta t$$

- The electric field has to be homogeneous and the drift velocity constant and known.
- Compared to MWPC: fewer wires and electronic channels, higher precision, but lower rate capability

Drift chambers

- A drift chamber (DC) consists of a region of moderate electric field, followed by a proportional counter
- Electrons produced by an ionizing particle at time t_0 migrate towards the anode, where the avalanche multiplication occurs at time t_1
- The position of the ionizing particle can be inferred by the space-time relationship: $x = \int_{t_0}^{t_1} w(t) dt$
 - In case of constant drift velocity: $x = w(t_1 - t_0)$
- The drift region is obtained with a set of cathode wires kept at increasing potentials

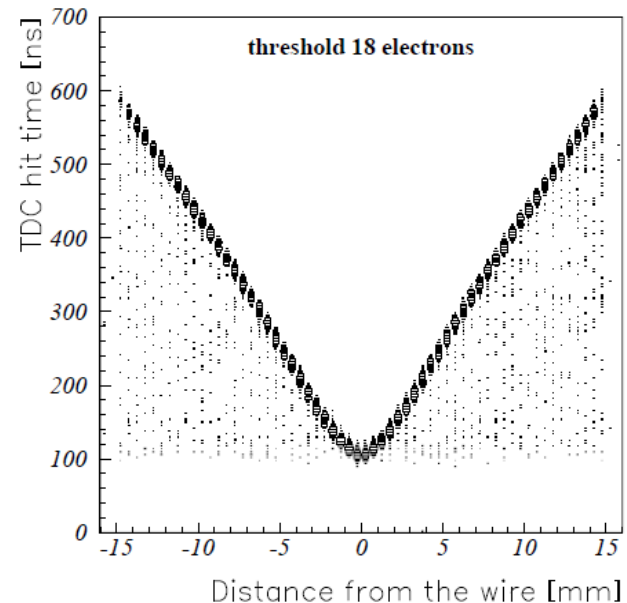
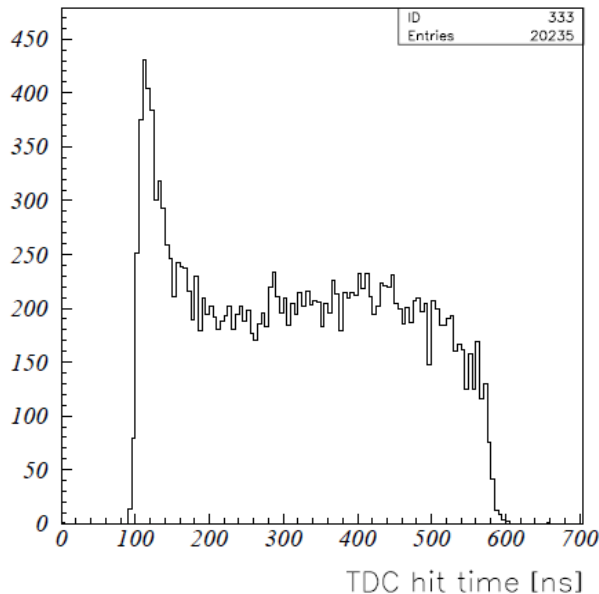


Position measurements

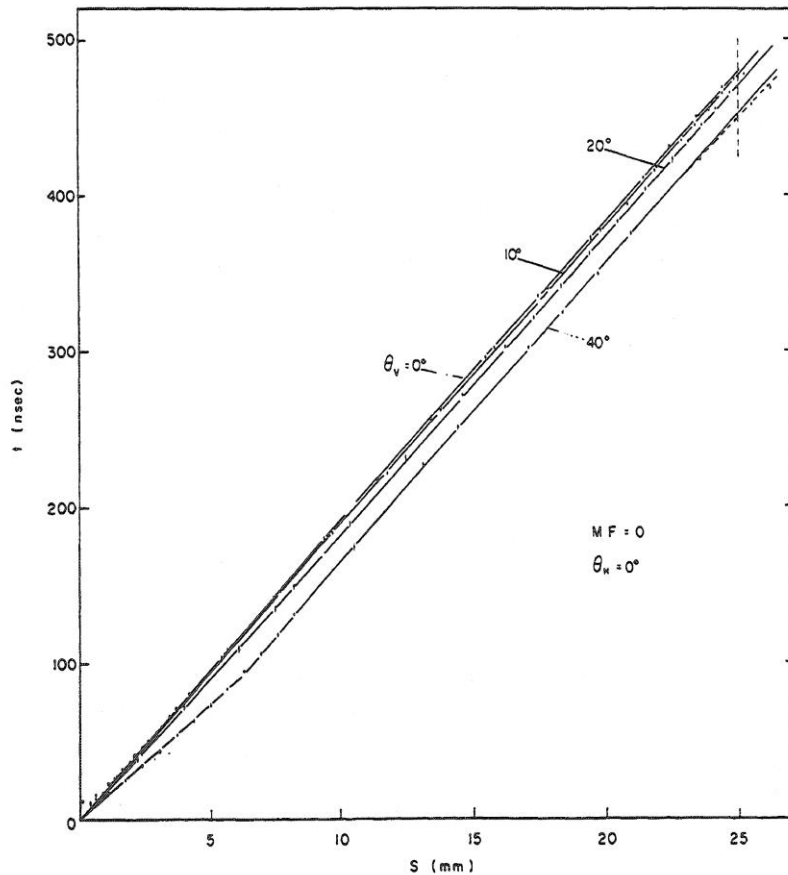
- The position resolution of a DC depends on:
 - Knowledge of the space-time relationship
 - Diffusion of electrons in the gas (intrinsic accuracy) $\rightarrow \sigma_x \propto \sqrt{x}$
- The space-time relationship can be measured by recording the time spectrum of a uniformly distributed beam of particles:

$$\frac{dN}{dt} = \frac{dN}{ds} \times \frac{ds}{dt} = kw(t) \Rightarrow \int \frac{dN}{dt} dt = k \int w(t) dt = ks(t)$$

a) Example of time spectrum obtained with a drift tube exposed to a uniform beam of particles
b) Example of space-time relationship



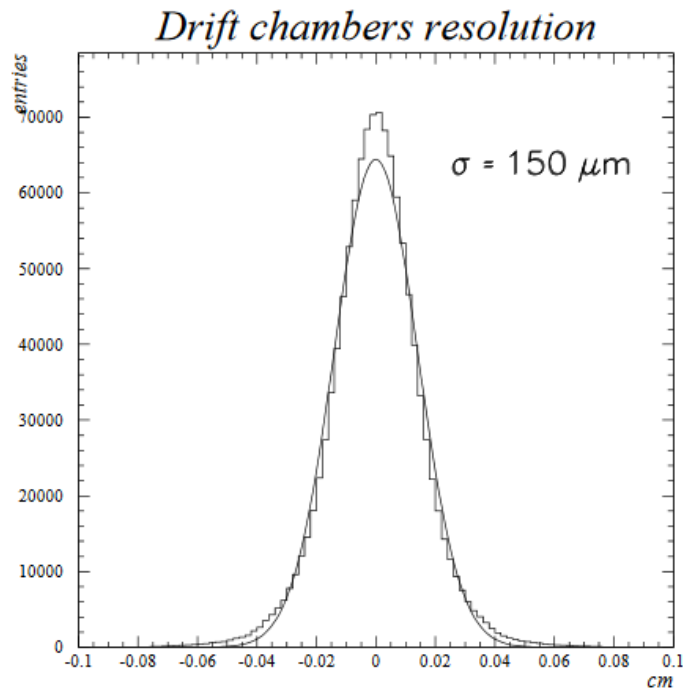
Space-time relationship



- The plot shows the space-time relationship for a drift chamber exposed to a uniform beam of minimum ionizing particles, crossing the chamber with different incidence angles
- Usually the space-time relationship is calculated by means of dedicated simulation codes (Garfield) which describe electron and ion transport in gases

Position resolution studies

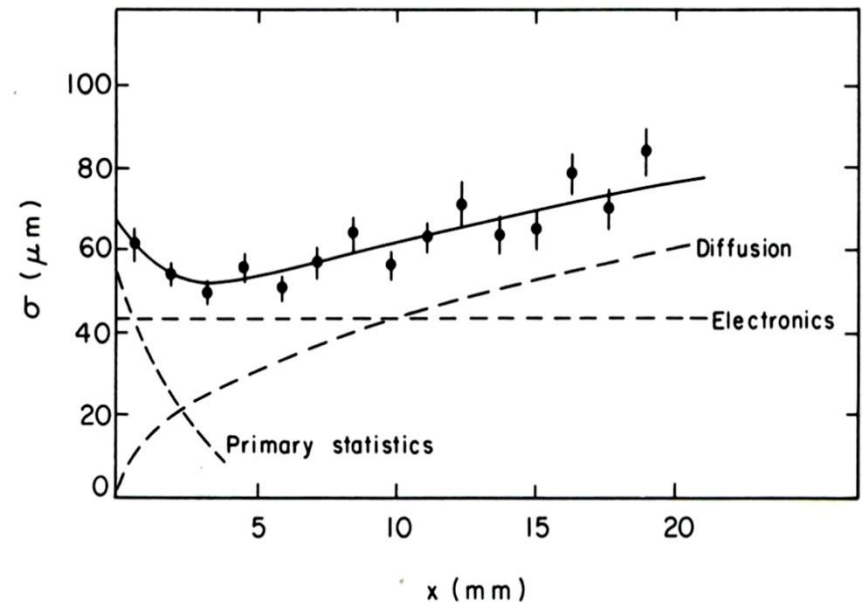
- The position resolution is usually studied with a telescope of drift chambers
- The drift chamber under investigation is placed in the middle of the telescope
 - The resolution is evaluated by studying the differences between the measured and fitted coordinates (with the other chambers)



The plot shows an example of a distribution of the residuals between the fitted and reconstructed positions

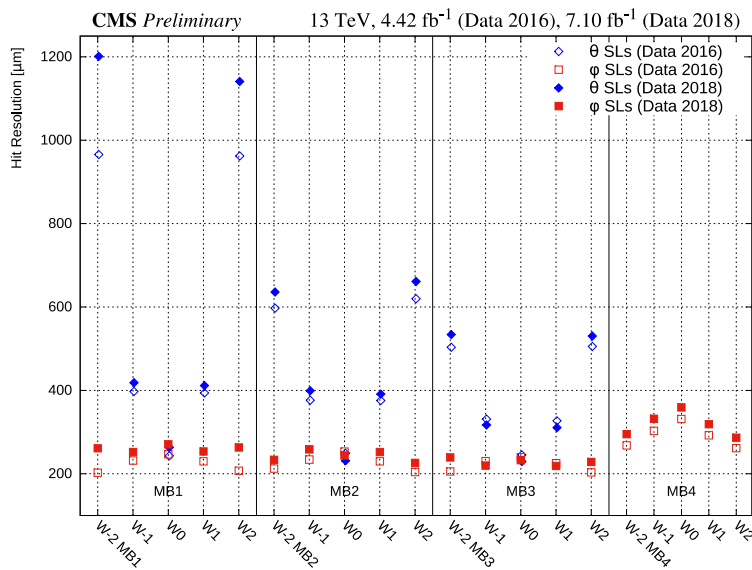
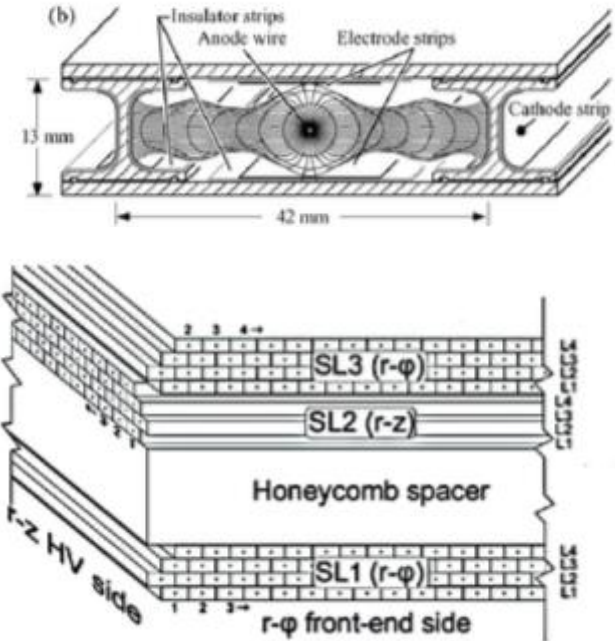
Position resolution studies

- The position resolution of a drift chamber depends on:
 - Accuracy of the time measurement
 - A good TDC can give an accuracy of $\sim 50\text{ps}$
 - Constant contribution to the resolution
 - Diffusion of electrons in the gas
 - The contribution to the resolution is $\propto \sqrt{x}$
 - Primary electron-ion pair production statistics
 - The contribution to the resolution is exponential
- The best possible resolution of a drift chamber is of a few tens of microns



CMS Drift Chambers

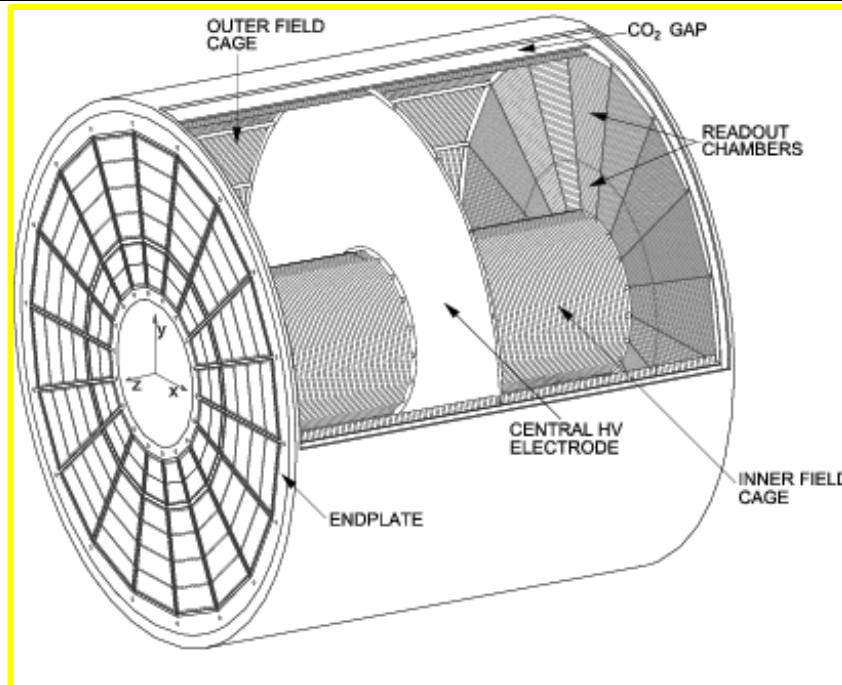
- CMS barrel stations are equipped by DTs
- The basic detector unit is a drift cell: a gas-filled tube with rectangular cross-section
- Four layers of tubes define **DT SuperLayers (SL)**
- DT chamber is done by two SLs with wires parallel to the beam direction, measuring muon position in the bending plane of the magnetic field and one in the longitudinal plane.
- **Gas mixture : 85% Ar + 15% CO₂**



- hit resolution in rφ : 200 to 250 μm
- hit resolution in rz : 400 to 600 μm

Time Projection Chambers

- The TPC is a cylindrical or square field cage filled with a detection medium
 - The medium can be a gas or a liquid
 - Liquid targets are used for neutrino detectors
- Charged particles produce tracks of ionization electrons that drift in a uniform electric field towards a position-sensitive amplification stage which provides a 2D projection of the particle trajectories
- The third coordinate is calculated from the arrival times of the drifted electrons
 - The start for this drift time measurement is usually derived from an external detector

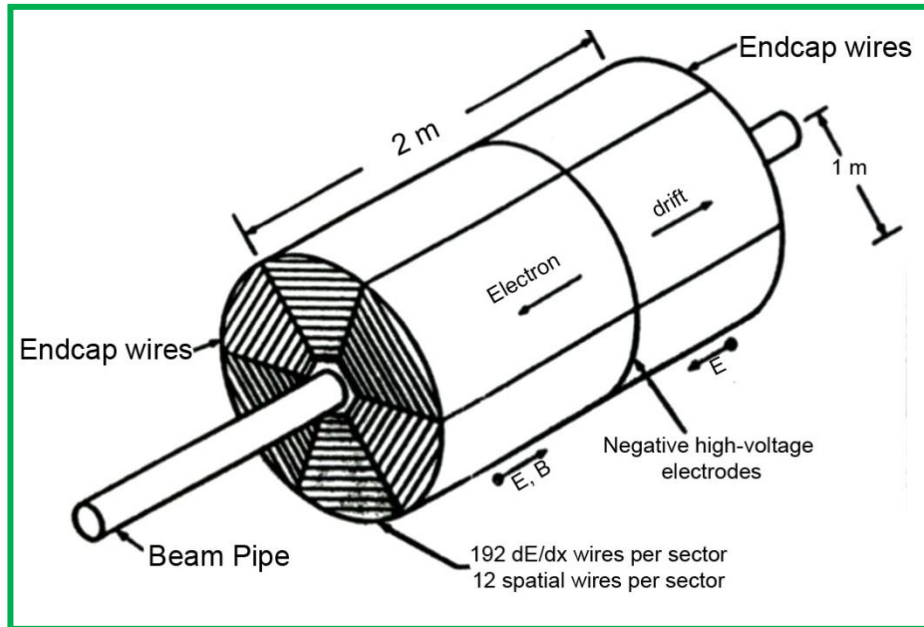


Schematic view of the ALICE TPC. The drift volume is a cylinder of 5m diameter

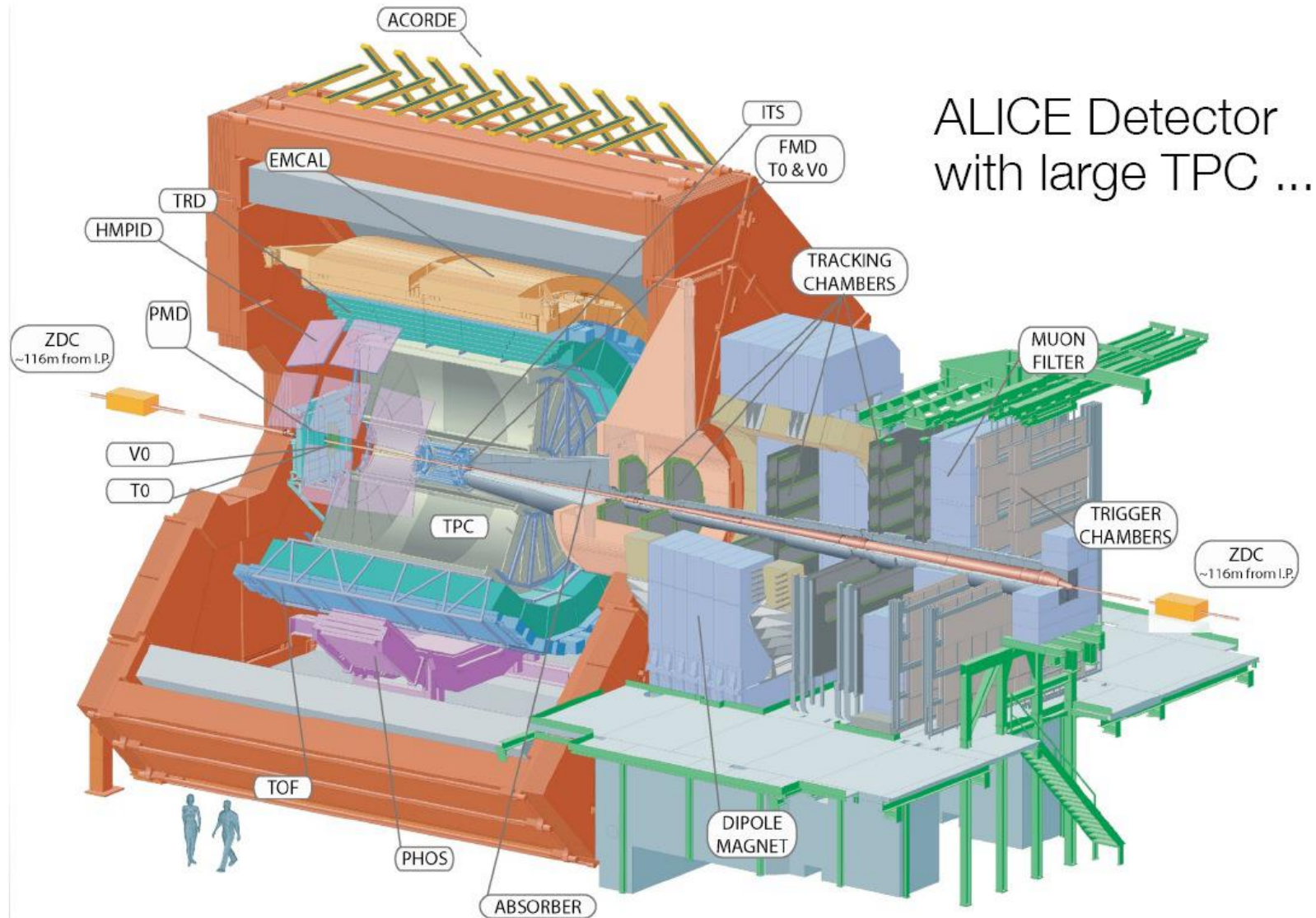
Time Projection Chambers

- The first TPC was developed by D. Nygren in 1978 for the PEP-4 experiment at SLAC
- It consisted of 2 contiguous cylindrical cells of a few m^3
 - The electric and magnetic fields are parallel to the axis
- Electrons drift towards the endcaps, equipped with proportional wires and cathode pads to reconstruct the (r, φ) coordinates
 - Resolution of $200\mu m$ on the x and y coordinates
- The z coordinate is reconstructed from the drift time
 - Resolution of $200\mu m$ on the z coordinate

Scheme of the TPC used in the PEP-4 experiment



ALICE TPC



ALICE TPC

Length: 5 meter

Radius: 2.5 meter

Gas volume: 88 m³

Total drift time: 92 μ s

High voltage: 100 kV

End-caps detectors: 32 m²

Readout pads: 557568

159 samples radially

1000 samples in time

Gas: Ne/CO₂/N₂ (90-10-5)

Low diffusion (cold gas)

Gain: > 10⁴

Diffusion: $\sigma_t = 250 \mu\text{m}$

Resolution: $\sigma \approx 0.2 \text{ mm}$

$\sigma_p/p \sim 1\%$; $\epsilon \sim 97\%$

$\sigma_{dE/dx}/(dE/dx) \sim 6\%$

Magnetic field: 0.5 T

Pad size: 5x7.5 mm² (inner)

6x15 mm² (outer)

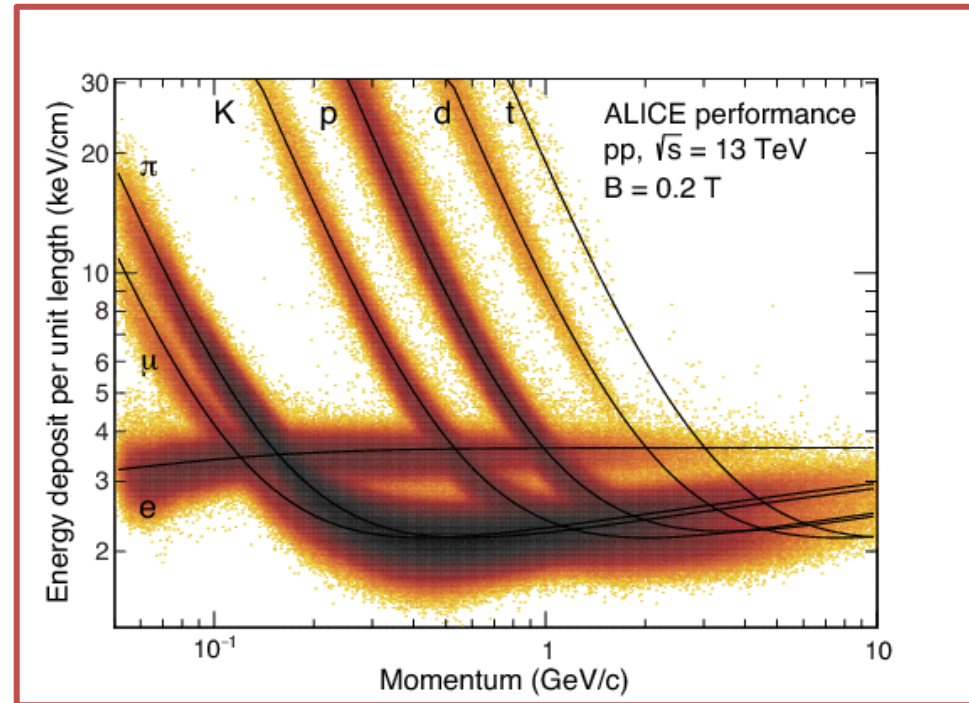
Temperature control: 0.1 K

[also resistors ...]



Particle Identification with TPCs

- Identification of the charged particles crossing the TPC is possible by simultaneously measuring their momentum and their dE/dx
- The momentum and the charge sign are calculated from a helix fit to the particle trajectory
- The dE/dx is estimated from many charge measurements along the particle trajectory (e.g. one measurement per anode wire or per row of readout pads)
 - The measured values are corrected for the effective length of the track segments and for variations of the gas temperature and pressure
 - The most probable value of the corrected signal amplitudes provides the best estimator for the specific energy deposit

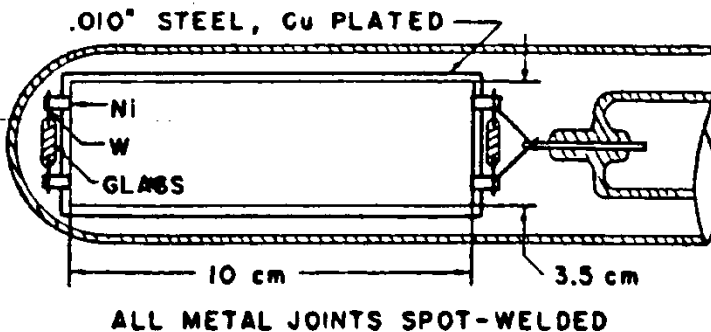
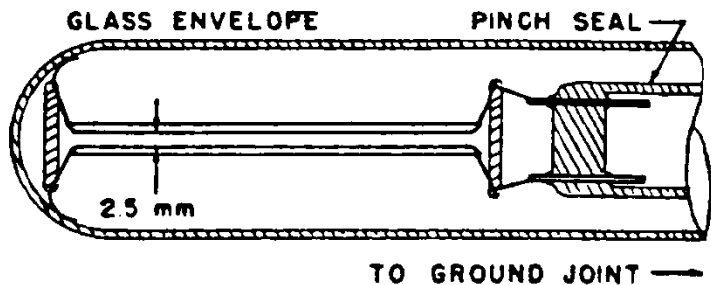


Now let's go back to the planar geometry

Remember: in principle detectors with planar geometry can achieve a quite good time resolution due to the absence of the jitter in the drift time

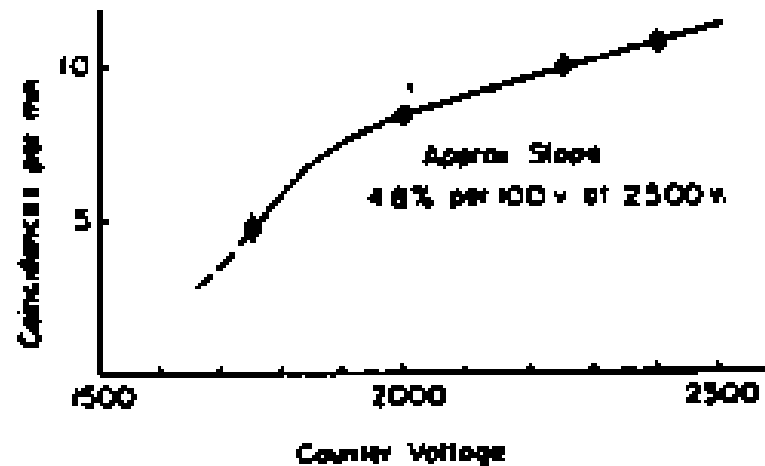
Keuffel's Parallel Plate Chambers

Basically, planar capacitors, with metal electrons, dating 1949

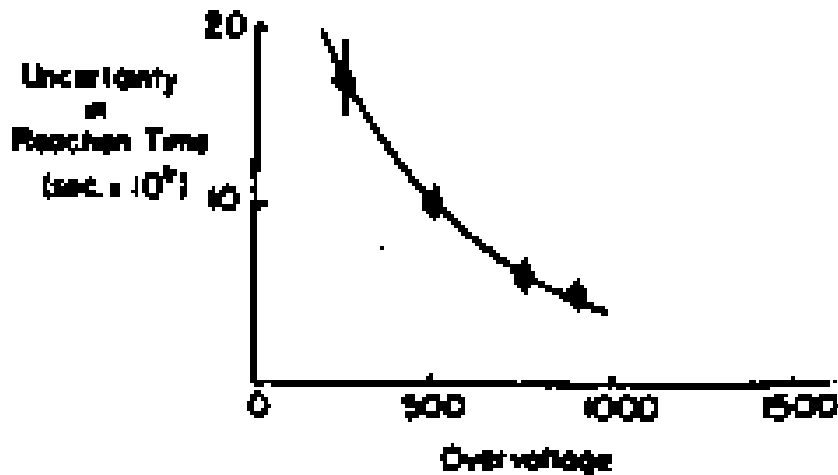


First prototype made in Molybdenum disks, later on Keuffel used Cu or Iron plated with Cu. $d=2.5$ mm, $A= 35$ cm²

Gas mixture: xilene $p_{\text{parz}} = 6$ mmHg
argon $p_{\text{tot}} = 0.5$ Atm



Keuffell's Parallel Plate Chambers



Around 1 ns time resolution:

→ world record at the time!

But: Life time of the detector: few months, limited by discharges setting up first in a point, then all over the detector plate surfaces.

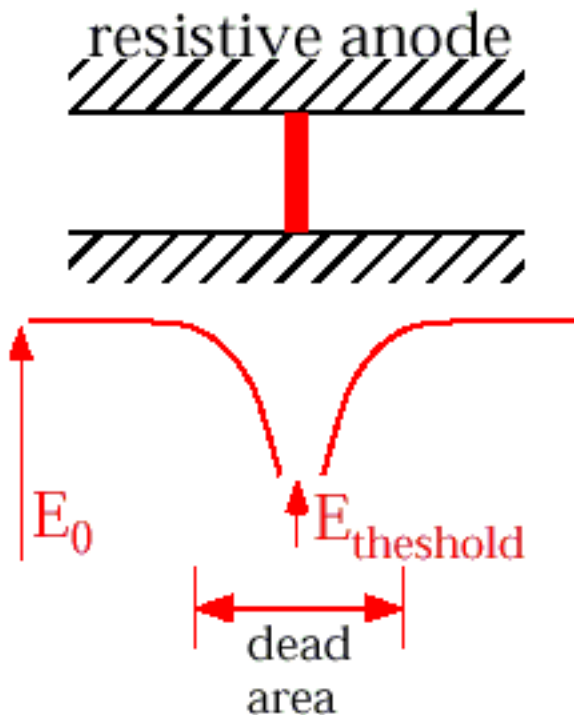


Need to introduce **auto-quenching mechanisms**

Resistive Plate Chamber

Self-extinguishing mechanism

The arrival of the electrons on the anode reduces the local electric field and therefore the discharge is extinguished. During the discharge the electrodes behave like insulators.



Avalanche duration related to the drift velocity and Townsend coefficient

Time constant for re-charging up related to the RC constant of the RPC elementary cell

$\eta = \alpha - \beta =$ effective Townsend coefficient

$$t_{dis} = \frac{1}{\eta v_d} \gg 10ns$$

$$t_{REC} = re_0 \left(e_r + \frac{2d}{g} \right) \approx 10ms$$

$$\tau_{dis} \ll \tau_{rec}$$

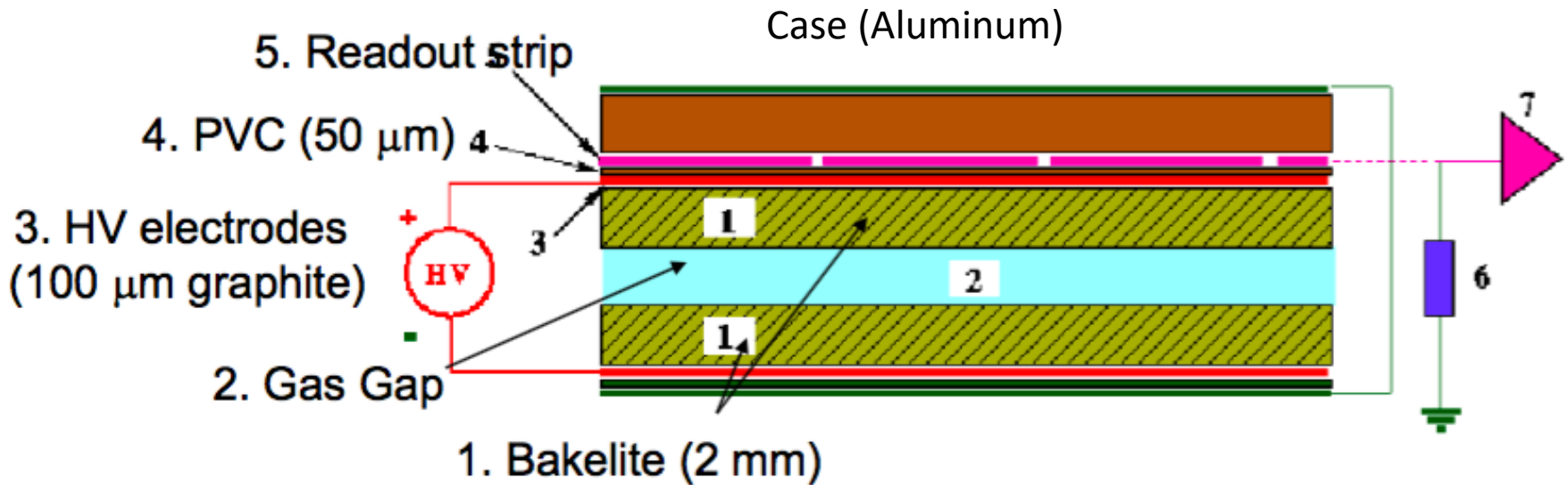
RPC basic elements

Gas mixture:

Argon, Iso-butane and Freon
at $P \approx 1 \text{ Atm}$

High Voltage contact: graphite coating on electrode outer surfaces

Pick up strips are used to collect the signal:
Al/Cu, $\sim \text{cm}$



Resistive Electrodes ($\rho \approx 10^{10} - 10^{12} \Omega \text{cm}$): **High Pressure Laminates (HPL)** “Bakelite” made by Kraft paper impregnated with melamine/phenol resins.
Internal electrode surface covered with a **thin linseed oil layer ($\sim \mu\text{m}$)**

Applications of the 1st generation RPCs

The first generation of RPC detectors was used in several HEP experiments:

'85: Nadir – 120 m² (Triga Mark II – Pavia)

'90: Fenice – 300 m² (Adone – Frascati)

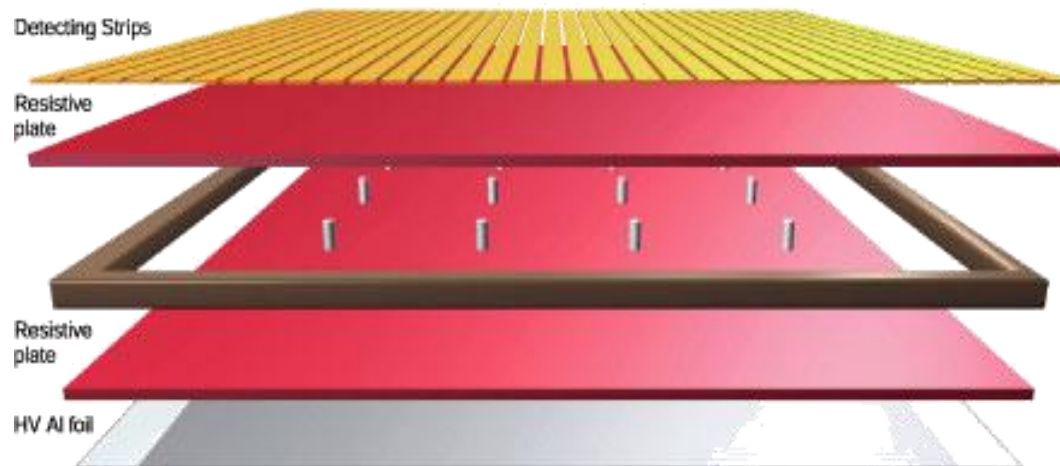
'90: WA92 – 72 m² (CERN SPS)

'90: E771 – 60 m²; E831 – 60 m² (Fermilab)

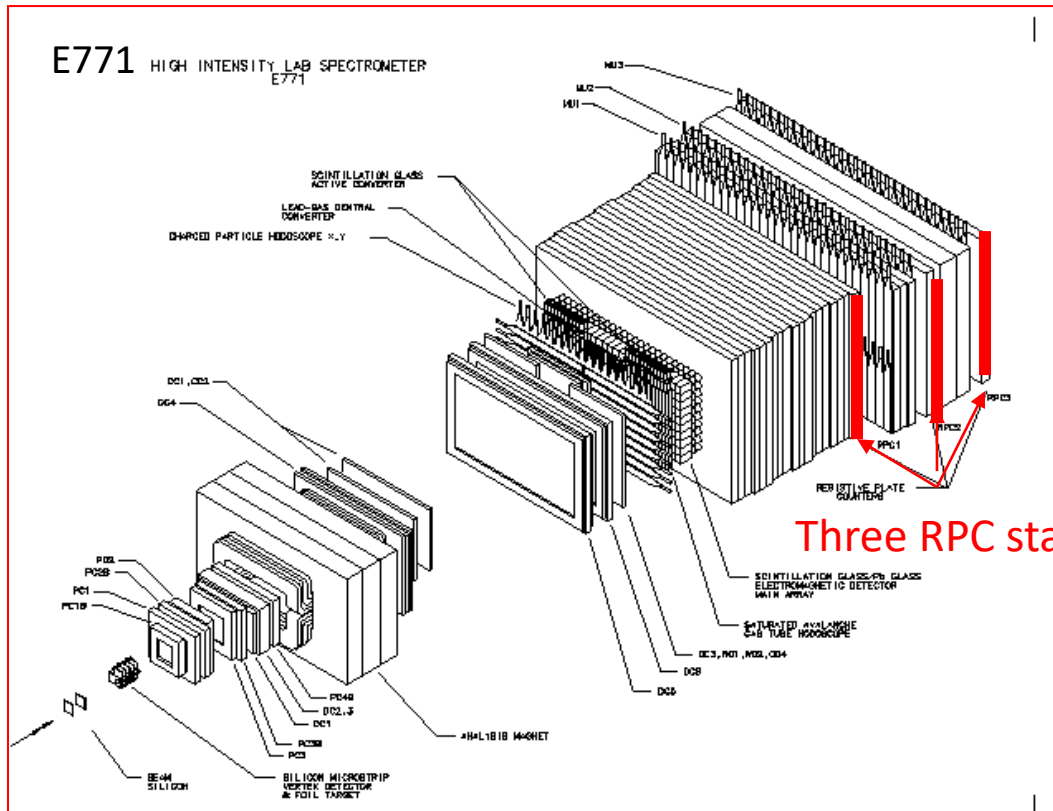
1994-1996: L3 – 300 m² (CERN-LEP)

1996-2002: BaBar – 2000 m² (SLAC)

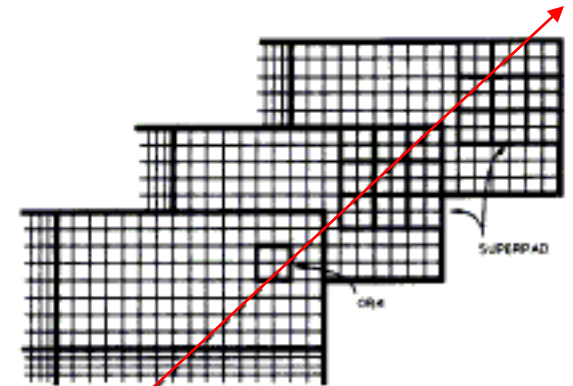
**Very large area of
muon detection**



The E-771 experiment



Three RPC stations



A triple coincidence to identify and track μ

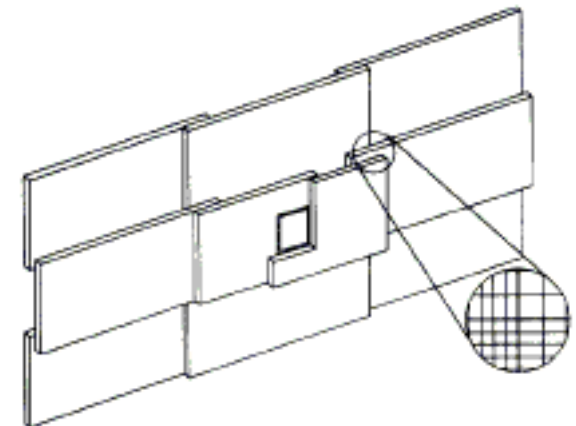
The RPC system did not cover the zone around the beam

Superimposed RPCs, with pad readout

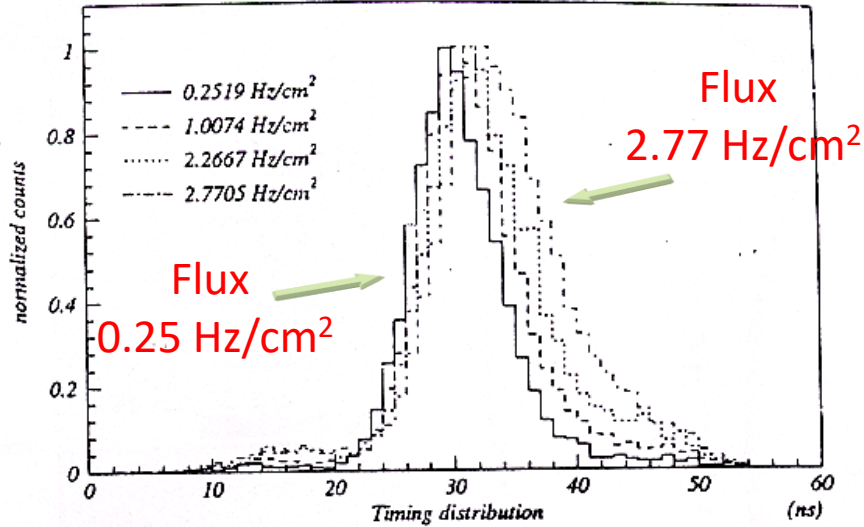
Streamer mode (Ar-isobutane-Freon)

HV 8 kV

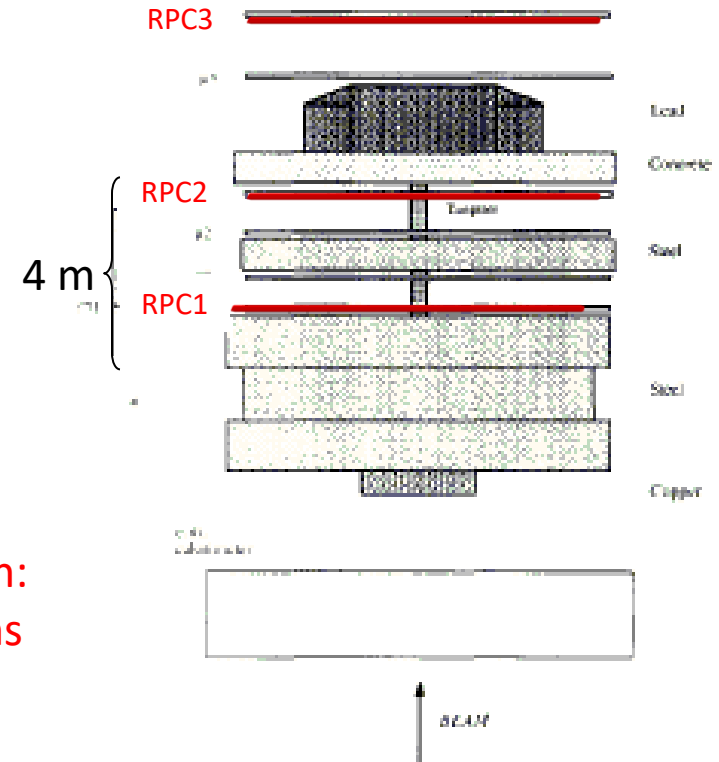
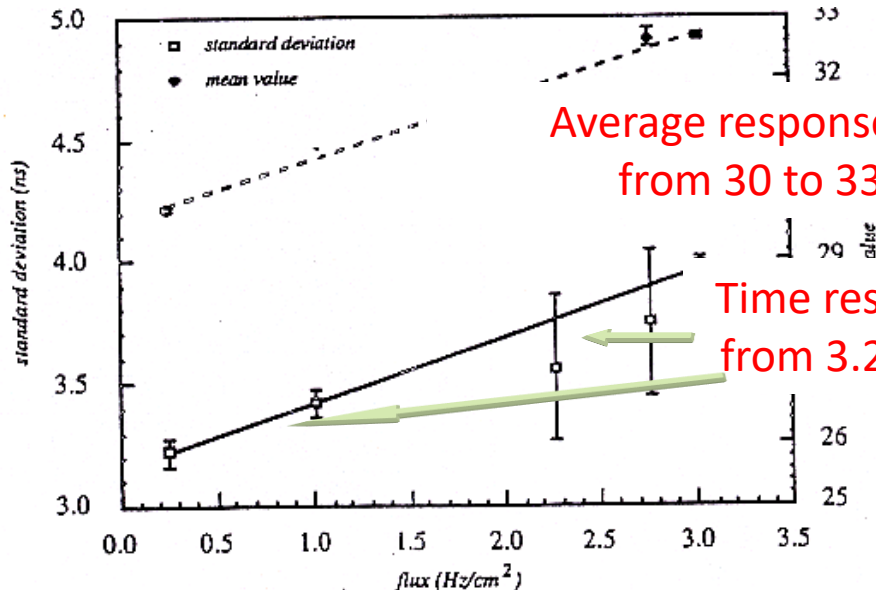
Maximum efficiency: 97%



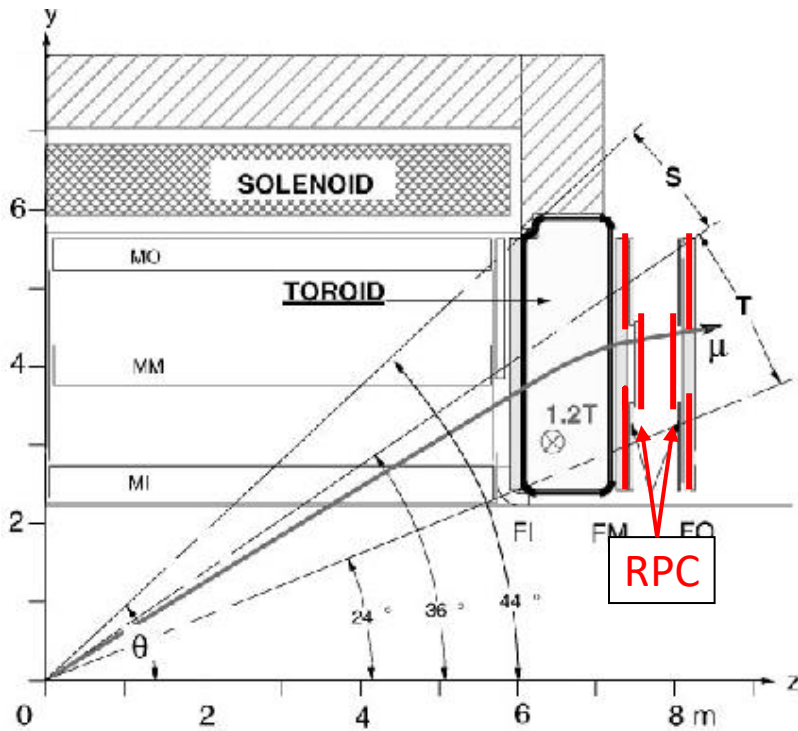
E-771: first hints of rate capability issues



It was the first experiment where performance variations due to the flux of particles impinging on RPCs were noticed and put in evidence.



The L3 experiment at LEP



Two layers of RPCs, each divide in 3 sections, trapezoidal in form and with different dimensions, superimposed at the edges.

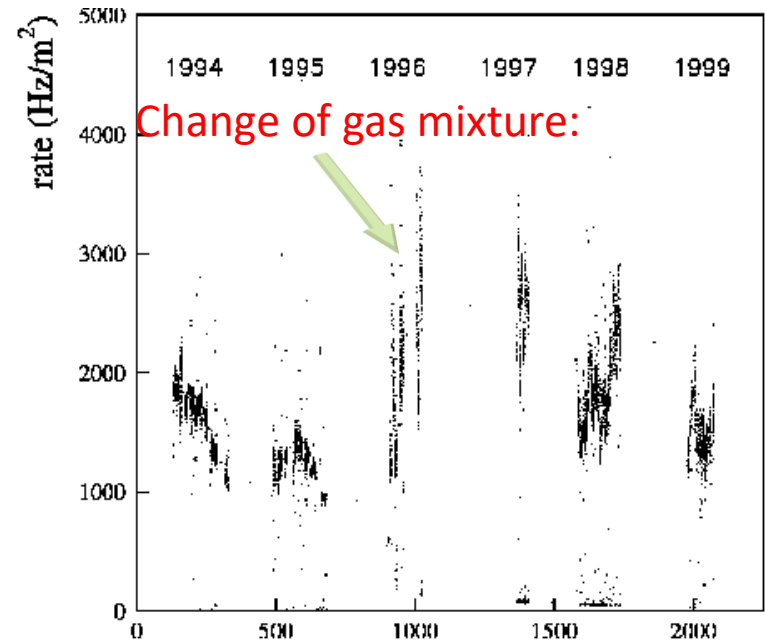
192 double gap RPC
total area > 300 m²
6144 strips, 29 mm strip pitch

Bakelite: $\rho \sim 2 \times 10^{11} \Omega\text{cm}$

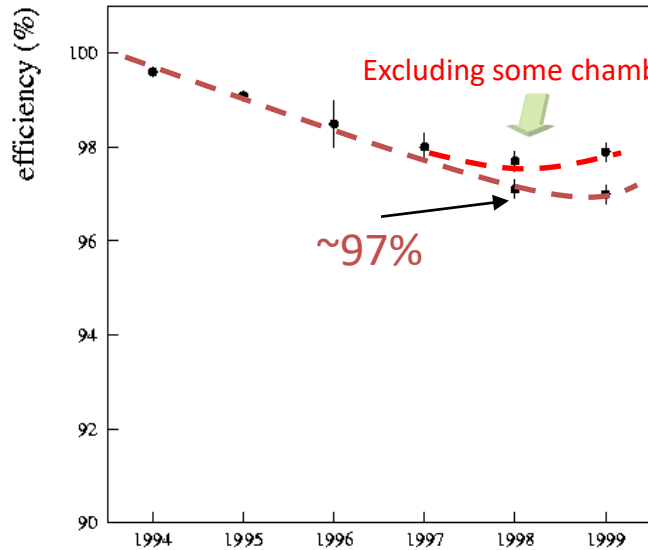
Gas: mixture

Argon/isobutane/CF₃Br (58/38/4) up to 1996
Argon/isobutane/C₂H₂F₄ (59:35:6) thereafter

Operating for 7 years (since 1994) in streamer mode



The L3 experiment at LEP

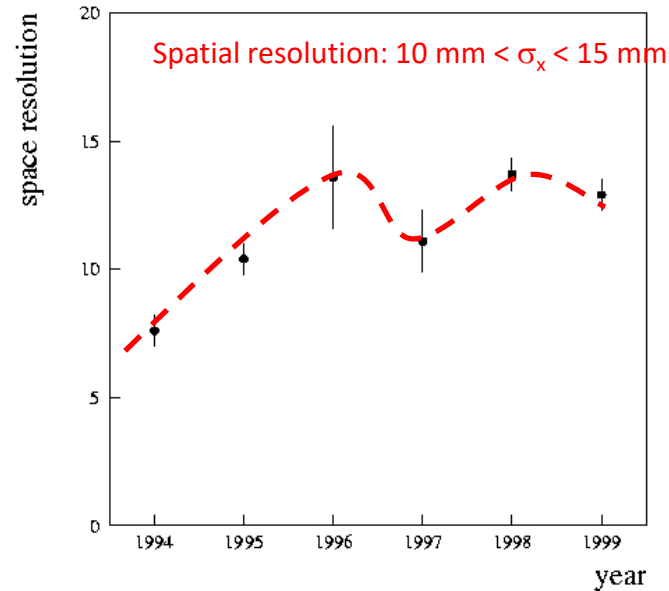


Chamber performance studied using:



Problems:

- electronic failures (large currents at high rate)
- increase of the chambers in some chambers
- gas leaks

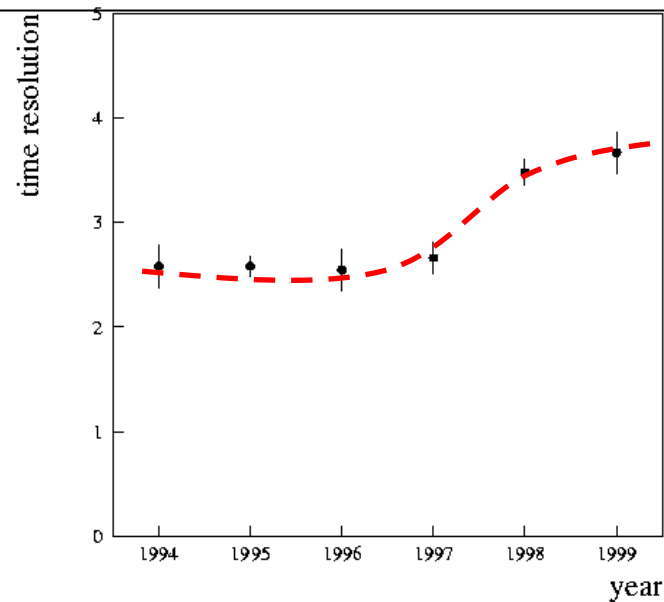


Expected:

$$\frac{L}{\sqrt{12}} \approx 8.3 \text{ mm}$$

Around 1.5-2 strips fired per track

No big problems but slow worsening of the performance



Significance of the first generation of the RPC

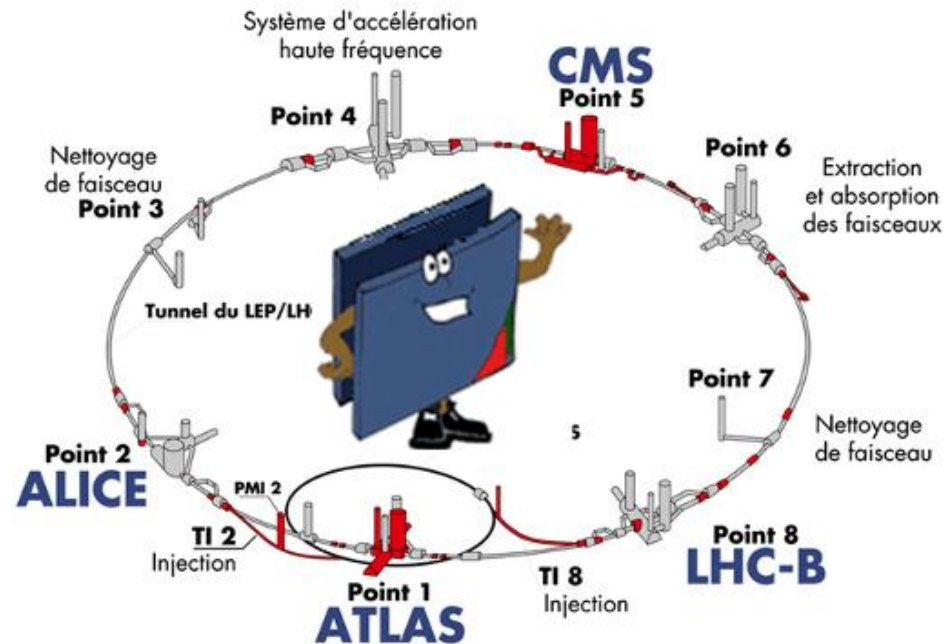
Why the RPCs were extensively used in HEP?

- **Golden parameter:** the time resolution (≈ 1 ns)
- **Good spatial resolution:** limited by strip dimensions
- **High muon efficiency** of the order of $> 96\%$ and **long term stability**
- **The cost** of RPC is much smaller as compared to other fast detector (like the scintillators)
- It is **easy** to construct and operate
- Simple signal pick up and readout system (just “strips”)
- Two dimensional readout (x and y)

BUT

rate capability < 50 Hz/cm²

RPCs at LHC



New detector need to sustain the expected background condition for 10 LHC year!

Detector requirements:

- **Maximum rate* $\approx 300 - 500 \text{ Hz/cm}^2$**
- **Improved time resolution ($< \text{ns}$) for TOF applications**

* *at the nominal LHC luminosity $10^{34} \text{ cm}^{-2} \text{ s}^{-1}$*

2nd generation of “classic” RPC

In late '90, a new generation of RPC was developed:

- **New working mode: *Avalanche mode (saturated avalanche)***
 - **New gas mixture: Freon-based mixture**
 - Total charge $\sim 20\text{-}40$ pC (from $0.1 - 1$ nC)
 - lower current in the detector \rightarrow better longevity
 - **New electronics** in order to transfer a large fraction of the amplification from the gas to the electronics
- \rightarrow good rate capability ~ 500 Hz/cm² with high efficiency ($> 95\%$) and stable conditions for 10 LHC years**

The issue of the rate capability

In the static condition the voltage applied to the chamber ΔV_{gap} is entirely transferred to the gas.

But, in the presence of a ϕ flux of particle, which creates a current I , the voltage inside the gas gap is reduced:

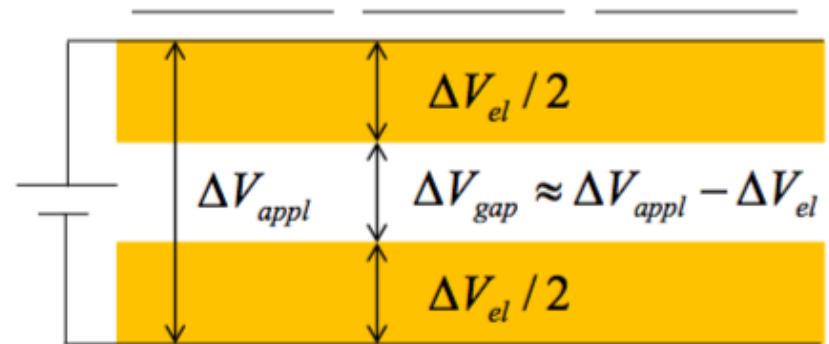
$$\Delta V_{gap} = \Delta V_{appl} - RI = \Delta V_{appl} - \Delta V_{el}$$

$$\Delta V_{el} = r d F \langle Q \rangle$$

Electrode
resistivity

Electrode
thickness

Particle flux counts/cm²

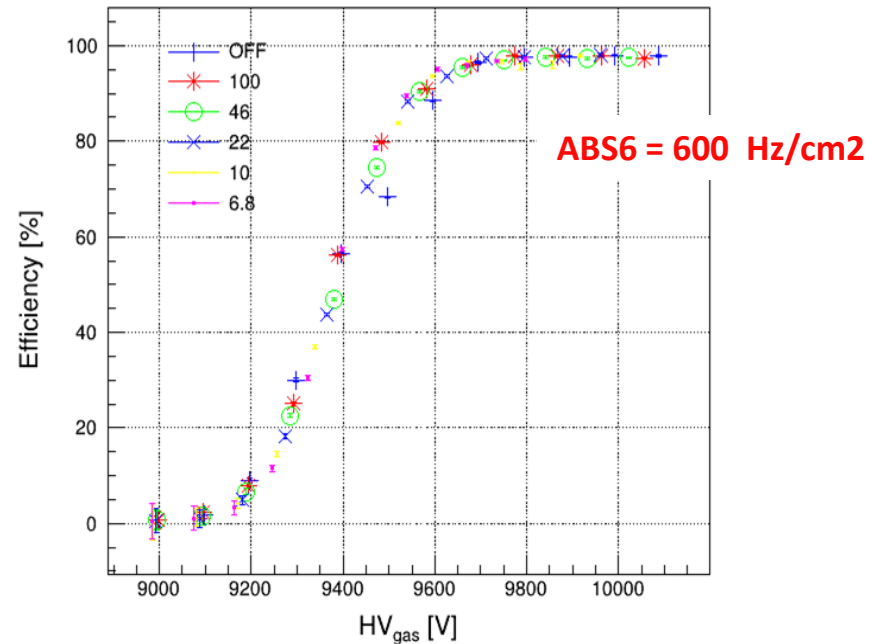
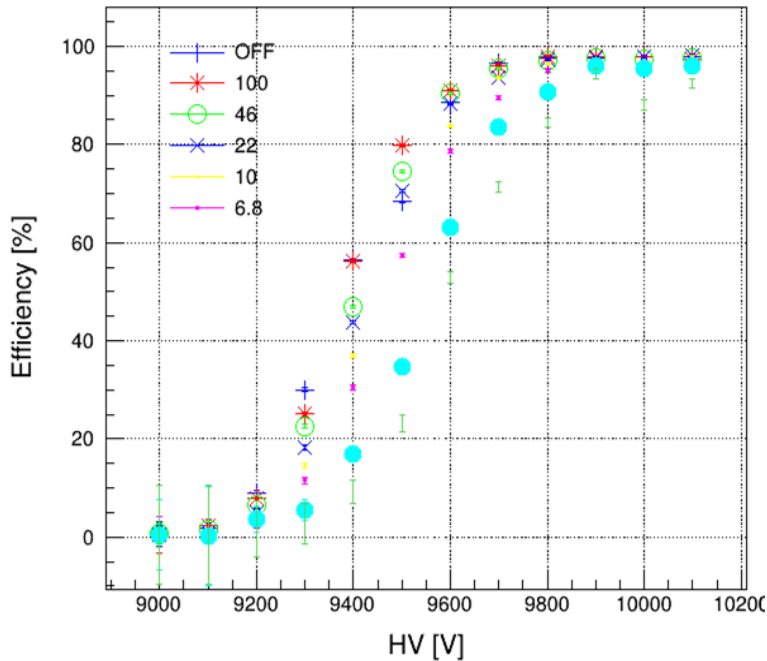


Average charge/hits

- To increase the rate capability (i.e the particle flux) the relevant parameters are $\langle Q \rangle$, ρ , d

Experimental results

Chamber efficiency as a function of HV_{gas} does not depend on the electrodes resistance once that ΔV_{el} has been gotten rid of : **the operation regime of the detector is invariant with respect to ΔV_{gas}**

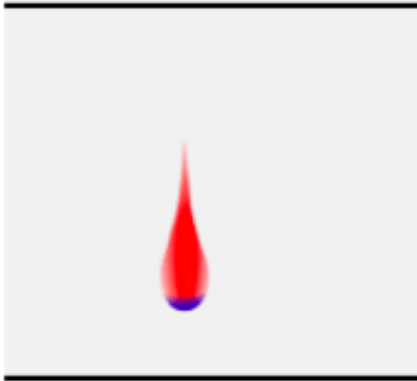


$$DV_{gap} = DV_{appl} - DV_{el} = DV_{appl} - r d F \langle Q \rangle$$

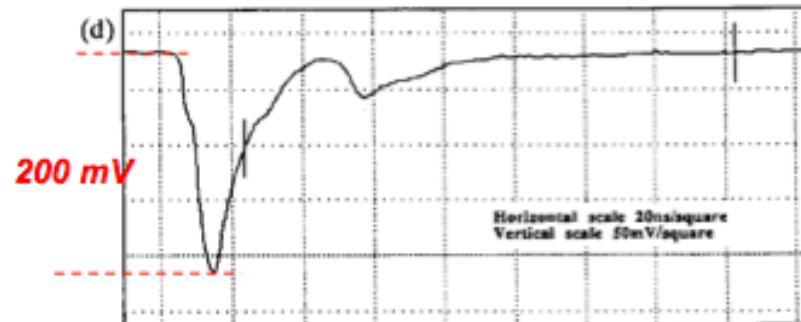
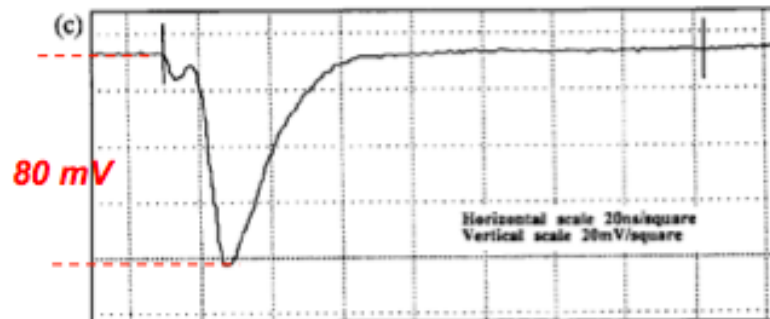
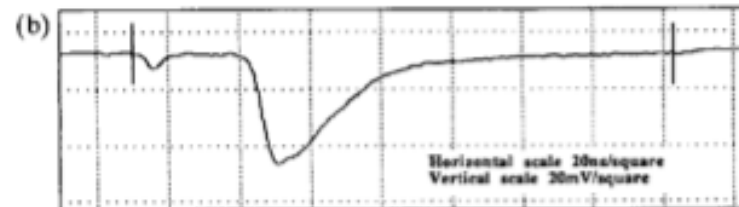
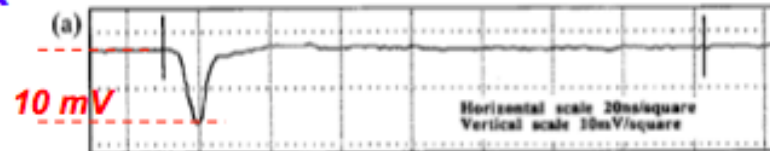
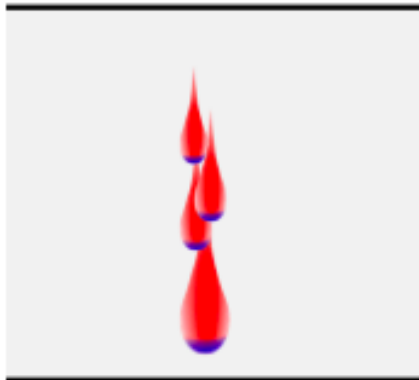
Change of the Operation mode

TRANSITION AVALANCHE TO STREAMER

NORMAL AVALANCHE



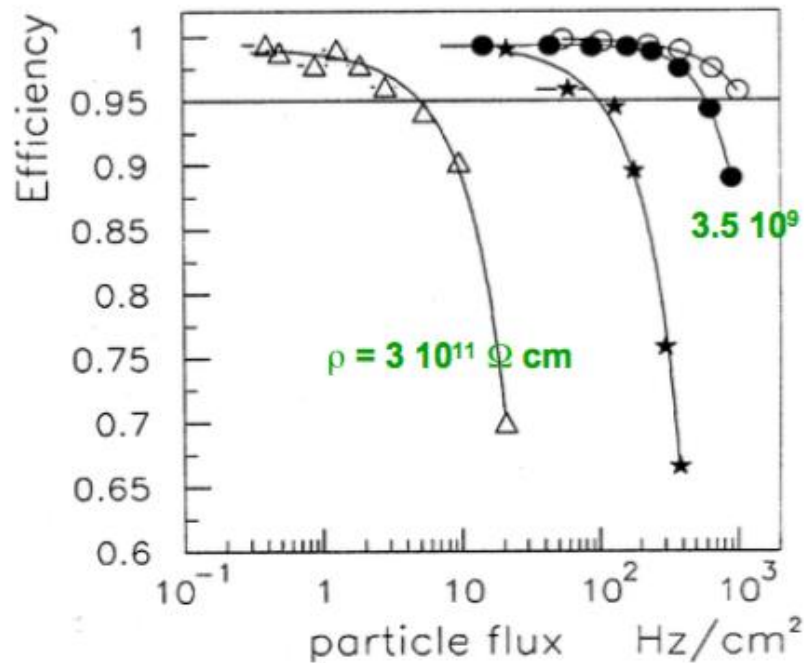
**PHOTON MEDIATED BACKWARD PROPAGATION:
STREAMER**



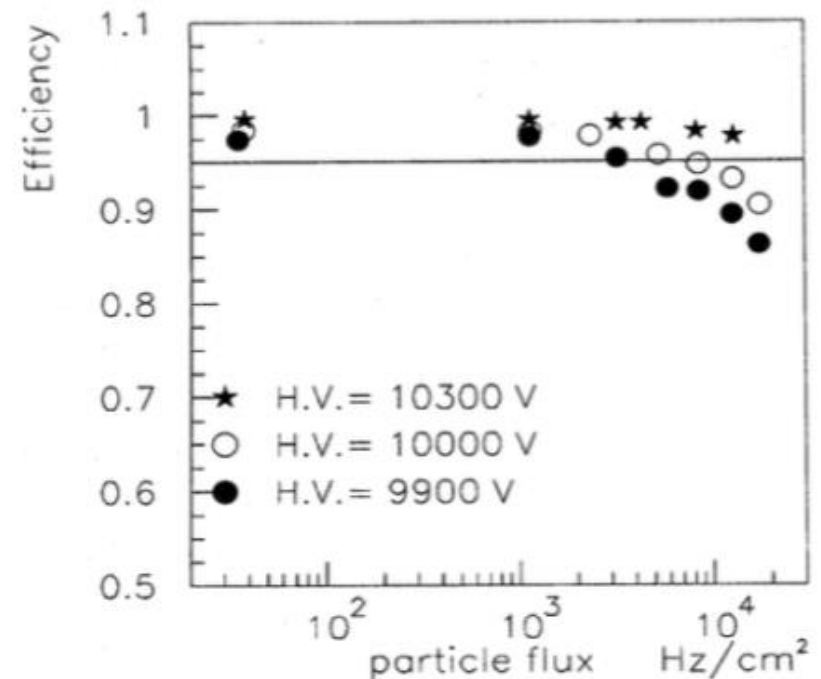
Change of the Operation mode

Average charge ~ 20-40 pC in Avalanche mode - 0.1 – 1 nC in streamer

STREAMER MODE:



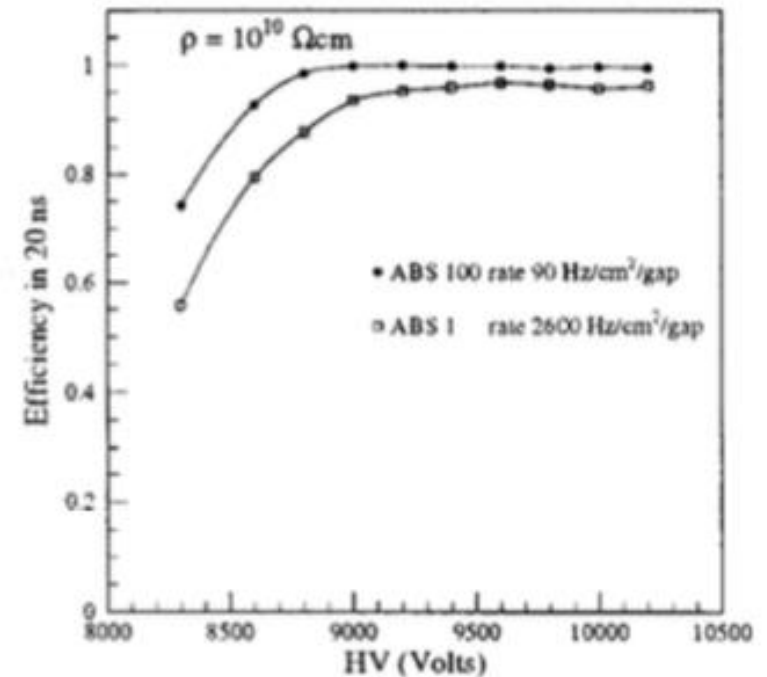
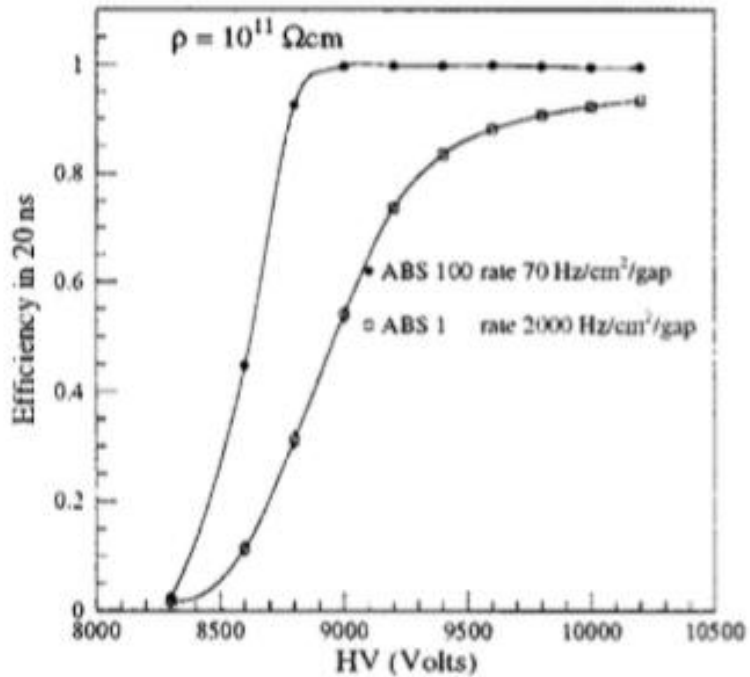
AVALANCHE MODE:



R. Araldi et al, Nucl. Physics B (Suppl) 78 (1999) 84

$$DV_{gap} = DV_{appl} - DV_{el} = DV_{appl} - r d F \langle Q \rangle$$

Reduced resistivity



M. Abbrescia et al. NIM, 434 (1999), 244-253

$$DV_{gap} = DV_{appl} - DV_{el} = DV_{appl} - r d F \langle Q \rangle$$

A new gas mixture

C₂H₂F₄ (95.4%), Iso-butane = 4.5%, SF₆ = 0.3 %

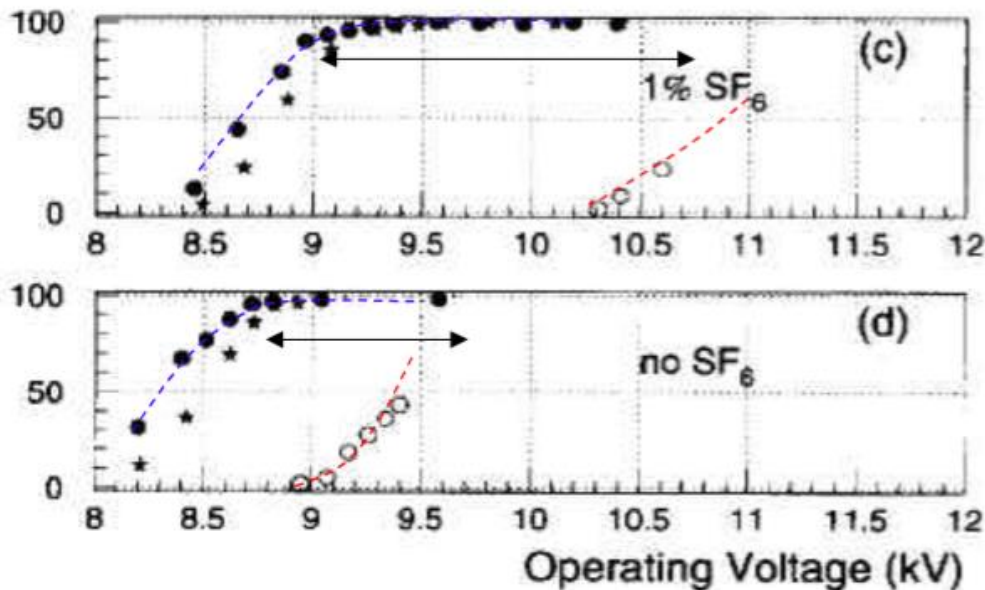
In a streamer mode, the main gas components should provide a **robust first ionization** signal and a **large avalanche multiplication** for a low electric field → **Argon based gas mixture ($\lambda = 2.5 \text{ mm}^{-1}$)**

In avalanche mode, the main component has to have high primary ionization but with small free path for electron capture. The high electronegative attachment coefficient limits the avalanche electron number → **Freon (C₂H₂F₄) based gas mixture ($\lambda = 5 \text{ mm}^{-1}$)**

Plus....a “**quenching gas**” like the **iso-butane** which has an high probability for absorbing ultra violet photons

A new gas mixture

... and a **strong electronegative** gas the **SF₆** is also used to control the excess number of electrons and extends the separation between streamer and avalanche

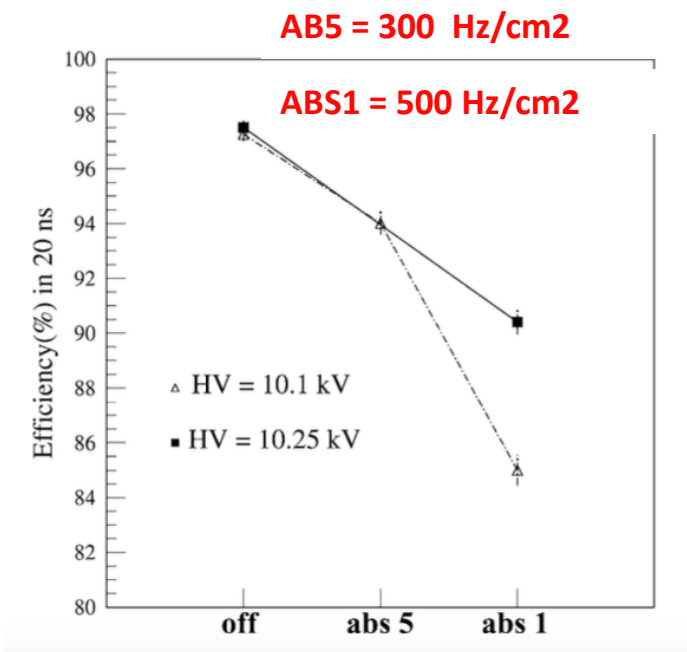


- EFFICIENCY (threshold = 30 mV)
- ★ EFFICIENCY (threshold = 100 mV)
- STREAMER FRACTION

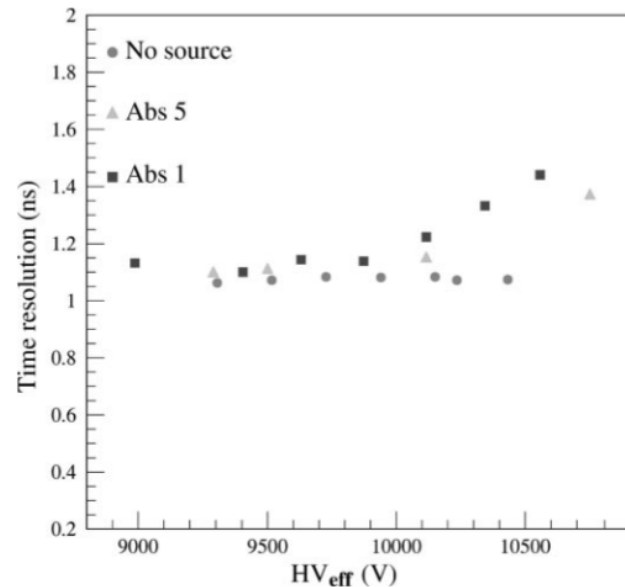
R. Santonico, Scient. Acta XII N2(1997)1

P. Camarri et al, Nucl. Instr. and Meth. A414(1998)317

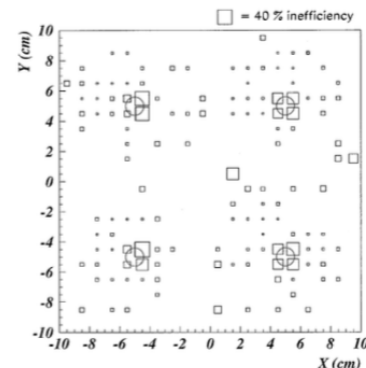
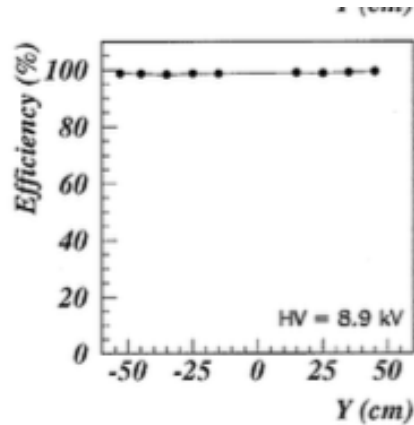
2nd generation RPC: Performance



Efficiency vs gamma hits rate

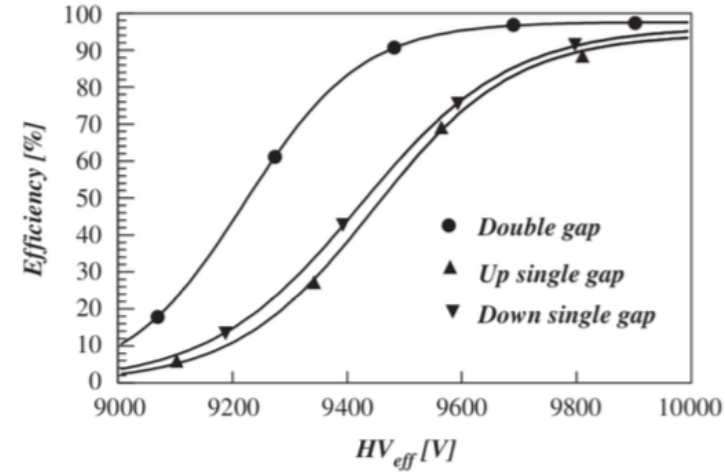
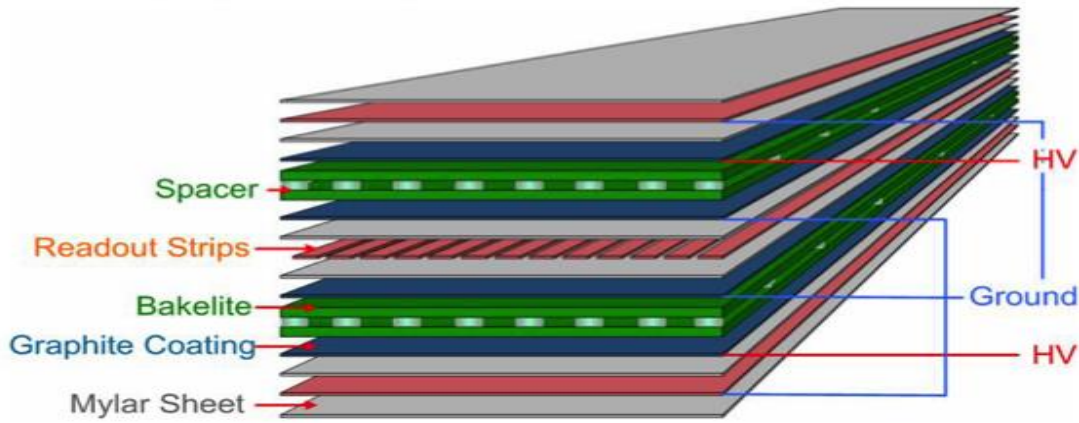


Time resolution vs HV at different gamma background



Uniform efficiency!

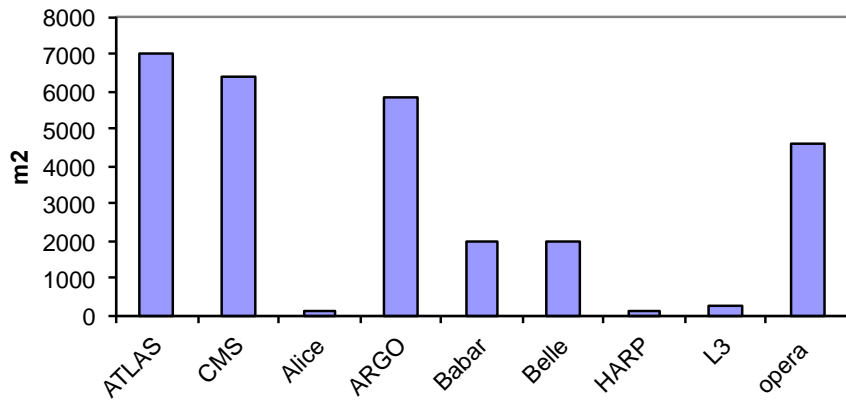
CMS RPC design



- **1056** chambers covering eta region up to 1.8
- Sensitive layers area: **3.200 m²**
- **Double gaps: 2mm gas gap width**
- **Working in avalanche mode**
- **Bakelite** bulk resistivity: $\rho = 2 - 5 \times 10^{10} \Omega\text{cm}$
- **Gas Mixture** 95.2% C₂H₂F₄+4.5% i-C₄H₁₀+ 0.3%SF₆
- **Strip read-out:** 2 ÷ 4 cm
- **Charge per hit** $\approx 20\text{-}30 \text{ pC}$



RPC CMS construction



Barrel Station



Forward Station



- CMS is one of the largest experiments equipped with RPC.

Key of the success:

- ➔ An “industrial approach”
- ➔ Quality control and acceptance criteria

World Wide RPC production

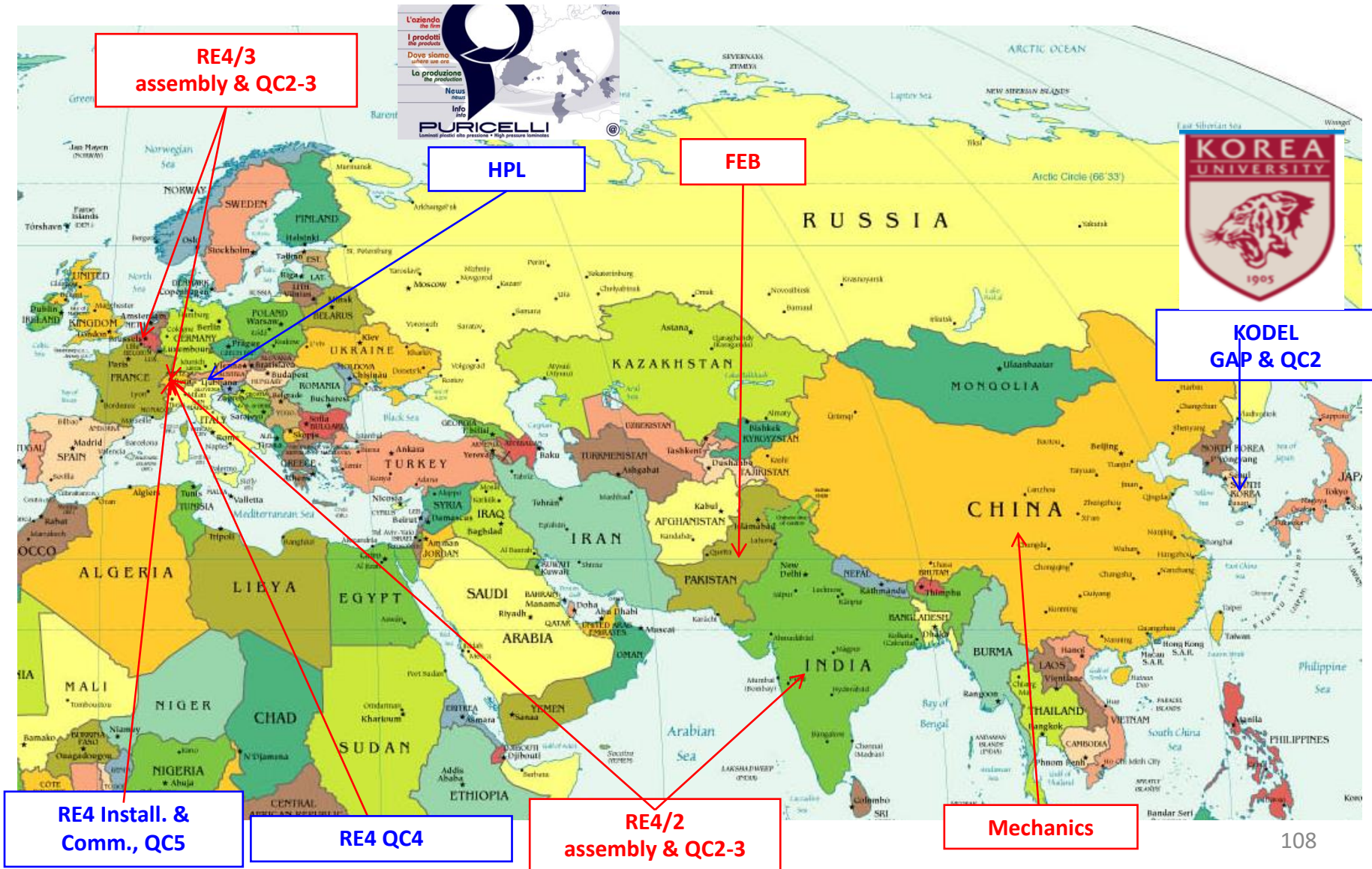
RPC mass production started in **early 2000**:

- **HPL**: PanPla (Italy)
- **Gaps**: General Tecnica (Italy) for the Barrel and Korea University for Endcap
- **Chambers** built and tested in several sites in Europe and Asia
- **Detector installation from 2004-2008**

RE4 stations construction and installation in 2012-14:

- **HPL**: Puricelli (Italy)
- **Gaps**: Korea University
- **Chambers**: India, Belgium and CERN

World Wide RPC production: RE4 CMS example



CMS RPC mass production

Key point: well defined Quality Control and Acceptance Criteria

Final chamber tests:

- Gas leak, connectivity, dark current tests
- Long term detector stability test

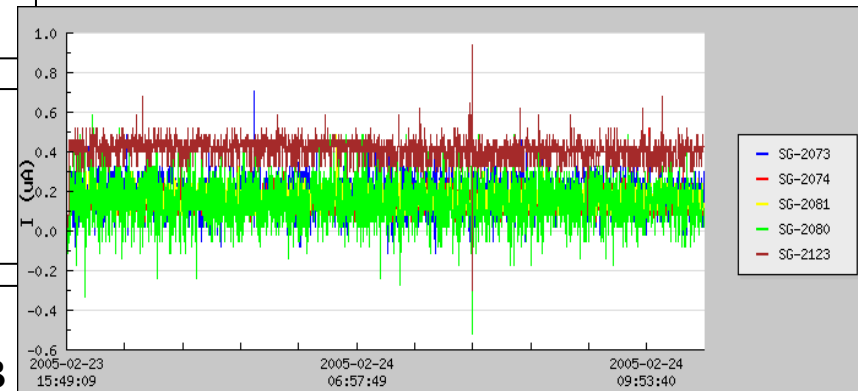
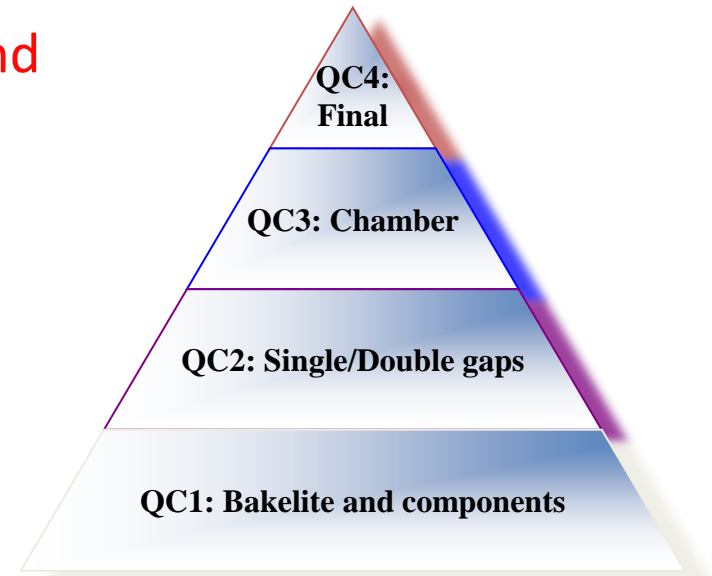
Chamber Assembly and tests

- Visual inspection, gas tightness, dark current test, connectivity test
- Performance study with cosmic muons

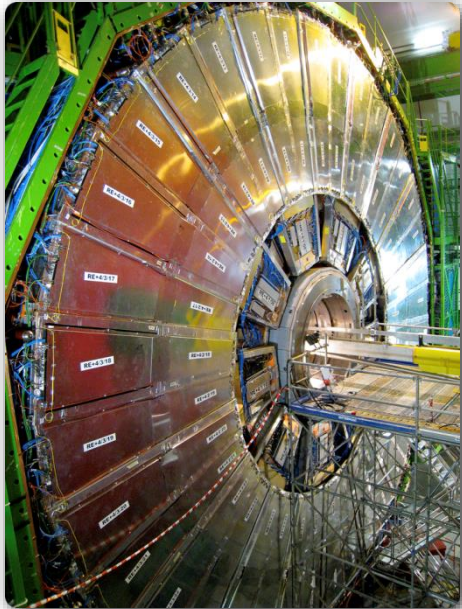
Gaps and Double production test

- Visual inspection, gas tightness and spacer test
- Electrical and dark current, resistivity measurement

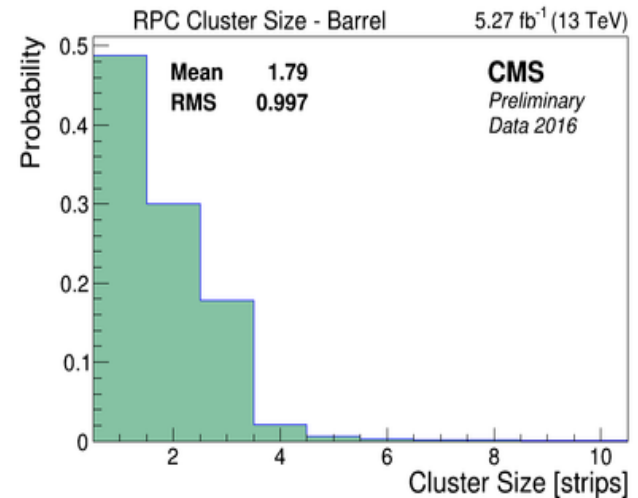
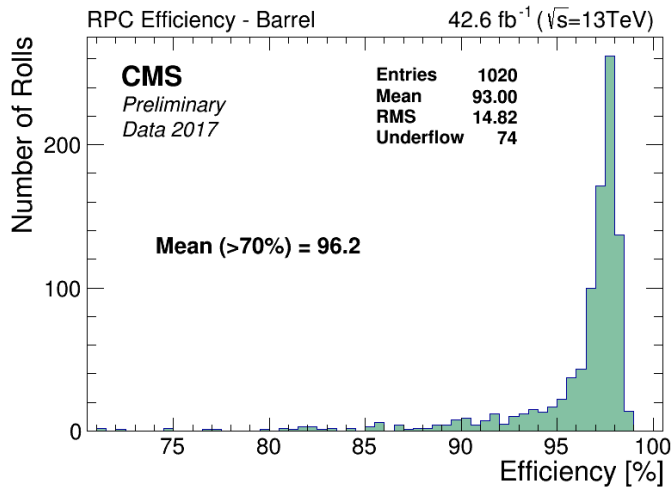
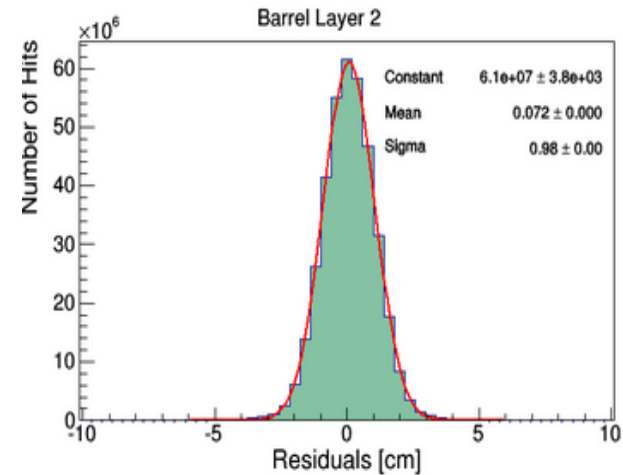
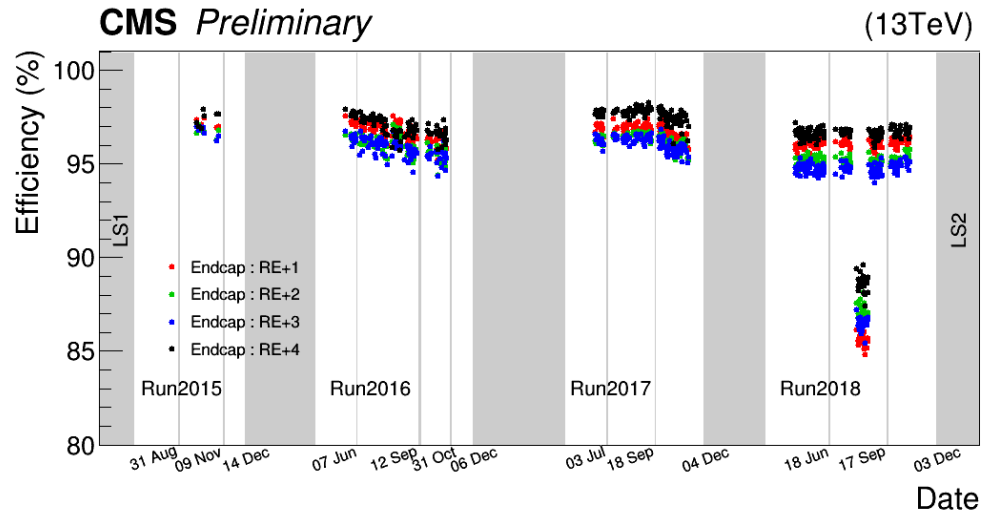
HPL production test: surface inspection, HPL resistivity
FEB test: PCB electrical integrity, FEB calibration, FEB +PCB calibration



From production to installation and commissioning



CMS RPC system performance @ LHC



Although the complexity of the systems, CMS chambers have excellent performance after “already” 10 year of RUNNING

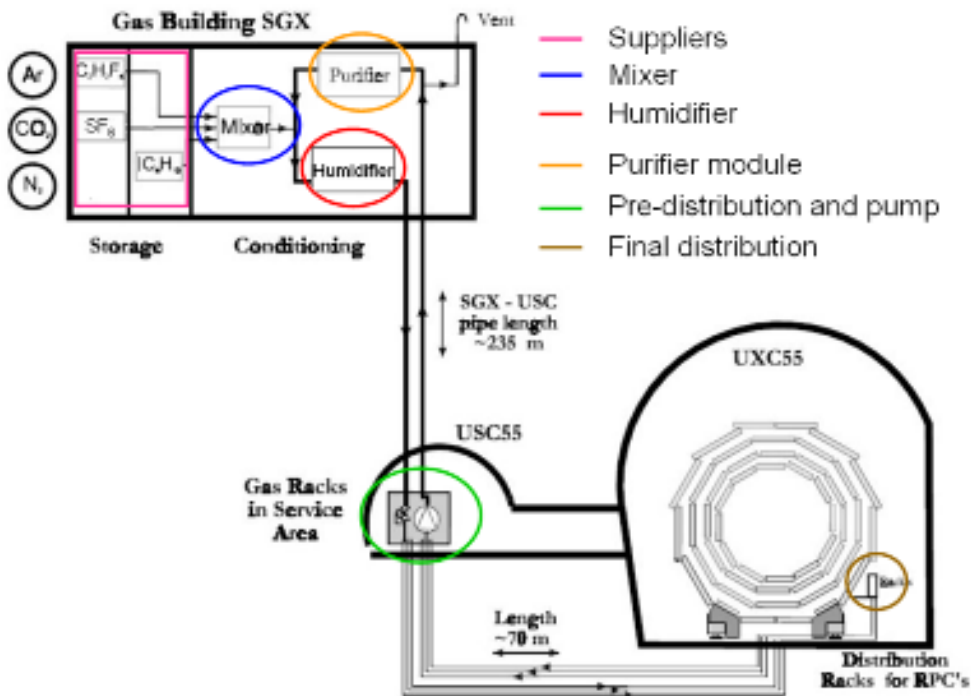
Closed loop gas system

CMS –RPC system has large detector volume (~13 m³ CMS).

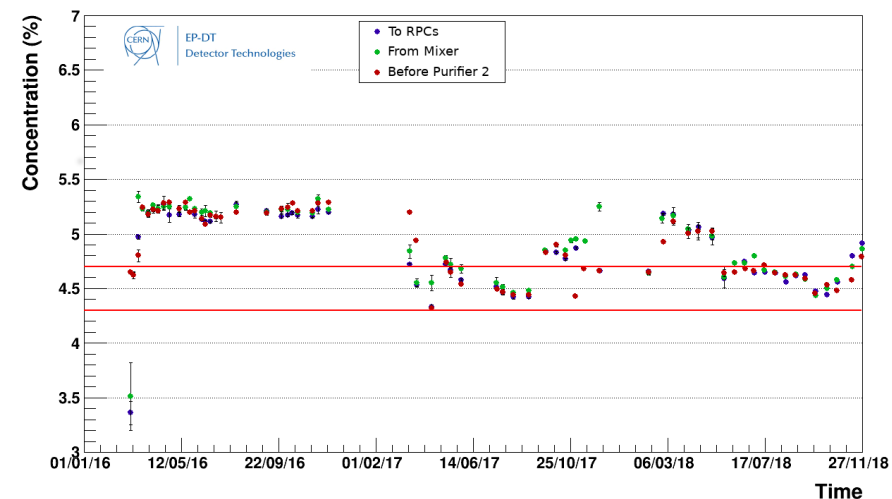
To maintain stable detector performance @ LHC conditions the gas flow should be around 1300 l/h corresponding to 1 exchange/hour

→ A closed-loop gas circulation system is unavoidable. Nowadays we are working with **10 % of fresh gas replenishing** rate

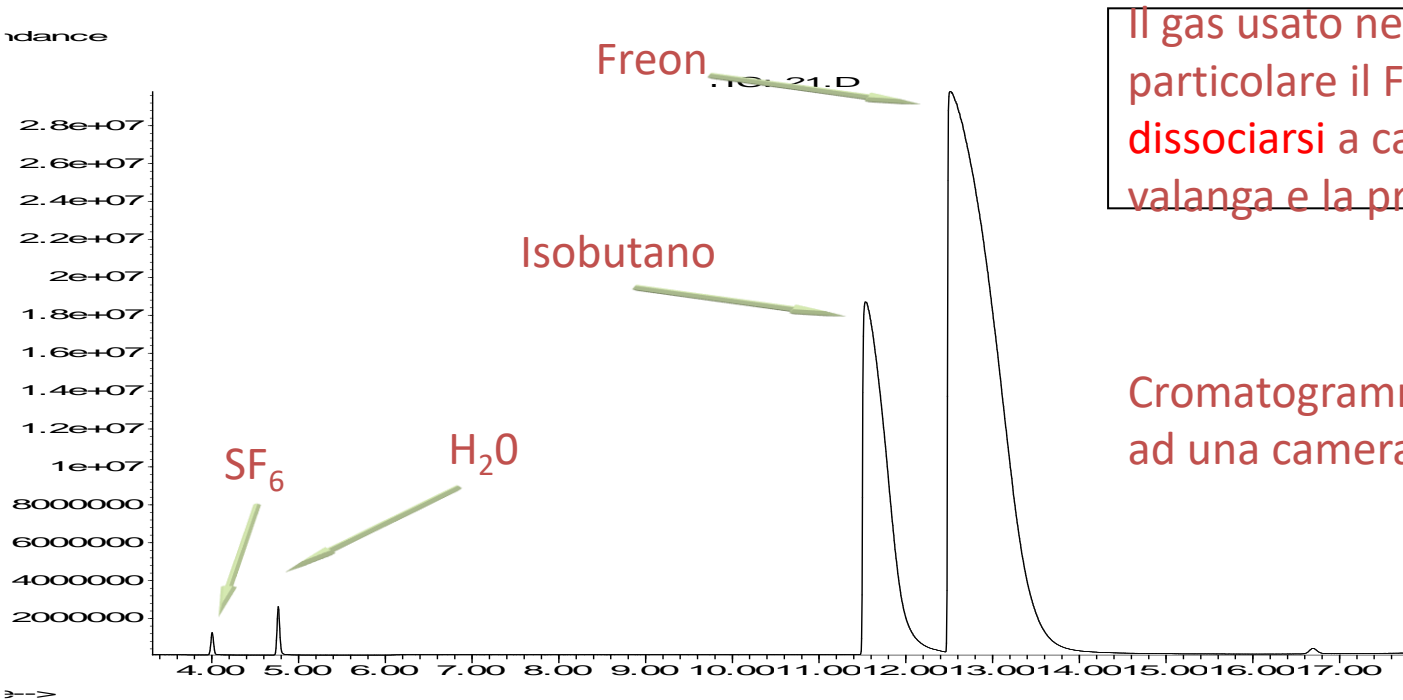
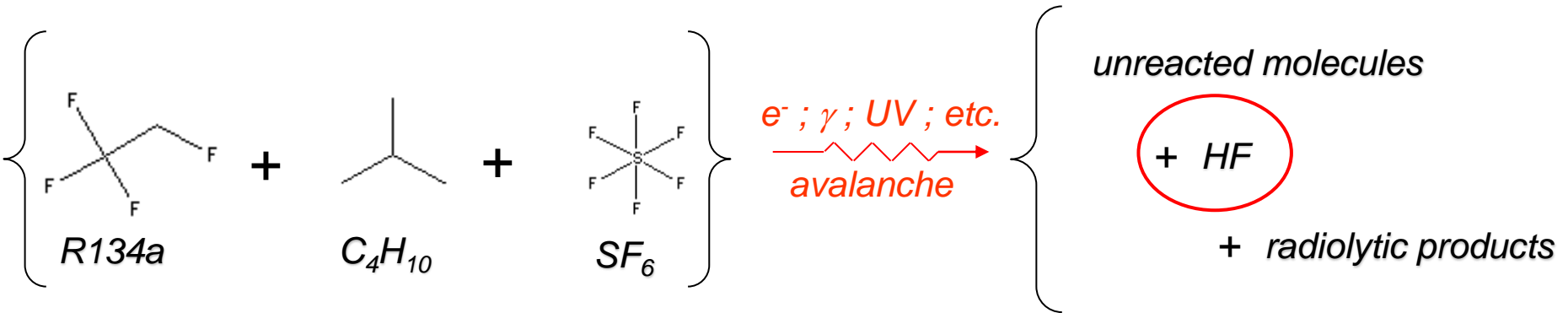
→ it is crucial to monitor the gas quality (chromatography)



RPC iC4H10



Gas issues



Il gas usato negli RPC (ed in particolare il Freon) può in parte dissociarsi a causa dei processi di valanga e la produzione di UV

Cromatogramma del gas in ingresso ad una camera

Gas issues

Chromatograph of the gas in output from one chamber

Perfluoro and hydrofluoro compounds

Saturated CHF_3 , C_2HF_5 , ...

Unsaturated C_2F_4 , $\text{C}_2\text{H}_2\text{F}_2$, ...

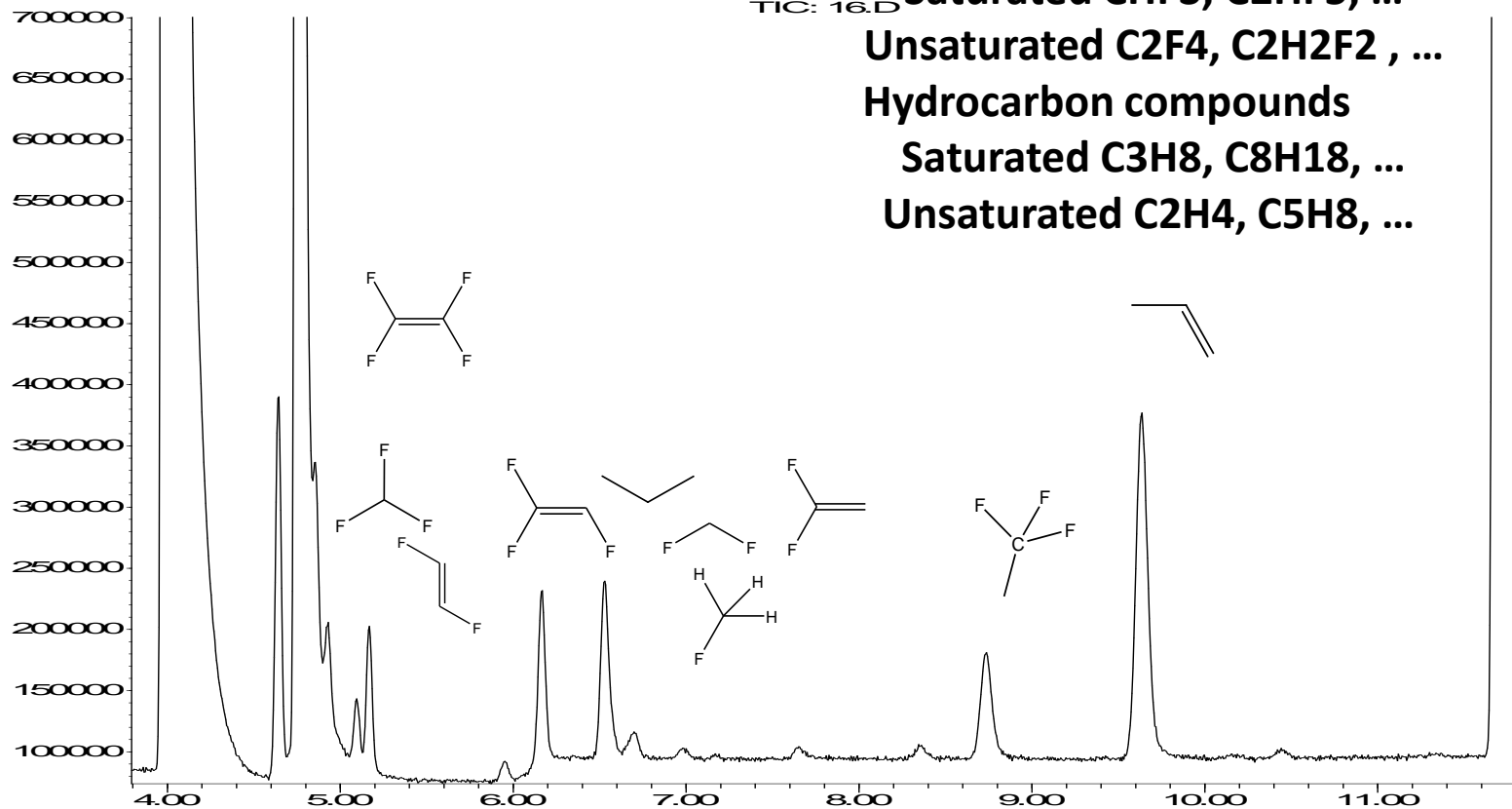
Hydrocarbon compounds

Saturated C_3H_8 , C_8H_{18} , ...

Unsaturated C_2H_4 , C_5H_8 , ...

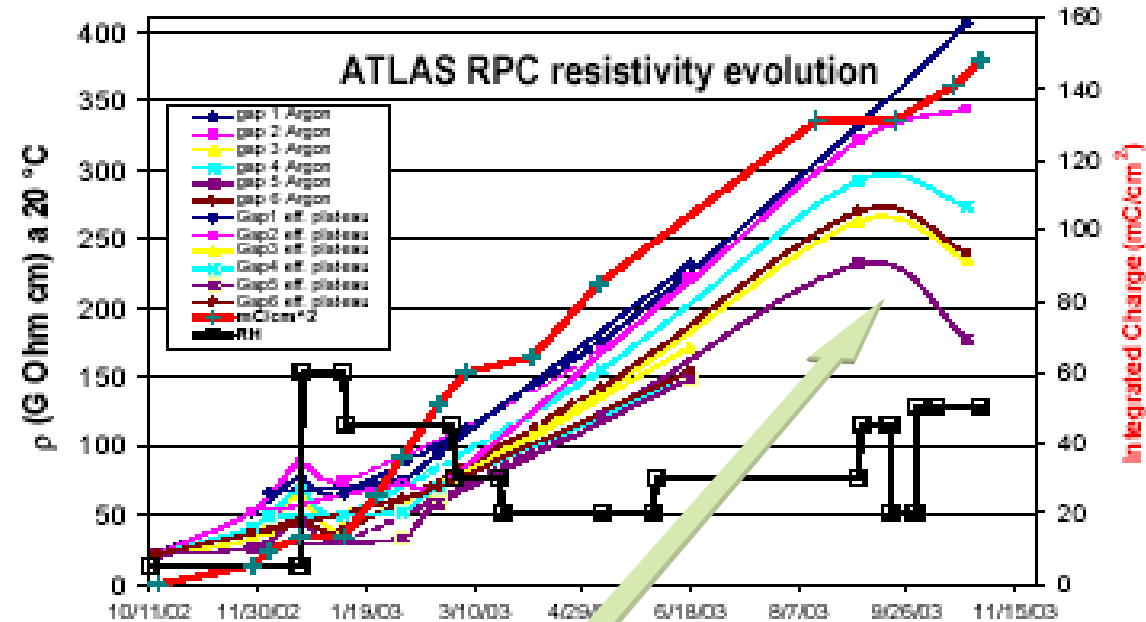
Abundance

TIC: 16.D



Time-->

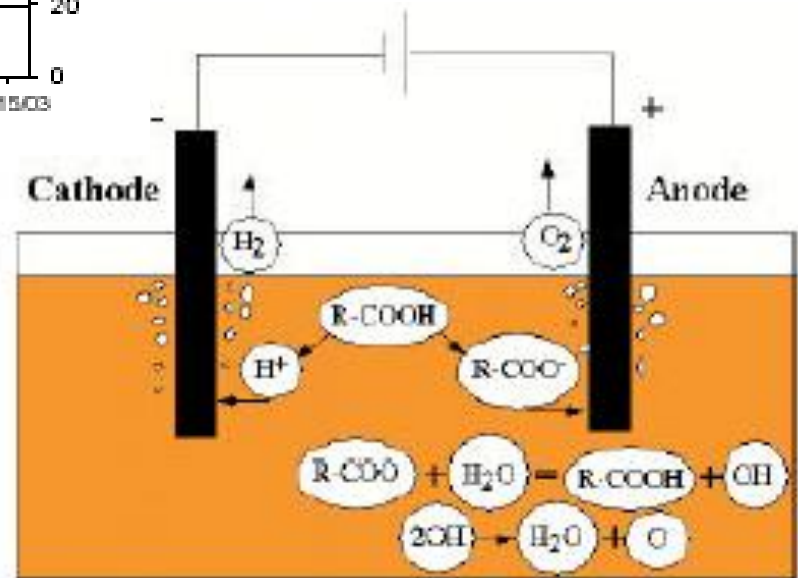
Water vapour issue



Bakelite resistivity has been experimentally found to depend on the amount of water vapour added to the mixture.

Time where the gas mixture was added with water vapour

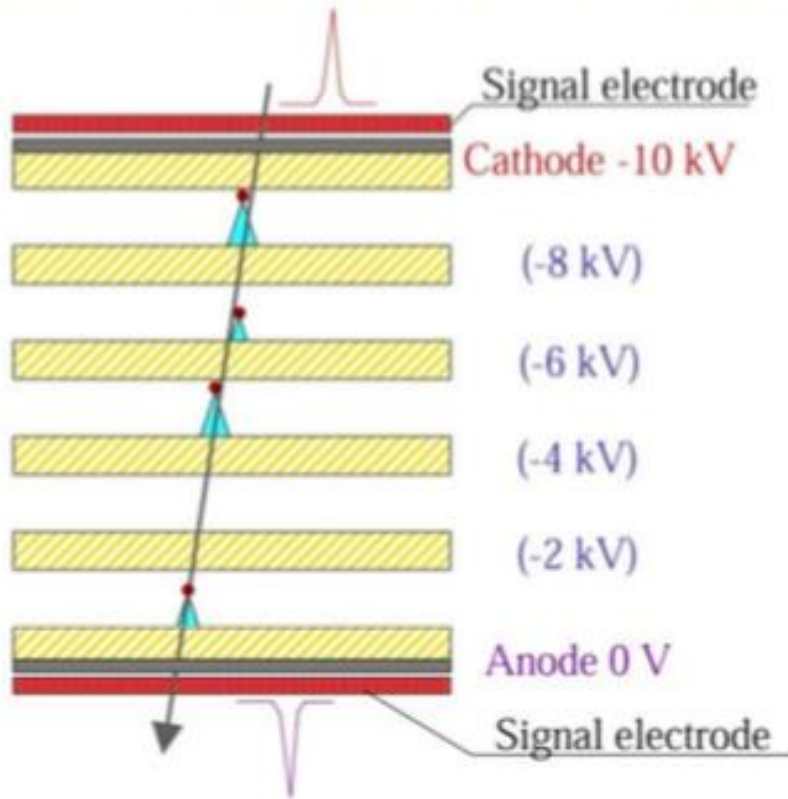
Conduction mechanism in bakelite is ionic, and therefore needs water to be sustained (J. Vavra)



Multi-gap RPCs

Multi-gap RPCs: developed by C. Williams for the ALICE experiment

MULTIGAP RESISTIVE PLATE CHAMBER

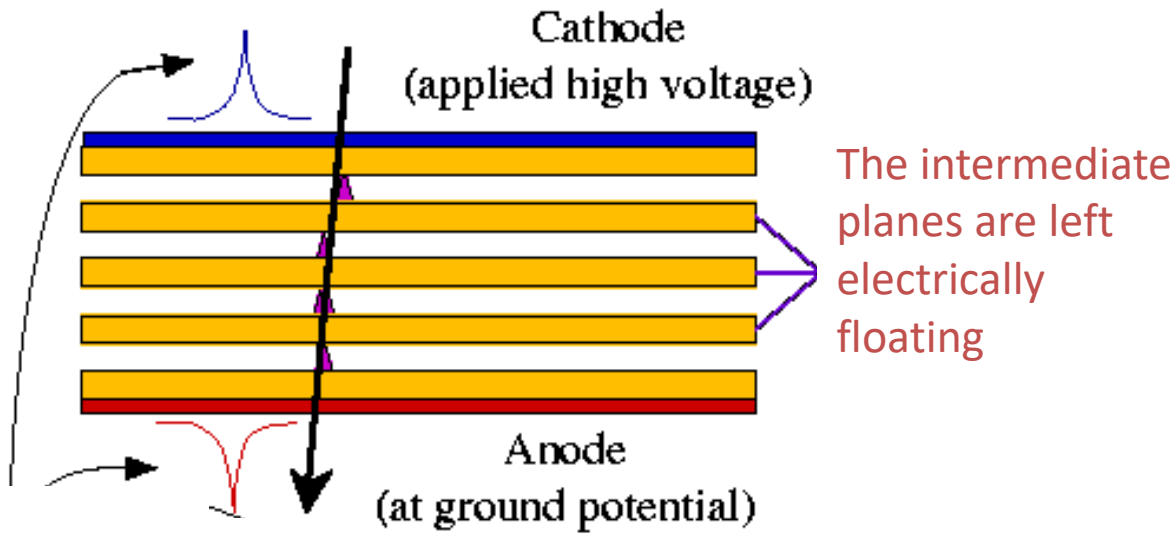


The **key point** to improve the timing is to use very thin gas gaps, in a multi-gap structure, to compensate the reduced primary ionization in the gas (high inefficiency).

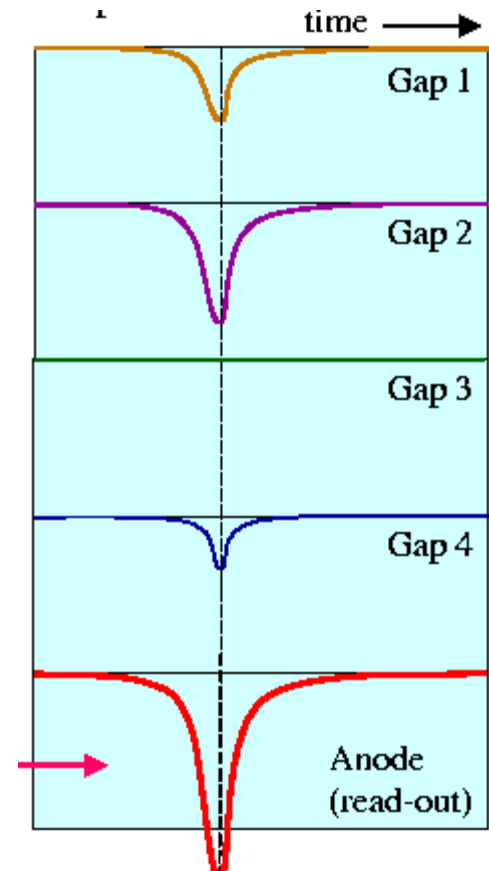
Design: the multi-gap is characterized by a number of floating (glass) electrodes whose potentials scales in such a way to equalize the field in all gaps.

Compared with the single gap design the average charge induced on the pickup electrodes does not change but gives a narrower charge distribution

Multi-gap RPCs



The intermediate planes are transparent to the induced signals



Avalanches in the various gaps take place (approximately) at the same time

The total signal is the analog sum of the signal from the various gaps

Possible configurations

'Planar' chamber of 8 x 8 cells

6 gaps of 220 μm melamine MRPC

MELAMINE

Cathode read-out pads

350 μm thick Mylar

Cathode pads at high voltage

1 mm thick Melamine-phenolic laminate

Anode read-out pads

6 gaps of 220 μm glass MRPC

GLASS

Cathode read-out pads

350 μm thick Mylar

Graphite layer to apply -ve high voltage

1 mm thick A14 glass fine ground finish

Anode read-out pads

Built with glass, bakelite, ceramics.

Single cell - 5 gaps of 220 μm

Schott A14
0.5 mm

GLASS
5 gap MRPC
5 gaps of 220 μm

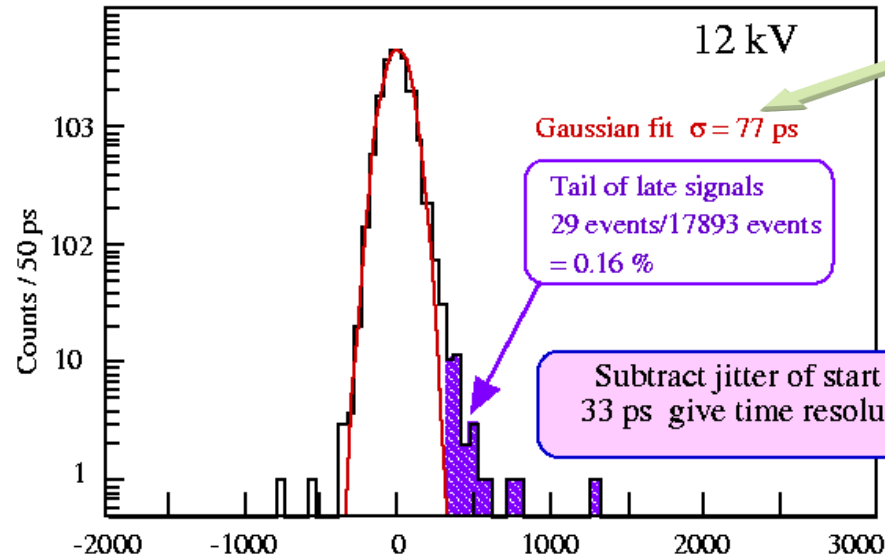
H.V.

Schott A2
0.5 mm thick

Schott 8540
2 mm thick

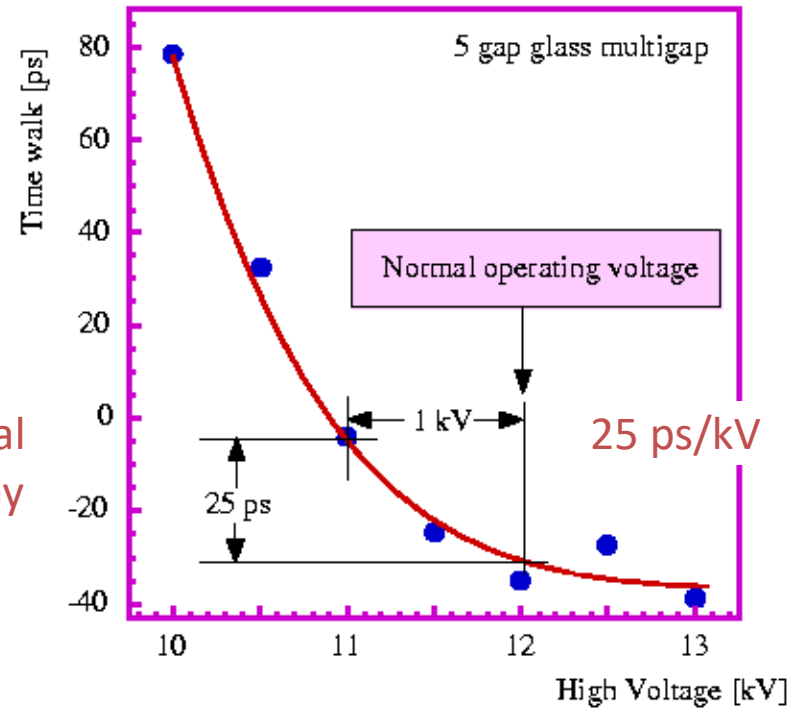
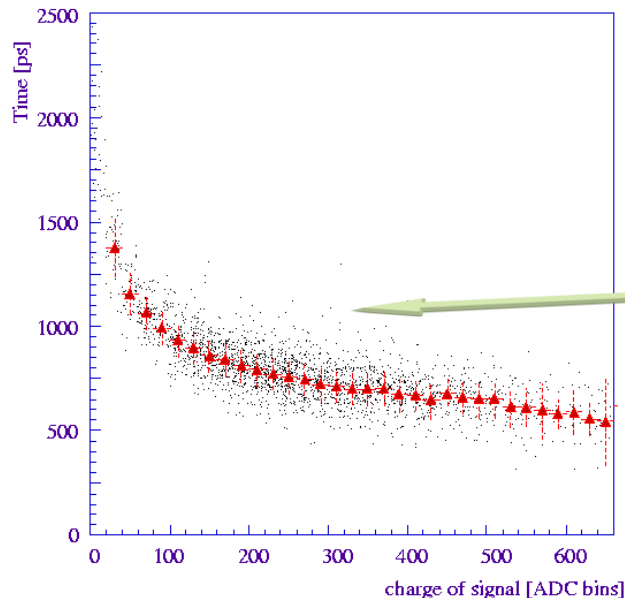
Read out

MRPC time resolution

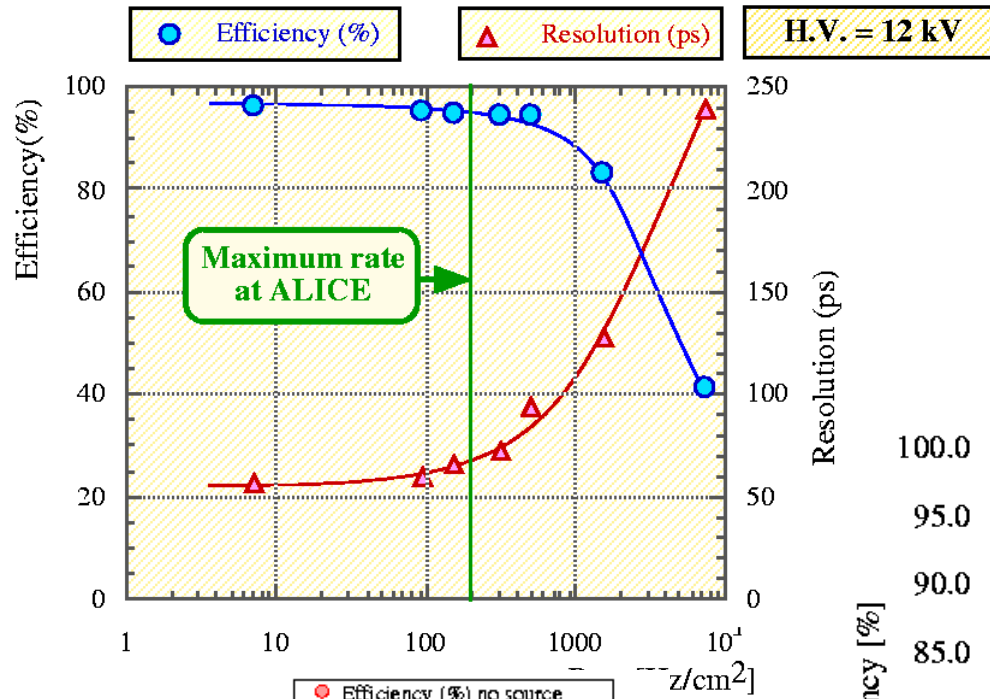


5 gaps, each 220 μm thick

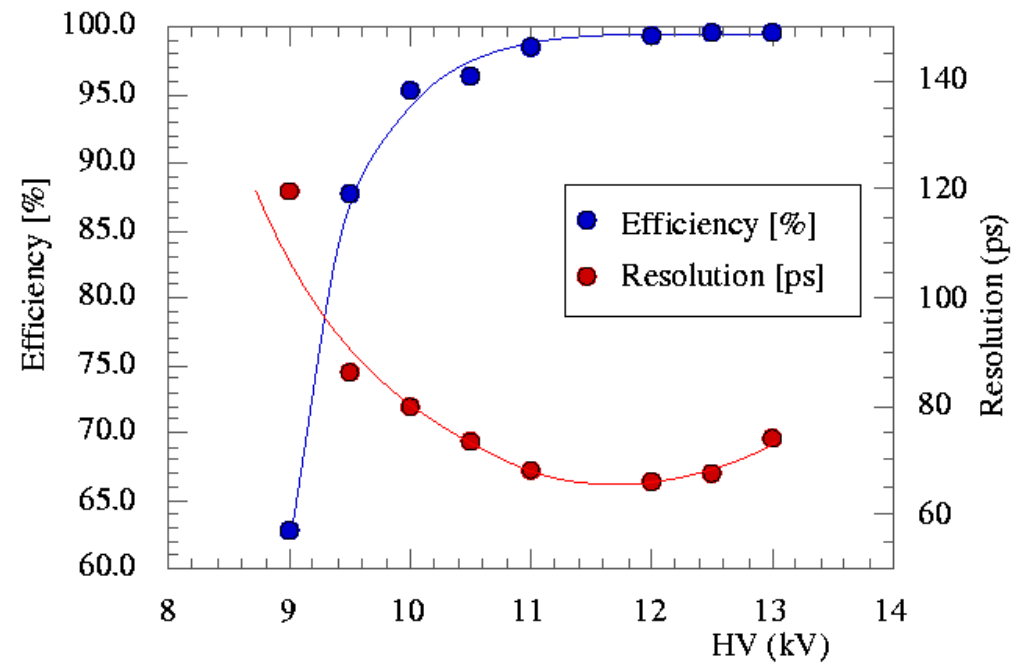
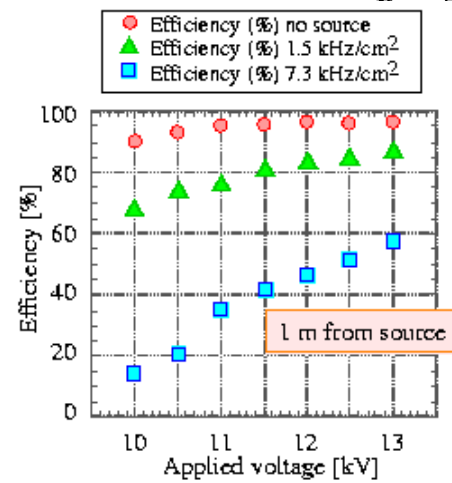
Detector time resolution ≈ 50 ps



Rate capability

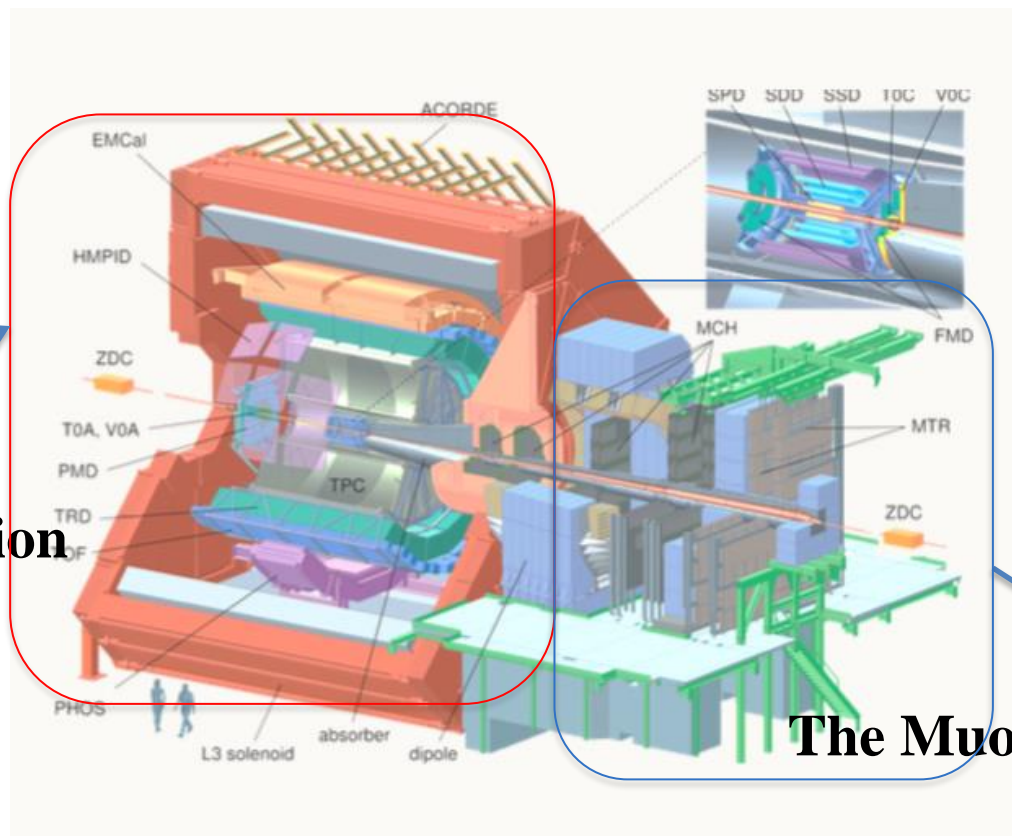


Efficiency measured in conditions of increasing background.



ALICE

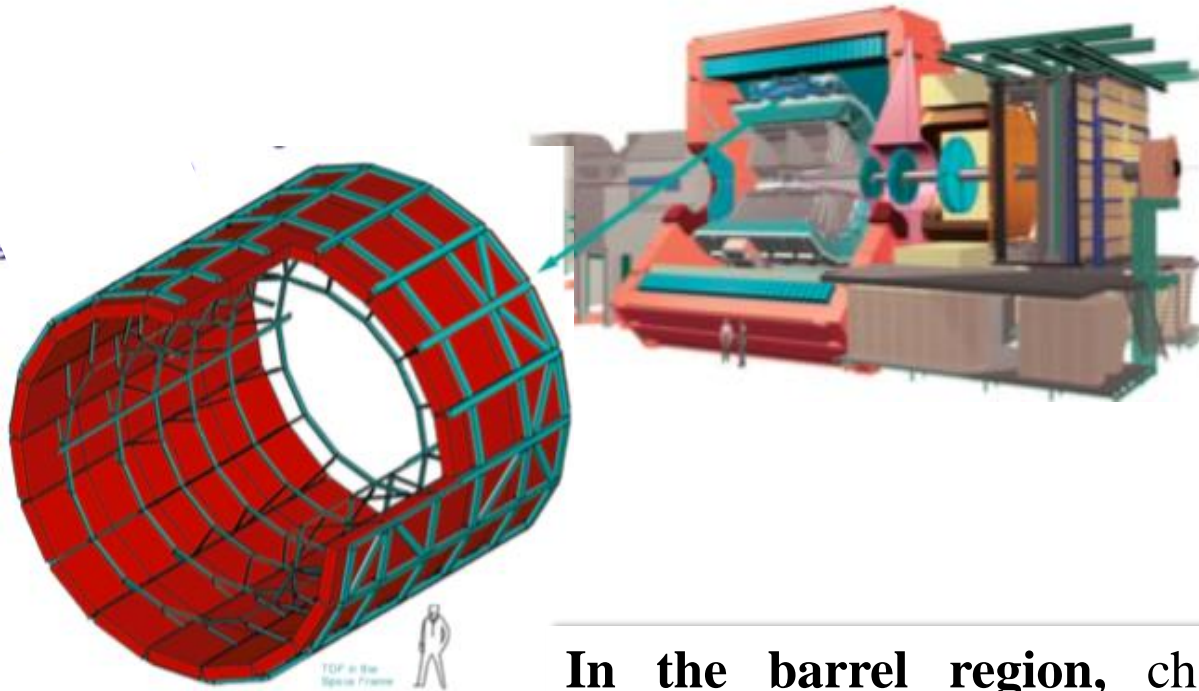
ALICE (A Large Ion Collider Experiment) is specialized in the detection of signatures of the Quark-Gluon Plasma state @ Heavy-ion collisions at ultra-relativistic energies (5.5 GeV). It is composed by two groups of detectors:



The Barrel region

The Muon Spectrometer

The Barrel region: ALICE TOF



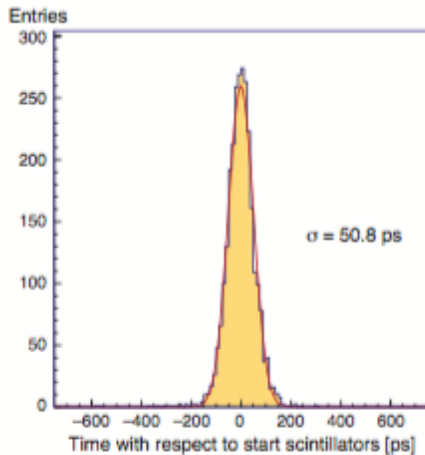
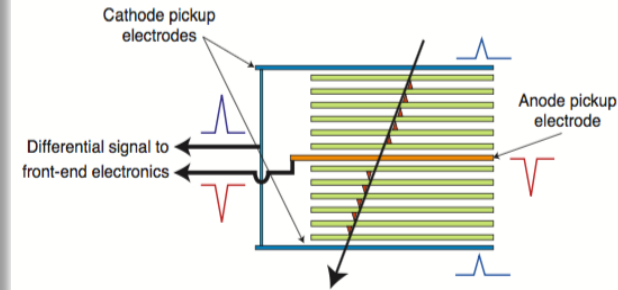
In the barrel region, charged particles in the intermediate momentum range (from 1 GeV/c to a few GeV/c) are identified by the **Time Of Flight (TOF) detector**.

The TOF is a large area detector covering a cylindrical surface of 141 m² with an inner radius of 3.7 m, a pseudo-rapidity interval [-0.9,+0.9] and full azimuthal coverage.

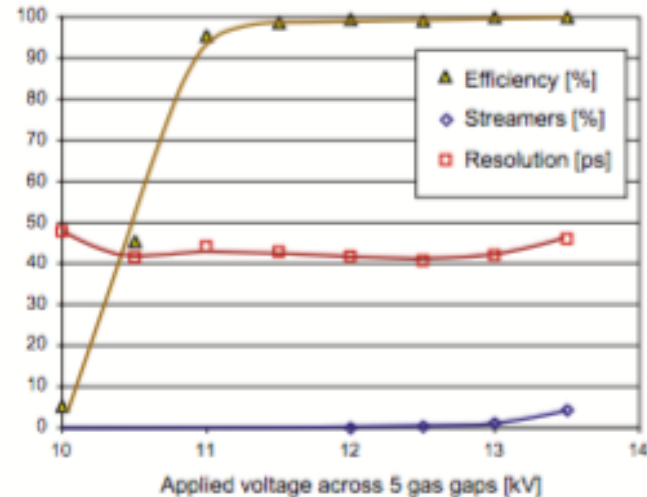
MRPC for the ALICE TOF

The TOF system is made of 1593 Multigap Resistive Plate Chamber (MRPC)

- Each MRPC consists of 2 stacks of glass, each with 5 gas gaps of 250 μm ; with an active area of $7.4 \times 120 \text{ cm}^2$
- Electrodes: high resistivity ($\approx 10^{13} \Omega\text{cm}$) float glass, 0.4 mm thick
- 96 readout pads of $2.5 \times 3.5 \text{ cm}^2$



Performance results



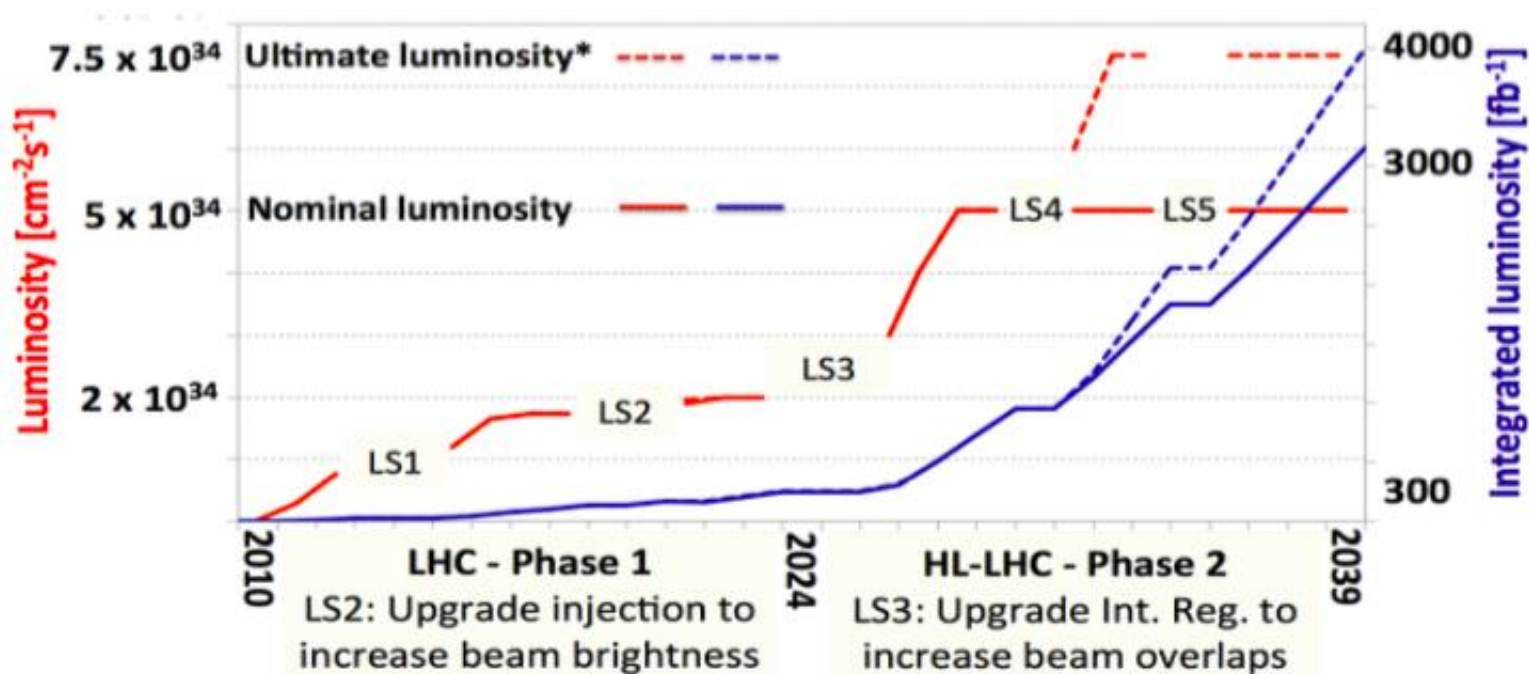
The time resolution of the TOF MRPC is in the 50 ps range. A typical efficiency and time resolution plateau as a function of the high voltage is more than 2 kV long before the onset of streamers, with efficiency reaching 99.9 %.

3th generation of RPC

New challenge: the HL-LHC



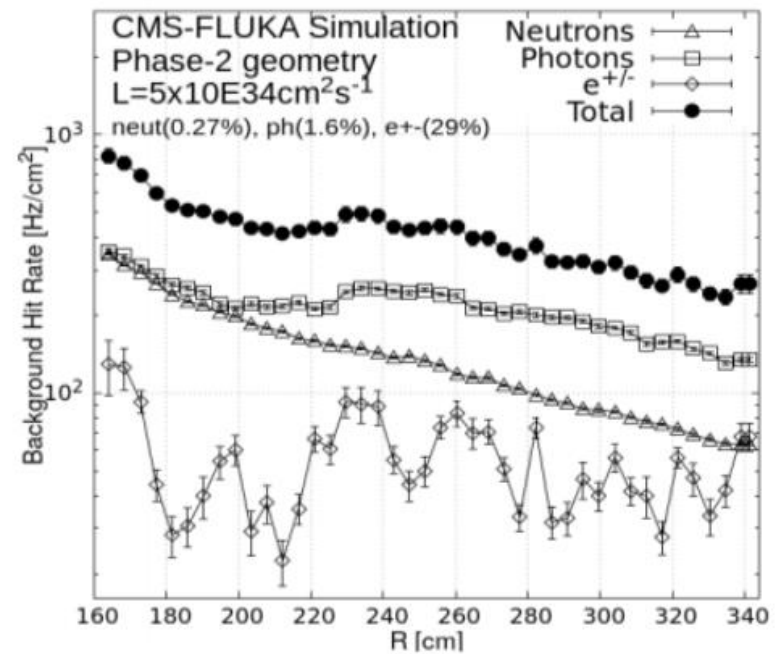
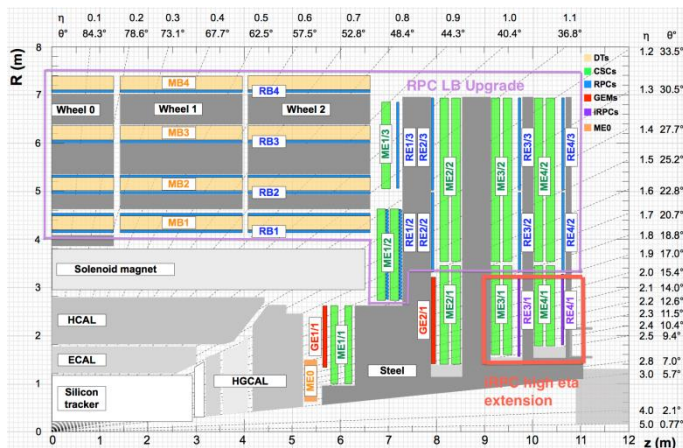
*“Europe’s top priority should be the **exploitation** of the **full potential** of the LHC, including the high luminosity upgrade of the machine and the detectors with a view to collecting 10 times more data than in the initial design, by around 2030”*



 **We are here**

The challenges for the RPC systems in the LHC experiments

- Confirm muon system performance at HL-LHC conditions: the RPC systems have to run at **5 times the expected LHC intensity** and for **30 years (instead of 10)**
- New RPC chambers needed to extend the CMS muon coverage up to $|\eta| < 2.8$ or to improve the trigger performance (ATLAS)
 - **Rate capability $\approx 1\text{-}2\text{ kHz/cm}^2$**



Further improve of the rate capability

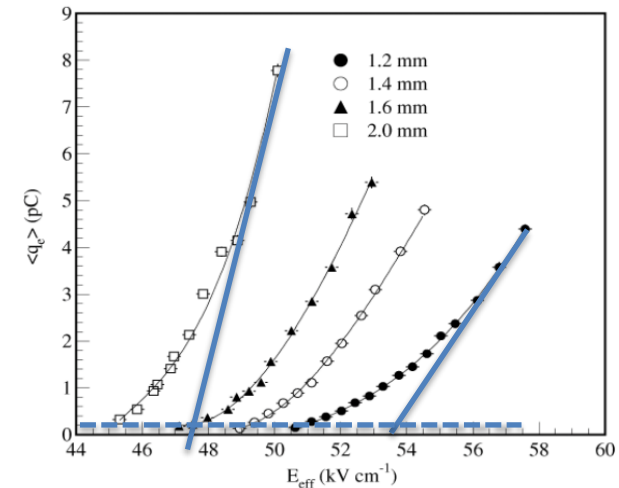
All relevant detector improvement factors have been investigated **to improve rate capability:**

- Reduced electrode resistivity
- **New detector geometry: gas gap and electrodes thickness**
- New Front-End electronics

The key points is to reduce:

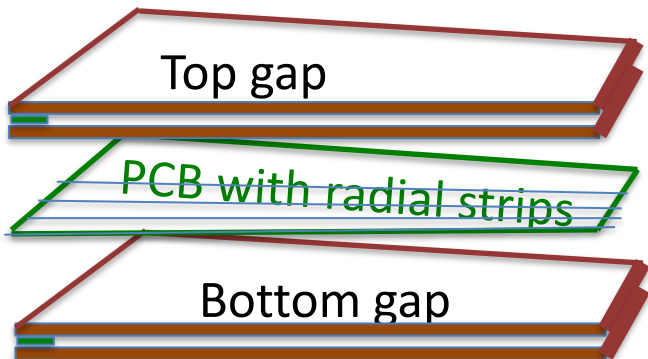
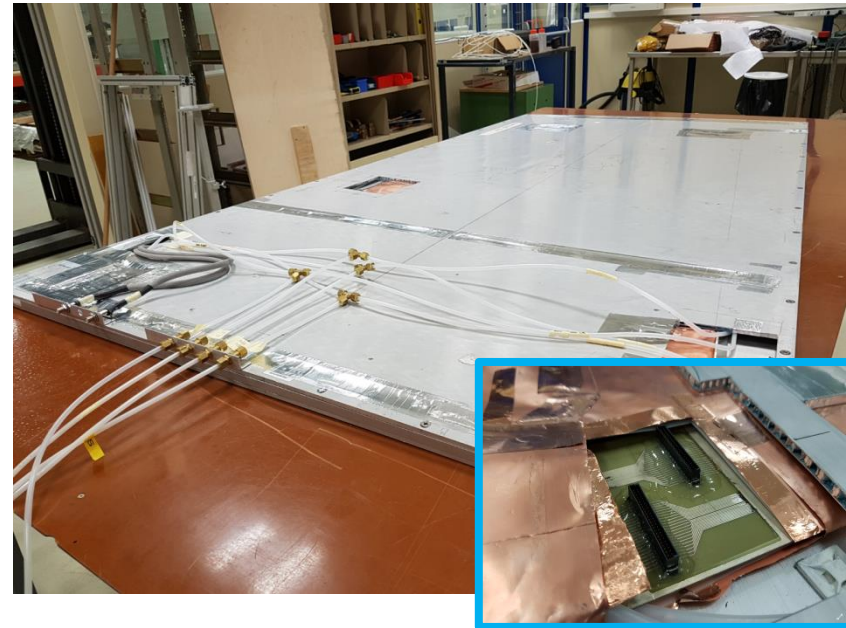
- the charge
 - thinner gas gaps: from 2 mm to 1 mm
 - lower electronics threshold
- Thinner electrodes: from 2 mm to 1mm

$$DV_{el} = r d F \langle Q \rangle$$



CMS improved RPC: new 2D design

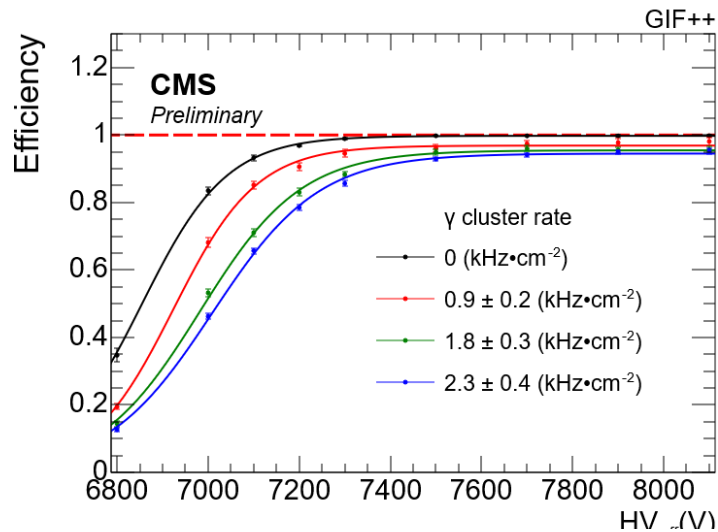
	iRPC	RPC
High Pressure Laminate thickness	1.4 mm	2 mm
Num. of Gas Gap	2	2
Gas Gap width	1.4 mm	2 mm
Resistivity (Ωcm)	$0.9 - 3 \times 10^{10}$	$1 - 6 \times 10^{10}$
Charge threshold	50 fC	150 fC
η segmentation	2D readout	3 η partitions



2D readout design:

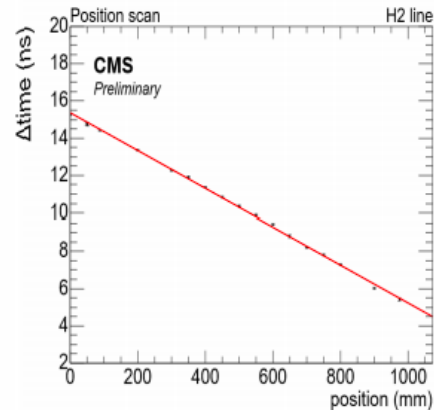
Readout Strips (with a pitch $\approx 0.6 \div 1.0$ cm) are readout from both-ends and connected to a new Front-End Boards equipped with a TDC

CMS improved RPC: new 2D design

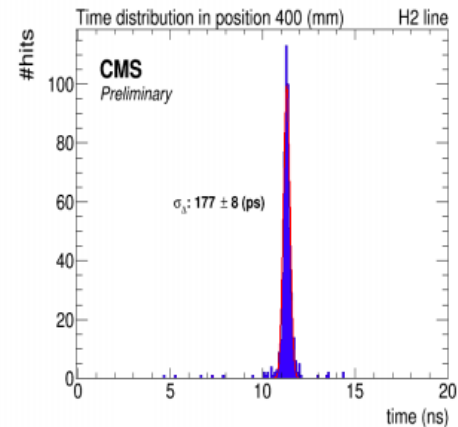


It has been proved:

- rate capability of 2 kH/cm 2
 - Spatial resolution along y coordinate 1.4cm
- Final validation of the new FEB ongoing..



**Uniformity in H2
using DESY table**



**Along-strip time resolution
and space resolution $\sigma_\eta \sim$
1.4 cm**

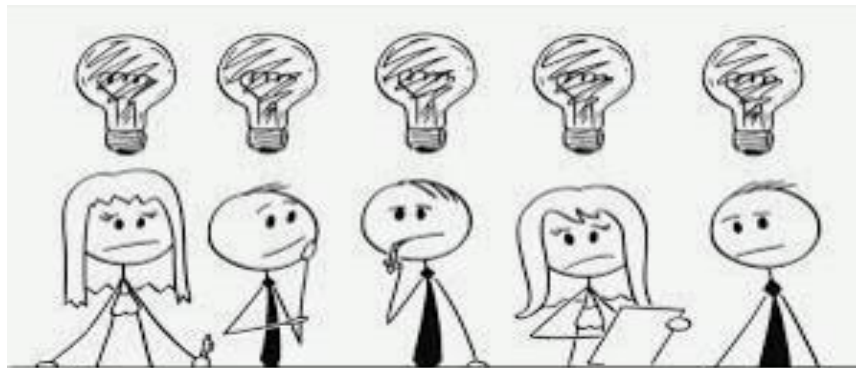
The eco-gas problem

We need to replace the R134a and SF₆ with more ecological gases, namely with a much lower GWP → limit the green house effect.

Difficult problem: gases are **the core of gas-filled detectors**

-It's like I would ask you to replace silicon in electronic devices (including smartphones, computers, TV sets, etc.) with another material, BUT:

- with the same performance
- at the same cost
- without changing anything of the rest of electronic circuits



A green choice

Note that EU is progressively banning greenhouse gases:

- but they are **still allowed** for research applications
- $C_2H_2F_4$ and SF_6 are **still allowed by law** to be used at CERN experiments
- nevertheless the green choice of the CERN community (and others) was to start asap research on ecofriendly gas mixtures

GREEN CHOICE

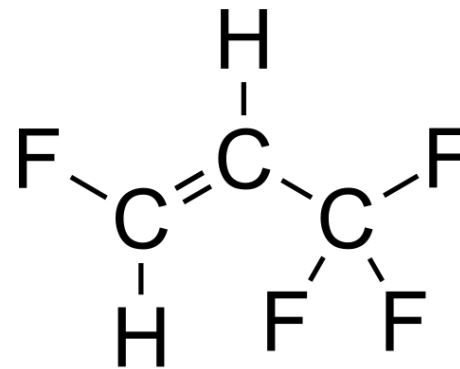
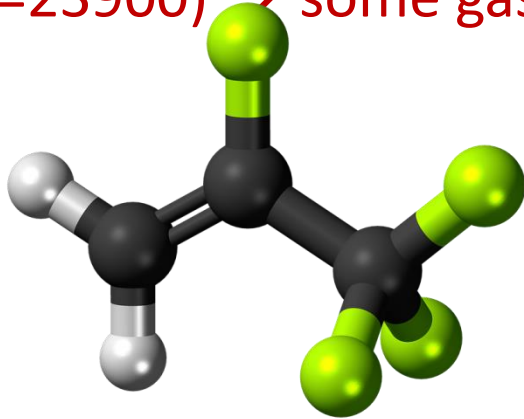


The smart (!?) idea

All high energy experiments (CMS, ATLAS, ALICE, LHCb, etc.) have started an **intense R&D program** to find suitable gas mixtures

-Practically **all research trendlines are concentrated** around the idea (by a smart guy) of replacing:

- $C_2H_2F_4$ (GWP=1430) \rightarrow $C_3H_4F_4ze$ (GWP=4)
- Adding some CO_2 to reduce the operating voltage
- SF_6 (GWP=23900) \rightarrow some gas still to be found



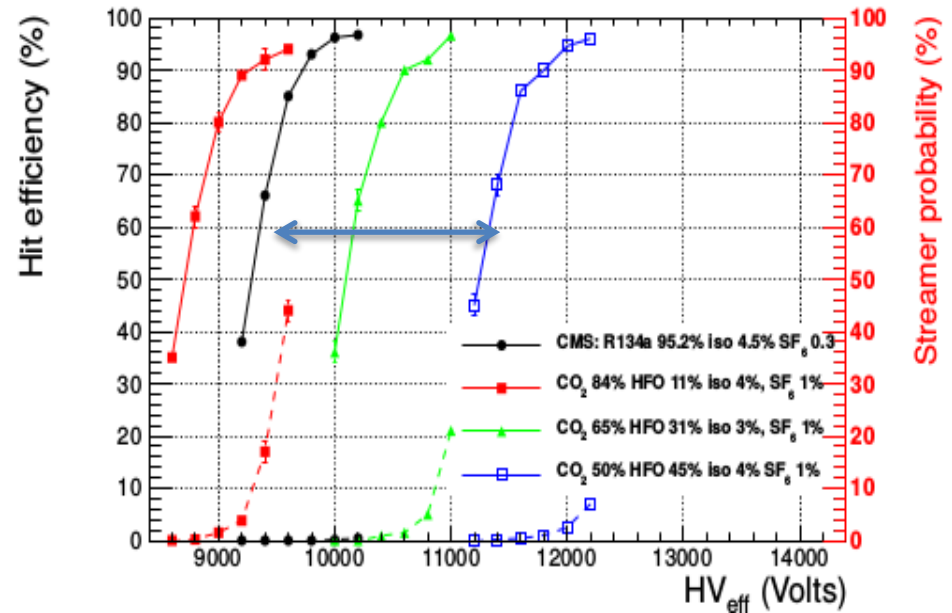
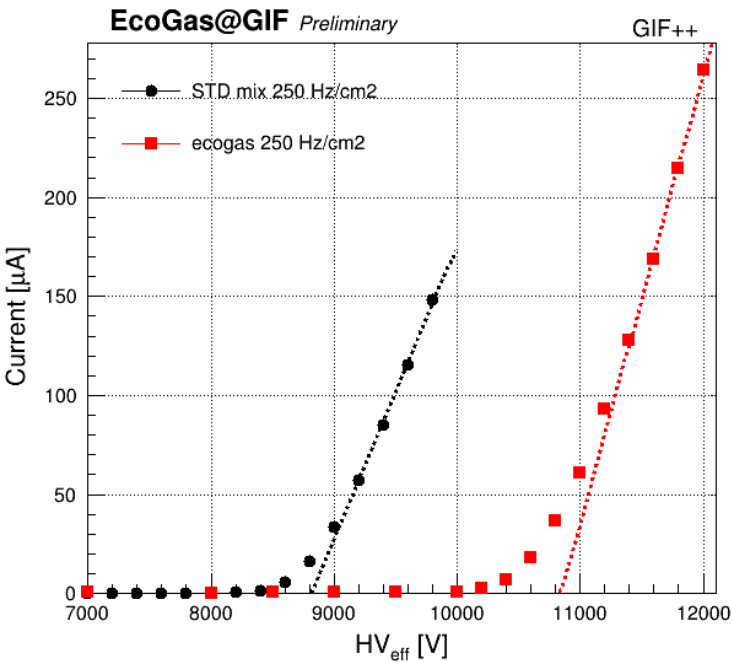
$C_3H_4F_4ze$ is the most similar molecule to $C_2H_2F_4$ but with a low GWP

Eco-gas mixtures

Validation of a **new ecological RPC gas mixture** started in GIF++ since April 2019.

- Five RPCs (2 CMS, 1 ATLAS, 1 ALICE, 1 EP-DT) are under test.
- One eco-gas mixture based on HFO 1234ze ($C_3H_2F_4$) (45%HFO, 50%CO₂, 1SF₆, 4%C₄H₁₀) under study

➤ **2 kV of HV shifts @ 250 Hz/cm² between the eco-gas was measured**



Detector performance stability ongoing ...

Conclusions

- Gaseous detectors were extremely successful in the past, and promise to be even more successful and wide spread in the future
- They are a fascinating topic to study, but, above all, there is so much work still to be done...



by YOU!

**We are thrilled to
have you on our team.**



WishesMsg.com



- prof. Marcello Abbrescia
- University of Bari, Italy
- Email: marcello.abbrescia@uniba.it,
marcello.abbrescia@ba.infn.it,
- Please do not hesitate to contact me for any information, request of additional material, or just a nice scientific discussion.



F. Sauli: **Principles of operation of multiwire proportional and drift chambers**, CERN Yellow Reports, CERN 77-09, 1977. - 92 p., 10.5170/CERN-1977-009

A. Peisert and F. Sauli: **Drift and diffusion of electrons in gases : a compilation (with an introduction to the use of computing programs)**, CERN Yellow Reports, CERN 84-08, 1984. - 127 p.

F. Sauli: **Gaseous Radiation Detectors: Fundamentals and Applications**, Cambridge University Press July 2014, ISBN: 9781107337701 , [hUps://doi.org/10.1017/CBO9781107337701](https://doi.org/10.1017/CBO9781107337701)

Glenn F. Knoll **Radiation Detection and Measurement, 4th Edition, Wiley ed.** ISBN: 978-0-470-13148-0, September 2010 864 Pages

W. Leo, **“Techniques for Nuclear and Particle Physics Experiments: A How-to Approach”**, Springer-Verlag, ISBN-13: 978-3540572800 , ISBN-10: 3540572805

Walter Blum, Werner Riegler, Luigi Rolandi, **Particle Detection with Drift Chambers**, Springer-Verlag 2008, ISBN: 978-3-540-76683-4











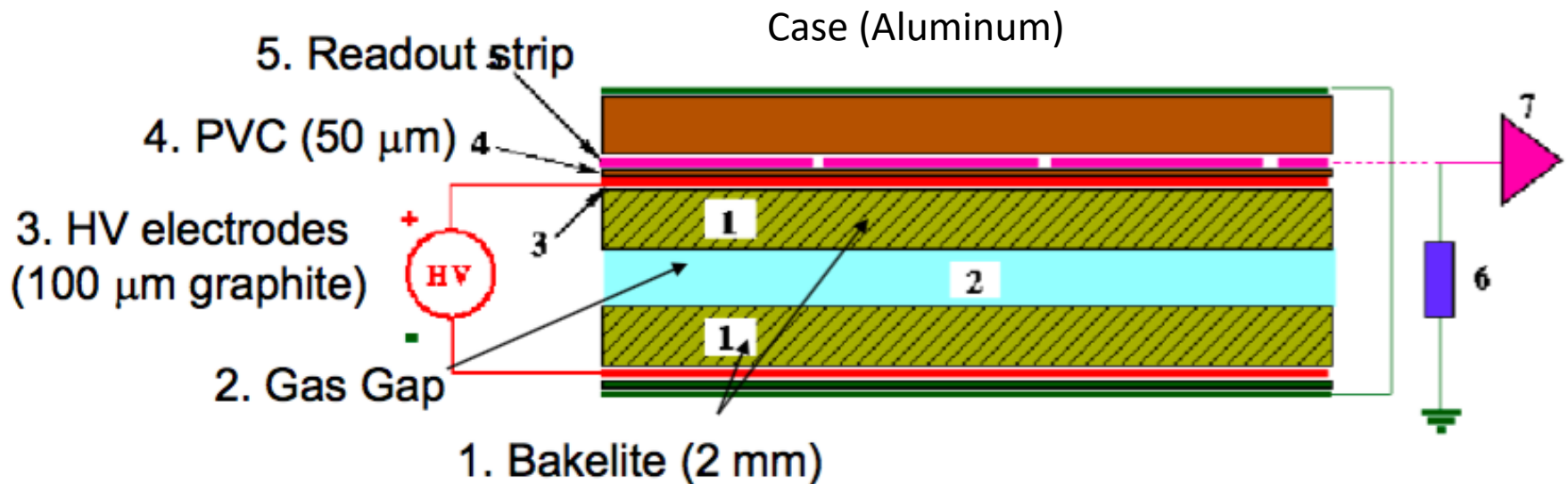
RPC basic elements (as in the 1st generation)

Gas mixture:

Argon, Iso-butane and Freon
at $P \approx 1 \text{ Atm}$

High Voltage contact: graphite coating on electrode outer surfaces

Pick up strips are used to collect the signal:
Al/Cu, $\sim \text{cm}$



Resistive Electrodes ($\rho \approx 10^{10} - 10^{12} \Omega \text{cm}$): **High Pressure Laminates (HPL)** "Bakelite" made by Kraft paper impregnated with melamine/phenol resins.
Internal electrode surface covered with a **thin linseed oil layer ($\sim \mu\text{m}$)**

Brief History of the Resistive Plate Chamber

- 1981: **1st generation** R. Santonico published the [paper "Development of Resistive Plate Counters"](#), Nucl. Instrum. Meth. N.187

Operated in **streamer mode** with an **Argon** based mixture
Performance: time resolution $\approx 1\text{ns}$ Efficiency $> 96\%$
Rate Capability $\approx 50\text{ Hz/cm}^2$

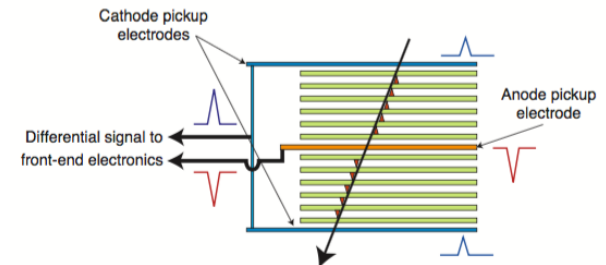
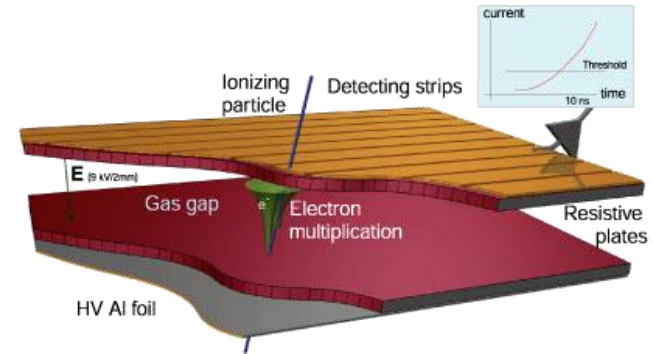
- 1992: **2nd generation** of RPC detector was developed for the LHC experiments (installed in ATLAS, CMS and ALICE).

Operated in **avalanche mode** with a **Freon** based mixture
Performance: time resolution $\approx 1\text{ ns}$ Efficiency $> 96\%$
Rate Capability $\approx 500\text{ Hz/cm}^2$

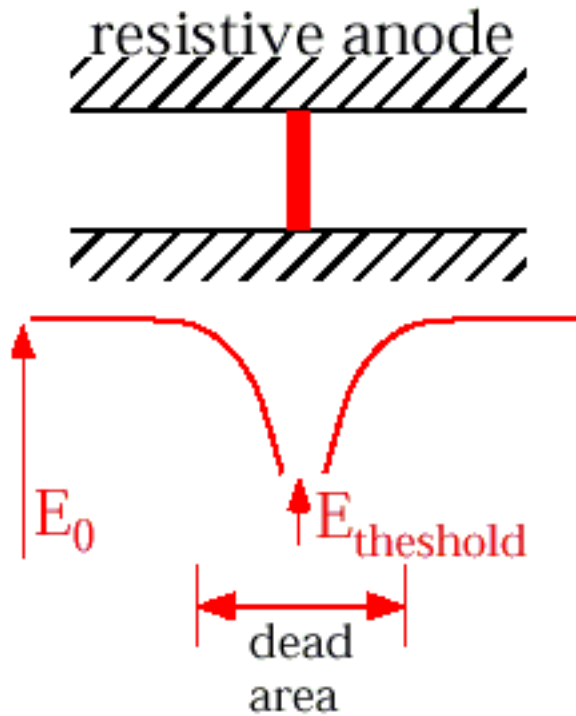
- 1995: **Multi-gap RPCs** developed by C. Williams (installed in ALICE and other experiments).

Operated in **avalanche mode** with a **Freon** based mixture
Performance: time resolution $\approx 60\text{ ps}$ Efficiency $> 96\%$

- 2015: **3rd generation of** RPC developed for HL-LHC



Resistive Plate Chamber



Discharging time linked to drift velocity and multiplication factor

Time constant for recharge related to the RC constant of the RPC elementary cell

$\eta = \alpha - \beta =$ effective Townsend coefficient

$$t_{dis} = \frac{1}{\eta v_d} \gg 10ns$$

$$t_{REC} = r e_0 \left(e_r + \frac{2d}{g} \right) \approx 10ms$$

$$\tau_{dis} \ll \tau_{rec}$$

Self-extinguishing mechanism

The arrival of the electrons on the anode reduces the local electric field and therefore the discharge will be extinguished.

During the discharge the electrodes behave like insulators.

Why Electrodes are “cured” with linseed oil ?

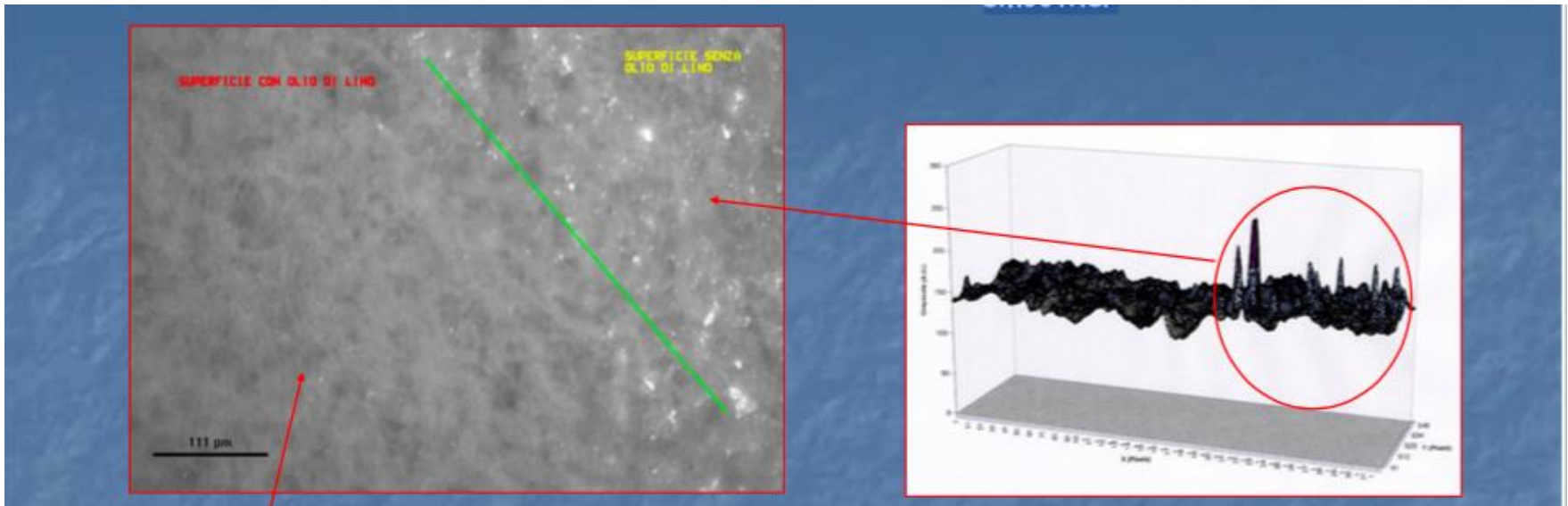
Linseed oil (If you look on Wikipedia..)

The Linseed oil is used as a painting medium. It was a significant advantage in the technology of oil painting!

Mixture of triglycerides, formed by one molecule of glycerol and three molecules of linear fatty acids. The oil is cured forming a hard stable film because of oxidation followed by polymerization.

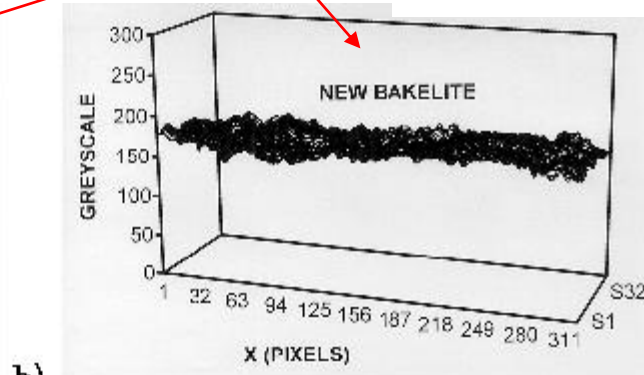
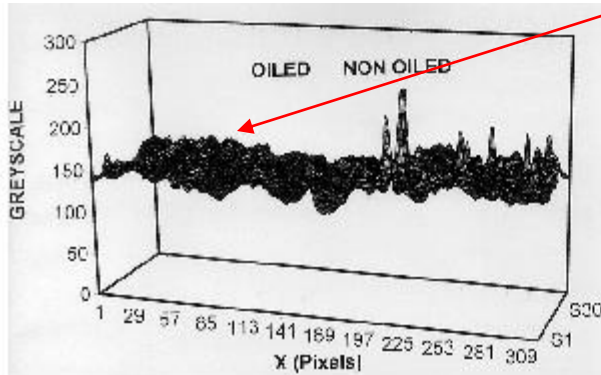
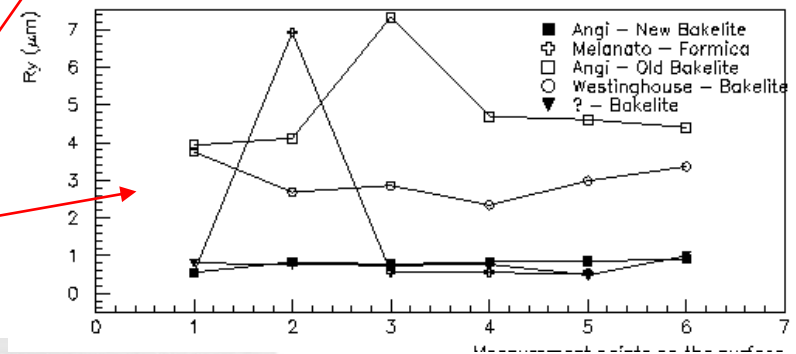
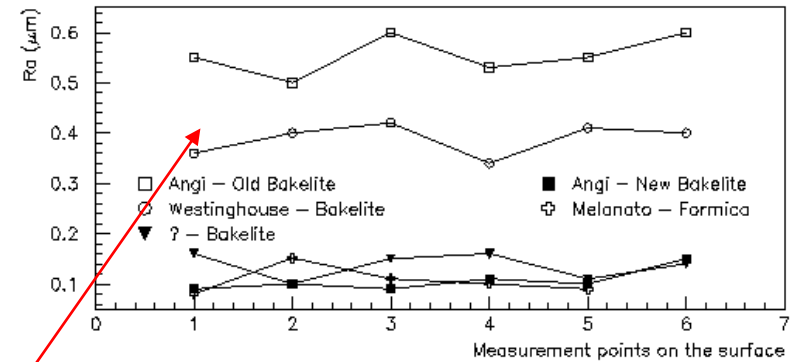
Linseed oil makes the surface smoother

The smoother the surface, the lower the intrinsic noise of the detector

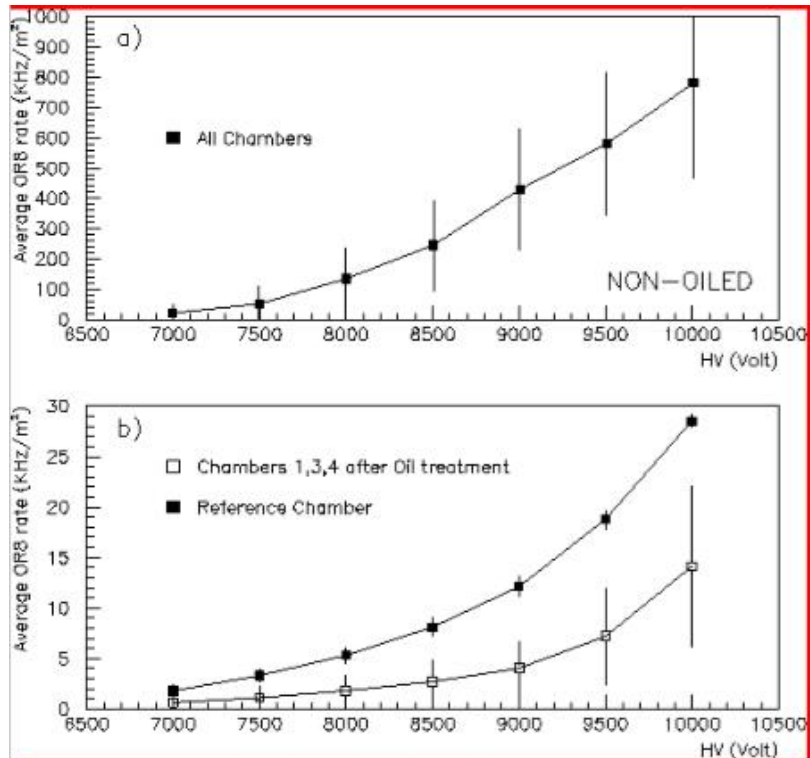


Comparison among not-oiled, oiled and smoother surfaces RPC

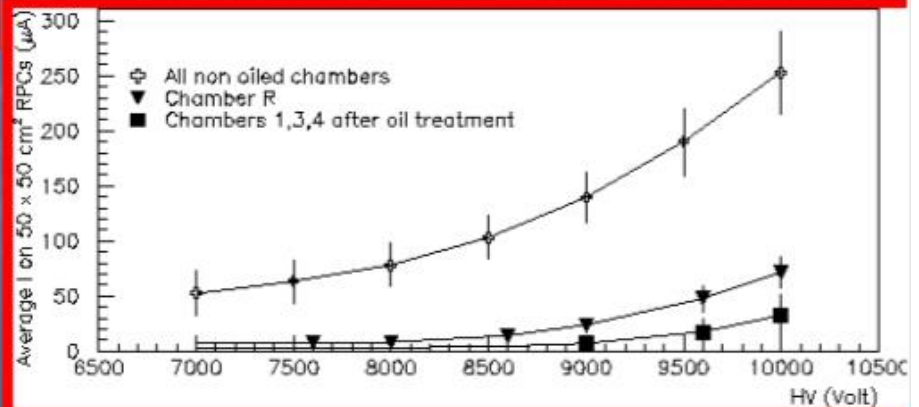
Direct measurements of surface roughness
 -mono-dimensional
 - bi-dimensional



RPC: the linseed Oil



Reduced Currents and Noise rate



Applications of the 1st RPC generation

The first generation of RPC detectors has been used in several HEP experiments:

'85: Nadir – 120 m² (Triga Mark II – Pavia)

'90: Fenice – 300 m² (Adone – Frascati)

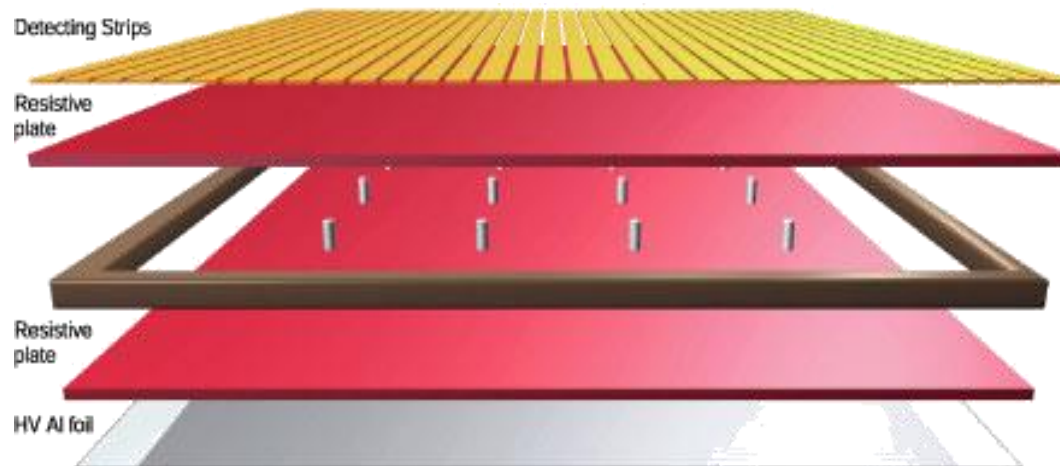
'90: WA92 – 72 m² (CERN SPS)

'90: E771 – 60 m²; E831 – 60 m² (Fermilab)

1994-1996: L3 – 300 m² (CERN-LEP)

1996-2002: BaBar – 2000 m² (SLAC)

**Very large area of
muon detection**



Experiments using RPCs

1st generation RPCs were immediately used in many physics experiments...

Veto

Nadir: 120 m² of double gap RPCs used as a veto on cosmic particles in an experiment on neutron-anti neutron oscillations

Fenice: 300 m² of RPC used as a cosmic vet in the reaction $J/\Psi \rightarrow n\text{-}n\text{ bar}$ at Adone

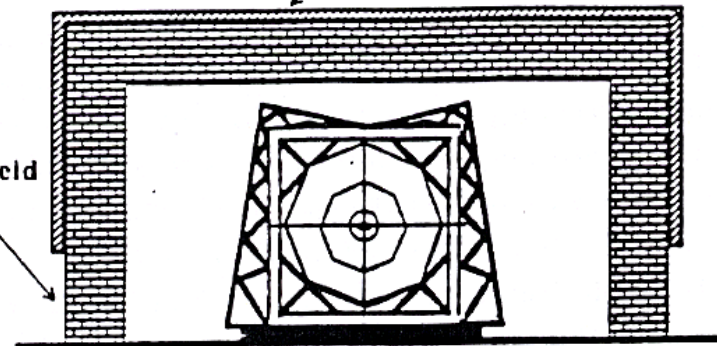
Operated in streamer mode
(Ar-isobutane-Freon)

HV 7-8 kV

Veto efficiency: 97-99%/plane

Concrete shield

Active veto system



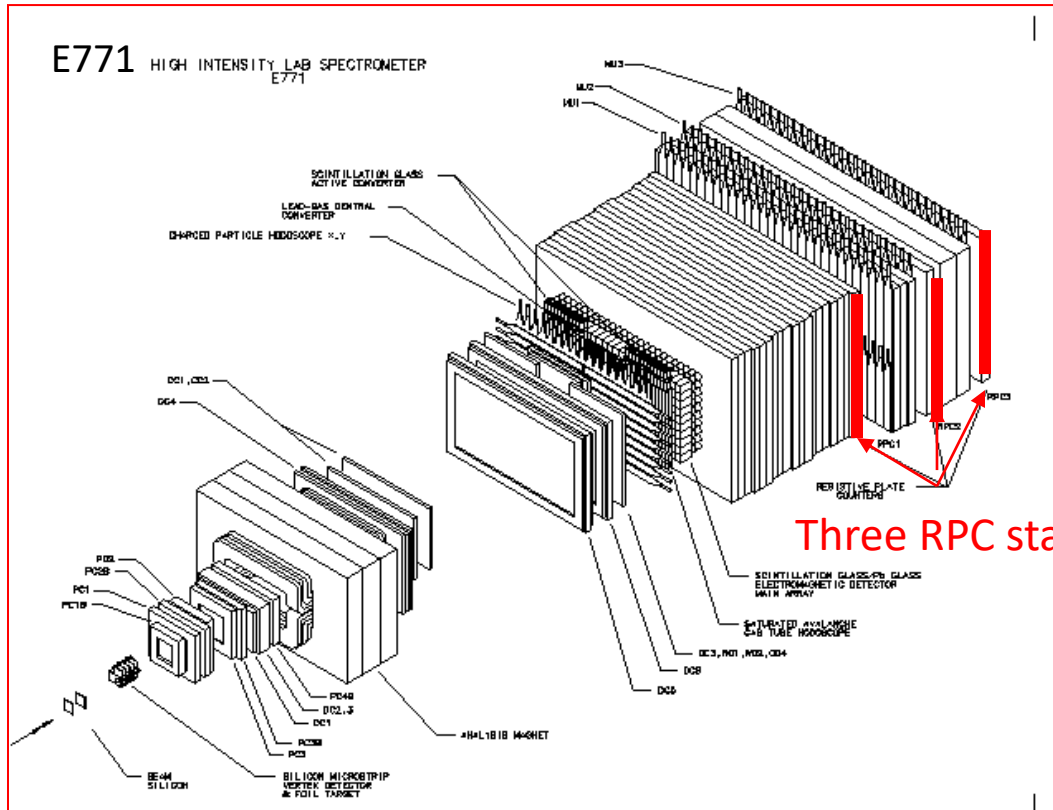
Trigger and tracking at accelerators

WA92: 72 m² of RPC used as trigger on μ events with high p_t in semi-leptonic decays of the B (SPS at CERN)

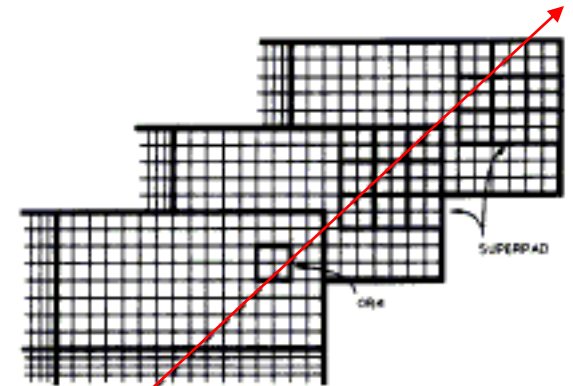
E771: 60 m² of RPC used as trigger and tracking come trigger on μ events with high p_t in semi-leptonic decays of the B (Fermilab)



The E-771 experiment



Three RPC stations



A triple coincidence to identify and track μ

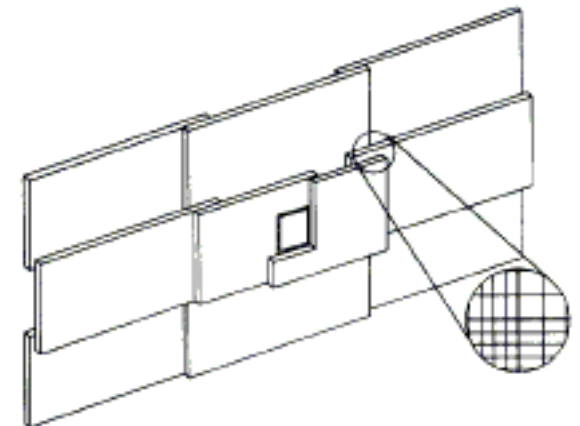
The RPC system did not cover the zone around the beam

Superimposed RPCs, with pad readout

Streamer mode (Ar-isobutane-Freon)

HV 8 kV

Maximum efficiency: 97%



ARGO-YBJ



Argo Panopte (who sees everything) is described as being very strong, since he had 100 eyes and was capable to sleep with only 50 of his eyes closed-

ARGO-YBJ (Astrophysical Radiation with Ground based Observatory at YangBaJing, Tibet) did never sleep.



Experiment to study with high efficiency and sensitivity Extensive Air Showers with energy $> 100 \text{ GeV}$

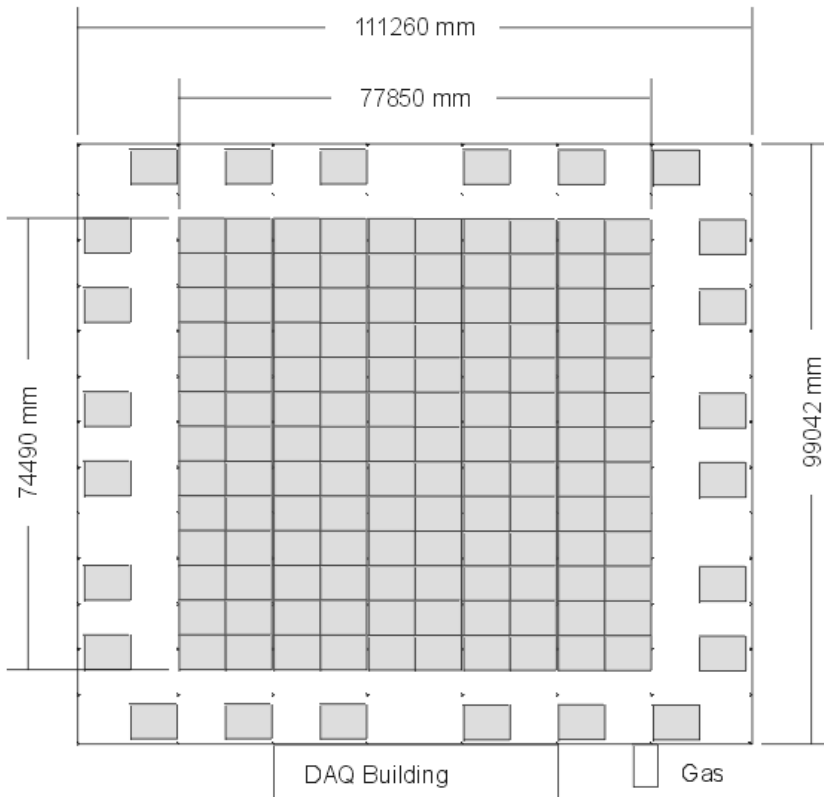


γ Astronomy $\sim 100 \text{ GeV}$
Diffuse γ rays
 γ -Burst
Ratio p/p bar
Spectrum of the primaries
Physics of Sun and atmosphere

ARGO-YBJ

Main Building with RPCs

ArgoN05



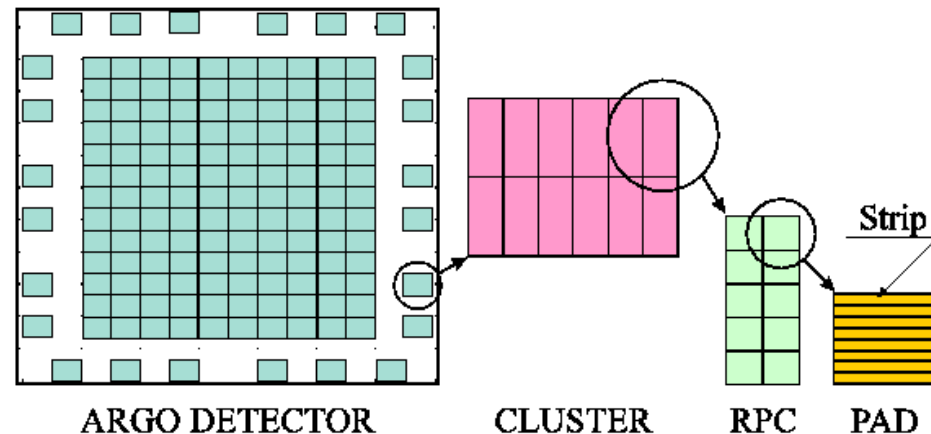
Detector carpet: 10 x 13 Clusters, 1560 RPC
 Sampling ring: 6 x 4 Clusters, 288 RPC
 Total: 154 Clusters, 1848 RPC
 For a complete coverage another 84 Clusters (1008 RPC) are needed



78 x 74 m² covered with RPCs

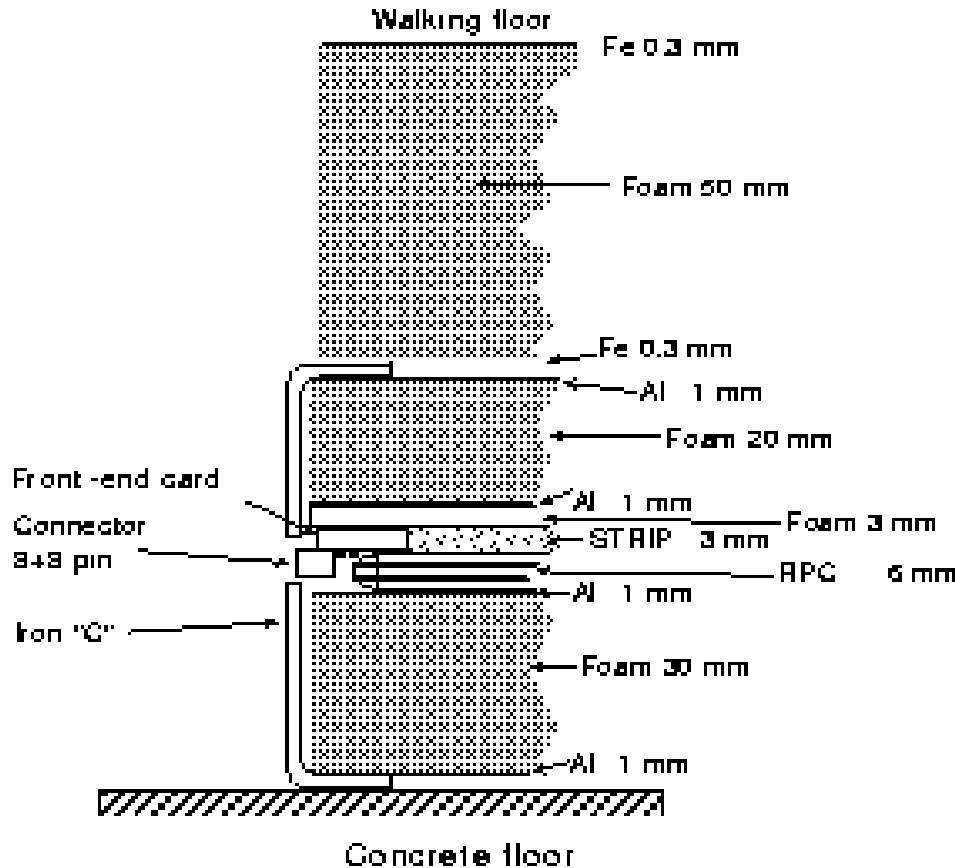
In addition a guard ring with partial cover up to 100 x 100 m²

“RPCs chosen because their low cost, large active area, excellent time and spatial resolution, easy of integration as a large system.”



ARGO-YBJ

ARGO detector cross section



Single gap RPCs

Volume resistivity $> 5 \cdot 10^{11} \Omega\text{cm}$

Area: $126 \times 285 \text{ cm}^2$

Aluminium strips $6 \times 56 \text{ cm}$

Fast-OR of 16 strips defining a PAD

10 pads ($56 \times 60 \text{ cm}^2$) covering a chamber (in total 18480 pads)

Streamer mode

Gas:

15% Argon,

10% Isobutane

75% Tetrafluoroethane $\text{C}_2\text{H}_2\text{F}_4$

Use of converters to increase the number of hits/event.

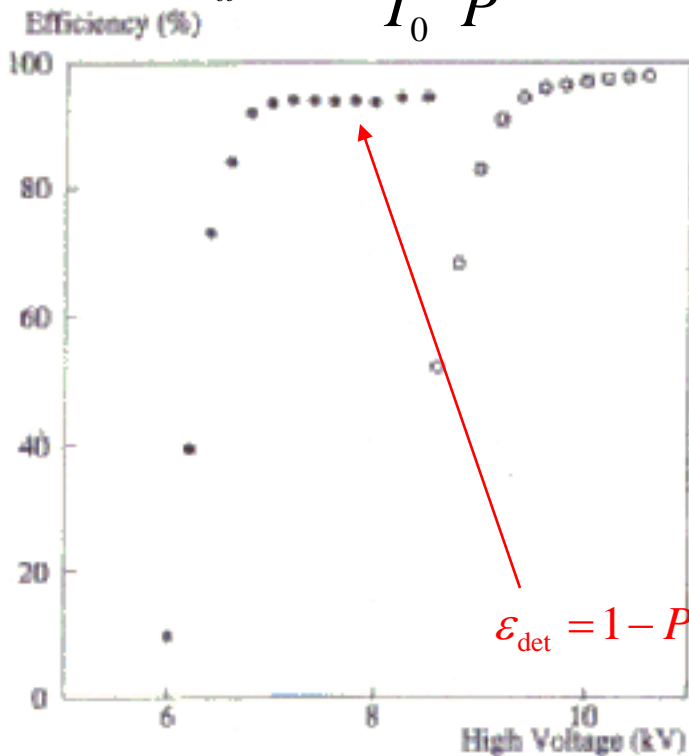
ARGO-YBJ

Operating at 4300 m above sea level

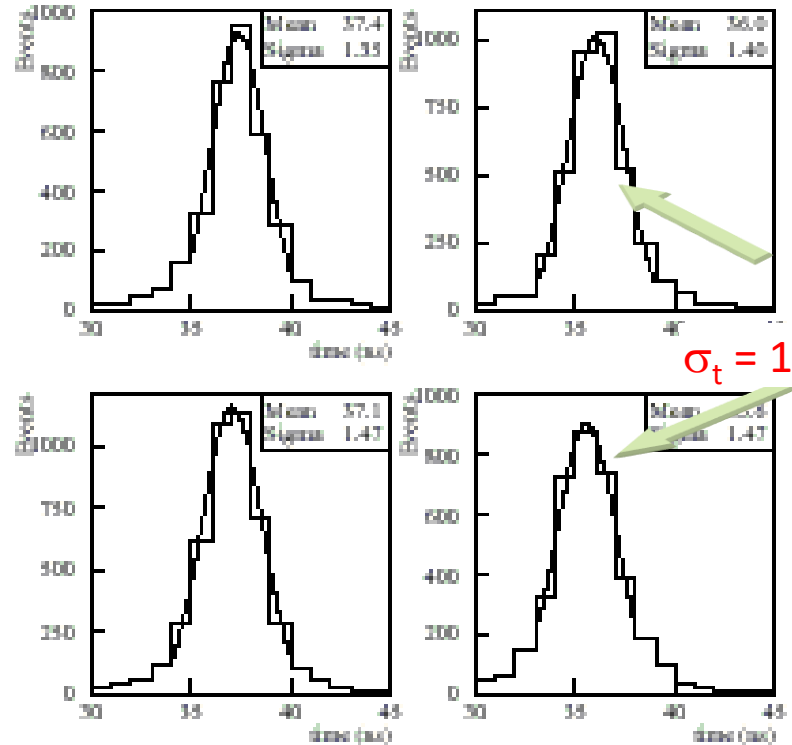


Low pressure ~ 600 mbar

$$V_{eff} = V_0 \frac{T}{T_0} \frac{P_0}{P}$$



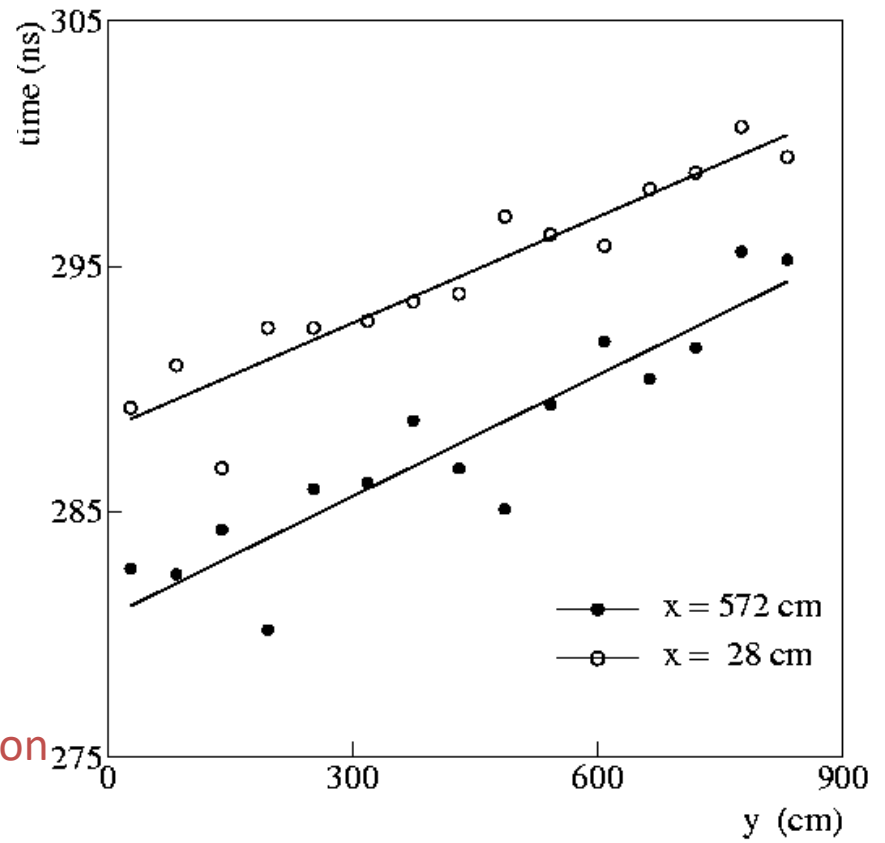
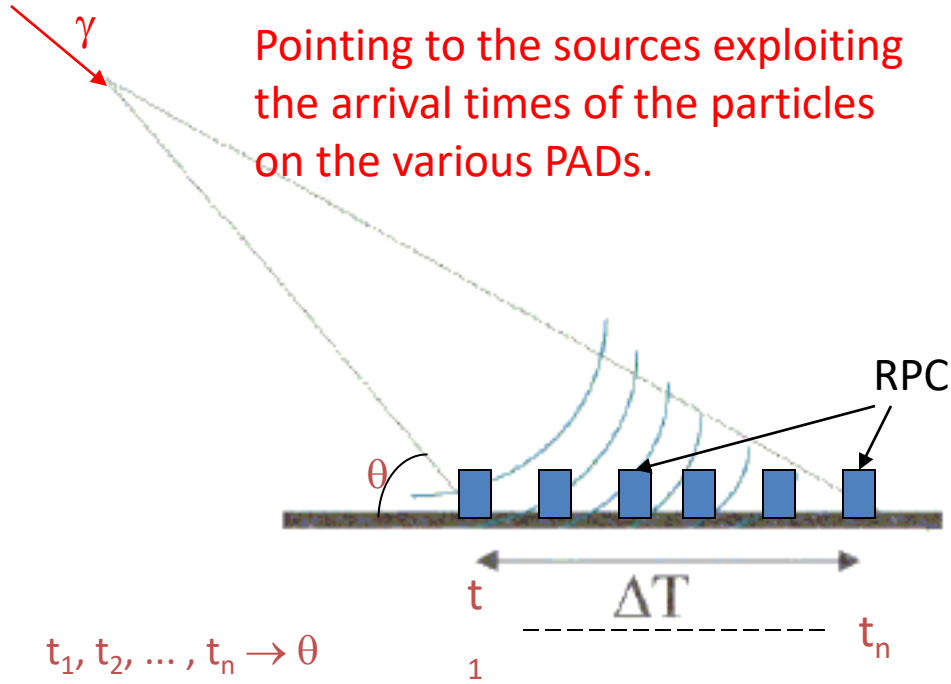
$$\epsilon_{det} = 1 - P(0) = 1 - e^{-\bar{n}}$$



$\sigma_t = 1.45$ ns

Time resolution

ARGO-YBJ

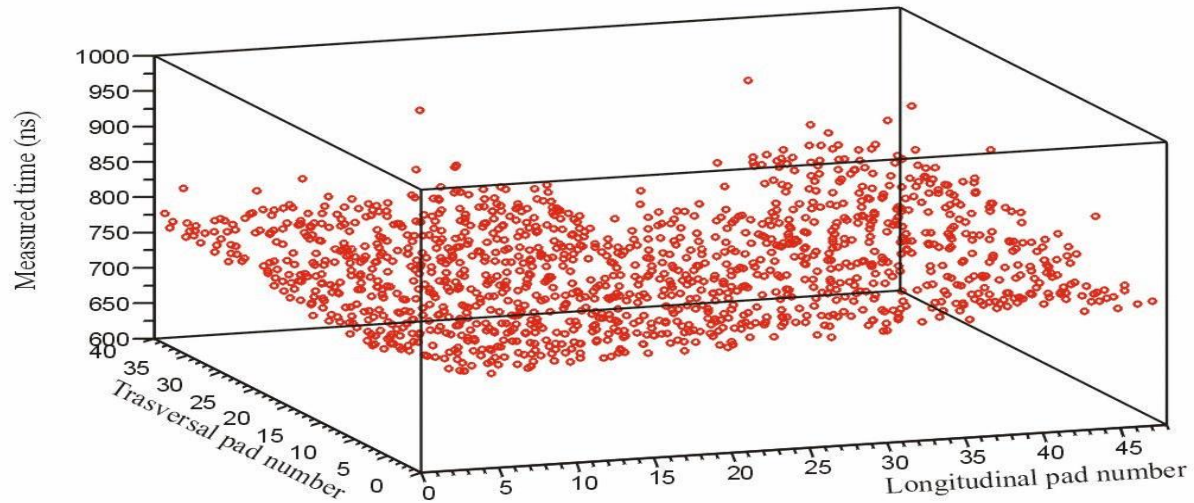


Interesting application where good time resolution is essential for a good tracking

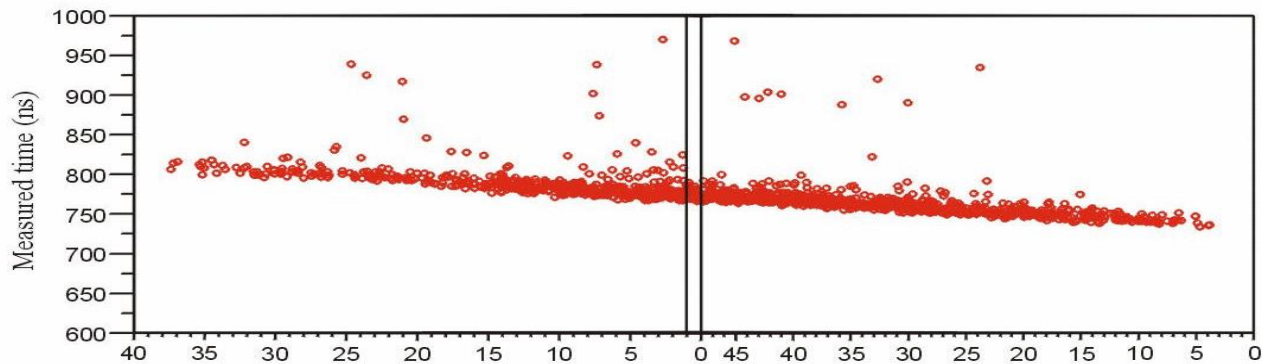
$\Delta t_{\text{RPC}} \sim 1\text{-}2 \text{ ns} \rightarrow \Delta\theta = 1 \text{ mrad}$

$$\frac{\text{Signal}}{\text{Background}} \propto \frac{1}{(\Delta\theta)^2}$$

ARGO-YBJ



Picture of an event on 16 clusters



The same event from such a point of view
to appear as a plane

Significance of the first generation of the RPC

Why the RPCs have been extensively used in several HEP experiments?

- **Golden parameter:** the time resolution (≈ 1 ns)
- **Good spatial resolution:** limited by strip dimensions
- **High muon efficiency** of the order of $> 96\%$ and **long term stability**
- **The cost** of RPC is much smaller as compared to other fast detector (like the scintillators)
- It is **easy** to construct and operate
- Simple signal pick up and readout system (just “strips”)
- Two dimensional readout (x and y)

BUT

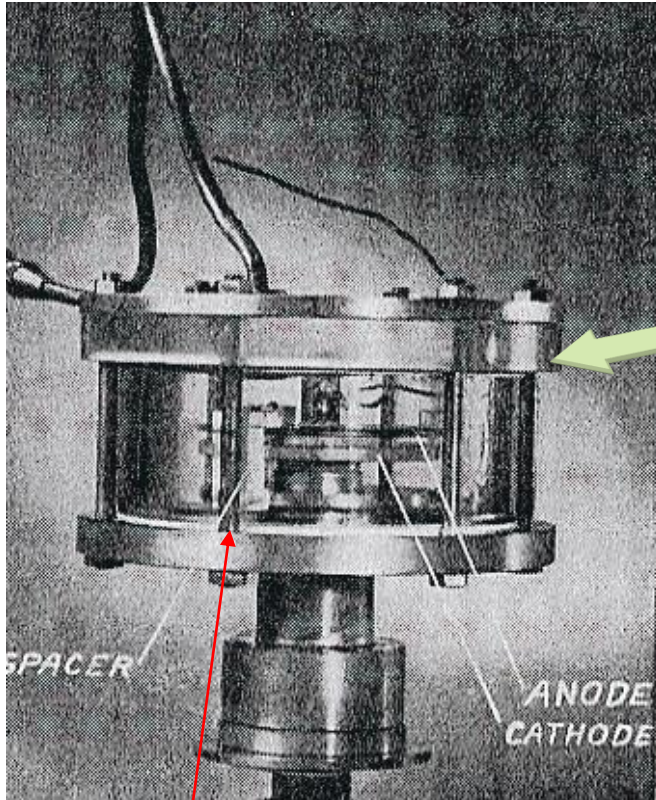
rate capability < 50 Hz/cm²





Le PPC di Madansky e Pidd

Sviluppati immediatamente dopo le PPC di Keuffel



uso di spaziatori di materiale isolante

Elettrodi circolari

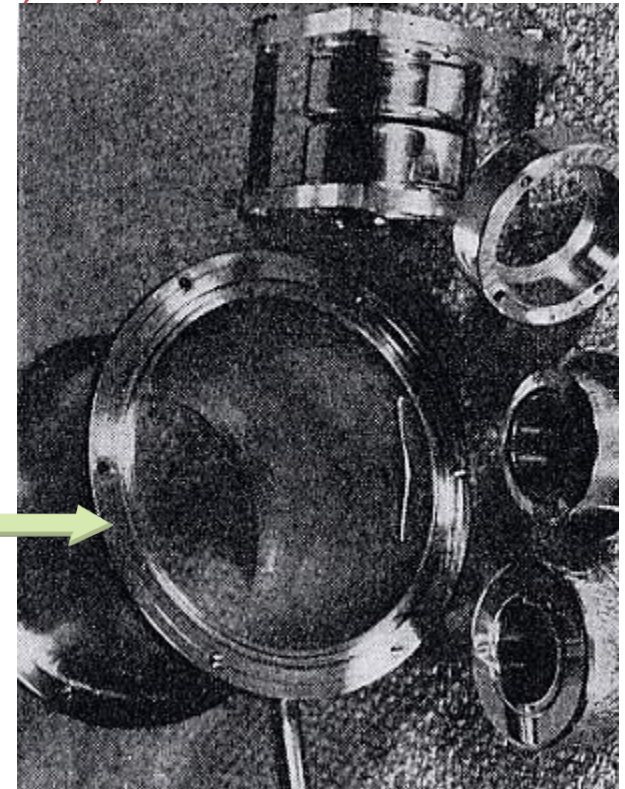
Anodo in Rame di dimensioni diverse: da 1 a 8 cm

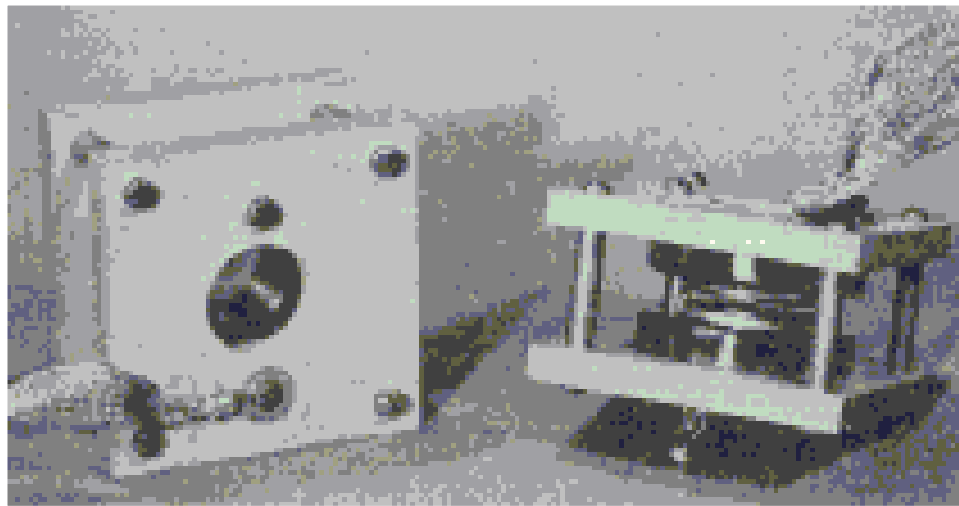
Catodo in Cu, Al, Au, Pt, Pb, etc.

distanza tra gli
elettrodi **variabile**
tra 0.5 e 5 mm

Variante:
entrambi gli
elettrodi in fogli di
rame, spessore 3
mm, tesi "come la
pelle di un
tamburo" su

un'intelaiatura di
qualche cm di

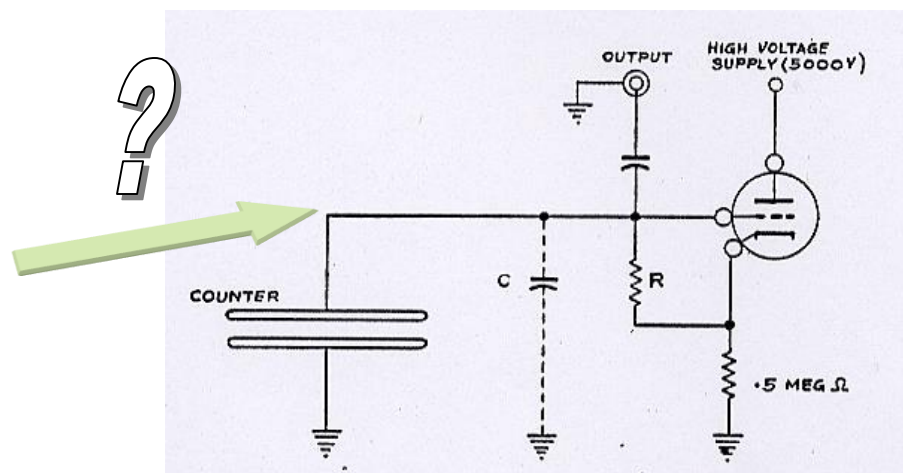


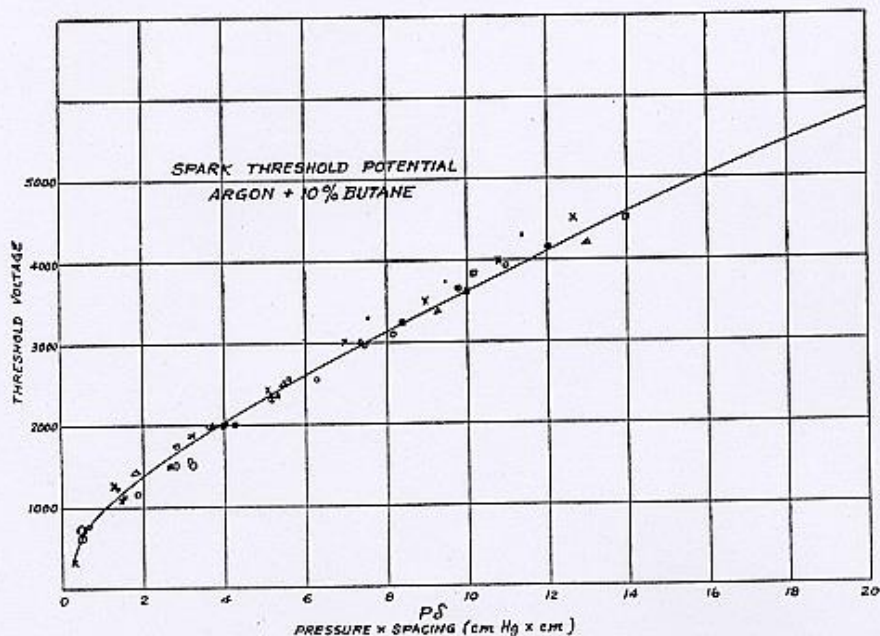


“il parallelismo degli elettrodi influisce sull'uniformità del campo elettrico (dichiarato entro lo 0.2%), sulla massima sovratensione permessa, ed, in generale, sulle prestazioni dei rivelatori”

miscela: 90% Argon, 10% iso-butano
pressione: studio sistematico tra 10 e 150 mmHg

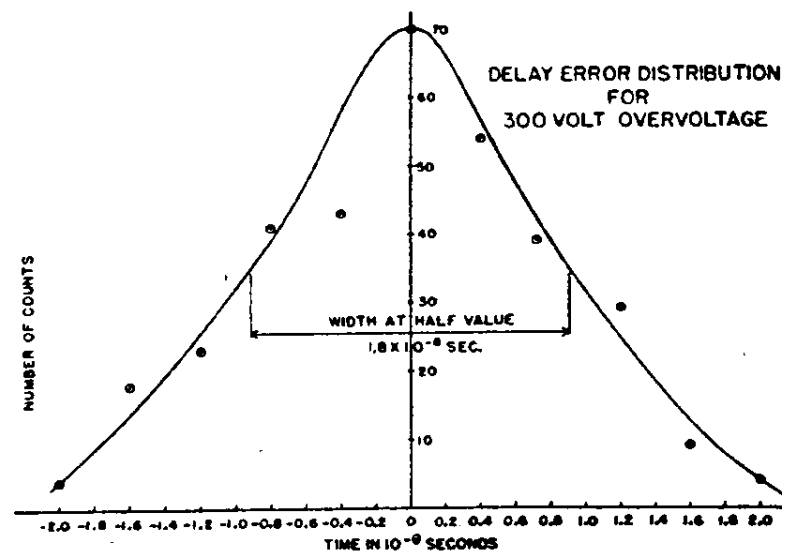
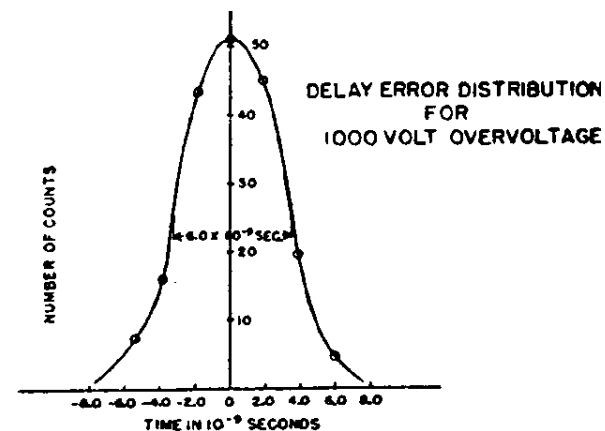
L'applicazione delle PPC passerà attraverso lo sviluppo di **elettronica sempre più sofisticata**: sia per la lettura del segnale, che per l'accensione-spegnimento del rivelatore





Prestazioni:

- segnali: ~ 100 V (su 50Ω)
- periodo di spegnimento: 0.1 - 0.001 s
- efficienza $\sim 98\%$ per particelle β
- risoluzione temporale: 6-18 ns, per sovratensione tra 300 e 1000 V





Il problema del “quenching” (3)

- Al contrario di ciò che avviene nei rivelatori a filo centrale, nei rivelatori a piani paralleli, una scarica perdura fino a quando la tensione applicata dall'esterno non viene in qualche modo rimossa.
- L'intero volume del rivelatore è attivo nei riguardi dello sviluppo di una scarica; essa tenderà a propagarsi verso l'esterno mediante fotoionizzazione UV e ionizzazione secondaria.

Si può:

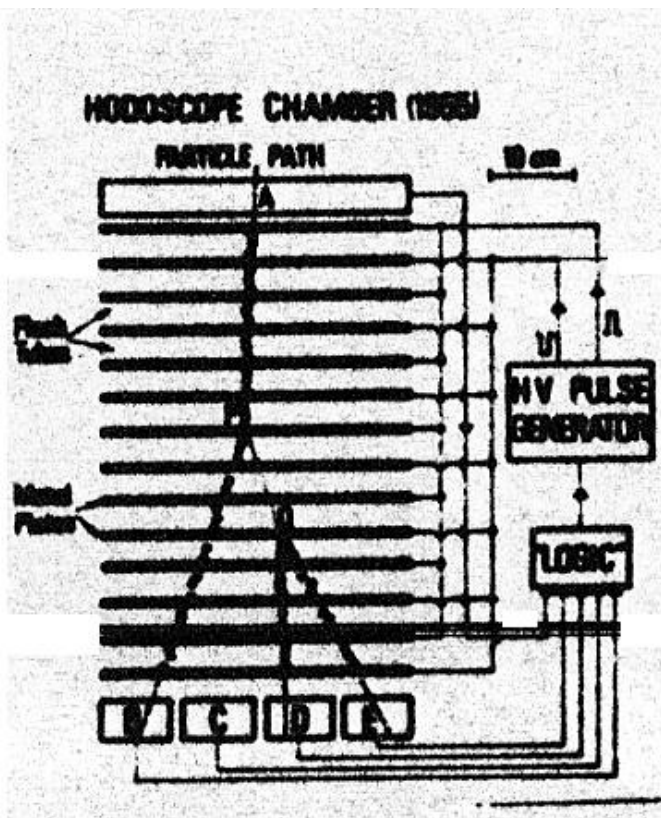
1. Dopo il passaggio di una particella ionizzante, rimuovere la tensione applicata per un certo tempo (0.01 - 0.05 s) → circuiti di spegnimento (Franzineti e Bella, Focardi, Torelli, Rubbia ...)

2. Applicare la tensione solo in coincidenza con il passaggio della particella ionizzante. Quanto rapidamente può essere ristabilita la HV fra gli elettrodi del rivelatore, dopo la scarica, senza causare conteggi spuri?

La frequenza massima di rivelazione delle particelle è quindi limitata: devo evitare le spurie ed, inoltre, il tempo di ricarica è correlato alla costante di tempo RC del sistema (compresi i piatti ...)

Le camere a Flash

Sviluppate a Pisa dal gruppo di M. Conversi, attorno al 1955

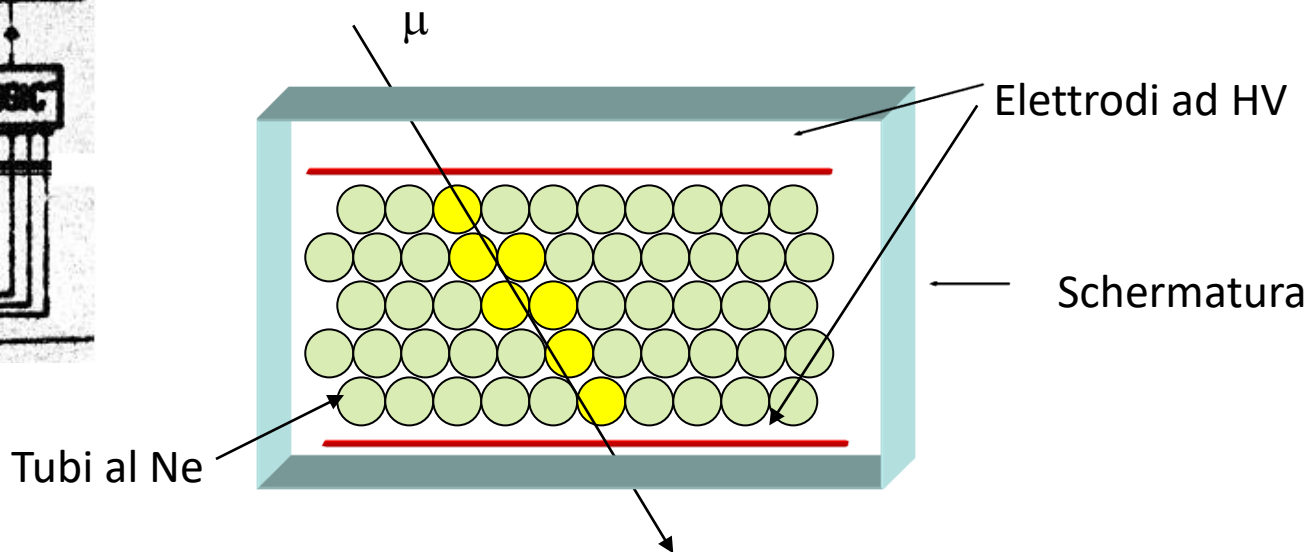


Elettronica molto
sostanziosa

Condensatore a piani paralleli riempito da un gran numero di tubi di vetro, diametro ~ 1 cm, senza filo

Miscela di Ar o Ne a 0.5 Atm

Qualche decimo di μ s dopo il passaggio della particella, applicazione di 10 kV/cm agli elettrodi di metallo, per 2 μ s



A causa della presenza del campo elettrico applicato nella regione fra le armature, sincronizzato con il passaggio di una particella ionizzante, si origina una scarica, accompagnata da emissione luminosa: gli elettroni prodotti nella valanga "accendono il neon"

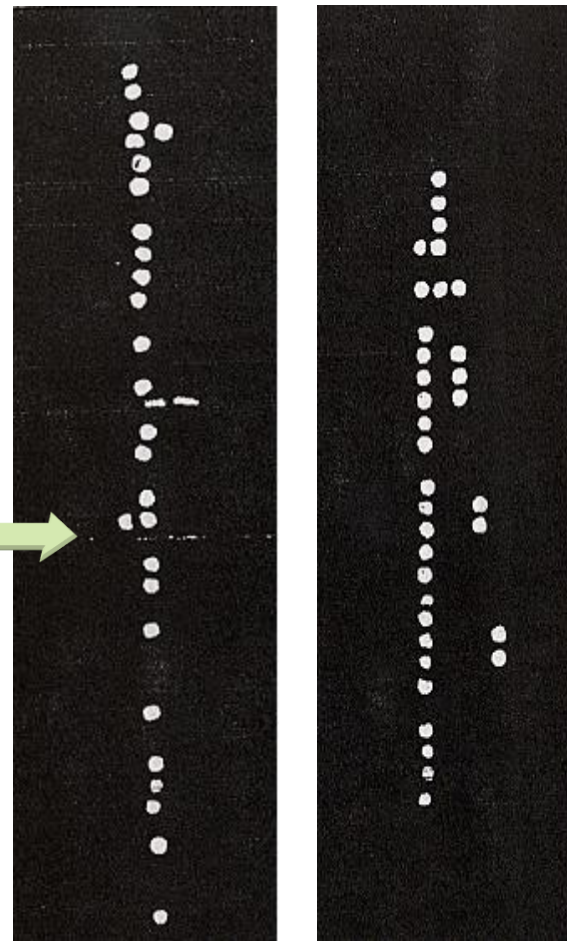
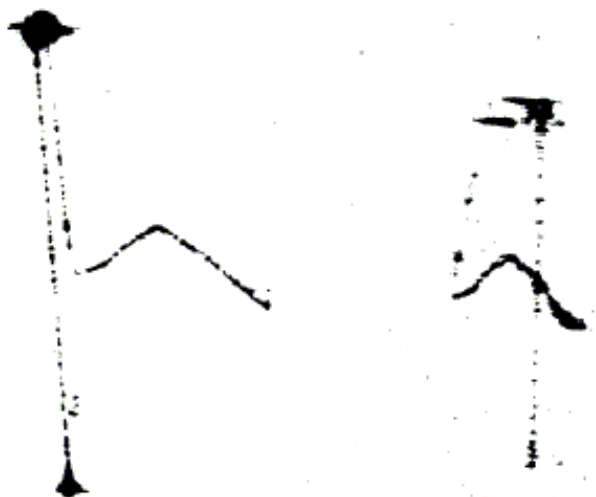


Gran numero di tubi, disposti
perpendicolarmente



ricostruzione 3D della traccia

Prime fotografie di μ cosmici o sciami elettromagnetici



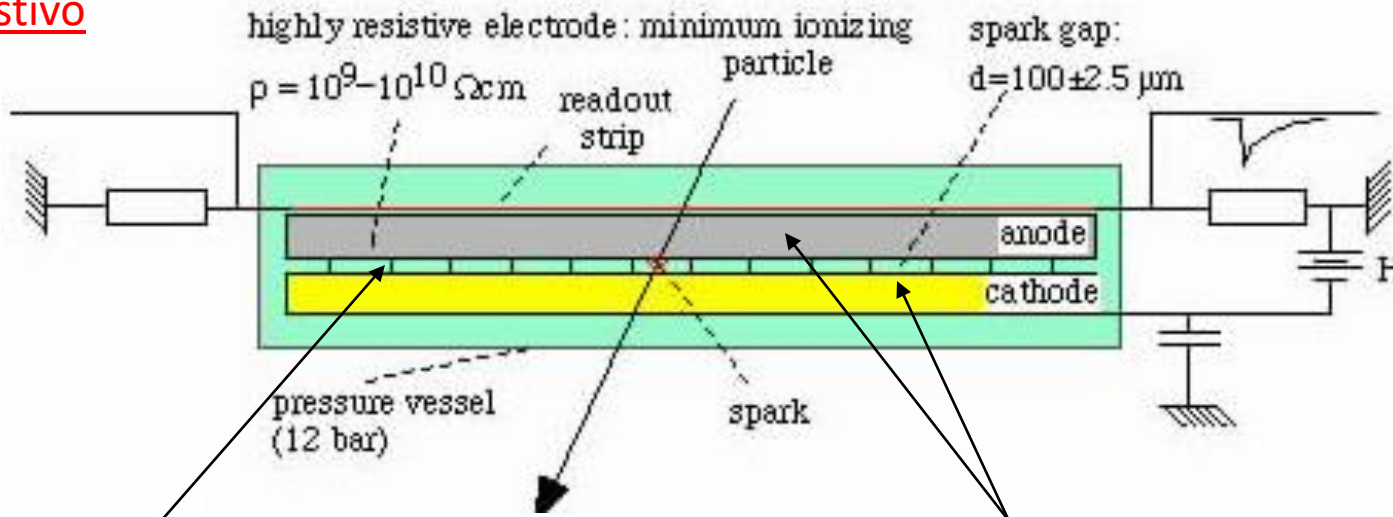
μ cosmico

$\gamma \rightarrow e^+e^-$

Le Planar Spark Chambers

Sviluppate da Yu. Pestov attorno al 1970, ed ancora usate attualmente

Le prime camere in cui uno degli elettrodi e' costituito non di metallo, ma da materiale resistivo



Gap tra 100 μm ed 1 mm, con una precisione di 1-5%

Elettrodi: catodo di vetro con pellicola di rame di 3 μm
anodo di **vetro semiconduttore** $\rho = 10^9 - 10^{10}$
 Ωcm
Campo elettrico 2×10^4
V/cm

Risoluzione temporale ~ 50 ps Miscela di gas a 10 Atm:

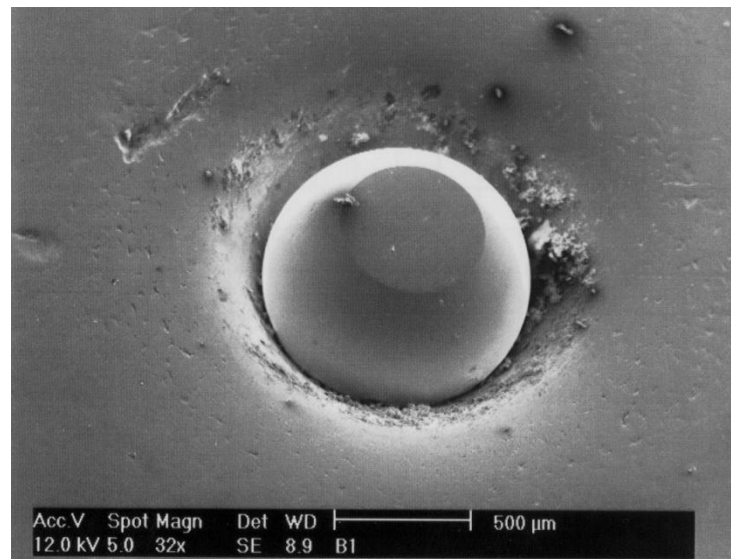
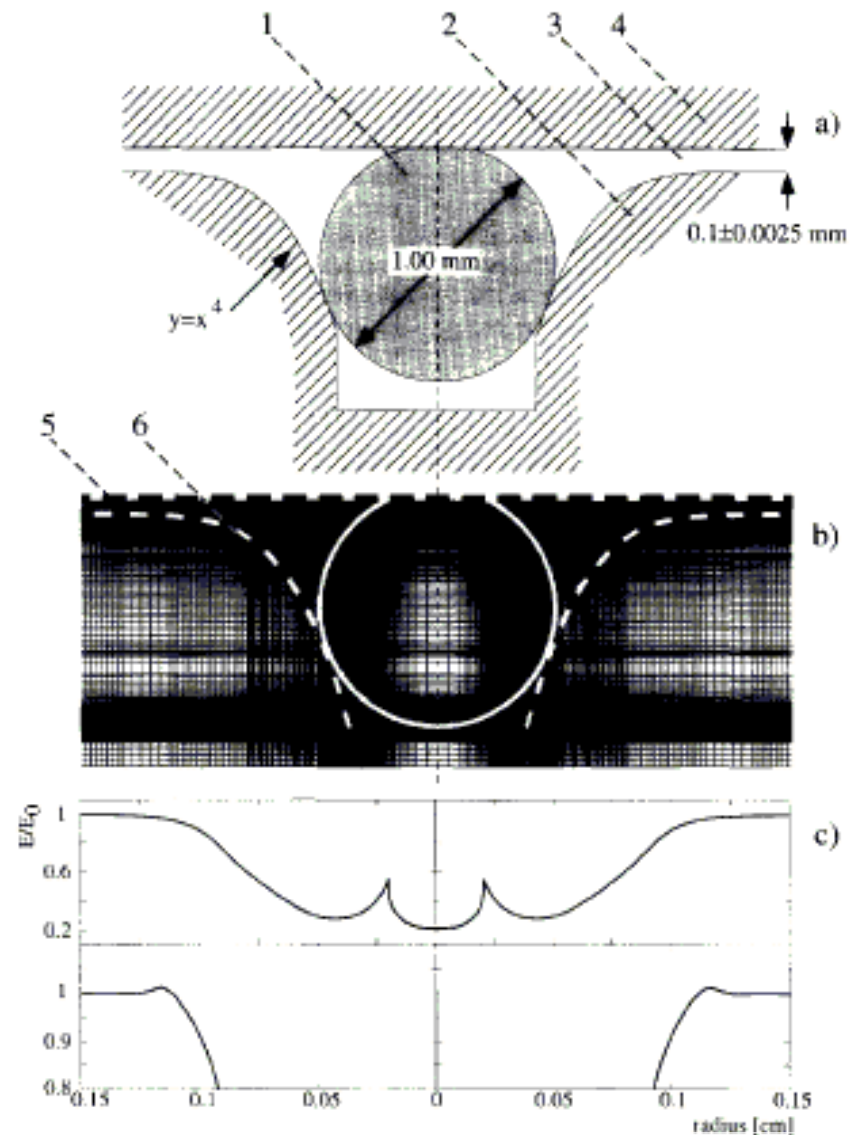
Argon-Neon, piu' gas di quenching (isobutano, etilene, butadiene, idrogeno, etere dietilico)

Le Planar Spark Chambers

Rivelatori “meccanicamente” estremamente critici

Poiche' il parallelismo e' critico:
Studio degli spaziatori **molto accurato**: possono
perturbare il campo elettrico in maniera
sostanziale

Foto di uno spaziatore in un catodo di Al

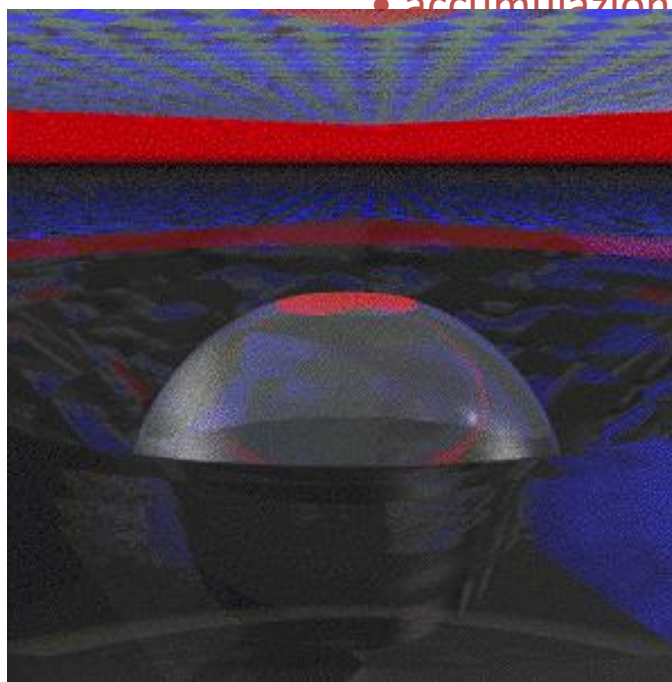
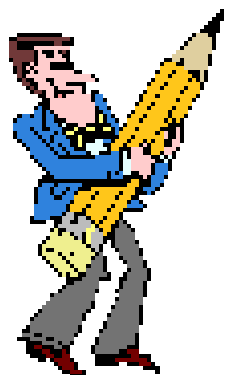


Trattamento delle superfici degli elettrodi:

- pulizia con ossido di cerio ed acqua filtrata e deionizzata
- uso di effetti di interferenza sulle superfici per individuare imperfezioni

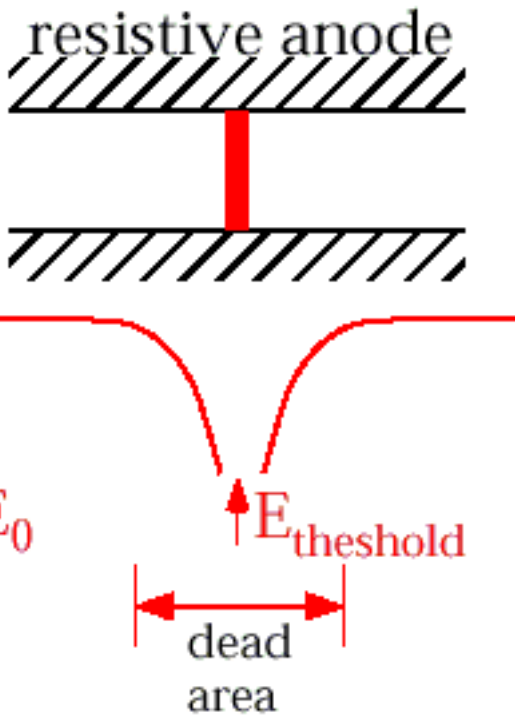
Condizionamento:

- per una settimana si aumenta gradualmente la tensione di lavoro mentre il rivelatore e' esposto ad una sorgente
- accumulazione di 10^6 scintille per cm^2
- pellicola di gas
- sugli elettrodi

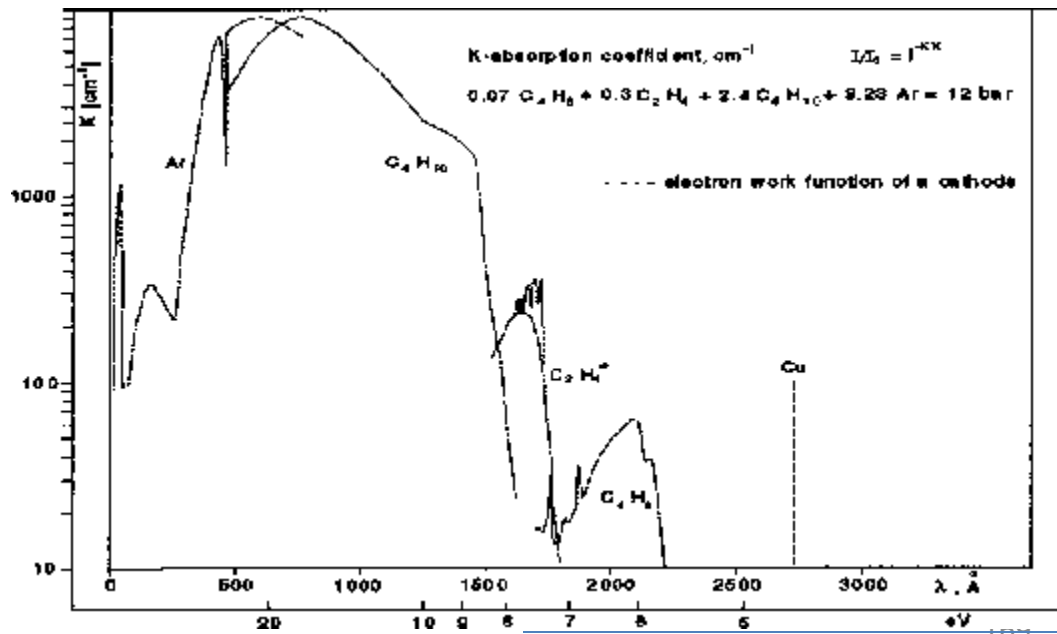
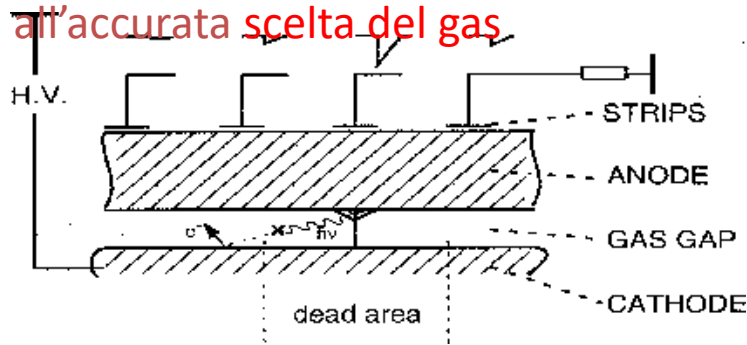


Veduta "d'artista" di uno spaziatore

Le Planar Spark Chambers



La scarica rimane (piu' o meno)
localizzata grazie agli elettrodi resistivi e
all'accurata scelta del gas.



Poiche' il tempo di ricarica
dell'elettrodo e' "grande" solo
una zona limitata di esso viene
interessata dal processo di
scarica

Le Planar Spark Chambers

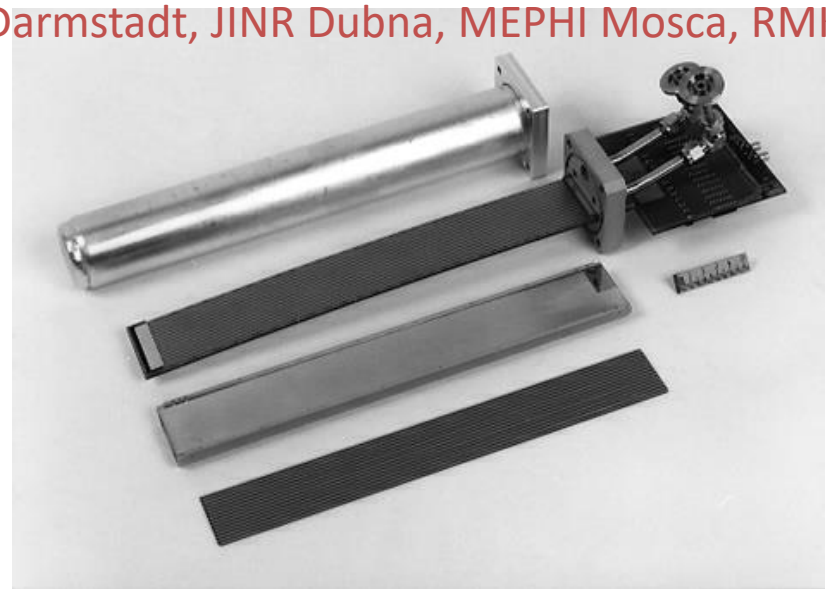
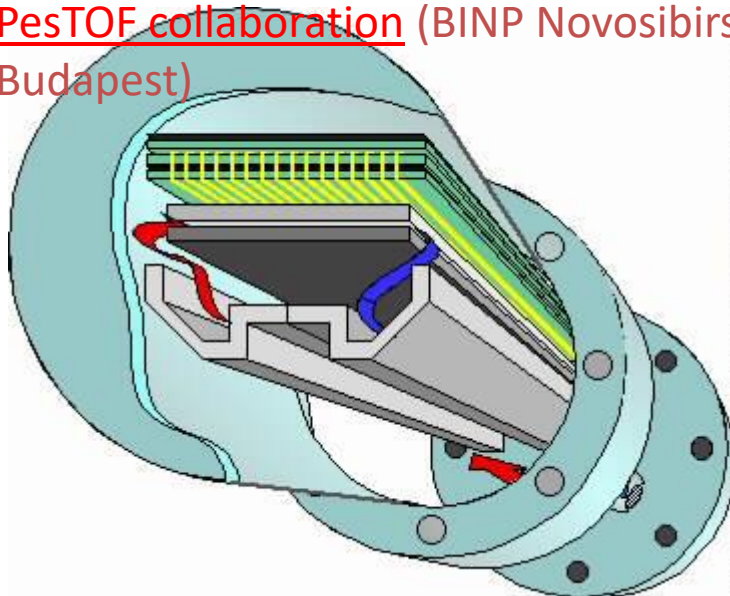
Idea di spark counters con scarica localizzata: Novosibirsk, 1971

prima applicazione ai collider e^+e^- : Novosibirsk 1982-85

continuazione dell'R&D ai collider e^+e^- : Novosibirsk, SLAC 1986-91

sviluppo degli spark counters (Pestov spark counters) per esperimenti con ioni pesanti:

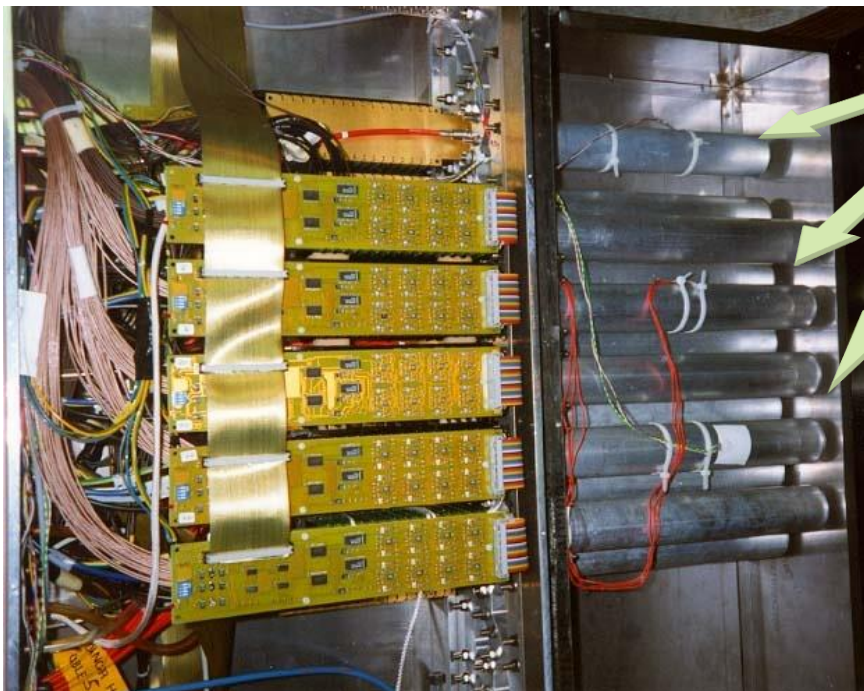
PesTOF collaboration (BINP Novosibirsk, GSI Darmstadt, JINR Dubna, MEPHI Mosca, RMKI Budapest)



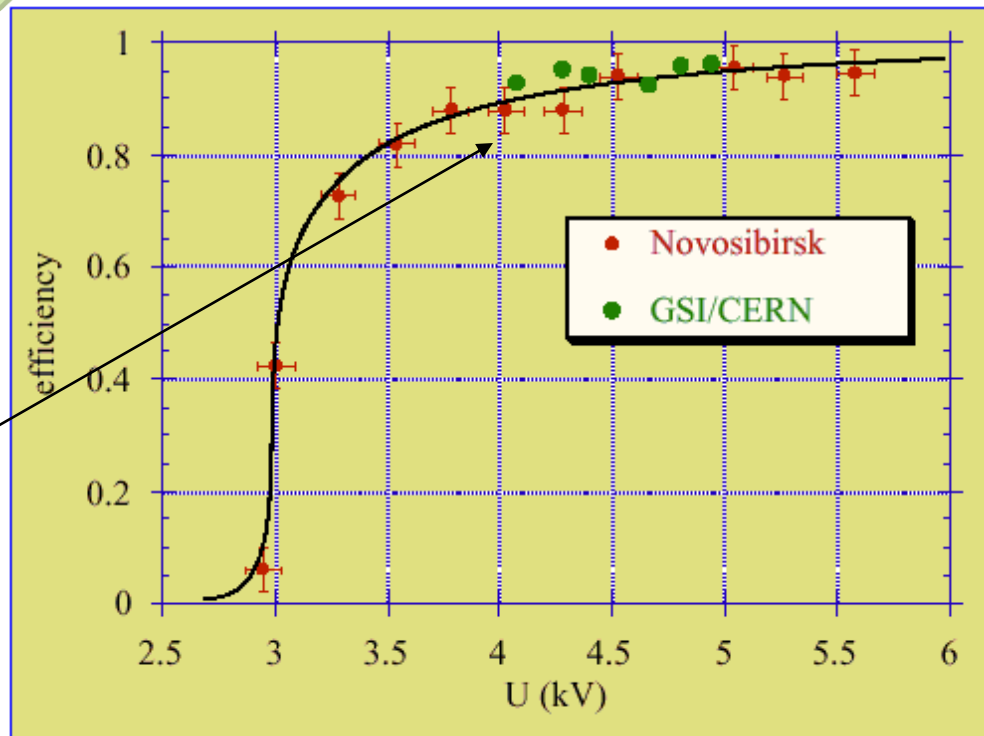
Attualmente tre grandi esperimenti hanno preso in considerazione l'uso di un grande array di spark counters:

ALICE, NA49 (CERN-SPS), FOPI al GSI

Le Planar Spark Chambers

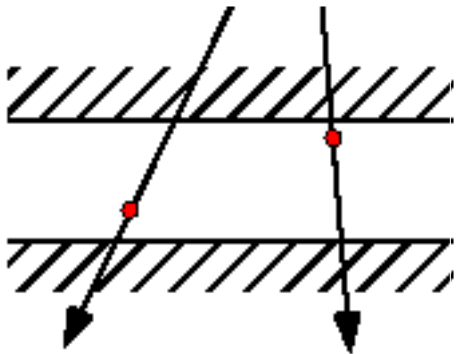


Una serie di 14 PSC ad NA49 al CERN



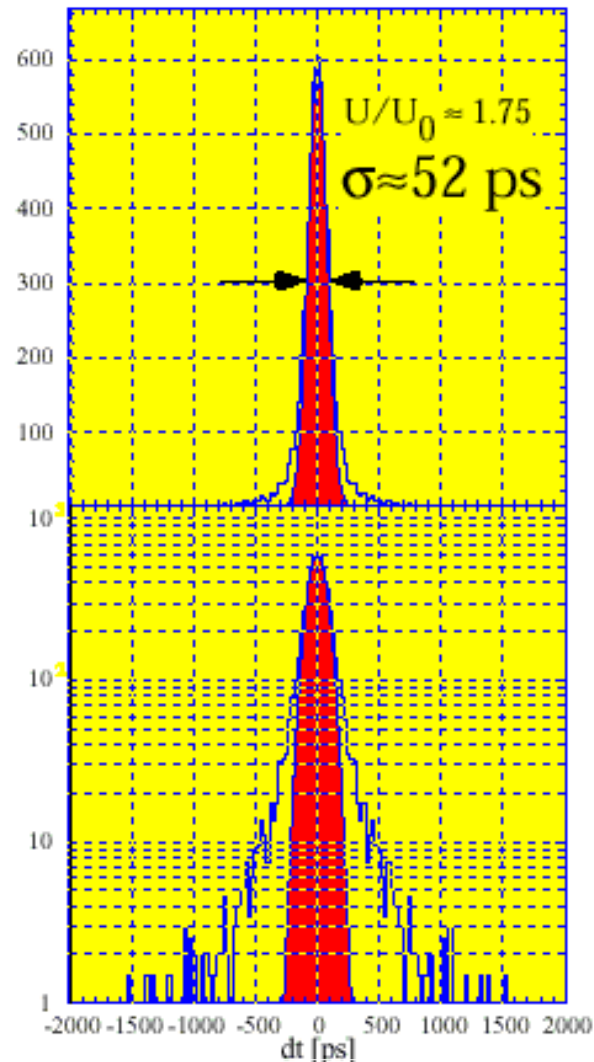
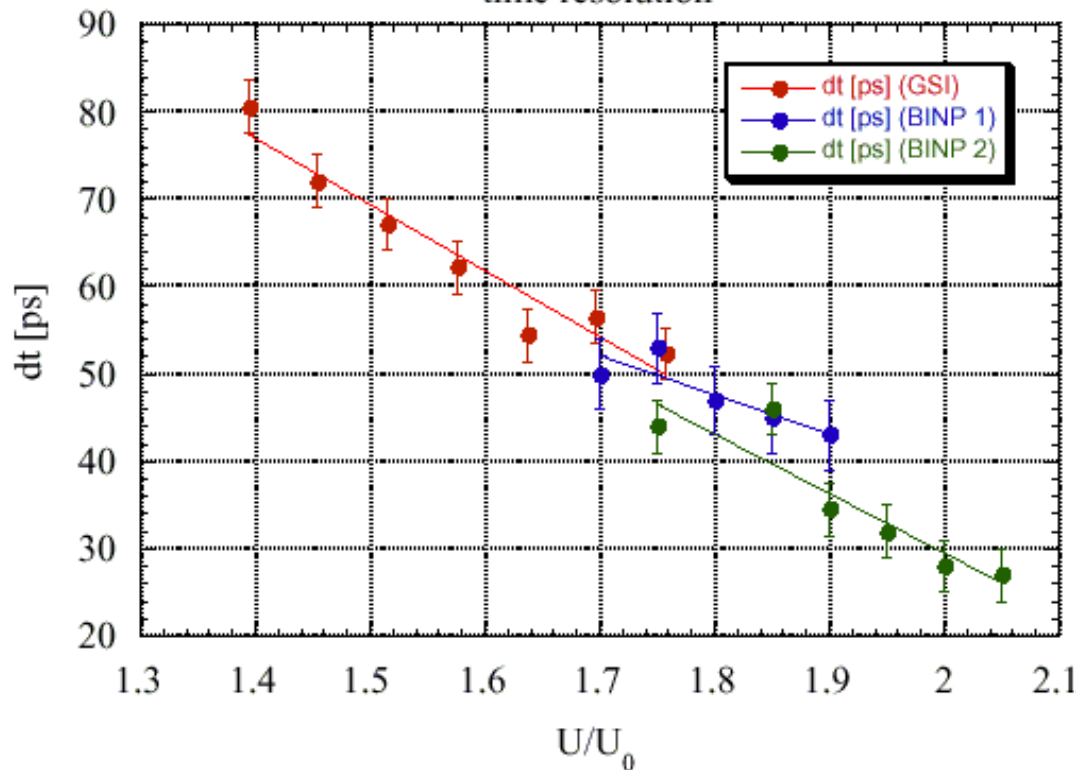
Efficienza elevata grazie al fatto
che ci sono Almeno 4-5 coppie
ione-elettrone nella gap (a 12

$$\epsilon_{\text{det}}^{(m)} = 1 - P(0) = 1 - e^{-\bar{n}}$$

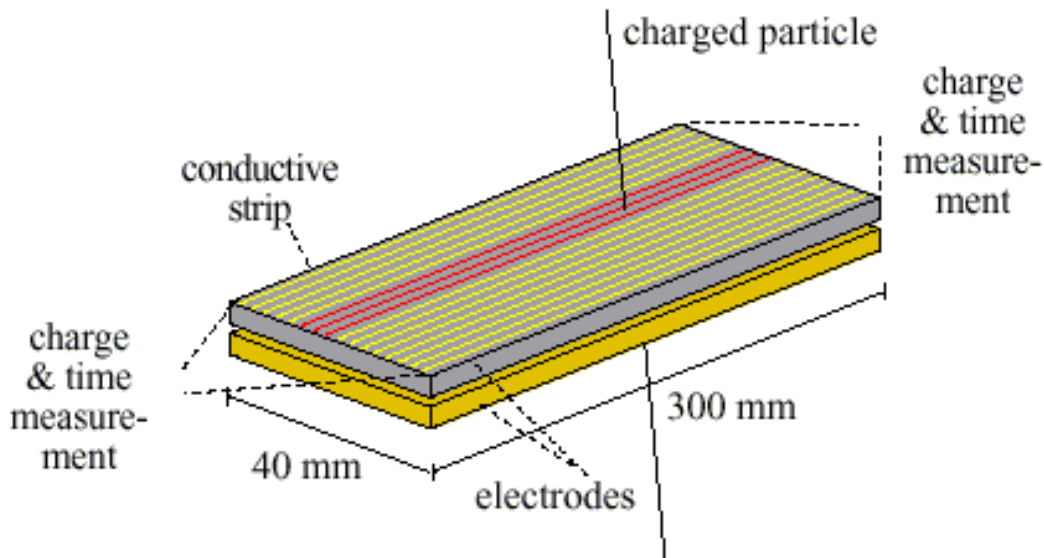


Risoluzione temporale
legata al tempo di
transito della particella
nella gap $\sim \mu\text{s}$

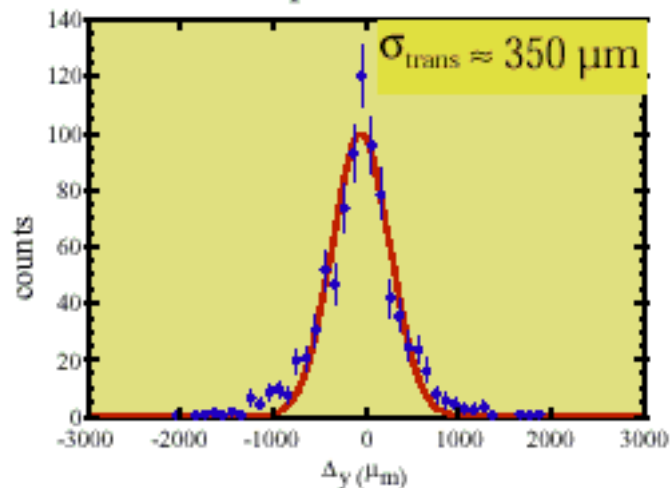
time resolution

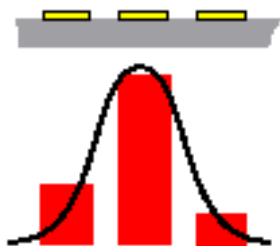



Le Planar Spark Chambers

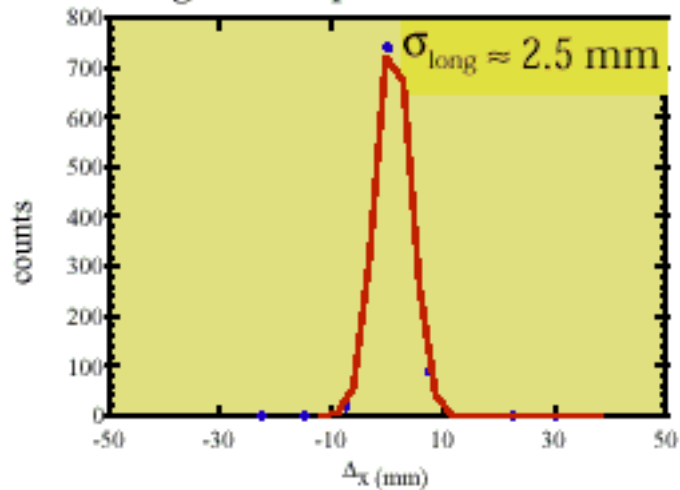


transverse position resolution

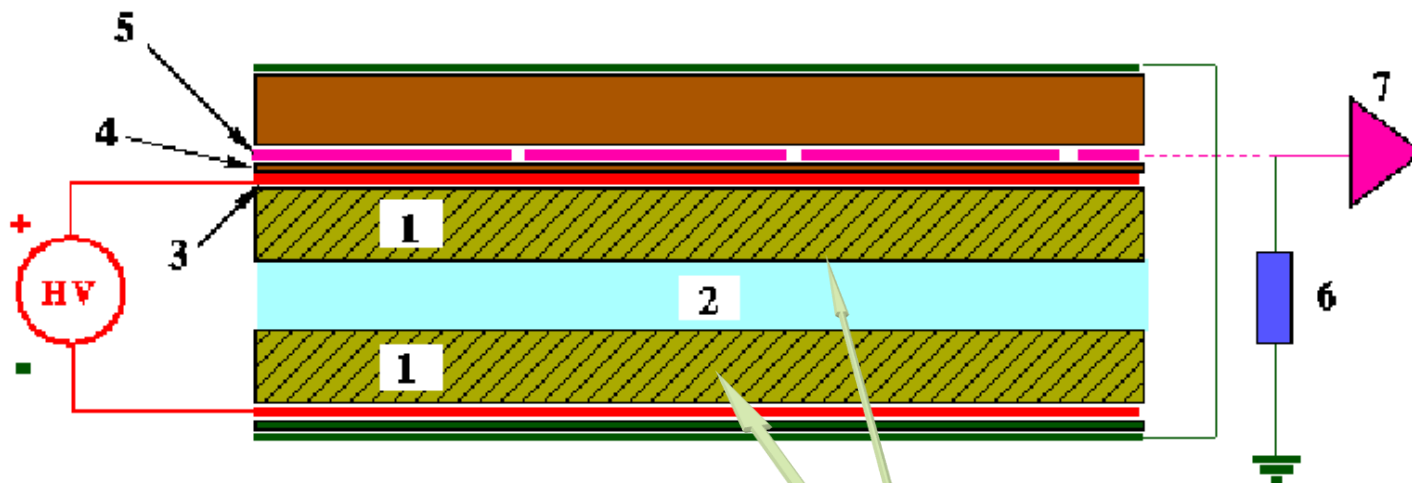


 <p>Posizione trasversale dalla media pesata della carica misurata sulle varie strip</p>	 <p>Posizione longitudinale determinata dalla differenza dei tempi destra-sinistra (limitata dalla risoluzione temporale)</p>
--	---

longitudinal position resolution



Sviluppati all'inizio degli anni '80 da R. Santonico (Roma)



bakelite di resistivita' 10^{10} - 10^{12} Ω cm
trattata con olio di lino

- Piani della gap: polimeri a base fenolica
- Gap: 2 mm
- Elettrodi di HV: 100 μ m di grafite
- Pressione di funzionamento: \sim 1 Atm
- Miscela di gas: 70% Ar, 29% iso-Butano, 1% Freon
- Gas flow: 0.1 vol/ora
- Dimensioni: Area: 1 x 2 m²
Spessore: 6 mm

- Strip di lettura in Al o Cu: larghe 1-3 cm

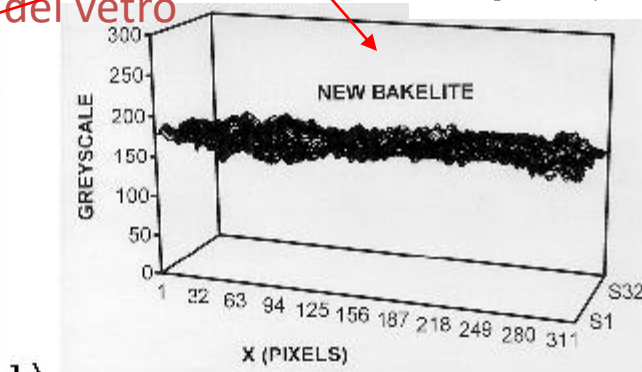
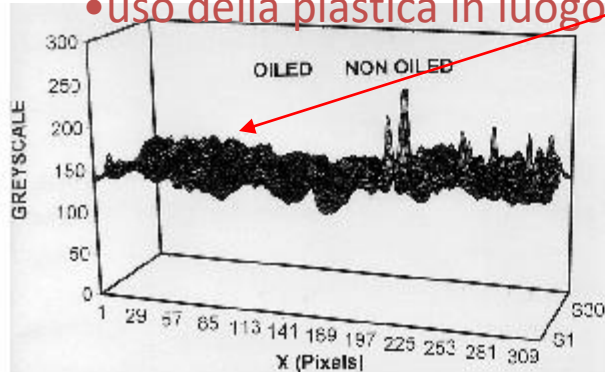
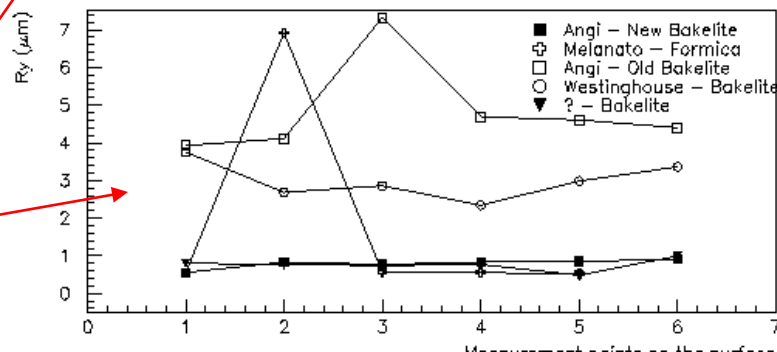
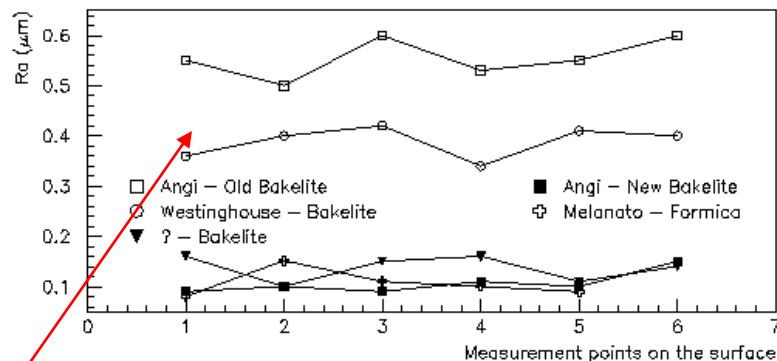
Paragone con gli scintillatori (R. Santonico):

- RPC meno costosi (10^5 lire/m²)
- Risoluzione temporale comparabile (1ns)
- Elettronica semplice
- Trasmissione del segnale su strip di lettura, cioè' bassa attenuazione su lunghe distanze

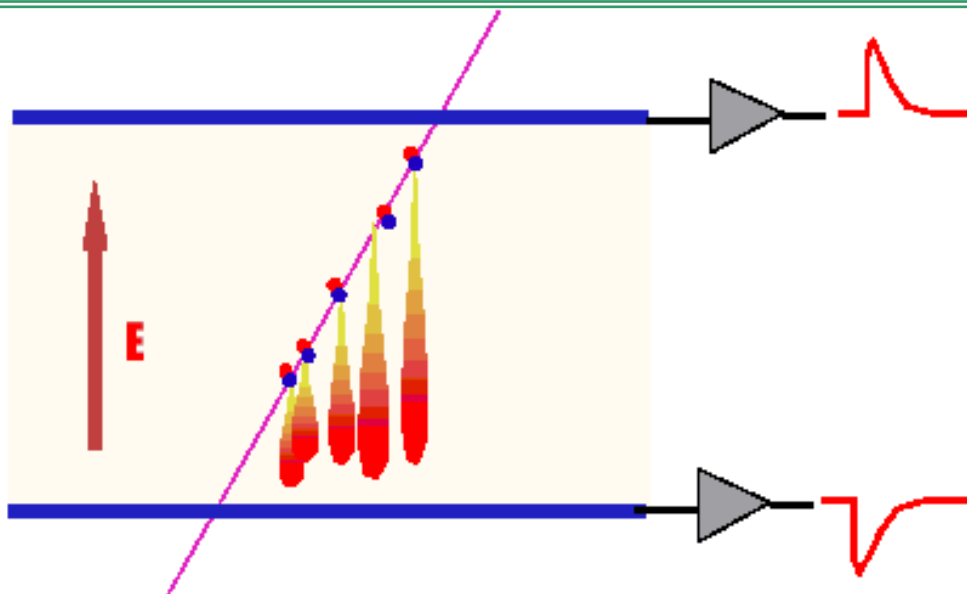
- Risoluzione spaziale determinata dalla dimensione delle strip (1-3 cm)

Rispetto alle PSC:

- assenza di gas ad alta pressione
- bassi requisiti di precisione nella meccanica
- uso della plastica in luogo del vetro



Regimi di funzionamento



Nel caso dei contatori a piani paralleli (e quindi anche degli RPC) la moltiplicazione della carica avviene in un **campo elettrico uniforme**.
La grandezza della **valanga** dipende dalla distanza dall'anodo



Non e' un contatore proporzionale

SPARK

STREAMER

AVALANCHE

Il segnale e' **indotto** sugli elettrodi di lettura

SPARK COUNTER

RESISTIVE PLATE CHAMBERS

AVALANCHE CHAMBERS

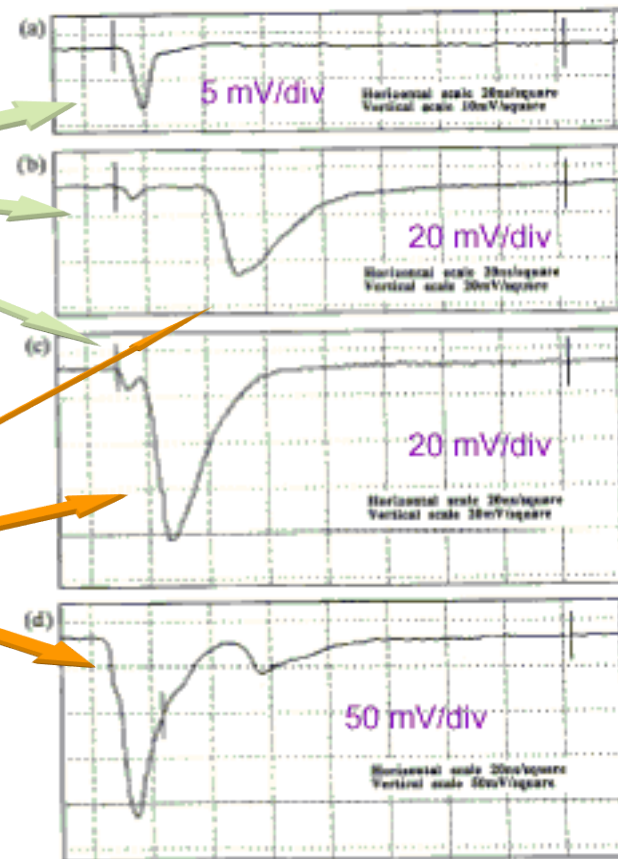
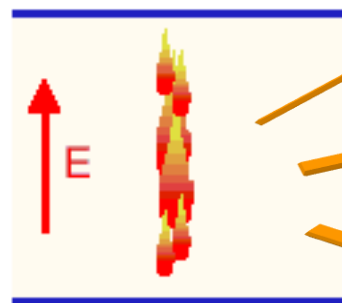
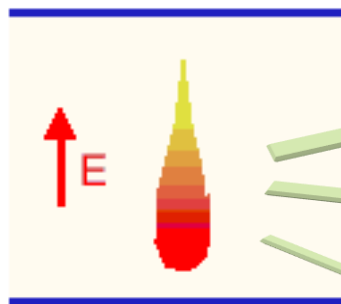
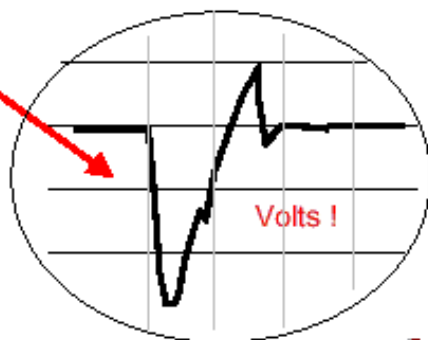
A seconda della **tensione** applicata opera con **regimi** di funzionamento **diverso**

Avalanche:

Il valore del campo elettrico E è tale che l'energia acquistata dall'elettrone è maggiore dell'energia di ionizzazione

Streamer

Spark



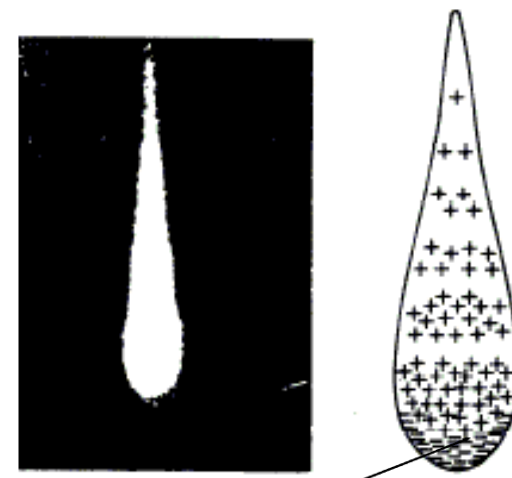
Nota: la separazione avalanche-streamer diminuisce all'aumentare della tensione

Streamer

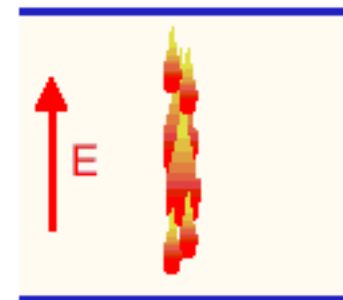
A campi elettrici piu' elevati la carica spaziale dovuta agli elettroni in testa alla valanga modifica il campo esterno fino ad annullarne gli effetti

- Ricombinazione di e^- -ioni
- Produzione di fotoni ultravioletti
- Produzione di ulteriori valanghe da ionizzazione di ultravioletti

Avviene quando gli elettroni nella valanga $\sim 10^8$ (criterio di Raether)



$E \sim 0$ se $\# e^- \sim 10^8$

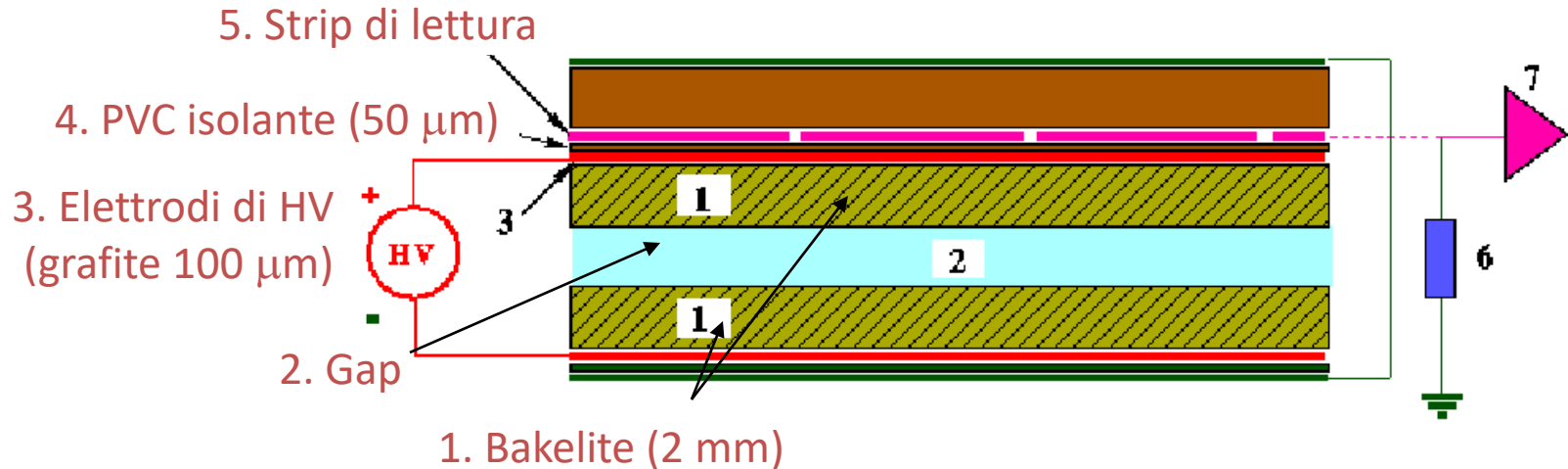


Filo centrale

Piani paralleli

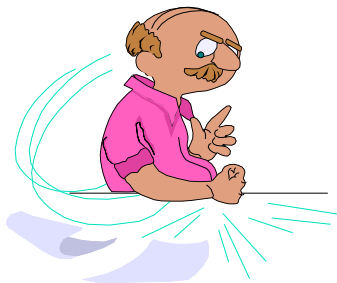
Come viene originato il segnale in un RPC?

In un RPC le strip sono completamente separate (isolate) dalla gap:



Gli elettroni della valanga o dello streamer non arrivano sulle strip:

il segnale e' indotto dal movimento delle cariche (elettroni e ioni) nella gap



La dizione popolare: "raccolta della carica" e', a volte, misleading

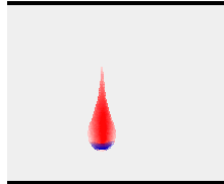


XVII Seminario Nazionale di Fisica Nucleare e Subnucleare

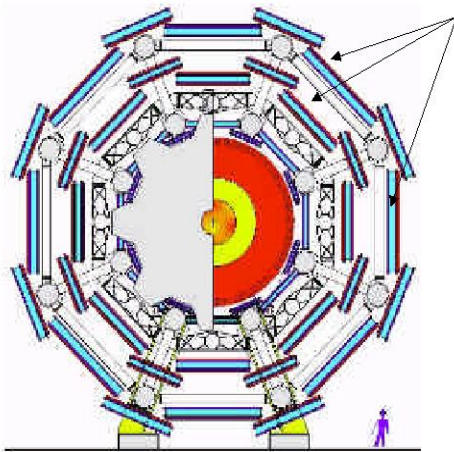
Otranto, Serra degli Alimini,
20-26 Settembre 2004

Cosa si vuole fare ...

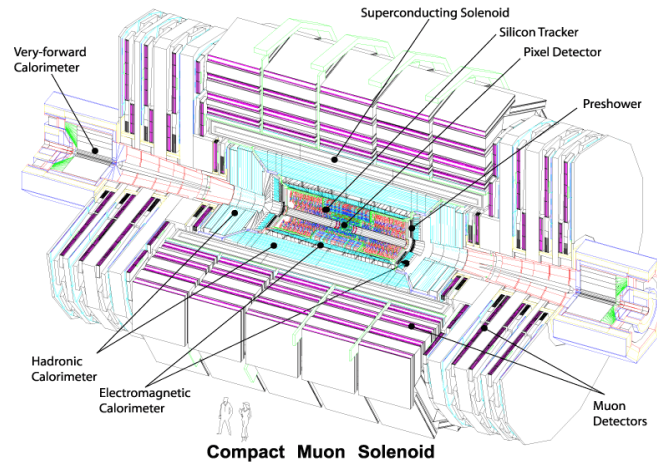
Avalanche mode



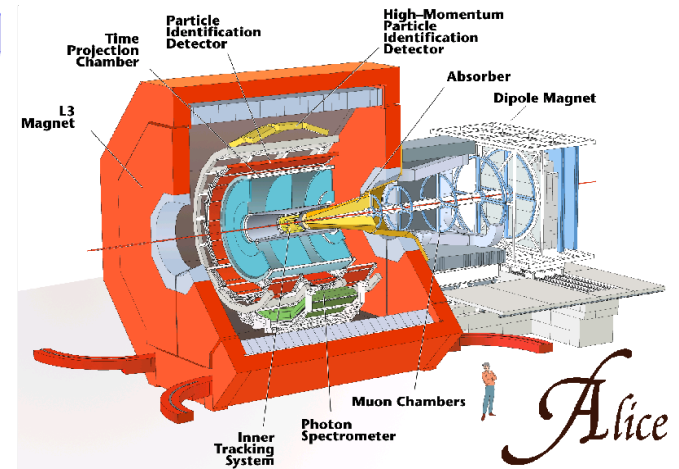
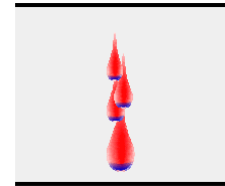
ATLAS



CMS



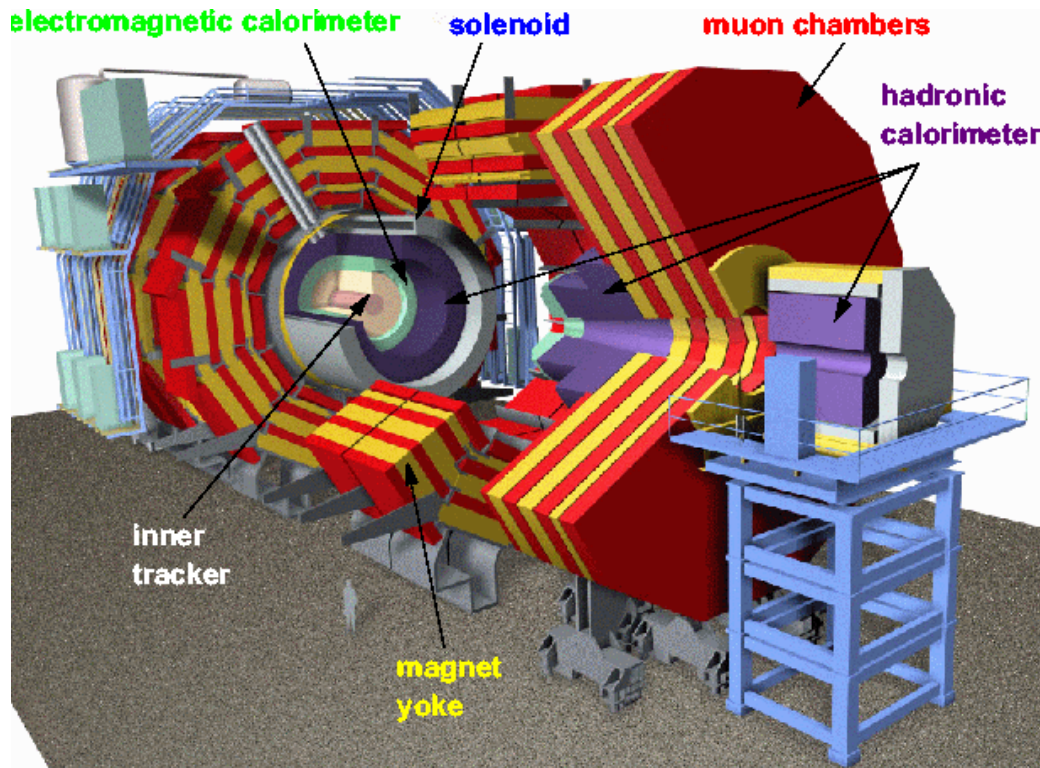
Streamer mode



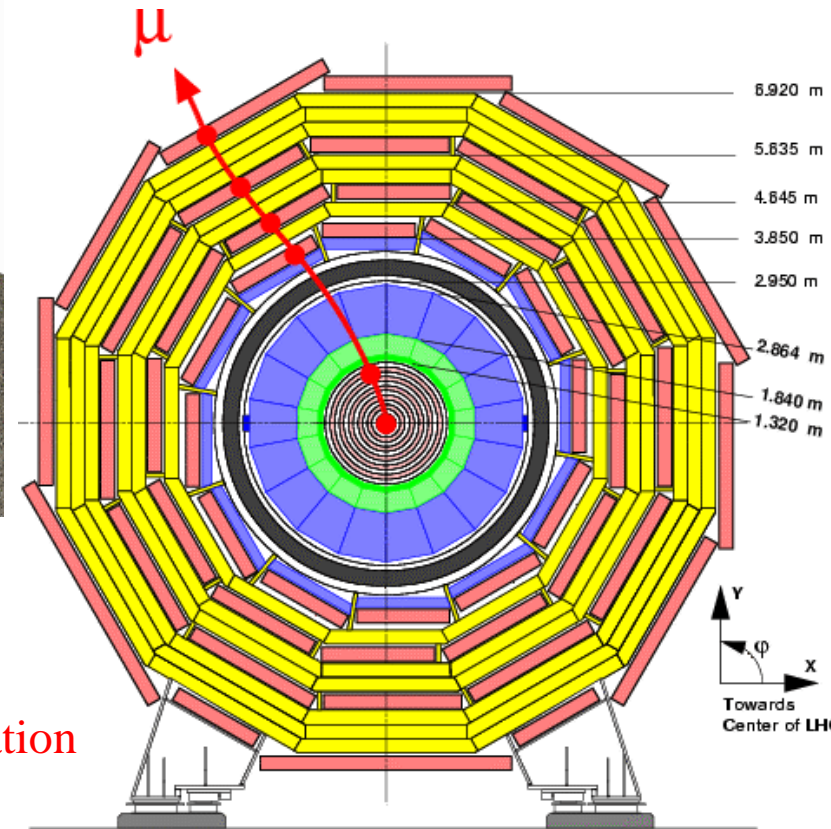
XVII Seminario Nazionale di Fisica Nucleare e Subnucleare

Otranto, Serra degli Alimini,
20-26 Settembre 2004

CMS



CMS sara' basato su:
"A very good redundant muon system"
(*Technical Proposal, CERN-LHCC 94-28, 15 Dec. 1999*)



Il trigger di primo livello dovra' garantire:

- Complete coverage of the solid angle
- Robustness: maximal use of available information
- Speed: decision time of the order of $1 \mu\text{s}$

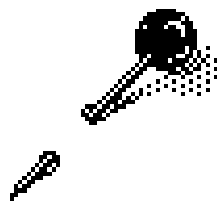
(*Letter of intent CERN-LHCC 92-3 1 Oct. 1992*)

Transverse View

Durante 10 anni LHC produrrà
 $\sim 10^{17}$ collisioni pp

Un'osservazione di 10 eventi
"esotici" potrebbe portare a
Nuova Fisica

Bisogna trovare 10 eventi tra 10^{17}



Un ago in un pagliaio?
Tipico ago: 5 mm^3
Tipico pagliaio: 50 m^3

$\text{ago/pagliaio} = 1/10^{10}$

Cercare nuova fisica ad LHC è
come cercare un ago in
1.000.000 di pagliai!







- prof. Marcello Abbrescia
- University of Bari, Italy
- Email: marcello.abbrescia@uniba.it,
marcello.abbrescia@ba.infn.it,
- Please do not hesitate to contact me for any information, request of additional material, or just a nice scientific discussion.



F. Sauli: **Principles of operation of multiwire proportional and drift chambers**, CERN Yellow Reports, CERN 77-09, 1977. - 92 p., 10.5170/CERN-1977-009

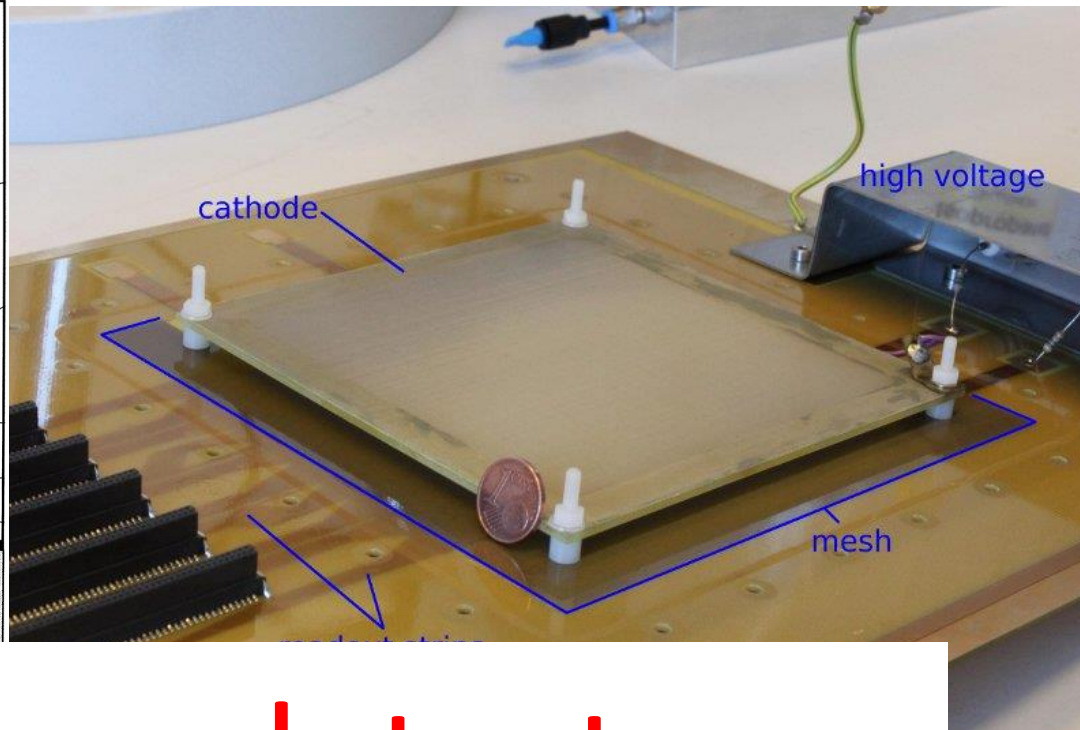
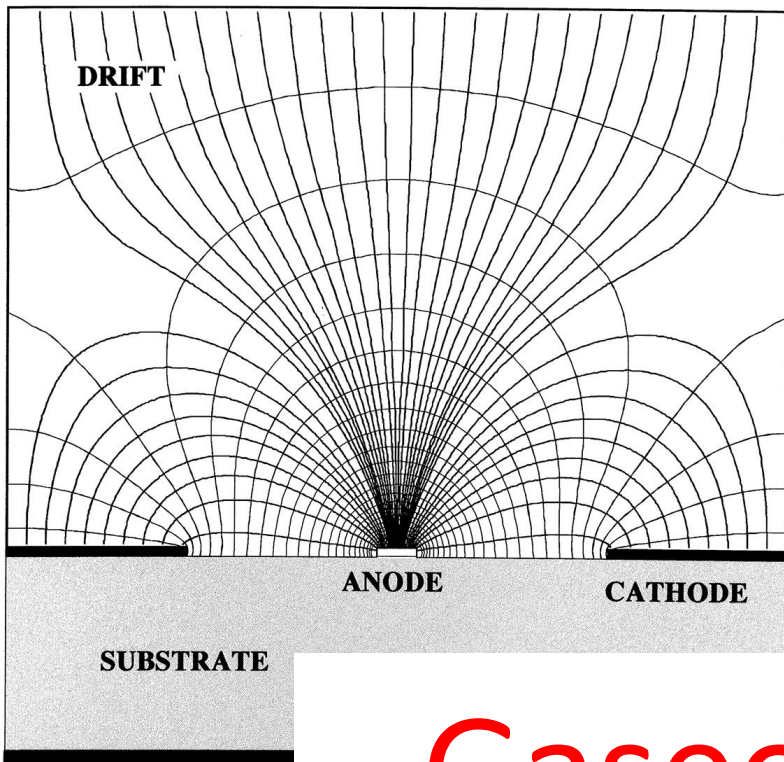
A. Peisert and F. Sauli: **Drift and diffusion of electrons in gases : a compilation (with an introduction to the use of computing programs)**, CERN Yellow Reports, CERN 84-08, 1984. - 127 p.

F. Sauli: **Gaseous Radiation Detectors: Fundamentals and Applications**, Cambridge University Press July 2014, ISBN: 9781107337701 , [hUps://doi.org/10.1017/CBO9781107337701](https://doi.org/10.1017/CBO9781107337701)

Glenn F. Knoll **Radiation Detection and Measurement, 4th Edition, Wiley ed.** ISBN: 978-0-470-13148-0, September 2010 864 Pages

W. Leo, **“Techniques for Nuclear and Particle Physics Experiments: A How-to Approach”**, Springer-Verlag, ISBN-13: 978-3540572800 , ISBN-10: 3540572805

Walter Blum, Werner Riegler, Luigi Rolandi, **Particle Detection with Drift Chambers**, Springer-Verlag 2008, ISBN: 978-3-540-76683-4



Gaseous detectors



Gaseous detectors



Gaseous detectors

M. Abbrescia

EURIZON School on particle detection technologies

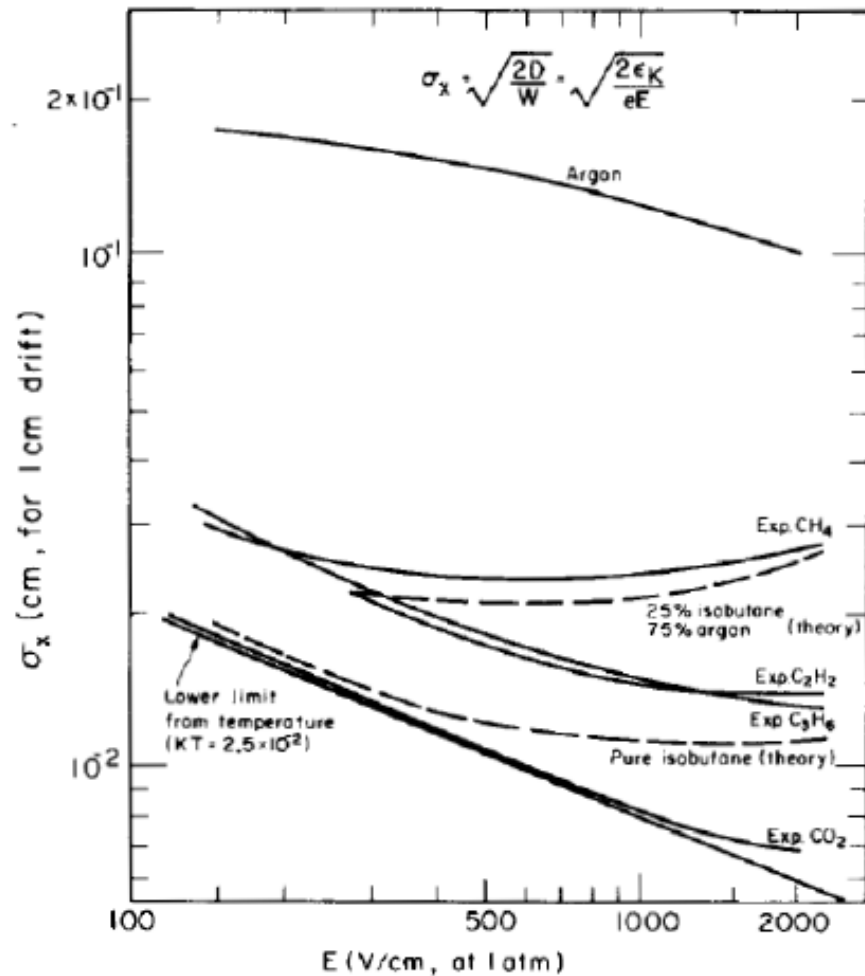
A blue and orange monorail train is traveling on a green steel truss bridge over a river. The bridge has a complex lattice structure. The train is moving from left to right. The river is in the foreground, and there are green trees and a building on the right side. The sky is blue with some clouds.

Gaseous detectors

M. Abbrescia

EURIZON School on particle detection technologies

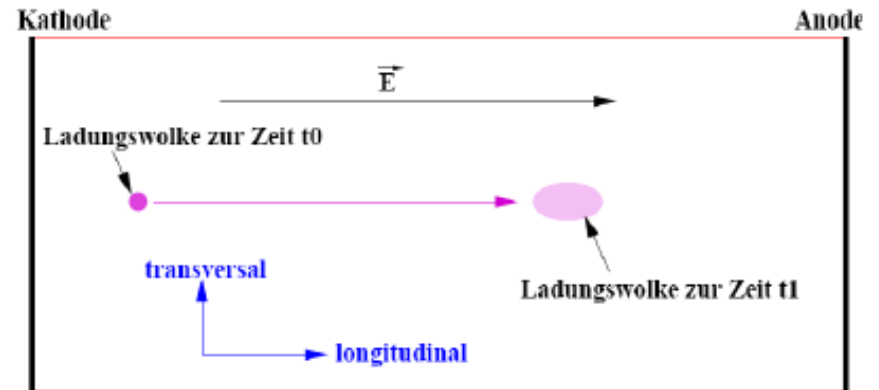
Diffusion in electric fields



Drift in direction of E-field superimposed to statistical diffusion

Extra velocity influences longitudinal diffusion

Transverse diffusion not affected



E-field reduced diffusion in longitudinal direction

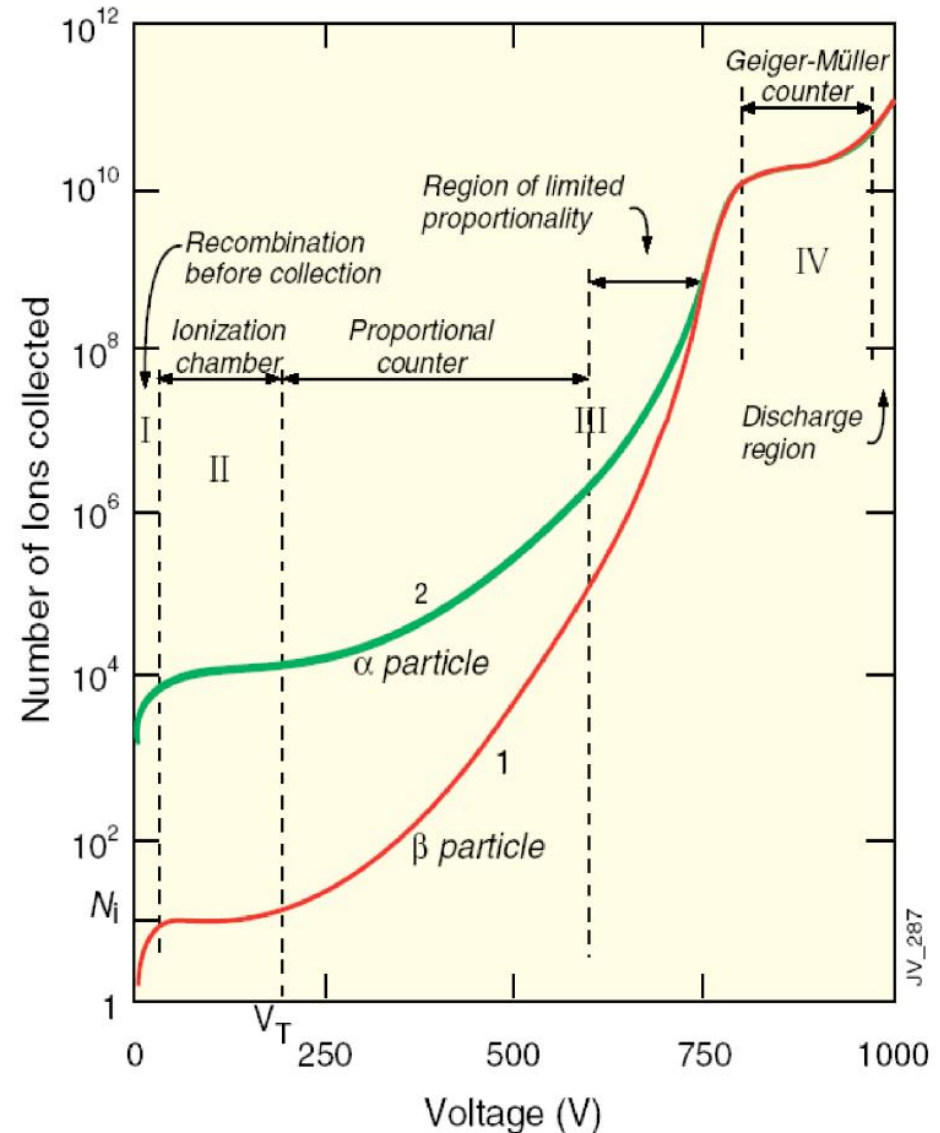
Historical background

- **First gaseous detector** invented by Ernest Rutherford, 1908 Nobel Laureate in Chemistry, with the help of Hans Geiger → proportional counter
 - Further developments by Geiger and Walther Muller permitted to detect single electrons (1928)
 - **Cloud chamber** by Charles Thomson Wilson, Nobel Laureate in 1927 (Bubble chamber by Donald Arthur Glaser, Nobel Laureate in 1960)
 - **Multi-Wire Proportional Chamber**, by George Charpak, Nobel Laureate in 1992
 - **Micro Pattern Gaseous Detectors** (MPGD), beginning of 2000
- ... and in between many many many other detector and successes

Operational regimes of gaseous detectors

Gaseous detectors operate differently depending on the voltage applied between cathode and anode:

- I. Recombination
- II. Charge collection (ionization chambers)
- III. Proportional regime
 - proportional counters
 - limited proportionality - saturation
- IV. Streamer region
 - limited streamer region
 - discharge region



Multi Wire Proportional Chamber

MWPC was developed 1968 by Georges Charpak and it was the first full electronic detector!

The Nobel Prize in Physics 1992 was awarded to Georges Charpak *"for his invention and development of particle detectors, in particular the multiwire proportional chamber"*.

Georges Charpak (1924-2010)

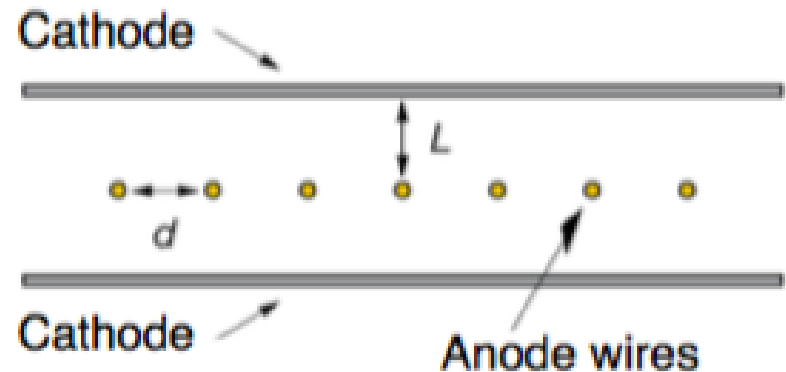
Nobelprize.org

<http://nobelprize.org/physics/laureates/1992/>



It consists of a set of parallel anode wires tightly spaced, between parallel cathodes

The signal is induced by the movement of e- and ions in the electric field.



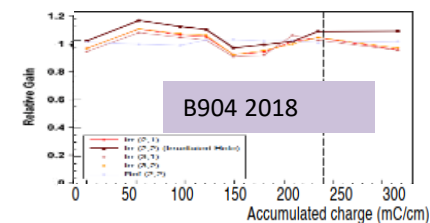
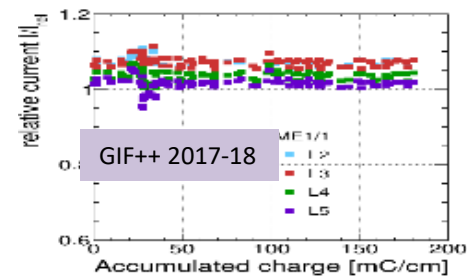
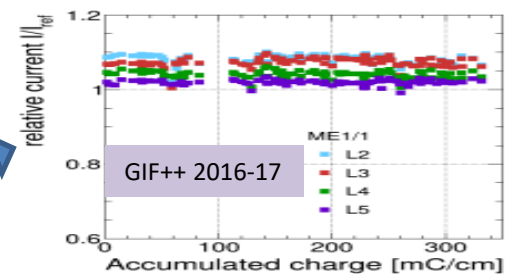
CMS CSC gas mixture

✓ 40% Ar + 50% CO₂ + 10% CF₄

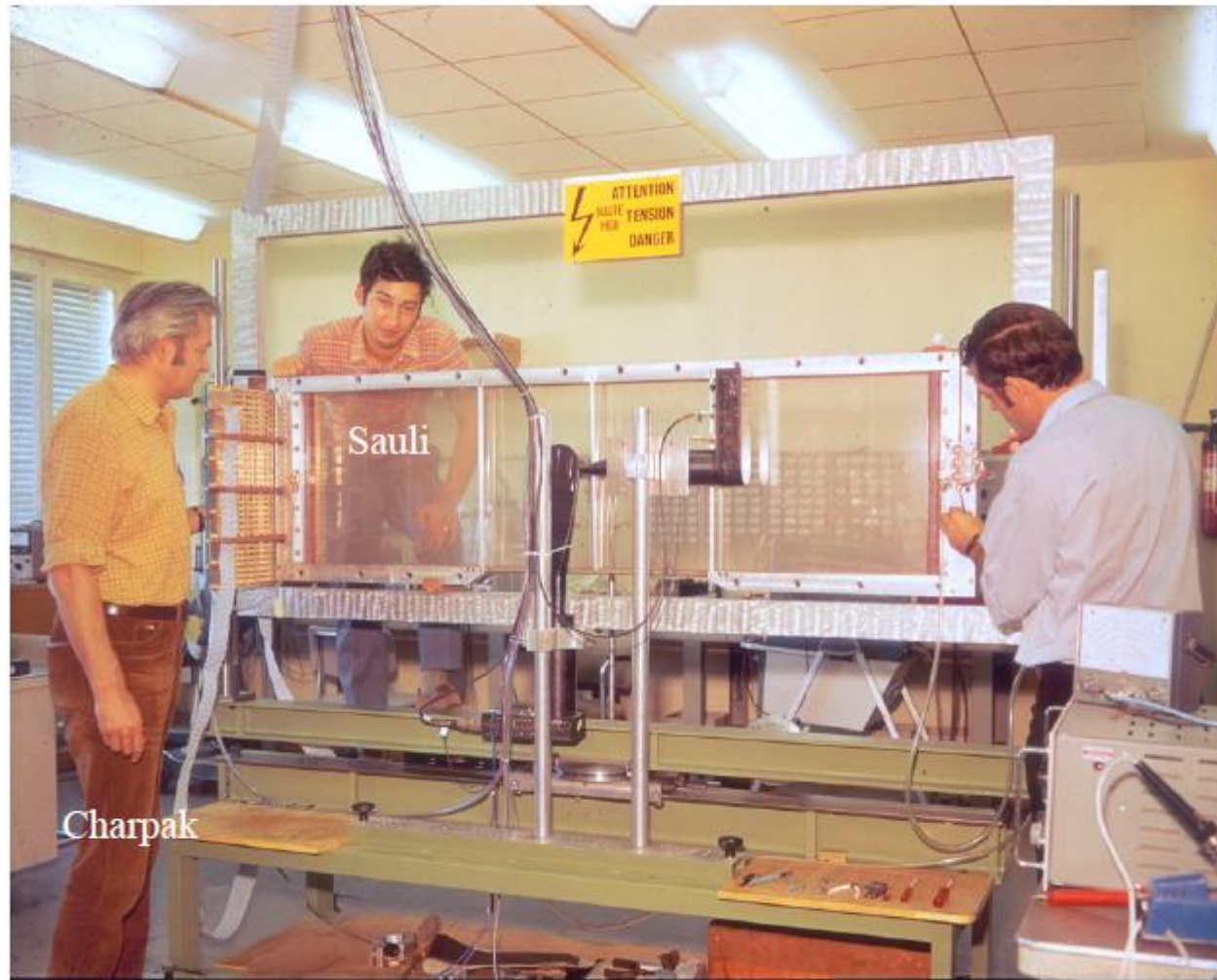
➤ CF₄ ensures good timing (higher v_{drift}), operation stability (avalanche quencher) and anti-aging properties

In view of a F-gas reduction consumption, tests have been done with reduced CF₄ concentration. They indicate stable operation and no degradation of performance is seen even after integrating the charge equivalent to HL-LHC plus a safety factor.

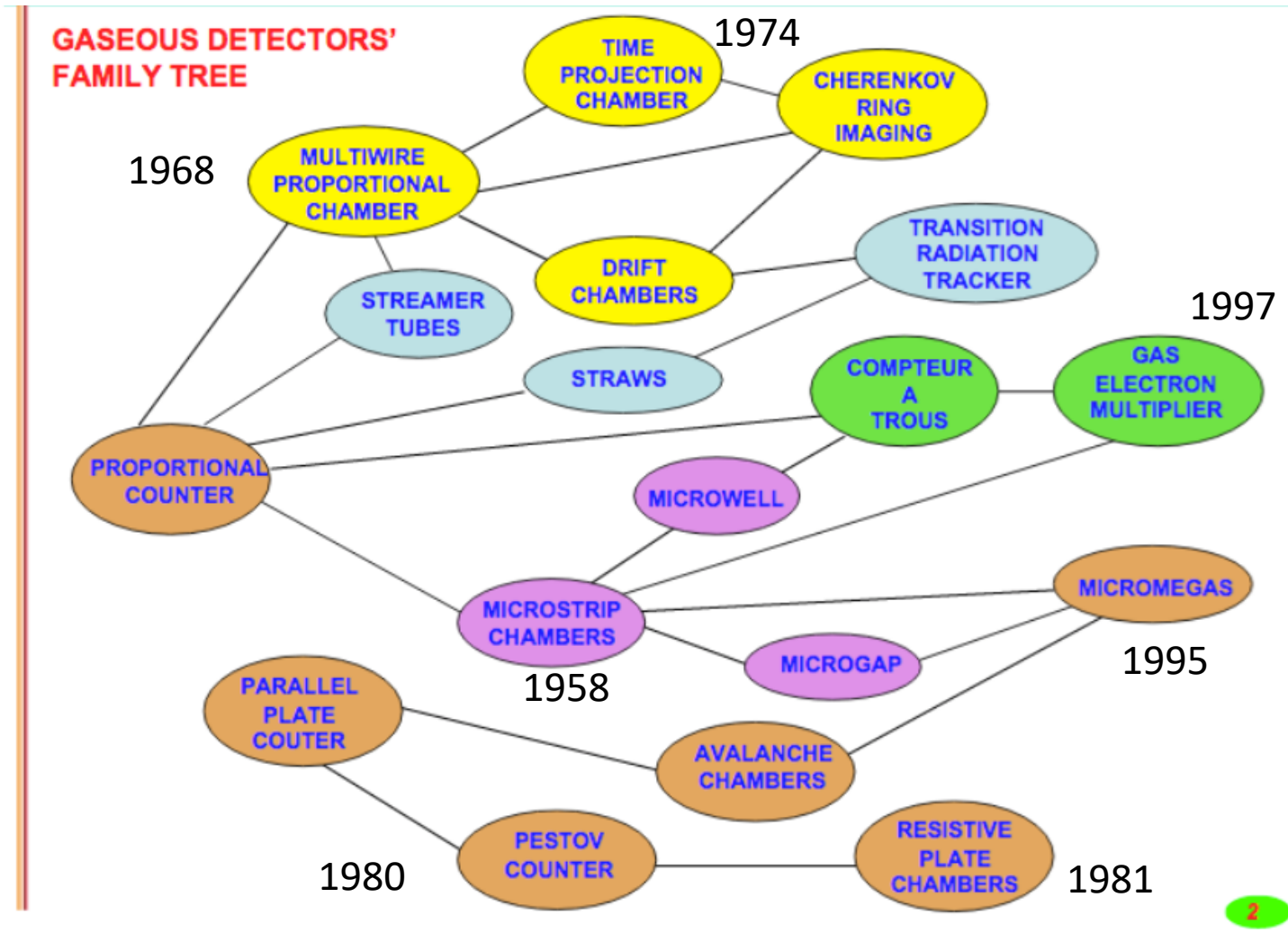
- CSCs irradiated at CERN GIF++ (2016-17) and PNPI (2016) with 10% CF₄ and Ar-CO₂ (40+50)% have shown no signs of aging up to >3x the charge of 3000fb⁻¹ integrated lumi at HL-LHC
- CSC irradiated at CERN GIF++ & B904 (2017-18) with 2% CF₄ and at PNPI (2017) with 1.6% CF₄ and Ar-CO₂ (40+58)% show stable gas gain after 3-4x HL-LHC.
- CSC prototypes irradiated at CERN B904 (2018) w/o-CF₄ and Ar-CO₂ (40+60)% show stable gas gain after 3x HL-LHC



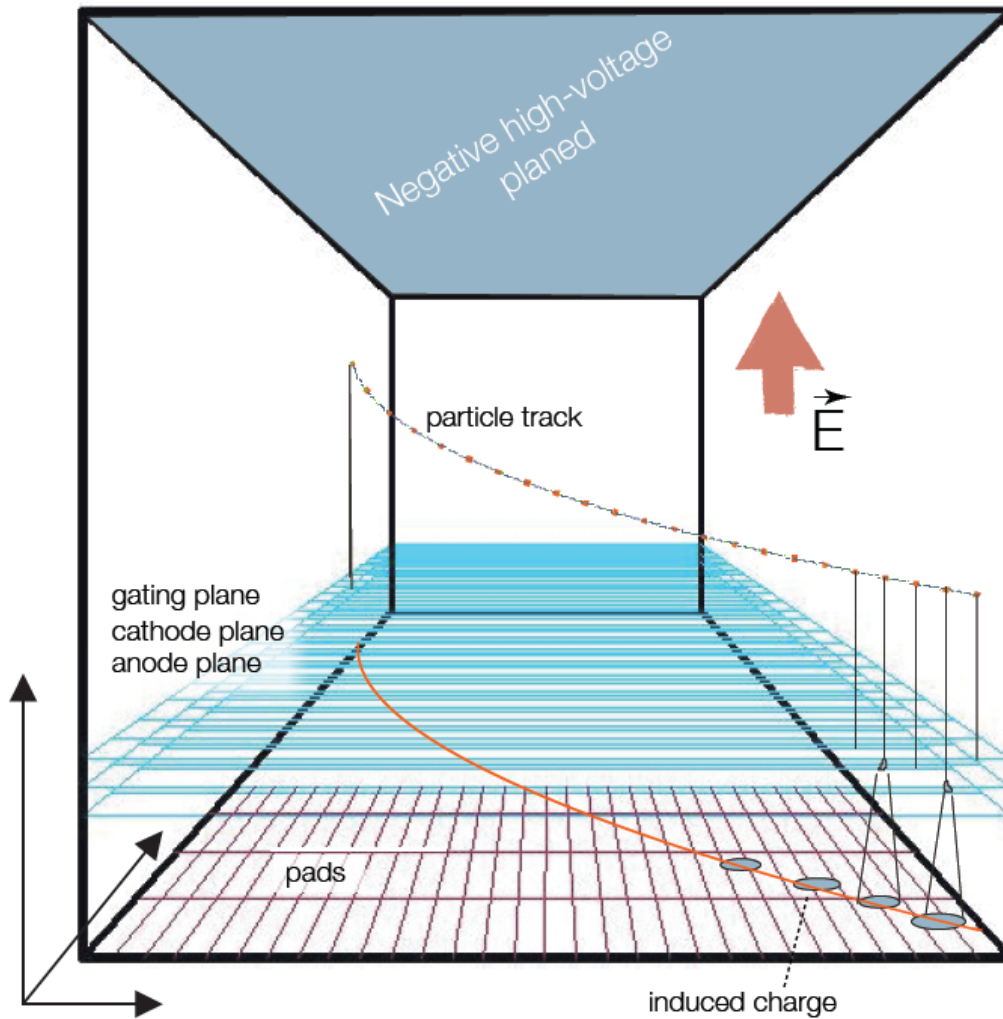
LARGE MWPC PROTOTYPE (1971)



Gaseous detectors family tree



TPCs pros and cons



Advantages:

- Complete track within one detector yields good momentum resolution
- Relative few, short wires (MWPC only)
- Good particle ID via dE/dx
- Drift parallel to B suppresses transverse diffusion by factors 10 to 100

Challenges:

- Long drift time; limited rate capability [attachment, diffusion ...]
- Large volume [precision]
- Large voltages [discharges]
- Large data volume ...
- Extreme load at high luminosity; gating grid opened for triggered events only ...

Typical resolution:

z : mm; x : 150 - 300 μm ; y : mm
 dE/dx : 5 - 10%

TPCs – technical solutions

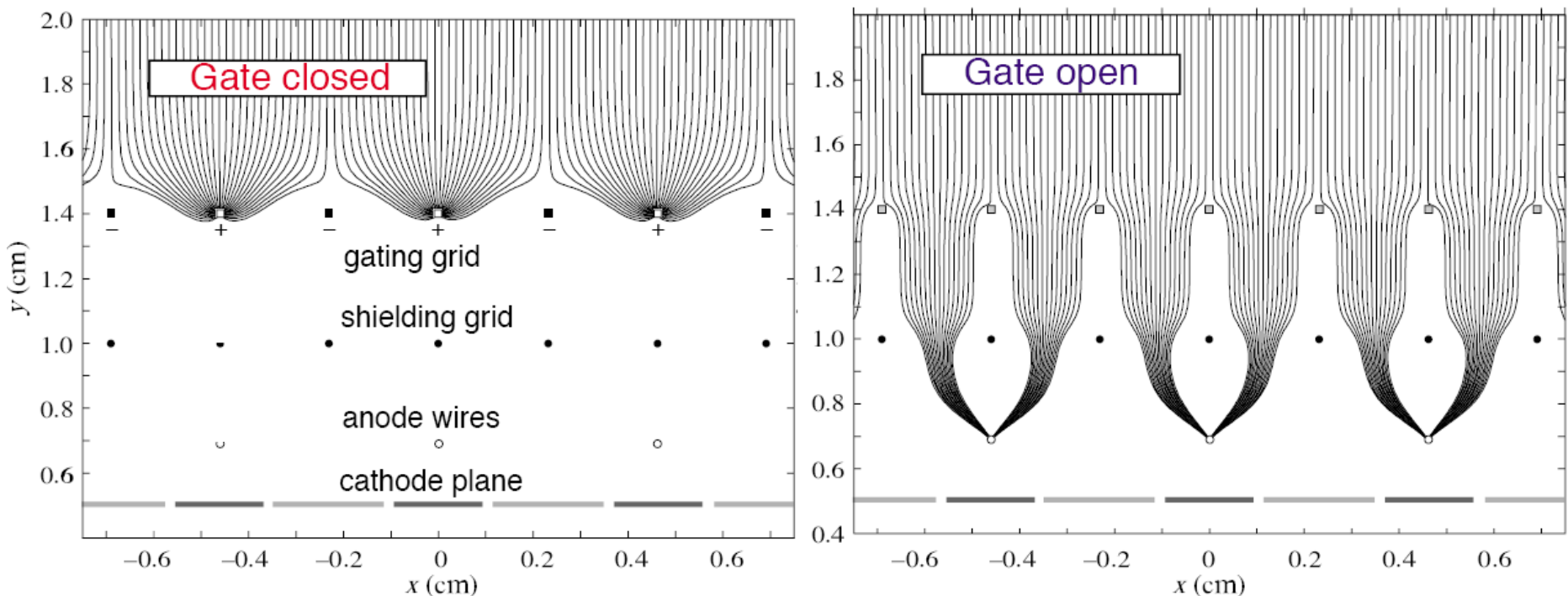
Difficulty: space charge effects due to slow moving ions
change effective E-field in drift region

Important: most ions come from amplification region

Solution: Invention of gating grid; ions drift towards grid ...

[Also: shielding grid to avoid sense wire disturbance when switching]

Requires external trigger to switch gating grid ...



Why Electrodes are “cured” with linseed oil ?

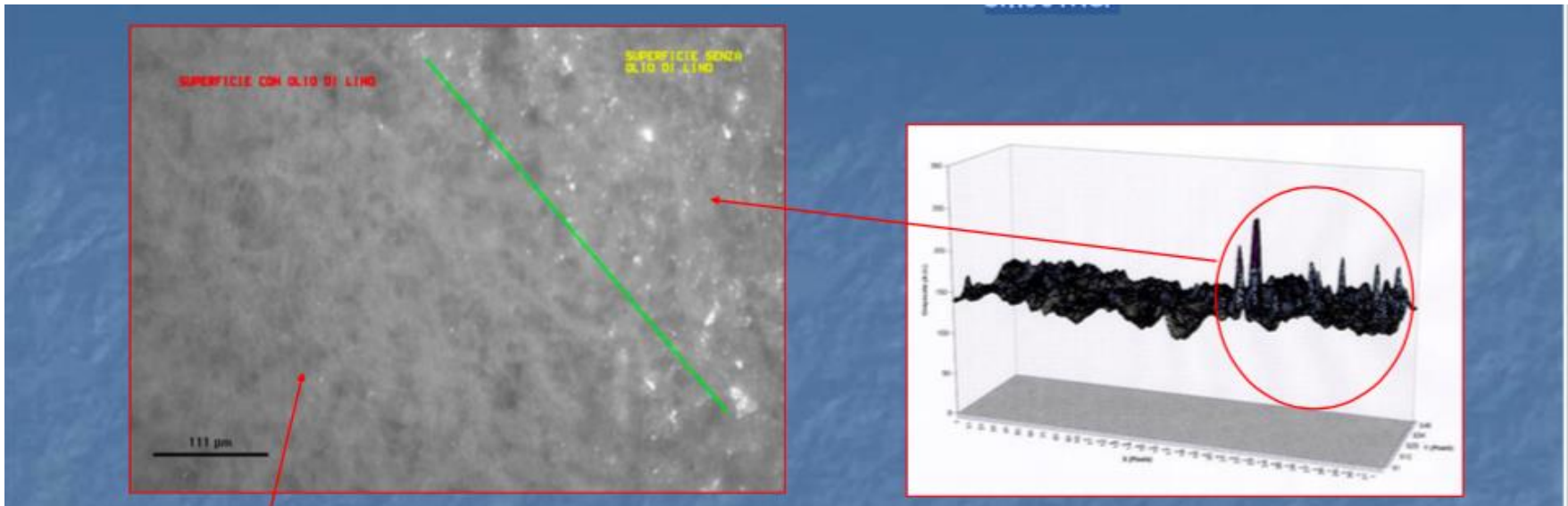
Linseed oil (If you look on Wikipedia..)

The Linseed oil is used as a painting medium. It was a significant advantage in the technology of oil painting!

Mixture of triglycerides, formed by one molecule of glycerol and three molecules of linear fatty acids. The oil is cured forming a hard stable film because of oxidation followed by polymerization.

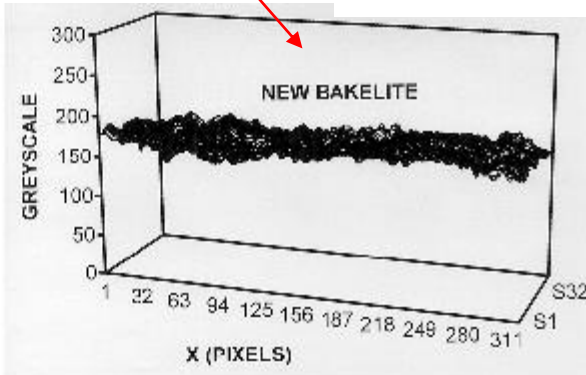
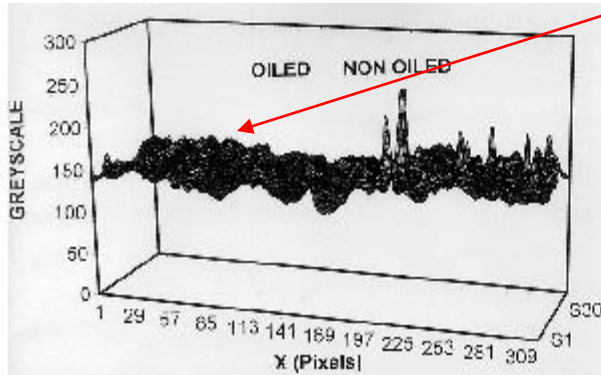
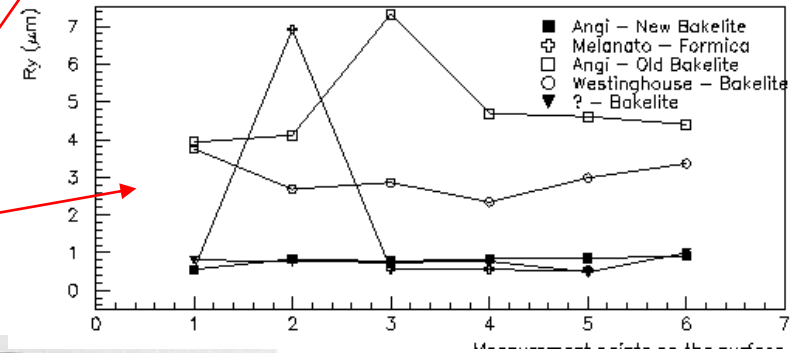
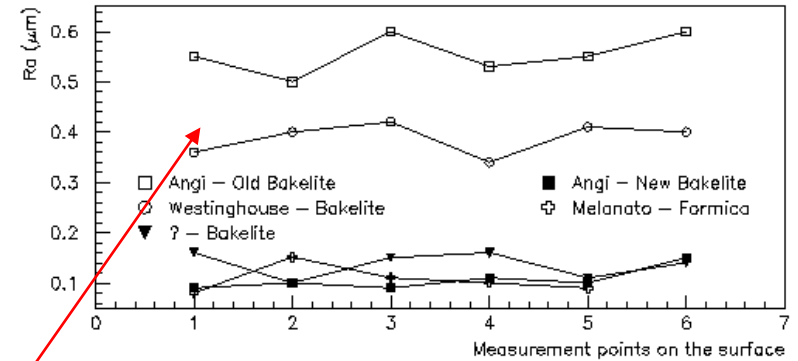
Linseed oil makes the surface smoother

The smoother the surface, the lower the intrinsic noise of the detector

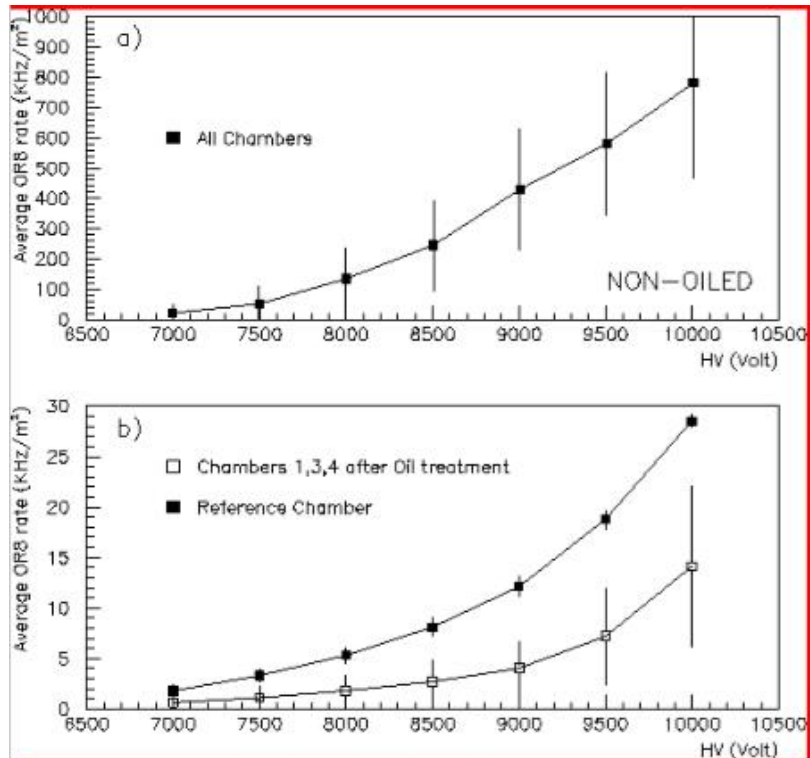


Comparison among not-oiled, oiled and smoother surfaces RPC

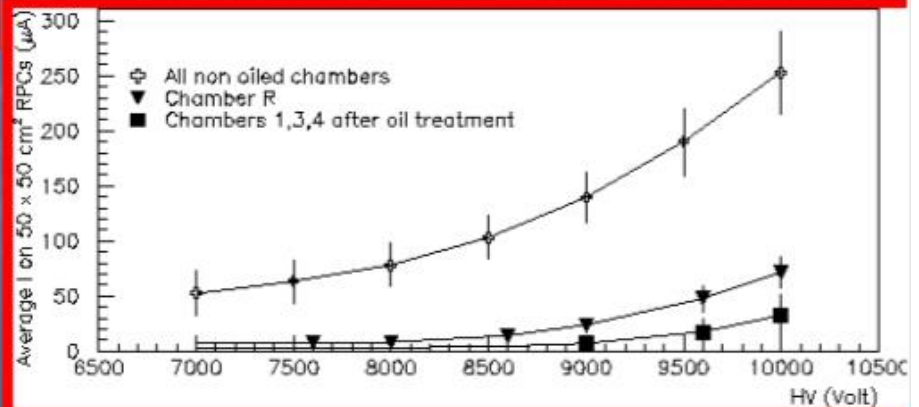
Direct measurements of surface roughness
 -mono-dimensional
 - bi-dimensional



RPC: the linseed Oil

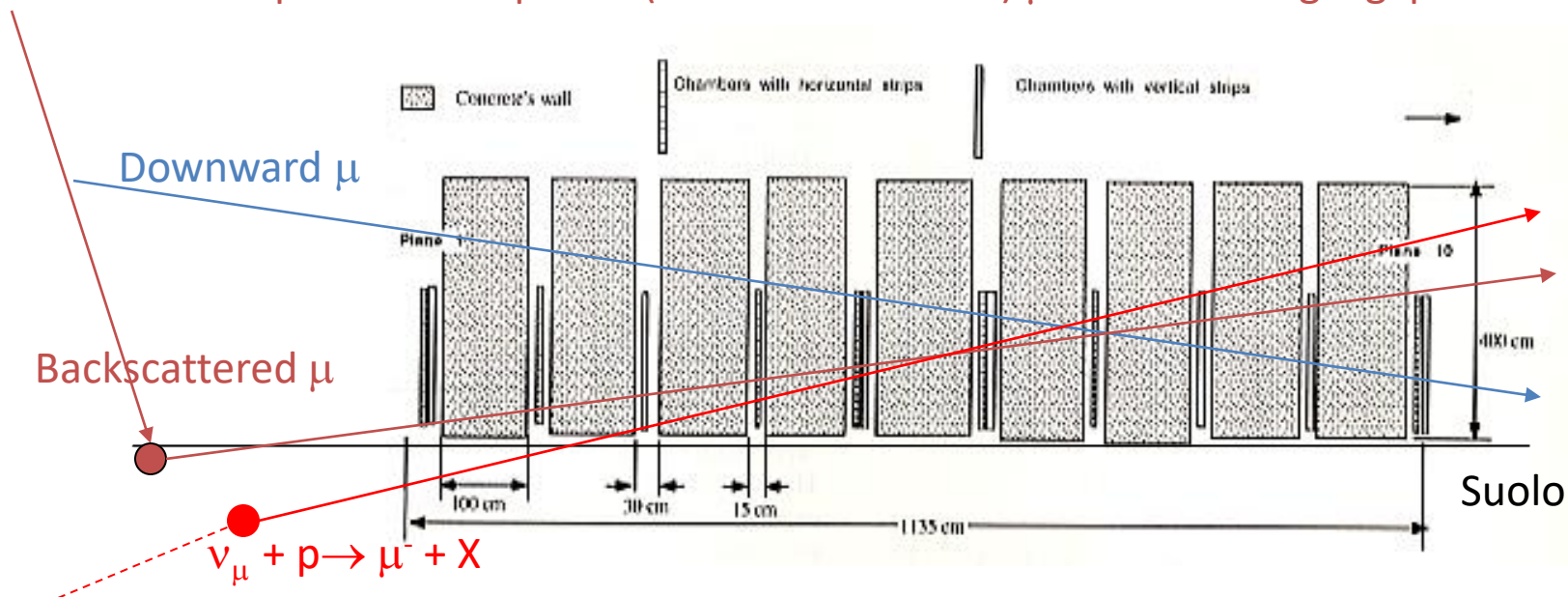


Reduced Currents and Noise rate



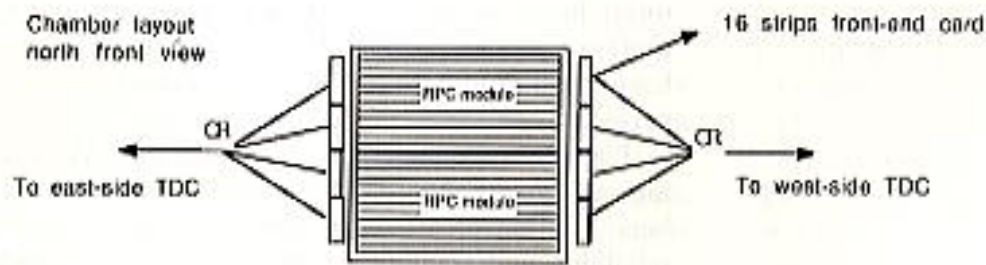
MINI: first experiment fully implemented with RPCs

MINI: telescope for atmospheric (and backscattered) μ : 64 m² of single gap RPC



Operating from since 1990 to 1996

10 stations, equipped with 14 chambers
 8 chambers with horizontal strips
 6 with vertical strips



Precise tracking!

MINI

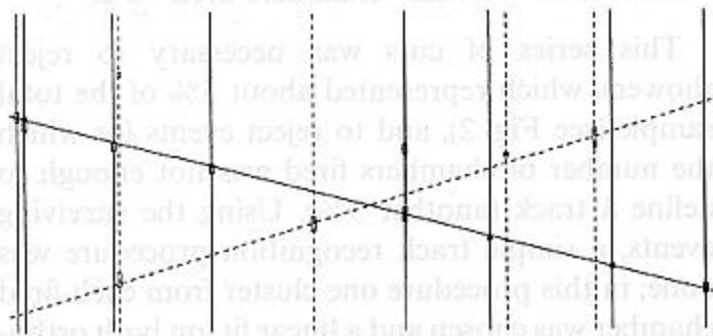
3D event reconstruction

Atmospheric shower

Single μ

Event n, 209

Classification: single muon event



Datafile: DAQ951207-1908

MINI was used both for physics and for studies on RPC performance

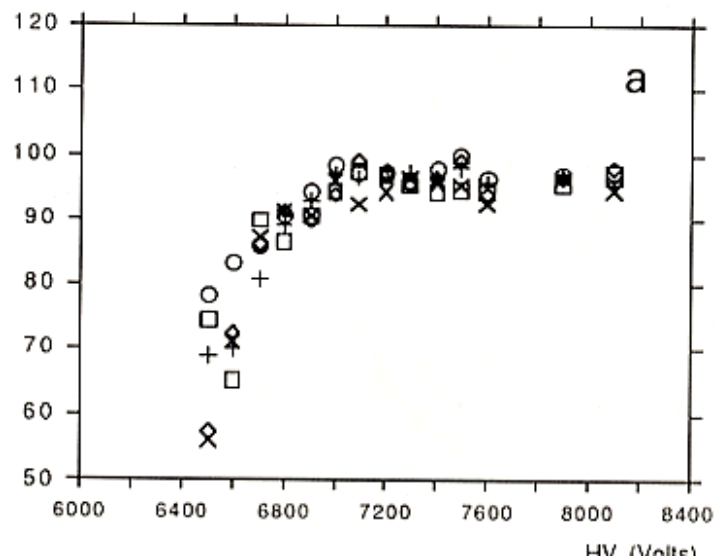
Efficiency uniformity

Event n, 1267

Classification: shower

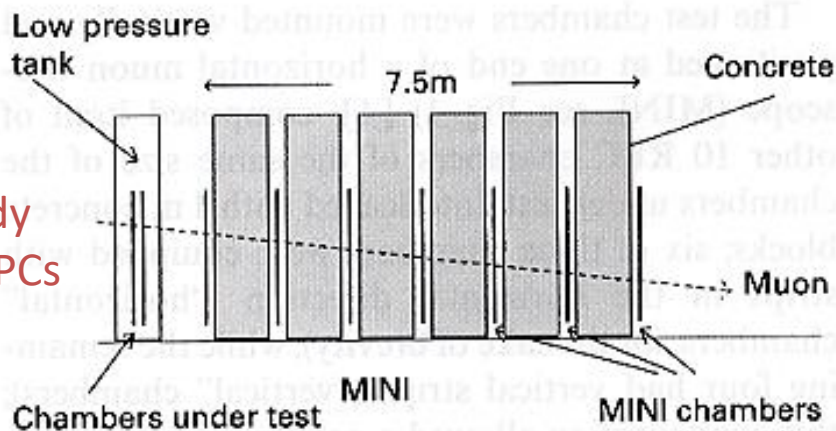


Lateral and upper view superimposed

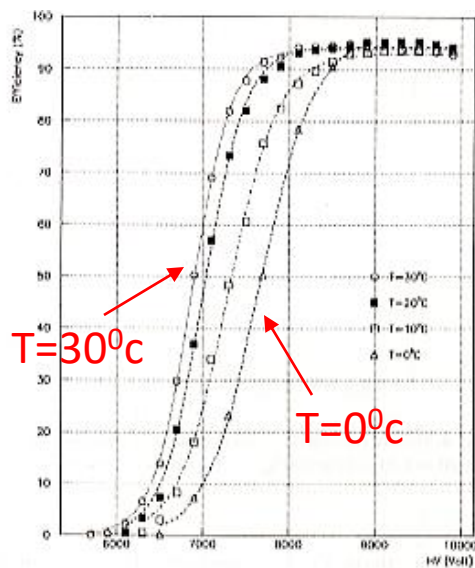


MINI

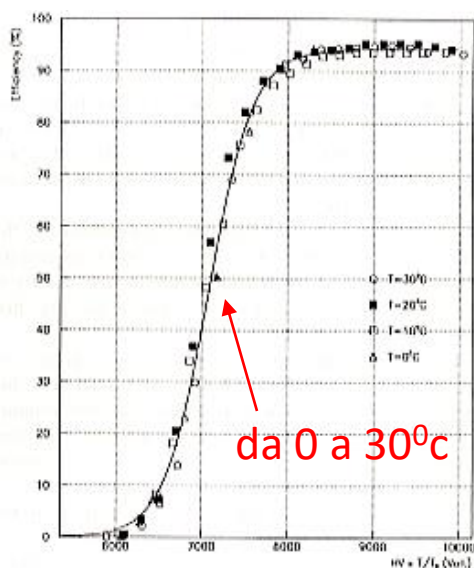
MINI was used to study the performance of RPCs vs. T and p



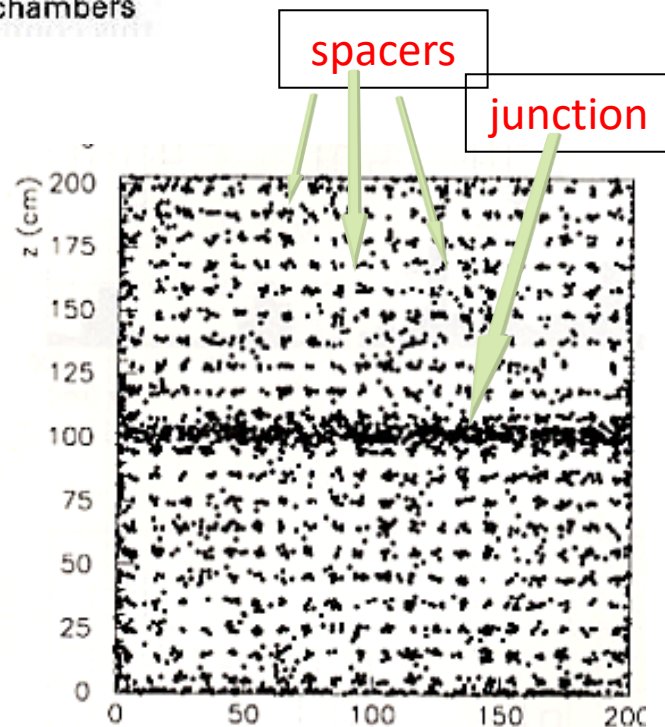
Prima "radiography" of a chamber using cosmic μ (inefficiency points due to the spacers and junctions)



HV



$HV \times \frac{T}{T_0}$



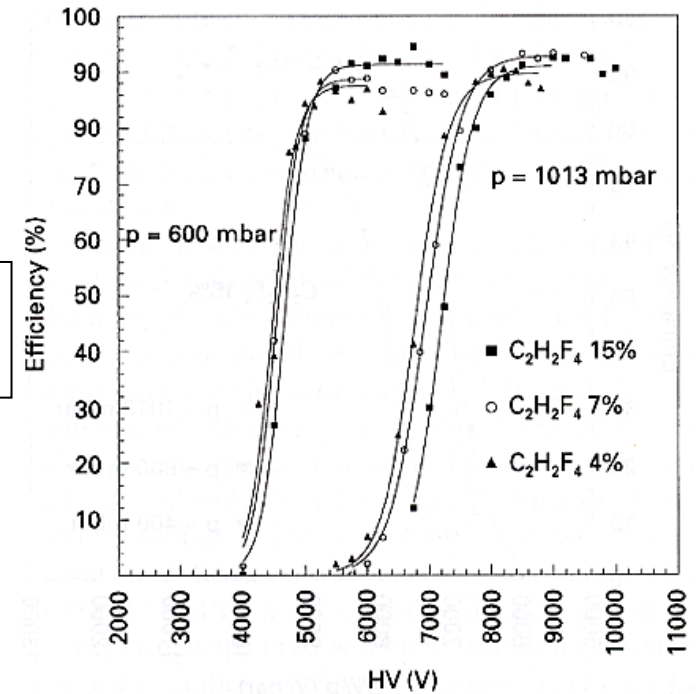
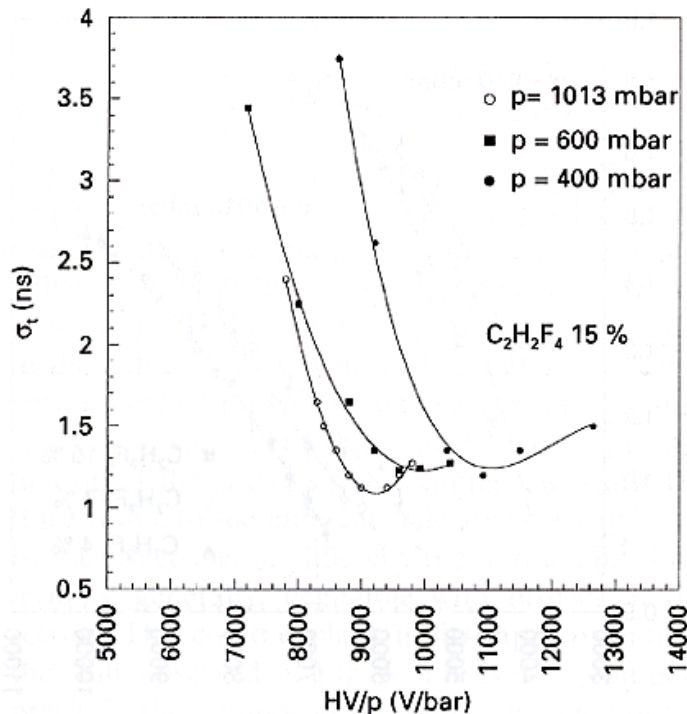
MINI

One of the most interesting results from MINI was checking that RPCs can operate at reduced pressure (down to 400 mbar)

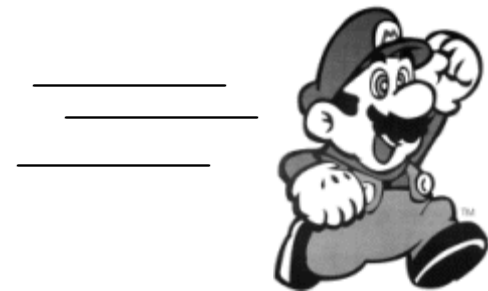
Not trivial, dealing with gaseous detectors...

Less primary pairs

Change in the mean free path, gas density ...



“Pilot” experiment for ARGO-0



ARGO-YBJ



Argo Panopte (who sees everything) is described as being very strong, since he had 100 eyes and was capable to sleep with only 50 of his eyes closed-

ARGO-YBJ (Astrophysical Radiation with Ground based Observatory at YangBaJing, Tibet) did never sleep.



Experiment to study with high efficiency and sensitivity Extensive Air Showers with energy $> 100 \text{ GeV}$

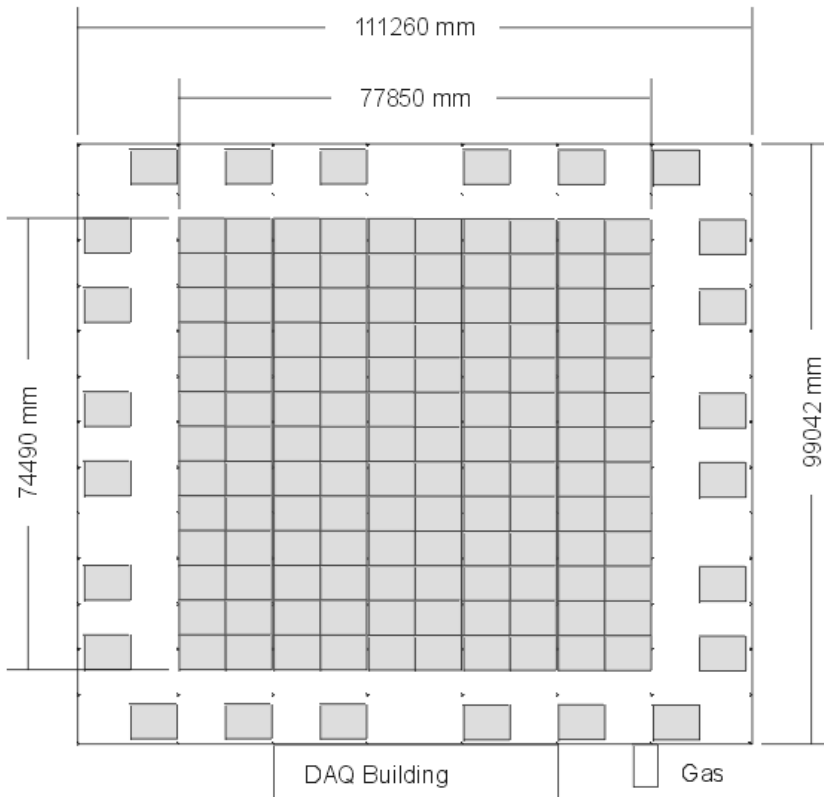


γ Astronomy $\sim 100 \text{ GeV}$
Diffuse γ rays
 γ -Burst
Ratio p/p bar
Spectrum of the primaries
Physics of Sun and atmosphere

ARGO-YBJ

Main Building with RPCs

ArgoN05



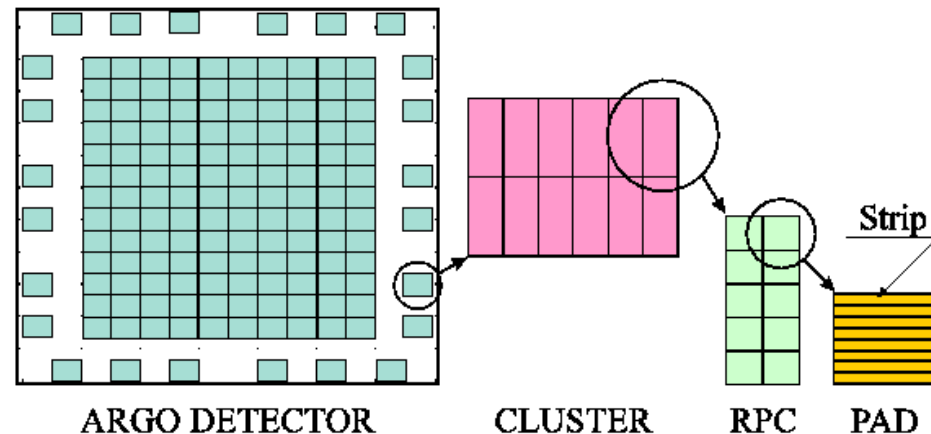
Detector carpet: 10 x 13 Clusters, 1560 RPC
 Sampling ring: 6 x 4 Clusters, 288 RPC
 Total: 154 Clusters, 1848 RPC
 For a complete coverage another 84 Clusters (1008 RPC) are needed



78 x 74 m² covered with RPCs

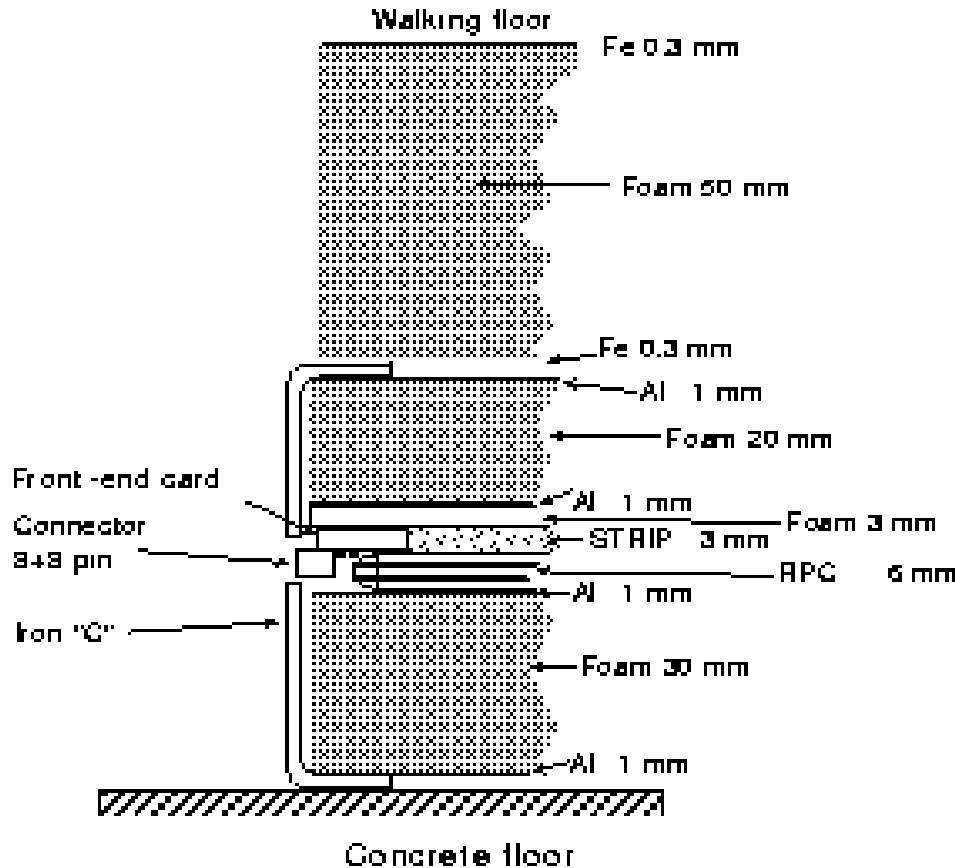
In addition a guard ring with partial cover up to 100 x 100 m²

“RPCs chosen because their low cost, large active area, excellent time and spatial resolution, easy of integration as a large system.”



ARGO-YBJ

ARGO detector cross section



Single gap RPCs

Volume resistivity $> 5 \cdot 10^{11} \Omega\text{cm}$

Area: $126 \times 285 \text{ cm}^2$

Aluminium strips $6 \times 56 \text{ cm}$

Fast-OR of 16 strips defining a PAD

10 pads ($56 \times 60 \text{ cm}^2$) covering a chamber (in total 18480 pads)

Streamer mode

Gas:

15% Argon,

10% Isobutane

75% Tetrafluoroethane $\text{C}_2\text{H}_2\text{F}_4$

Use of converters to increase the number of hits/event.

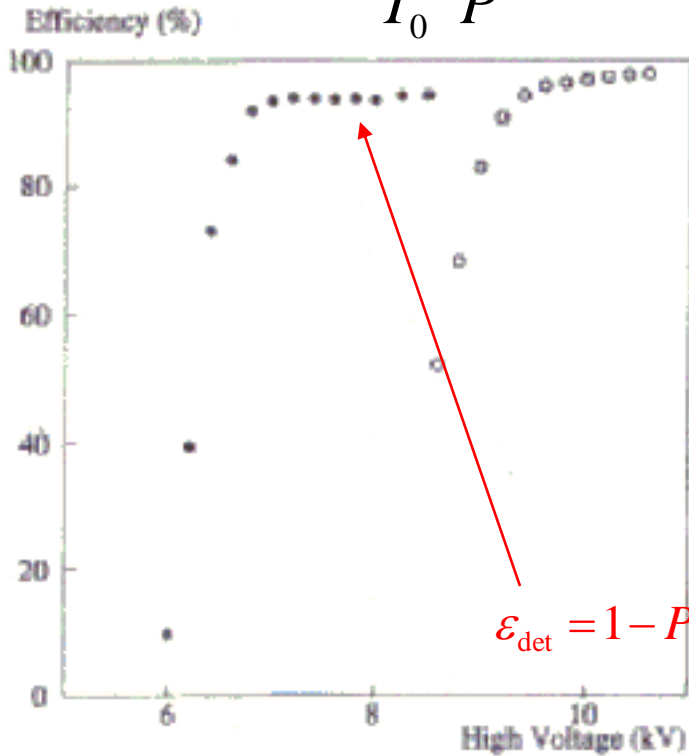
ARGO-YBJ

Operating at 4300 m above sea level

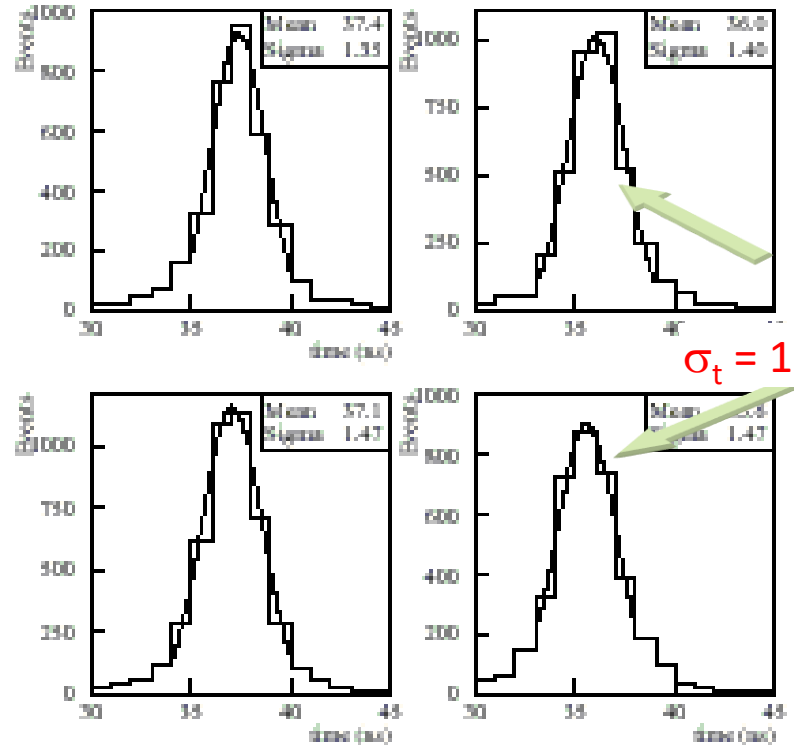


Low pressure ~ 600 mbar

$$V_{eff} = V_0 \frac{T}{T_0} \frac{P_0}{P}$$



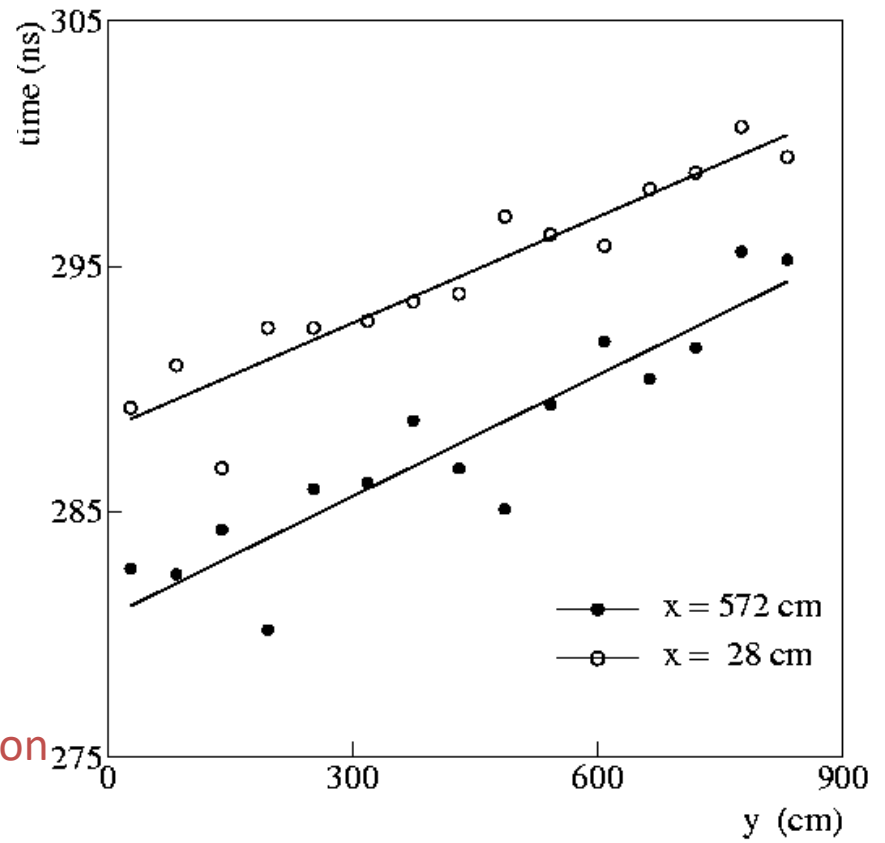
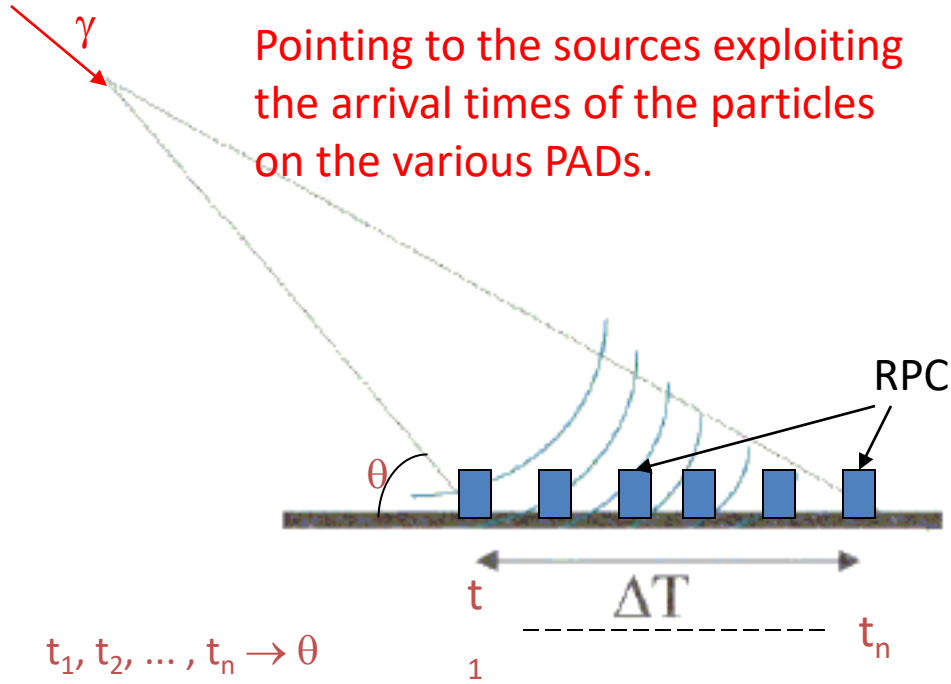
$$\epsilon_{det} = 1 - P(0) = 1 - e^{-\bar{n}}$$



$\sigma_t = 1.45$ ns

Time resolution

ARGO-YBJ



Interesting application where good time resolution is essential for a good tracking

$$\Delta t_{\text{RPC}} \sim 1\text{-}2 \text{ ns} \rightarrow \Delta\theta = 1 \text{ mrad}$$

$$\frac{\text{Signal}}{\text{Background}} \propto \frac{1}{(\Delta\theta)^2}$$

Experiments using RPCs

1st generation RPCs were immediately used in many physics experiments...

Veto

Nadir: 120 m² of double gap RPCs used as a veto on cosmic particles in an experiment on neutron-anti neutron oscillations

Fenice: 300 m² of RPC used as a cosmic vet in the reaction $J/\Psi \rightarrow n\bar{n}$ at Adone

Operated in streamer mode
(Ar-isobutane-Freon)

HV 7-8 kV

Veto efficiency: 97-99%/plane

Concrete shield

Active veto system



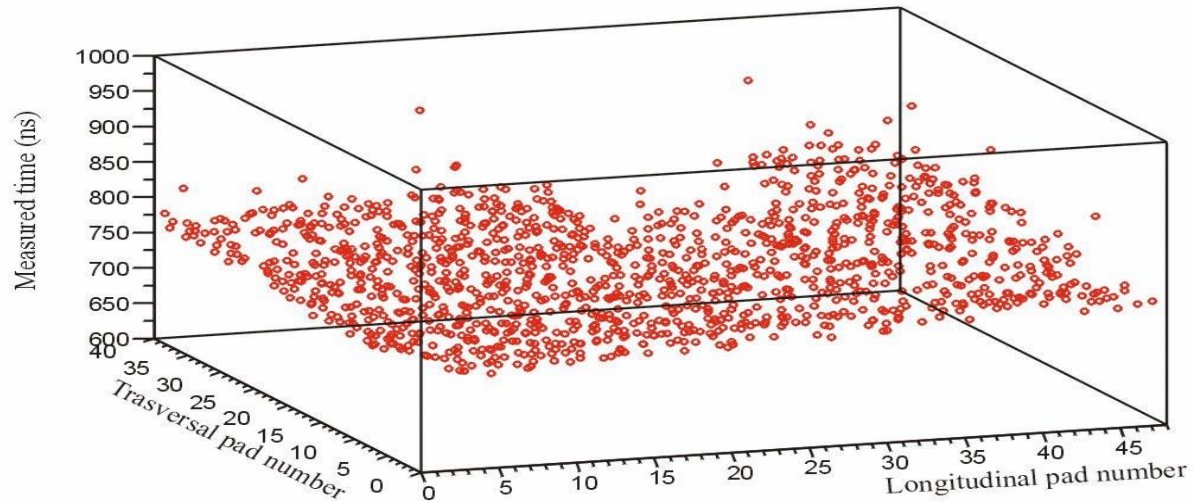
Trigger and tracking at accelerators

WA92: 72 m² of RPC used as trigger on μ events with high p_t in semi-leptonic decays of the B (SPS at CERN)

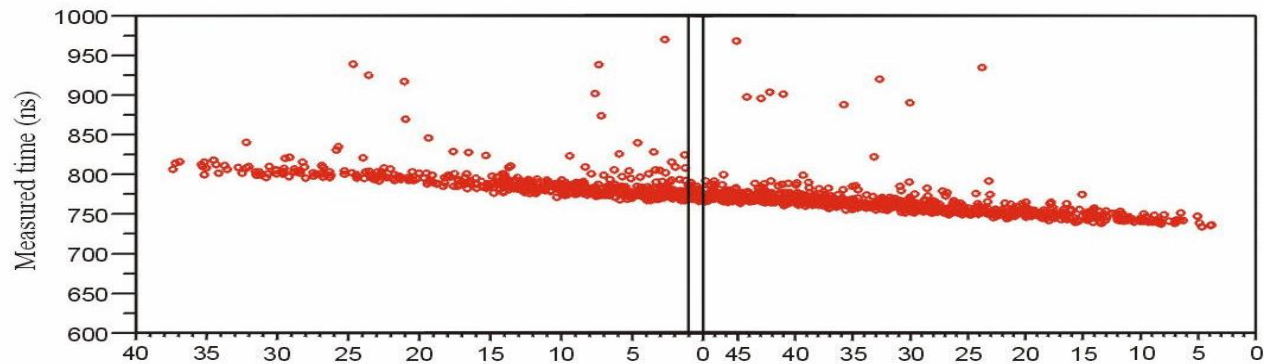
E771: 60 m² of RPC used as trigger and tracking come trigger on μ events with high p_t in semi-leptonic decays of the B (Fermilab)



ARGO-YBJ



Picture of an event on 16 clusters



The same event from such a point of view to appear as a plane

NCP contribution on CMS R&D

Pakistan was actively involved in the CMS RPC project since the R&D phase

- **PK-01/99** 400*400 mm² double gap RPC, Italian bakelite 1999. (non-oiled)
- **PK-02/00** Full size RE2/2 chamber, tested at GIF in 2000, phenolic bakelite gaps fabricated in Italy ($\rho \approx 10^{10}\Omega$, not-oiled)
- **PK-03/01** Full size RE2/2 chamber, tested at GIF in 2001, melaminic bakelite gaps ($\rho \approx 10^{10}\Omega$, not-oiled)
- **PK-04/02** Full size RE2/2 chamber, tested at GIF in 2002, gaps supplied from Korea ($\rho \approx 10^{10}\Omega$ cm, not oiled)
- **PK-05/03** Full-size RE2/2, tested at GIF in 2003, gaps supplied from Korea ($\rho \approx 10^{10}\Omega$ cm, oiled))



1999 (400*400 mm²)



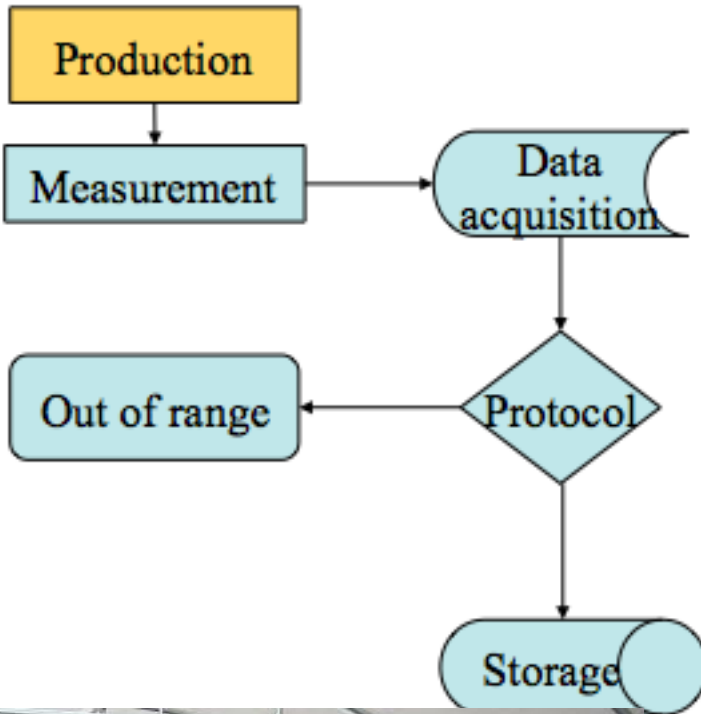
2000 Full Size



2003 Full Size

Bakelite quality control

CMS example



Bulk resistivity ρ

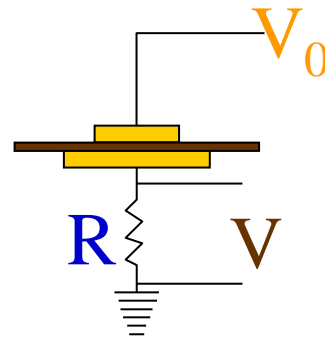
Determines the time constant of an elementary RPC cell and the rate capability

Average roughness R_a

It is related to the quality of the surface. A small R_a reduces spontaneous discharges which might affect the RPC rate capability

Dielectric constant ϵ_p

It is related to τ and to the average fast charge q_e of a single avalanche



$$\rho = k \frac{V_0}{(V/R)}$$

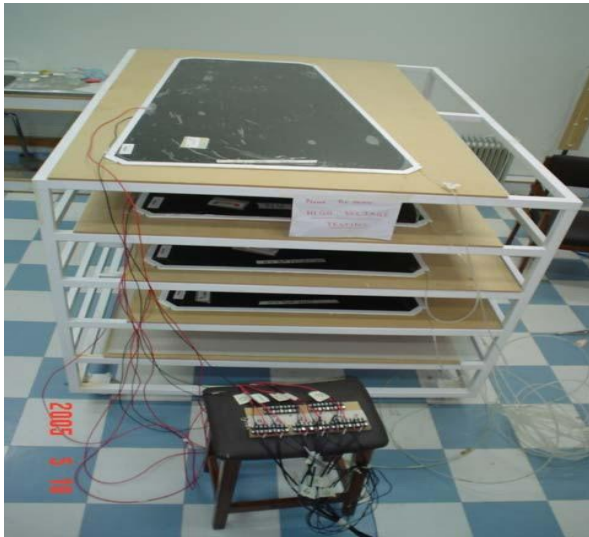
k = geometrical factor (98.17)

$V_0 = 500 \text{ V}$

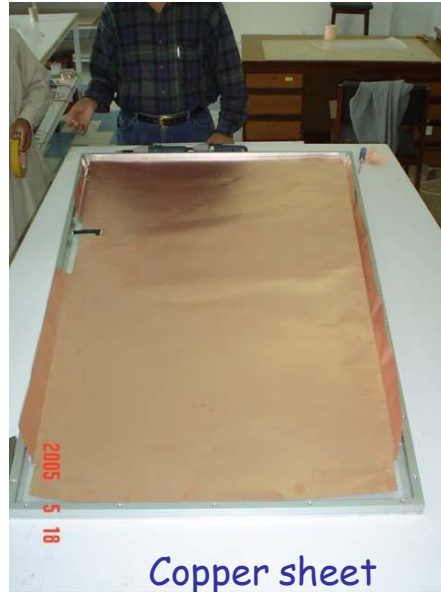
$R = 10 \text{ or } 100 \text{ k}\Omega$

CMS RPCs production @ NCP

66% of Endcap chambers (288 + 10 % contingency) have been produced in NCP lab...



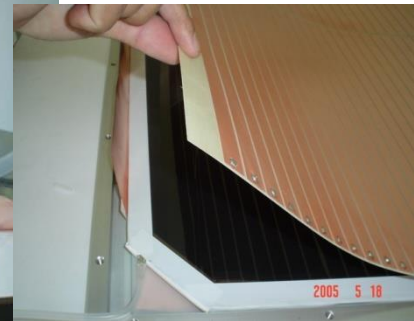
Gas leak test, Spacer test and HV vs Dark Current test on the gas gaps



Copper sheet

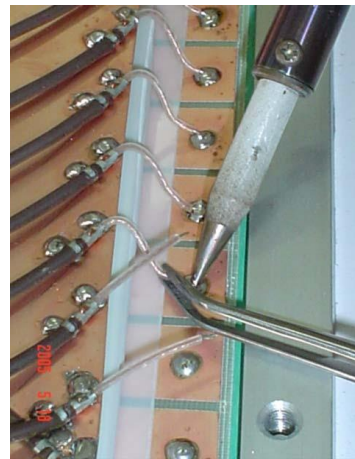


Gas pipes at inlet



Readout strips sheet

Assembly Procedure



Soldering



Mounting of FEBs

Conclusions: the RPC from 1981 to nowadays

The RPC are gas detector are extensively used in several experiments

A lot of progress on detector performance done:

- **Rate capability** from 10 Hz/cm² to 30000 Hz/cm²
- **Time resolution** from 1 ns to 50 ps
- **Space resolution** from 1 cm to 0.01cm
- **Stable detector performance at LHC experiment**
- ...while keeping the same simple structure which always allowed to scale the detector to large surfaces

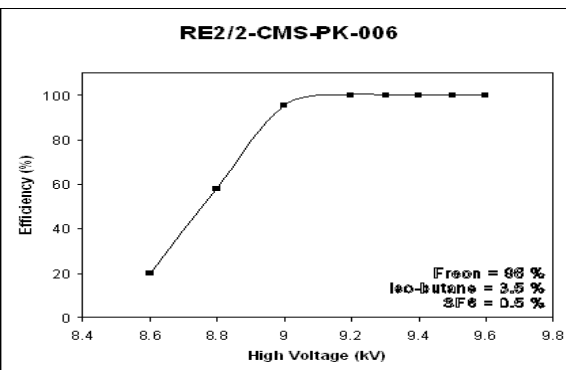
The Secret?

- Right choice of materials and electronics
- Severe QC and AQ during construction
- Continuously monitoring of the detector performance during the LHC operation and maintenance during the LHC shutdown

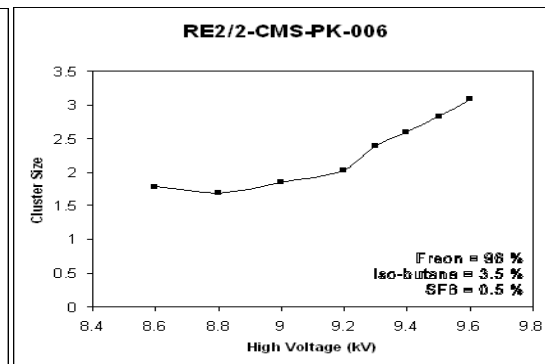
Looking forward for future applications of the RPCs

CMS RPCs validation @ NCP

... tested in NCP cosmic test lab....



Efficiency



Cluster size

...and Shipped to CERN